

**DOKUZ EYLÜL UNIVERSITY**  
**GRADUATE SCHOOL OF NATURAL AND APPLIED SCIENCES**

**SEASONAL VARIATION OF DISSOLVED  
ORGANIC MATTER IN İZMİR BAY**



**by**  
**Hakan ALYÜRÜK**

**February, 2018**  
**İZMİR**

# **SEASONAL VARIATION OF DISSOLVED ORGANIC MATTER IN İZMİR BAY**


**A Thesis Submitted to the  
Graduate School of Natural and Applied Sciences of Dokuz Eylül University  
In Partial Fulfillment of the Requirements for the Degree of Doctor of  
Philosophy in Marine Sciences and Technology Program**

**by  
Hakan ALYÜRÜK**


**February, 2018  
İZMİR**

## PhD THESIS EXAMINATION RESULT FORM

We have read the thesis entitled “SEASONAL VARIATION OF DISSOLVED ORGANIC MATTER IN İZMİR BAY” completed by HAKAN ALYÜRÜK under supervision of PROF.DR. AYNUR KONTAŞ and we certify that in our opinion it is fully adequate, in scope and in quality, as a thesis for the degree of Doctor of Philosophy.

  
.....  
Prof.Dr. Aynur KONTAŞ

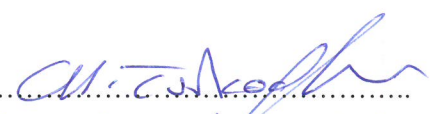
Supervisor

  
.....  
Prof.Dr. Hasan Baha BÜYÜKİŞİK

Thesis Committee Member

  
.....  
Prof.Dr. Esin SUZER

Thesis Committee Member

  
.....  
Prof. Dr. Muhammed TÜRKÖLÜ

Examining Committee Member

  
.....  
Doç. Dr. E. Yesim ÖZKON

Examining Committee Member

  
.....  
Prof.Dr. Kadriye ERTEKİN

Director

Graduate School of Natural and Applied Sciences

## ACKNOWLEDGEMENTS

I am very grateful to my supervisor Prof.Dr. Aynur KONTAŞ for her guidance and support. I am thankful to researchers, Prof.Dr. Esin SUZER, Res.Assist.Dr. Enis DARILMAZ, Dr. Oya ALTAY and Ph.D. student Mustafa BİLGİN from Institute of Marine Sciences and Technology for their support. I also thank to R/V K. Piri Reis captains and crews for their support at field studies. I thank to the Scientific and Technological Research Council of Turkey for scholarship (TÜBİTAK-BİDEB 2228). This thesis had only been funded by OYP Research Project Funds of The Turkish Council of Higher Education. However, amino acid analyses were performed on the HPLC system that was formerly funded by two TÜBİTAK projects. I want to thank TÜBİTAK-COST ES 1003 project (Project No: 110Y193, Project Name: Biodiversity properties in Aegean Sea ecosystem: Plankton, Benthos and Bacteria) and I want to thank TÜBİTAK 1001 Project (Project No: 113Y447, Project Name: Determination of organic matter and pollutant levels in water, sediment and organisms from Edremit Bay). I am also grateful to my family, they have always supported and encouraged me.

Hakan ALYÜRÜK

# SEASONAL VARIATION OF DISSOLVED ORGANIC MATTER IN İZMİR BAY

## ABSTRACT

Seasonal variations and spatial distributions of nutrients, Chl-a, DOC, dissolved carbohydrates and amino acid concentrations were investigated in seawater from the İzmir Bay. Samples were collected from surface, subsurface and bottom depths at seven different stations. Dissolved nitrogen concentrations were found remarkably higher at middle-inner bays and highest levels observed at station 1. Ortho-phosphate levels were only higher in summer and autumn at middle-inner bays. N/P ratios were relatively high at outer bay and nitrogen is the limiting element for middle-inner parts of the İzmir Bay. According to TRIX, high eutrophication risks were observed at winter-spring. However, eutrophication was observed in summer-autumn at Middle-Inner Bays. There were no eutrophication risks at Outer Bay. In general, DOC, POC and TOC levels increased from winter to summer, then slightly decreased in autumn. DOC, MCHO, PHCO and TDCHO levels were found higher in middle-inner bays, under the influence of anthropogenic inputs. DFAA, TDHAA and PHAA levels were found higher at Middle-Inner Bays. DFAA, TDHAA and PHAA levels were observed highest in spring and summer. For Middle-Inner and Outer Bays, principal component analyses were performed on bulk chemical composition. Amino acids, dissolved carbohydrates, PP, PN and Chl-a were found in the same component group at Middle-Inner Bays. For Outer Bay, PHAA, dissolved carbohydrates, PP, PN and Chl-a were found in the same group. Dissolved and total nutrients, DOC, TOC, Chl-a, dissolved carbohydrates and amino acid levels were increased from outer to middle-inner bay due to anthropogenic and terrestrial inputs.

**Keywords:** Nutrients, TRIX, organic matter, carbohydrate, amino acid, seawater

# İZMİR KÖRFEZİNDE ÇÖZÜNMÜŞ ORGANİK MADDENİN MEVSİMSEL DEĞİŞİMİ

## ÖZ

İzmir Körfezi deniz suyunda nutrient, Chl-a, DOC, çözünmüş karbohidrat ve amino asit konsantrasyonlarının mevsimsel ve bölgesel değişimleri araştırılmıştır. Örnekler 7 istasyondan yüzey, yüzeyaltı ve dip derinliklerinden alınmıştır. Çözünmüş azot konsantrasyonları orta-iç körfezde belirgin olarak daha yüksek bulunmuş ve en yüksek azot düzeyleri 1 nolu istasyonda gözlenmiştir. Orto-fosfat düzeyleri orta-iç körfezde sadece yaz ve güz mevsiminde daha yüksek bulunmuştur. N/P oranları dış körfezde daha yüksek bulunmuş ve iç körfezde azotun limitleyici element olduğu gözlenmiştir. TRIX indeksine göre, orta-iç körfezlerde kış-bahar mevsimlerinde yüksek ötrifikasyon riski ve yaz-güz mevsimlerinde ötrifikasyon düzeyleri saptanmıştır. Dış körfezde ise ötrifikasyon riski bulunmamıştır. Genel olarak, DOC, POC ve TOC düzeyleri kıştan yaza artmış ve güzde düşüş göstermiştir. DOC, MCHO, PCHO ve TDCHO düzeyleri, antropojenik girdilerin etkisi altındaki orta-iç körfezlerde daha yüksek bulunmuştur. DFAA, TDHAA ve PHAA düzeyleri orta-iç körfezlerde daha yüksek bulunmuştur. En yüksek DFAA, TDHAA ve PHAA düzeyleri bahar ve yaz mevsimlerinde gözlenmiştir. Orta-iç ve dış körfezler için deniz suyundaki kimyasal bileşenler üzerinde temel bileşen analizi gerçekleştirilmiştir. Orta-iç körfezde, amino asitler, çözünmüş karbohidratlar, PP, PN ve Chl-a aynı bileşen grubu içerisinde yer almıştır. Dış körfezde ise PHAA, çözünmüş karbohidratlar, PP, PN ve Chl-a aynı grupta bulunmuştur. Çözünmüş ve toplam nutrientler, DOC, TOC, Chl-a çözünmüş karbohidratlar ve amino asit düzeylerinin antropojenik ve karasal girdiler nedeniyle dış körfezden orta-iç körfeze doğru artış gösterdiği düşünülmektedir.

**Anahtar kelimeler:** Nutrientler, TRIX, organik madde, karbohidrat, amino asit, deniz suyu

## CONTENTS

	<b>Page</b>
Ph.D. THESIS EXAMINATION RESULT FORM .....	ii
ACKNOWLEDGEMENTS .....	iii
ABSTRACT .....	iv
ÖZ .....	v
LIST OF FIGURES .....	ix
LIST OF TABLES .....	xv
<b>CHAPTER ONE – INTRODUCTION .....</b>	<b>1</b>
1.1 Organic Matter in the Marine Environment .....	1
1.2 Composition of the Organic Matter .....	1
1.3 Sources and Fate of the Organic Matter .....	3
1.4 Analysis Methods of the Organic Matter .....	4
1.5 Carbohydrates in the Marine Environment .....	5
1.6 Amino Acids in the Marine Environment .....	6
1.7 Physical & Chemical Characteristics of the Water Column in the İzmir Bay ..	8
1.8 A Review of the Literature .....	11
<b>CHAPTER TWO – MATERIALS AND METHODS .....</b>	<b>17</b>
2.1 Sampling Methods & Stations .....	17
2.2 Hydrographic Analyses .....	17
2.3 Determination of pH and Dissolved Oxygen .....	18
2.4 Analyses of Chlorophylls and Pheopigments .....	19
2.5 Analyses of Dissolved Nutrients .....	19
2.5.1 Nitrite Nitrogen Analysis .....	20
2.5.2 Nitrate Nitrogen Analysis .....	20
2.5.3 Ammonium Nitrogen Analysis .....	20
2.5.4 Inorganic Phosphate Phosphorus Analysis .....	21

2.6 Analyses of Dissolved Total & Total Nitrogen & Phosphorus .....	21
2.6.1 Dissolved Total and Total Nitrogen Analysis .....	21
2.6.2 Dissolved Total and Total Phosphorus Analysis .....	21
2.7 Analyses of Dissolved & Total Organic Carbon .....	22
2.7.1 Dissolved Organic Carbon Analysis .....	22
2.7.2 Total Organic Carbon Analysis .....	22
2.8 Determination of Eutrophication Level by TRIX and UNTRIX Indexes .....	22
2.9 Analyses of Carbohydrates .....	23
2.9.1 Dissolved Free Carbohydrate Analysis .....	23
2.9.2 Dissolved Total Carbohydrate Analysis .....	24
2.10 Analyses of Amino Acids .....	24
2.10.1 Sampling .....	24
2.10.2 Hydrolysis .....	24
2.10.3 Principle of Amino Acid Analysis .....	25
2.10.4 Modifications Applied in the Amino Acid Analysis .....	25
2.11 Statistical Analyses .....	31
<b>CHAPTER THREE – RESULTS .....</b>	<b>32</b>
3.1 Results of Hydrographic Analyses .....	32
3.2 Results of pH, Dissolved Oxygen, Chlorophyll and Pheopigment Analyses ..	41
3.3 Results of Dissolved Nutrient Analyses .....	49
3.4 Results of Dissolved & Total Organic Carbon Analyses .....	64
3.5 Results of Eutrophication Level Determination by TRIX and UNTRIX Indexes .....	69
3.6 Elemental C/N/P Ratios .....	72
3.7 Results of Carbohydrate Analyses .....	74
3.7.1 Seasonal Variations .....	74
3.7.2 Spatial Distribution .....	78
3.7.3 Correlation Analysis .....	78
3.7.4 Factor Analysis of Dissolved Carbohydrates .....	85
3.8 Results of Amino Acid Analyses .....	87



3.9 D/L Ratios and Degradation Index Results for Amino Acid Analyses.....	102
3.10 Molecular Composition of Dissolved Organic Carbon, Nitrogen and Total Phosphorus .....	105
3.11 Statistical Analyses and Plots.....	109
<b>CHAPTER FOUR – DISCUSSION AND CONCLUSION.....</b>	<b>142</b>
<b>REFERENCES.....</b>	<b>154</b>
<b>APPENDICES .....</b>	<b>172</b>
APPENDICE 1: Abbreviations List.....	172

## LIST OF FIGURES

	<b>Page</b>
Figure 2.1 The sampling stations in the İzmir Bay .....	18
Figure 2.2 The reaction of an L-amino acid with OPA and IBLC to form a stereomeric fluorescent complex .....	25
Figure 2.3 Chromatograms belong to D/L-amino acid analysis. a) 50 nM L-amino acid mix analyzed with both IBLC and IBDC methods. b) Sample of dissolved free amino acid analysis from the İzmir Bay .....	28
Figure 3.1 Depth profiles of temperature at the sampling stations .....	33
Figure 3.2 Depth profiles of salinity at the sampling stations .....	34
Figure 3.3 Depth profiles of conductivity at the sampling stations .....	35
Figure 3.4 Depth profiles of potential density at the sampling stations.....	36
Figure 3.5 The map showing the path of vertical contour maps of seawater temperature, salinity and density at five adjacent stations .....	37
Figure 3.6 Vertical transect profiling maps of temperature for five stations at a) winter, b) spring, c) summer, and d) autumn seasons.....	38
Figure 3.7 Vertical transect profiling maps of salinity for five stations at a) winter, b) spring, c) summer, and d) autumn seasons .....	39
Figure 3.8 Vertical transect profiling maps of seawater densities for five stations at a) winter, b) spring, c) summer, and d) autumn seasons .....	40
Figure 3.9 Seasonal pH profiles of seawater at sampling stations.....	42
Figure 3.10 Chl-a, Chl-b, Chl-c, Pheophytin and DO profiles of seawater at sampling stations in winter .....	43
Figure 3.11 Chl-a, Chl-b, Chl-c, Pheophytin and DO profiles of seawater at sampling stations in spring.....	44
Figure 3.12 Chl-a, Chl-b, Chl-c, Pheophytin and DO profiles of seawater at sampling stations in summer.....	45
Figure 3.13 Chl-a, Chl-b, Chl-c, Pheophytin and DO profiles of seawater at sampling stations in autumn.....	46
Figure 3.14 pH, O <sub>2</sub> % and Chl-a profiles of seawater at surface waters in winter .....	47
Figure 3.15 pH, O <sub>2</sub> % and Chl-a profiles of seawater at surface waters in spring.....	47

Figure 3.16 pH, O <sub>2</sub> % and Chl-a profiles of seawater at surface waters in summer...	48
Figure 3.17 pH, O <sub>2</sub> % and Chl-a profiles of seawater at surface waters in autumn....	48
Figure 3.18 NO <sub>2</sub> , NO <sub>3</sub> , TNO <sub>x</sub> and NH <sub>4</sub> profiles of seawater at sampling stations in winter .....	52
Figure 3.19 NO <sub>2</sub> , NO <sub>3</sub> , TNO <sub>x</sub> and NH <sub>4</sub> profiles of seawater at sampling stations in spring .....	53
Figure 3.20 NO <sub>2</sub> , NO <sub>3</sub> , TNO <sub>x</sub> and NH <sub>4</sub> profiles of seawater at sampling stations in summer .....	54
Figure 3.21 NO <sub>2</sub> , NO <sub>3</sub> , TNO <sub>x</sub> and NH <sub>4</sub> profiles of seawater at sampling stations in autumn .....	55
Figure 3.22 DIN, DTN, DON, PN and TN profiles of seawater at sampling stations in winter.....	56
Figure 3.23 DIN, DTN, DON, PN and TN profiles of seawater at sampling stations in spring.....	57
Figure 3.24 DIN, DTN, DON, PN and TN profiles of seawater at sampling stations in summer .....	58
Figure 3.25 DIN, DTN, DON, PN and TN profiles of seawater at sampling stations in autumn.....	59
Figure 3.26 DIP, DOP, DTP, PP and TP profiles of seawater at sampling stations in winter.....	60
Figure 3.27 DIP, DOP, DTP, PP and TP profiles of seawater at sampling stations in spring.....	61
Figure 3.28 DIP, DOP, DTP, PP and TP profiles of seawater at sampling stations in summer .....	62
Figure 3.29 DIP, DOP, DTP, PP and TP profiles of seawater at sampling stations in autumn.....	63
Figure 3.30 DOC, POC and TOC profiles of seawater at sampling stations in winter .....	65
Figure 3.31 DOC, POC and TOC profiles of seawater at sampling stations in spring .....	66
Figure 3.32 DOC, POC and TOC profiles of seawater at sampling stations in summer .....	67

Figure 3.33 DOC, POC and TOC profiles of seawater at sampling stations in autumn .....	68
Figure 3.34 Seasonal TRIX and UNTRIX profiles at Middle-Inner Parts of the İzmir Bay .....	70
Figure 3.35 Seasonal TRIX and UNTRIX profiles at Outer Part of the İzmir Bay ...	71
Figure 3.36 MCHO, PCHO and TDCHO profiles of seawater in winter .....	79
Figure 3.37 MCHO, PCHO and TDCHO profiles of seawater in spring .....	80
Figure 3.38 MCHO, PCHO and TDCHO profiles of seawater in summer .....	81
Figure 3.39 MCHO, PCHO and TDCHO profiles of seawater in autumn .....	82
Figure 3.40 Linear relationships between MCHO, PCHO, Chl-a, and TDCHO/DOC (%) for a) middle-inner bay and b) outer bay.....	84
Figure 3.41 Biplots of factor loadings indicating the explained proportions of variances for salinity, Chl-a, DOC, MCHO, and TDCHO in the bay: a) middle-inner bay, b) outer bay.....	86
Figure 3.42 Seasonal and spatial variations of mean molecular DFAA concentrations at all sampling depths in the İzmir Bay.....	88
Figure 3.43 Seasonal variations of DFAA mol percentages at all depths and stations in the İzmir Bay .....	89
Figure 3.44 Seasonal and spatial variations of total DFAA concentrations at the İzmir Bay .....	90
Figure 3.45 Seasonal variations of DFAA concentrations with depth at the İzmir Bay. Data are represented as Mean±SD.....	90
Figure 3.46 Biplot of PCA loadings for DFAA .....	91
Figure 3.47 Seasonal and spatial variations of mean molecular TDHAA concentrations at all sampling depths in the İzmir Bay.....	93
Figure 3.48 Seasonal variations of TDHAA mol percentages at the İzmir Bay .....	94
Figure 3.49 Seasonal and spatial variations of total TDHAA concentrations at the İzmir Bay .....	95
Figure 3.50 Seasonal variations of TDHAA concentrations with depth at the İzmir Bay. Data are represented as Mean±SD .....	95
Figure 3.51 Biplot of PCA loadings for TDHAA .....	96

Figure 3.52 Seasonal and spatial variations of mean molecular PHAA concentrations at all sampling depths in the İzmir Bay.....	98
Figure 3.53 Seasonal variations of PHAA mol percentages at the İzmir Bay.....	99
Figure 3.54 Seasonal and spatial variations of total PHAA concentrations at the İzmir Bay.....	100
Figure 3.55 Seasonal variations of PHAA concentrations with depth at the İzmir Bay. Data are represented as Mean±SD.....	100
Figure 3.56 Biplot of PCA loadings for PHAA.....	101
Figure 3.57 Seasonal D/L-Ratios of Asp, Glu, Ser and Ala at all depths and stations (Mean±SD).....	103
Figure 3.58 Seasonal variations of Degradation Index values (Mean±SD).....	104
Figure 3.59 Seasonal variations of identified DOC components: a) Inner bay, b) Outer bay.....	106
Figure 3.60 Seasonal variations of identified DON components: a) Inner bay, b) Outer bay.....	107
Figure 3.61 Seasonal variations of identified TP components: a) Inner bay, b) Outer bay.....	108
Figure 3.62 Pearson correlation coefficient results between Chl-a and bulk chemical parameters at Middle-Inner Bays.....	111
Figure 3.63 Pearson correlation coefficient results between Chl-a and bulk chemical parameters at Outer Bay.....	111
Figure 3.64 Pearson correlation coefficient results between TRIX and bulk chemical parameters at Middle-Inner Bays.....	112
Figure 3.65 Pearson correlation coefficient results between TRIX and bulk chemical parameters at Outer Bay.....	112
Figure 3.66 Linearity between DIN and DON at Middle-Inner and Outer Bays.....	113
Figure 3.67 Linearity between DOC and DON at Middle-Inner and Outer Bays ...	113
Figure 3.68 Linearity between Chl-a and DOC at Middle-Inner and Outer Bays ...	114
Figure 3.69 Linearity between TP and TN at Middle-Inner and Outer Bays .....	114
Figure 3.70 Linearity between DOC and TDHAA at Middle-Inner and Outer Bays .....	115

Figure 3.71 Linearity between Chl-a and TDHAA at Middle-Inner and Outer Bays .....	115
Figure 3.72 Linearity between DON and TDHAA at Middle-Inner and Outer Bays .....	116
Figure 3.73 Linearity between TDCHO and TDHAA at Middle-Inner and Outer Bays .....	116
Figure 3.74 Linearity between C/N (DOC/DON) and TDCHO at Middle-Inner and Outer Bays .....	117
Figure 3.75 Linearity between C/N (DOC/DON) and TDHAA at Middle-Inner and Outer Bays .....	117
Figure 3.76 Linearity between C/N (DOC/DON) and $DI_{TDHAA}$ at Middle-Inner and Outer Bays .....	118
Figure 3.77 Linearity between POC/PON and $DI_{PHAA}$ at Middle-Inner and Outer Bays .....	118
Figure 3.78 Linearity between $C_{TDHAA}/DOC$ and $N_{TDHAA}/DON$ at Middle-Inner and Outer Bays .....	119
Figure 3.79 Linearity between $DI_{TDHAA}$ and $C_{TDHAA}/DOC$ at Middle-Inner and Outer Bays.....	119
Figure 3.80 Seasonal and spatial variations of o-PO4 .....	120
Figure 3.81 Seasonal and spatial variations of DOP .....	120
Figure 3.82 Seasonal and spatial variations of PP .....	121
Figure 3.83 Seasonal and spatial variations of TP .....	121
Figure 3.84 Seasonal and spatial variations of DIP/TP.....	122
Figure 3.85 Seasonal and spatial variations of DOP/TP .....	122
Figure 3.86 Seasonal and spatial variations of DOP/TP .....	123
Figure 3.87 Seasonal and spatial variations of DIN.....	123
Figure 3.88 Seasonal and spatial variations of DON .....	124
Figure 3.89 Seasonal and spatial variations of PN.....	124
Figure 3.90 Seasonal and spatial variations of TN .....	125
Figure 3.91 Seasonal and spatial variations of DIN/DIP .....	125
Figure 3.92 Seasonal and spatial variations of DON/DOP .....	126
Figure 3.93 Seasonal and spatial variations of TRIX .....	126

Figure 3.94 Seasonal and spatial variations of UNTRIX.....	127
Figure 3.95 Seasonal and spatial variations of DOC .....	127
Figure 3.96 Seasonal and spatial variations of POC .....	128
Figure 3.97 Seasonal and spatial variations of TOC.....	128
Figure 3.98 Seasonal and spatial variations of DOC/DON.....	129
Figure 3.99 Seasonal and spatial variations of Chl-a.....	129
Figure 3.100 Seasonal and spatial variations of MCHO.....	130
Figure 3.101 Seasonal and spatial variations of PCHO .....	130
Figure 3.102 Seasonal and spatial variations of TDCHO .....	131
Figure 3.103 Seasonal and spatial variations of MCHO/TDCHO.....	131
Figure 3.104 Seasonal and spatial variations of PCHO/MCHO .....	132
Figure 3.105 Seasonal and spatial variations of MCHO/DOC .....	132
Figure 3.106 Seasonal and spatial variations of PCHO/DOC.....	133
Figure 3.107 Seasonal and spatial variations of TDCHO/DOC .....	133
Figure 3.108 Seasonal and spatial variations of DFAA.....	134
Figure 3.109 Seasonal and spatial variations of DCAA .....	134
Figure 3.110 Seasonal and spatial variations of PHAA.....	135
Figure 3.111 Seasonal and spatial variations of TDHAA.....	135
Figure 3.112 Seasonal and spatial variations of $DI_{DFAA}$ .....	136
Figure 3.113 Seasonal and spatial variations of $DI_{PHAA}$ .....	136
Figure 3.114 Seasonal and spatial variations of $DI_{TDHAA}$ .....	137
Figure 3.115 PCA results for bulk parameters at Middle-Inner Bays.....	139
Figure 3.116 PCA results for bulk parameters at Outer Bay .....	139

## LIST OF TABLES

	<b>Page</b>
Table 2.1 Eutrophication risk evaluation criteria for TRIx index scales .....	23
Table 2.2 Chromatographic separation parameters for 20 nM D/L-amino acid standards ( $t_R$ : retention time, $k$ : retention factor, $w$ : peak width, $N$ : theoretical plate number, $h$ : reduced plate height, $n$ : peak capacity) .....	29
Table 2.3 Separation factors ( $\alpha$ ) and peak resolutions ( $R$ ) for 20 nM D/L-amino acid standards (Criteria: $\alpha \geq 1.05$ , $R \geq 1.5$ ) .....	30
Table 2.4 Modules of HPLC system used in amino acid analysis .....	31
Table 2.5 Gradient elution program for Mobile Phase B .....	31
Table 3.1 Seasonal variations of dissolved, dissolved total and total N/P ratios .....	73
Table 3.2 Seasonal variations of C/N/P ratios in dissolved and particulate matter ...	73
Table 3.3 Seasonal variations of MCHO, PCHO and TDCHO in the water column of the İzmir Bay ( $n=7$ for each range) .....	75
Table 3.4 Results of One Way ANOVA tests for seasonal changes of salinity, Chl-a, DOC, MCHO, TDCHO and PCHO (Values represent Mean $\pm$ SD; $n=6$ for inner bay; $n=15$ for outer bay; $p<0.05$ ) .....	76
Table 3.5 Seasonal variations for MCHO/TDCHO, MCHO/DOC and TDCHO/DOC ratios in the water column of the İzmir Bay ( $n=7$ for each range) .....	77
Table 3.6 Correlations between MCHO, PCHO, TDCHO, DOC, Chl-a and salinity ( $n=21$ for all tests, $\rho$ is the Spearman's rank correlation coefficient, $p$ is the significance level, * means significance level of 0.05, ** means significance level of 0.01, *** means significance level of 0.001) .....	83
Table 3.7 Two-Way ANOVA results (Season and location vs. bulk parameters, Win: Winter, Spr: Spring, Sum: Summer, Aut: Autumn, Out: Outer Bay, MidIn: Middle-Inner Bays) .....	138
Table 3.8 PCA results of bulk parameters at Middle-Inner and Outer Bays (PC: Principal Component represents standardized loadings based on correlation matrix) .....	140
Table 3.9 Proportional and cumulative variances explained by each Principal Component .....	141



Table 3.10 K-Means Clustering results of PCA loadings for bulk parameters at Middle- Inner and Outer Bays .....	141
Table 4.1 Nutrient, chlorophyll and organic matter concentrations in the İzmir Bay .....	146
Table 4.2 Comparison of DOC, MCHO and TDCHO levels of the İzmir Bay with different parts of the world.....	147
Table 4.3 Comparison of organic and inorganic chemical concentrations in the İzmir Bay with different parts of the world .....	149



# CHAPTER ONE

## INTRODUCTION

### 1.1 Organic Matter in the Marine Environment

The organic matter found in marine or terrestrial environments is primarily produced by autotrophs. Sequentially, the utilizable fraction of the organic matter is transferred to other organisms like heterotrophs as an energy source for the metabolic reactions and maintenance of the metabolism. Consequently, a considerable fraction of the organic matter is oxidized to smaller molecules or metabolized to more inert compounds in biochemical reactions. Another fraction is directly used by marine organisms and released into the environment after biodegradation or as a consequence of metabolism. However, production and utilization of the organic matter is not only carried out by marine organisms but also by the terrestrial organisms. Therefore, the organic matter found in the marine environments could be originated from terrestrial processes (called as allochthonous) or *in situ* marine (called as autochthonous) sources (Hedges, 2002; Libes, 2009). The terrestrial organic matter could be transported to the marine environments by rivers, rain runoffs or winds. However, the amount of organic matter originated from terrestrial sources (0.4 Pg C/y) is comparatively lower than *in situ* primary production in the marine environment (40-50 Pg C/y) (Libes, 2009). The organic matter found in seawater can be classified as dissolved organic matter (DOM) and particulate organic matter (POM) based on the molecular size distribution (Hedges, 2002). Practically, the part of seawater that passes through 0.45-1.00  $\mu\text{m}$  glass fiber filters contain DOM, whereas the fraction that remained on the filter is defined as POM (Hedges, 2002). This traditional definition is useful, since small particles ( $<1.0 \mu\text{m}$ ) do not sink in water column.

### 1.2 Composition of the Organic Matter

DOM can also be further separated into two main fractions as high molecular weight (HMW) and low molecular weight (LMW). The size limit that separates these fractions is approximately 1 nm (1000 daltons). The separation of HMW and LMW

DOM from each other is mainly achieved by tangential flow ultrafiltration technique (Libes, 2009). DOM can also be classified based on its solubility and light absorption properties. Humic acids and fulvic acids can be isolated from DOM by changing the pH of mobile phase through ion exchange columns (XAD type) (Libes, 2009). Separation is depended on the solubility of fulvic acids at all pH ranges, however humic acids are not soluble under pH 2. DOM contains different types of molecules that are able to absorb light including almost the entire solar spectrum reaching the sea surface (Libes, 2009). The fraction of DOM that absorbs light at specific wavelengths is called as chromophoric DOM (CDOM). This fraction of the DOM is beneficial to the planktonic organisms through regulating the limits of euphotic zone and absorbing the harmful solar radiation. The most abundant element within DOM and POM is carbon. Due to the presence of technical difficulties, DOM and POM are measured as dissolved organic carbon (DOC) and particulate organic carbon (POC), respectively, or in the form of other elements (DON, DOP, PON, POP). Some difficulties faced in the characterization of organic compounds within DOM pool are the presence of very large number of organic molecules, the large and complex structure of these molecules and the interferences arisen from high salt content of seawater (Libes, 2009). Due to these restrictions, a very limited fraction of the surface ocean (<10%) and deep ocean (<5%) DOC has been characterized (Libes, 2009). In the surface water, DOC concentrations in tropical and temperate regions are higher (60-90  $\mu\text{M C}$ ) compared to deep waters (35-45  $\mu\text{M C}$ ) (Benner, 2002). Based on average values, the following stoichiometric ratios are calculated for surface waters: C/N=13.6, C/P=300 and C/N/P=300/22/1. These ratios indicate that DOM is poor in terms of N and P than that of marine plankton (C/N/P=106/16/1) (Redfield et al., 1963; Benner, 2002).

A great amount of POM is produced by primary producers like phytoplankton, macroalgae and bacteria found in seawater (Libes, 2009). Especially photoautotrophic nanoplankton (2 – 20  $\mu\text{m}$ ) and picoplankton (0.2 – 2  $\mu\text{m}$ ) provide higher contribution to the production of organic matter. The photoautotrophic bacteria such as *Synechococcus* and *Prochlorococcus* use bacteriochlorophylls and phycoerythrins as pigments in primary production. Another marine bacterium, *Pelagibacter ubique* Hasle, 1950, is one of the most abundant organism in seawater and use rhodopsin

molecule in its energy metabolism. Proteins are the most abundant biomolecules found in phytoplankton and bacteria and approximately half of their dry weight is composed of proteins. Also, bacteria have high ribonucleic acids (RNA) and deoxyribonucleic acids (DNA) content compared to phytoplankton. Therefore, the nitrogen containing molecules are more abundant in bacteria. Bacterial cell walls and membranes contain various types of biomolecules including peptidoglycans, lipopolysaccharides and porins. These molecules become part of the dissolved organic matter after the death of bacteria (Libes, 2009).

### **1.3 Sources and Fate of the Organic Matter**

The organic carbon fixed by primary producers has several fates. About one third of the fixed carbon is respired by the primary producers; some fractions are released into the seawater as extracellular substances or as a consequence of viral lysis and sloppy feeding by the grazers. For example, protozooplankton (foraminiferans, radiolarians, etc.) utilize and release biomass of pico- and nanoplankton into the marine food web. The mesozooplankton and macrozooplankton consume primary producers and heterotrophic prokaryotes and produce fast sinking fecal pellets that contribute to the POM pool in deep sea (Libes, 2009). Most zooplankton species are able to excrete ammonium and other low molecular weight DON. This process contributes to remineralization of nitrogen and provides inorganic nitrogen for photoautotrophs. Viral infections kill marine bacteria and phytoplankton in the surface waters. This results with lysis of cell membrane and release of cell content to the marine food web as DOM. A similar process is generated during sloppy feeding by grazers that involves lysis of bacterial and eukaryotic cell membranes. About one third of the DOM generated from primary production is consumed by marine bacteria. However, the utilized fraction of the DOM is returned back to seawater by the feeding of protozooplankton on marine bacteria. This process is called as microbial loop (Libes, 2009).

Primary production, and therefore, the export of POM are seasonally affected by availability of light and nutrients in mid- and high latitudes. While the annual cycle of

planktonic production is controlled by a spring bloom and a secondary fall bloom in mid-latitudes, summer blooms in high latitude is depended on the delivery of iron (Libes, 2009).

Following the death of marine organisms, their biomass becomes part of the detrital POM which also includes molts, cast-off feeding nets, egg cases, fecal pellets, and marine snow. The concentration of detrital POM is generally decreased exponentially with increasing depth. This means POM is produced in the surface waters and consumed in the deep waters. Different classes of organic molecules are produced by degradation of the detrital POM. Degradation of POM is mostly depended on enzymatic catabolic reactions generated by marine organisms inside or outside of their cells. Some extracellular enzymes involved in these reactions are nucleases (for breakdown of DNA and RNA to nucleotides), phosphatases (for removal of phosphate groups), proteases, lipases, and glucosidases.

#### **1.4 Analysis Methods of the Organic Matter**

Qualitative and quantitative investigations of DOM have importance for biogeochemical studies. Due to the complexity of molecules in DOM, it is most frequently studied through analysis of its carbon (DOC) or nitrogen (DON) composition. There are three widely applied methods for determination of DOC concentrations: high temperature catalytic combustion (using TOC analyzers), low temperature chemical oxidation (using peroxodisulphate under acidic conditions) or photochemical oxidation (using both UV and peroxodisulphate treatment) (Bauer and Bianchi, 2011; Statham & Williams, 1999; Wangersky, 2000). These methods give similar quantitative results when applied properly. Qualitative methods for characterization of DOC are stable carbon isotope analysis ( $\delta^{13}\text{C}$ ), NMR analysis ( $^1\text{H}$ - and  $^{13}\text{C}$ -NMR), optical analyses including absorbance and fluorescence methods and compound specific analyses (amino acid, carbohydrate, lipid or other biomolecules) (Bauer & Bianchi, 2011). Stable carbon isotope analyses give important information on the sources and dynamics of DOC (Lang et al, 2007). For example, lighter carbon stable isotope ( $\delta^{13}\text{C}$ ) is found higher in terrestrial C3 plants than in phytoplankton

(Osburn & Stedmon, 2011).  $^1\text{H}$ - and  $^{13}\text{C}$ -NMR analyses are useful for determination of functional groups in bulk form of DOC. Absorbance and fluorescence methods are used to characterize chromophoric DOC (mainly humic or protein like molecules) found in riverine, estuarine and coastal areas. As stated for the quantification DOC, determination of DON concentrations is also possible by using high temperature catalytic combustion, low temperature chemical oxidation or photochemical oxidation methods (McCarthy & Bronk, 2008; Sharp et al., 2002). Specific components of DON like urea, humic (N-containing) substances, amino acids, amino sugars and nucleic acids have been investigated in seawater (McCarthy & Bronk, 2008). It is possible to characterize DON by  $^{15}\text{N}$ -NMR stable isotope technique; however, this method is meaningful when applied together with  $^1\text{H}$ - and  $^{13}\text{C}$ -NMR techniques (McCarthy & Bronk, 2008). In this thesis, DOM concentrations (in terms of total and dissolved carbon, nitrogen and phosphorus) and its specific components (total carbohydrates and amino acids) were investigated in the İzmir Bay for the first time.

### **1.5 Carbohydrates in the Marine Environment**

Carbohydrates are one of the major groups that is commonly utilized by the microorganisms. Also, they are the products of photosynthesis process that takes place within phytoplankton and marine algae. Qualitative and quantitative studies have been performed for understanding the biogeochemical cycling of dissolved carbohydrates including its molecular and polymeric forms. Dissolved carbohydrates could be divided as monosaccharides and polysaccharides or neutral and acidic sugars based on the analysis methods and their structures (Benner & Opsahl, 2001; Chanudet & Filella, 2006; Hedges et al., 1994; Lin & Guo, 2015; Mykkestad et al., 1997). Dissolved carbohydrates are one of the well identified components of DOC that constitutes up to 3-30% of bulk DOC (Benner, 2002; Hung et al., 2003; Pakulski & Benner, 1994; Wang et al., 2006). This fraction contains mono-, oligo- and polysaccharides, the latter one is used as storage material, cell wall components and extracellular exudates (He et al., 2015; Mykkestad & Børsheim, 2007). Polysaccharides have been studied extensively due to their aggregation and colloidal properties. It has been reported that they were responsible from biofilm production, mucilage events (Baldi et al., 1997; Leppard,

1997; Penna et al., 2003; Penna et al., 2009; Pettine et al., 1999), complexation with trace metals (Jang et al 1990, 1995), and marine snow formation (Alldredge et al., 1993; He et al., 2015; Passow et al., 1994; Skoog et al., 2008).

In the water column, concentrations of the carbohydrates change both vertically and horizontally based on their rate of production and utilization by the organisms, and also by terrestrial inputs (He et al., 2015; Zhang, 2010). Carbohydrate concentrations were reported to be highest at estuaries, gulfs and bays, whereas they were found at intermediate concentrations in coastal waters and lowest at oligotrophic ocean waters (Amon & Benner, 2003; Handa, 1966; Handa, 1967; He et al., 2015; Hung et al., 2003; Wang et al., 2006; Khodse et al., 2010; Pakulski & Benner, 1994; Yang et al., 2010).

## **1.6 Amino Acids in the Marine Environment**

Amino acids are one of the important components in DOM pool. Proteins in marine micro-organisms account up to 50% of organic carbon and 80% of organic nitrogen. Amino acids and proteins are mostly released into the seawater by excretion of extracellular enzymes and viral lysis (Repeta, 2015).

Early studies on dissolved amino acids at nanomolar concentrations were first performed between 1960s and 1970s (Lee & Bada, 1975, 1977). More recent dissolved amino acid analyses depend on the reaction of o-phthaldialdehyde (OPA) with primary amines (Lindroth & Mopper, 1979; Mopper & Lindroth, 1982). This reaction is conducted at basic conditions and it gives fluorescent products with amino acids. This enables detection of amino acids with high performance liquid chromatography (Repeta, 2015).

Amino acid forms in seawater are classified according to methods used in sample preparation. Dissolved free amino acids (DFAA) are directly measured in filtered seawater and this form represents monomeric (unbonded) amino acids. Total dissolved hydrolysable amino acids (TDHAA) are measured in filtered seawater after an acid digestion step and this form contains peptides, proteins and DFAA form. Dissolved

combined amino acids (DCAA) are found from the difference between TDHAA and DFAA. This form represents peptides, proteins and other polymeric forms of amino acids dissolved in seawater. Particulate hydrolysable amino acids (PHAA) are found from acid digestion of particulate matter retained on filters used to filter seawater. This form represents free and polymeric (peptides and proteins) amino acids found in particulate matter (Repeta, 2015).

DFAA concentrations at surface waters of open ocean are generally found between 10-40 nM, whereas DFAA concentrations at deep-waters are found at lower values (<10-20 nM) and represent a constant profile. TDHAA concentrations are found at higher levels and changed with depth similar to DFAA. While TDHAA concentrations found between 200-450 nM at surface waters, TDHAA levels decreases to 100-200 nM below euphotic zone (Kaiser & Benner, 2009; Lee & Bada, 1975, 1977; McCarthy et al., 1996; Yamashita & Tanoue, 2003). Compared to open-ocean, DFAA and TDHAA concentrations found higher at coastal zones, near-shore areas and semi-enclosed bays (Repeta, 2015).

Spatially, changes in TDHAA concentrations reflect similar patterns with DOC concentrations. Ratio of TDHAA carbon to DOC ( $C_{TDHAA}/DOC$ ) changes from site to site and with depth. This ratio is generally found between 1-4% at surface waters and decreases to range of 0.4-0.8% at deep-waters greater than 1000 m (Kaiser & Benner, 2009; McCarthy et al., 1996; Yamashita & Tanoue, 2003). TDHAA ratio in DON is much higher (1.4-11%) and it is the largest molecule group in DON (Kaiser & Benner, 2009; McCarthy et al., 1996; Tada et al., 1998). This ratio has been reported to decrease from coastal waters to open ocean (Yamashita & Tanoue, 2003). Similar observations were also reported from Baltic Sea, Chesapeake Bay, Biscaye Bay and Laptev Sea (Mopper & Lindroth, 1982). High TDHAA to DOC ratio might be influenced from nutrient and chlorophyll concentrations at near shore sites with high productivity and higher organic matter cycling rates (Repeta, 2015).

Major amino acids contributing more than 90% to TDHAA pool are glycine, aspartic acid, glutamic acid, alanine, serine, threonine and arginine. Compared to



PHAA, mol fractions of aspartic acid and glycine in TDHAA are generally high, but leucine, isoleucine and arginine are found at lower concentrations (Repeta, 2015).

In nature, amino acids have two enantiomeric forms as D- and L-amino acids. Proteins are made up of L-amino acids, but, D-amino acids are used by bacteria in cellular functions and cell walls (Cava et al., 2011). Variations in composition and distributions of D-amino acids in TDHAA pool have been used in the assessment of bacterial contribution to DOM (Kaiser & Benner, 2006; Lee & Bada, 1977; McCarthy et al., 1998).

### **1.7 Physical & Chemical Characteristics of the Water Column in the İzmir Bay**

The İzmir Bay is located at western coast of the Anatolia. Its structure is L shaped which is oriented to north with its longer part and connected to the Aegean Sea. The Bay could be divided into three parts as Outer, Middle and Inner Bay due to their different characteristics. The Outer Bay is composed of three sub-parts; Outer 1, Outer 2, and Outer 3. There are several islands located at Outer 1 and 2 regions. According to Sayin (2003), the hydrography of the İzmir Bay is influenced from several factors; freshwater inputs that carry anthropogenic loads to the bay, exchanges between the atmosphere and the sea, exchange of water between the Aegean Sea and the bay, topography of the bay, the sea level changes, movement of waters directed by wind-driven circulation and winter convection. As a result of these factors, there are five different water masses in the İzmir Bay: Inner Bay water (anthropogenically polluted), Outer Bay water (influenced from the Gediz River and the Aegean Sea) (Outer 3), upwelling water in Gülbahçe Bay (Outer 2), Outer I water (located at salt production area), and Middle Bay water (connects Outer I to Inner Bay) (Sayin, 2003).

Under the influence seasonal warming and evaporation, a thermohaline layer is formed in the İzmir Bay at the end of spring. It reaches to 20–25 m depth in summer. In the fall, due to turbulences driven by the winds, it exceeds 30 m. The halocline and pycnocline layers are observed nearly at the same depth of thermocline. Vertical distribution of density is homogeneous in winter as a result of convection and wind

mixing processes, except in the Inner Bay where fresh water discharges affect vertical density profile (Sayin, 2003).

The average temperature of surface seawater is about 16 °C in winter and it reaches about 24 °C in summer. The average salinity of the Bay is 39.1±0.51 psu. However, the average salinity is about 38.0 psu in the Inner Bay. The high freshwater input could be the main factor for the considerable low salinity values of Inner Bay both in summer and winter seasons. On the other hand, the highest salinity values are observed at the Middle Bay where a salt production facility is located in the area (Sayin, 2003).

In the İzmir Bay, the horizontal and vertical stratification of the water column is also influenced by the winds. The winds from the west cause an upwelling in the Gülbahçe Bay and a downwelling at Urla and Güzelbahçe. Contrastly, the winds from the east cause upwelling to at Güzelbahçe and Urla coasts. The transport of Aegean Sea water is also driven by the winds from the west and north directions. Contrarily, the winds from the south prevent the entrance of Aegean seawater into the Bay. Southerly winds also cause upwelling at the east coast of the Uzun Island (Sayin, 2003).

The geochemical structure of the Bay was studied by Duman et al. (2004). The sediments, particle size lower than 2 µm, are abundantly composed of smectite and illite, whereas kaolinite, chlorite, vermiculite and smectite–illite (mixed-layer minerals) are found in lesser percentages. The source of illite could be Gediz River since it could carry the debris of Neogene sediments and metamorphic rocks to the bay (Aksu et al., 1998; Duman et al., 2004). Smectite is also possibly supplied by Gediz River to the İzmir Bay surface sediments. Some of the heavy minerals found at the sediment surfaces are garnet, opaque, amphibole, apatite and pyroxene which are also consistent with the geologic structure of Gediz river drainage basin (Aksu and Piper, 1983; Duman et al., 2004). Quartz-schist, mica-schist, phyllite, quartz and gneiss are some gravel types found in the İzmir Bay (Duman et al., 2004; İzdar, 1971).

In the surface sediments, total calcium carbonate levels ( $\text{CaCO}_3$  %) were found between 15.9% and 48.3%. The carbonate levels were higher in the western side of the central bay. This case could be associated with detritus of gastropods and bivalves (remnants of shells or skeletons) (Duman et al., 2004).

Total organic carbon concentrations in the sediments of the İzmir Bay changed from 0.40% to 3.12% (Outer Bay: 0.5-0.8%; Middle Bay: 1.0-1.5%; Inner Bay: 1.5-3.1%). Higher organic carbon content was frequently observed in polluted sediments with silt content (Balkaş & Juhasz, 1993; Duman et al., 2004). The upper level of organic carbon content for the İzmir Bay was higher than that of the Eastern Mediterranean Sea (0.11%–0.85%), Aegean Sea (0.30%–0.70%), and the Marmara Sea (0.37%–2.16%) (Duman et al., 2004; Emelianov & Romankevich, 1979; Ergin et al., 1993; Voutsinou-Taliadouri & Satsmadjis, 1982). Relatively higher abundance of organic carbon (>1.5%) in southwest part of the bay could be attributed to presence of terrigenous inputs, marine organic production and local sewage pollution (Duman et al., 2004).

The inorganic nutrients, particulate organic matter and dissolved organic carbon composition of the İzmir Bay was investigated by Kucuksezgin et al. (2005) during cruises in March, July, November 2000 and January 2001. It was found that  $\text{TNO}_x\text{-N}$  and dissolved inorganic phosphate (DIP) concentrations increased with depth, whereas  $\text{NH}_4\text{-N}$  and dissolved oxygen (DO) decreased in the outer bay. Due to the presence of phytoplankton blooms, nitrate and phosphate levels decreased in spring, while an increase was observed in November in the outer bay. On the other hand, the nutrients were highly abundant at the surface layers around middle bay (close to the Gediz River estuary) during spring season. During the summer, ammonium and phosphate concentrations were higher in the middle and inner bay which may be attributed to the presence of bacterial activity and as a result, lower N:P ratios were observed within summer period (IMST, 2000; Kucuksezgin et al. 2005). Consequently, the nutrients levels were higher in the middle-inner bays than in the outer bay. According to Kucuksezgin et al. (2005), DOC and TOC (Total organic carbon) concentrations were found in the range of 37-97 and 43-113  $\mu\text{M}$  in the water column of outer bay,

respectively. Highest DOC concentrations were observed in the middle and inner bay which are characterized by relatively low salinity values and a significant correlation was found between DOC and salinity ( $\text{DOC} = -18.57S + 799.17$ ,  $r = 0.4988$ ,  $p < 0.05$ ). The particulate matter concentrations were ranged from 3.2 to 22.6  $\mu\text{M}$  for POC, 0.32 to 2.1  $\mu\text{M}$  for PON and 0.02 to 0.21  $\mu\text{M}$  for PP in the outer bay for all sampling seasons. The particulate matter concentrations were found higher in the middle and inner bays during the summer period and ranged from 12.3 to 197  $\mu\text{M}$  for POC, 1.7 to 29.6  $\mu\text{M}$  for PON, and 0.11 to 1.9  $\mu\text{M}$  for PP.

## 1.8 A Review of the Literature

In the literature, qualitative and quantitative analyses of the dissolved and particulate organic matter have been studied (Harvey & Mannino, 2001; Jaffé et al., 2012; Jørgensen et al., 2011; Kaiser & Benner, 2008, 2009; Kim & Kim, 2013; Letscher et al., 2013; Meador et al., 2010; Murphy et al., 2008; Panagiotopoulos et al., 2013; Penru et al., 2013; Sannigrahi et al., 2006; Suksomjit et al., 2009; Romera-Castillo et al., 2013; Van Beusekom & de Jonge, 2012; Van Engeland et al., 2010; Yamashita & Tanoue, 2003; Zhang et al., 2009). These studies were focused on the characterization of the DOM such as its molecular size distribution and its light absorption properties, the origin of the DOM (terrestrial or marine origin), classification of the DOM, and determination of the specific compound classes such as amino acids, carbohydrates, and amino sugars in the DOM. In the following paragraphs, selected recent studies related to the DOM were discussed.

Murphy et al. (2008) investigated the sources of DOM in oceanic waters based on the optical properties of CDOM. They applied PARAFAC analysis to the fluorescence data of CDOM and classified DOM into eight classes composed of humic like and protein like signals. Humic components of the DOM originated from terrestrial sources and it was tractable in the open ocean up to 1.5% of riverine concentrations.

Jørgensen et al. (2011) studied the characteristics and distributions of the DOM. Different compound classes identified by fluorescence spectra in the DOM were two

humic like, four amino acid like and one chemically uncharacterized. Amino acids like peaks were identified as tryptophan, tyrosine and phenylalanine. The fluorescence intensities of amino acid like peaks were higher in the surface waters, whereas the intensities of humic acid like peaks were lower.

Van Engeland et al. (2010) studied the DON dynamics in the North Sea from 1995 to 2005. The DON concentrations were measured with an average of 11 and 5  $\mu\text{mol/L}$  in the coastal and open ocean, respectively. The organic nitrogen fractions within the total dissolved nitrogen (TDN) was 38 and 71% for the coastal and open ocean waters, respectively. In the coastal ocean, seasonal variations were observed due to the presence of DON cycle and high DON values were observed in spring and summer seasons. However, seasonality of the DON values in the open ocean was weak.

Van Beusekom & de Jonge (2012) investigated the seasonal and inter-annual variations of dissolved organic phosphorus (DOP) in the southern Wadden Sea (five stations, 1991-2007) and the northern Wadden Sea (one station, 2000-2009). A seasonal cycle was observed for DOP concentrations between winter (average of 0.1-0.2  $\mu\text{M}$ ) and summer (average of 1.6  $\mu\text{M}$ ) seasons. The regional comparison of DOP values in summer seasons between years of 2000 and 2007 showed that average DOP values were consistently changed with chlorophyll-a (from phytoplankton) in summer and ammonium concentrations in autumn.

Kaiser & Benner (2008) studied the chemical composition and diagenetic processing of suspended POM (>100 nm), HMW DOM (1-100 nm) and LMW DOM (<1 nm) by the analysis of amino acids (AA), neutral sugars (NS) and amino sugars (AS) at the stations close to Bermuda and Hawaii. The AA, NS and AS concentrations decreased with depth in unfiltered seawater. The molecular size of the organic matter was dominantly small. The total biomolecule content of the surface POM was composed of 55% of organic carbon.

Meador et al. (2010) investigated the chemical composition and cycling of the DOM in the Eastern Mediterranean Sea. Abundance, composition and distribution of

the ultrafiltrated DOM (UDOM) collected from deep basins at depths from 2 to 4350 m were similar to that of previous reports except for a sample from the North Aegean Sea. The UDOM samples were analyzed in terms of bulk and molecular composition (amino acid and monosaccharide). It was found that the amino acid content of UDOM was correlated with apparent oxygen utilization and prokaryotic activity.

Sohrin et al. (2014) have investigated the DOC and DON concentrations in the Okhotsk Sea to understand the driving forces and amount of DOC export from the Okhotsk Sea to North Pacific Intermediate Water (NPIW). High DOC and DON concentrations were found close to Amur River at depths near to surface. These DOC and DON concentrations were correlated positively with Chl-a and negatively with salinity which indicated the influence of the Amur River on the area. The ratios of DOC to DON in the Okhotsk Sea Mode Water (OSMW) were found higher in the Bussol' Strait and the Kuril Basin. This difference was attributed to the possible diapycnal mixing of sedimentary terrigenous organic carbon transported along the water masses. It was also found that fresh DOM could be transported by diapycnal mixing from the surface to OSMW.

Kaiser et al. (2014) have studied the dynamics of particulate organic matter in the Lianzhou Bay, under the influence of the Nanliu River and human activities, in southern China. Suspended, sedimentary and particulate organic matter were sampled along the land-ocean transect and analyzed for elemental (C/N), isotopic ( $\delta^{13}\text{C}$  and  $\delta^{15}\text{N}$ ) and amino acid composition. It was found that suspended particulate organic matter (SPOM) in the Nanliu River system was dominated by autochthonous production rather than terrestrial inputs. The SPOM was influenced from the variability in primary production and precipitation regimes. In addition, it was reported that marine and riverine productivity were greatly influenced by anthropogenic inputs. Also, the anthropogenic inputs dispersed along the coastal area by the effects of currents, topographic and hydrographic properties.

Lu et al. (2014) have investigated the temporal dynamics of dissolved free amino acid (DFAA) and short-chained aliphatic polyamine (PA) concentrations and their

contributions to DON pool along water column in Gray's Reef National Marine Sanctuary (GRNMS). DFAA concentrations were 10-fold higher than PA concentrations. Also, DFAA and PA concentrations changed more than 5-fold during diurnal cycles and between seasons. Glycine and spermidine were the highest abundant molecules for DFAA and PA classes, respectively. While the DFAA concentrations were correlated with Chl-a concentrations, PA concentrations were highly correlated with bacterial cell abundance.

Bianchi et al. (2014) have studied the temporal and spatial dynamics of amino acids (AA) and other dissolved and particulate matter in Mississippi River Plume (MRP). It was found that abiotic factors like particle adsorption and sediment re-suspension were highly dominant on dissolved and particulate AA dynamics. The positive correlation between acidic AA (e.g. aspartic acid and glutamic acid) and basic AA (e.g. histidine and arginine) as well as negative correlation between dissolved AA and salinity could possibly be some evidences of partitioning of amino acids with suspended sediments. It was reported that bulk DOC and POC decreased with distance from river plume area. Due to the presence of highly abundant bacterial production and freshly produced matter, carbon normalized amino acid levels showed a better proxy for degradation in coastal surface water near to the river plume.

Jørgensen et al. (2014) have studied the combined neutral sugar and amino acid levels found in DOM which was formerly produced by bacteria and also the concentrations of remaining molecules after 32 days of bacterial degradation. It was reported that the levels of biomolecules were not affected from initial substrate concentrations or bacterial community in bacterial degradation bioassays conducted with natural and artificial seawater samples. The neutral sugars were composed of high glucose content (47 mol %) and lower contributions of other neutral sugars (3-14 mol %). Following the bacterial degradation of DOM, its remaining content was characterized by a high galactose (33 mol %), glucose (22 mol %) and the other neutral sugars (7–11 mol %). During the bacterial degradation period, the ratios of D-amino acids to L-amino acids were increased. At the end of 32 days of degradation period,

D/L ratios of aspartic acid, glutamic acid, serine and alanine were found as 0.79, 0.32, 0.30 and 0.51 for all experiments, respectively.

Escoubeyrou & Tremblay (2014) have studied the development of an amino acid analysis method with simple sample preparation and new chromatographic conditions for hybrid C18 column. It was found that the high salt content and treatment of the samples were not altered the AA levels or their separation. The limits of detection for AAs were in the range of 0.007–3.6 nM. The developed method allows the quantification of all AA forms including free, dissolved combined, particulate, and total in most natural waters.

Hasumi & Nagata (2014) have studied the development of a three-dimensional numerical model for the evaluation of marine biogeochemical cycles. The couplings between planktonic and microbial processes were obtained by adding the production and consumption of dissolved organic matter (DOM) to the model. The results of the model indicated that contribution of the refractory DOM to global biogeochemical cycles is negligible over a long-time scale; high DOM concentrations suppresses the global marine primary productivity and the DOM produced by plankton enhanced the primary productivity in subtropical regions as a consequence of its remineralization to nutrients.

Suzuki et al. (2015) have studied the vertical and horizontal dissolved and particulate nutrient distribution in the Campos Basin, Brazil. It was found that the vertical profiles of the nutrients followed the stratified tropical water pattern. Higher concentrations of nutrients were observed on the continental shelf rather than the continental slope. It was also found that as the N/P ratio for nutrients showed slight limitation of nitrogen for primary production, organic and particulate matter presented a strong phosphorus limitation.

Wu et al. (2016) have investigated the seasonal variation of suspended organic matter in coastal waters and Changjiang Estuary, China together with enantiomeric amino acid analysis in July, August and November 2011. They found higher



concentrations of particulate organic carbon, particulate nitrogen and hydrolysable particulate amino acids (PAA) in July and August than in November. It was reported from the results of PAA analysis that the *in situ* production was determined as the key factor for seasonal variation of PAA. The positive effect of microbial organic matter was linked to a decrease in glutamic acid and increase in D-alanine and total suspended matter.

Lin & Guo (2015) have studied the spatial and vertical distributions of dissolved carbohydrate species from the northern Gulf of Mexico after the oil spill event. Carbohydrate concentrations decreased from continental shelf to basin regions and found in the range of 4-27  $\mu\text{M C}$  for monosaccharides, 4-34  $\mu\text{M C}$  for HCl-hydrolysable polysaccharides and 0-42  $\mu\text{M C}$  for dilute HCl-resistant polysaccharides. It was reported that the carbohydrates produced in the upper water column and transformed interchangeably from monosaccharide to polysaccharide or vice versa during transport in the water column.

In this thesis, the aim was to investigate seasonal variations and spatial distributions of nutrients, bulk DOM levels (total and dissolved organic carbon, nitrogen and phosphorus) and specific components of DOM (dissolved total and free carbohydrates, dissolved free, total dissolved and particulate amino acids) in the İzmir Bay. The study area, İzmir, is a highly industrialized and high populated city. The İzmir Bay has dense shipping activity and the bay was under the pollution threat by anthropogenic sources until 2000's. Also, the Gediz River is an important area for wild life near the İzmir and it is opened to the İzmir Bay from the North side of the bay. According to our knowledge, this thesis will be the first study in the İzmir Bay for the determination of seasonal and biogeochemical dynamics of the DOM after running of Wastewater Treatment Plant.

## **CHAPTER TWO**

### **MATERIALS AND METHODS**

#### **2.1 Sampling Methods & Stations**

The seawater samples were collected from 7 different stations in the İzmir Bay (Figure 2.1). The samples were collected from the surface (0-2 m), subsurface (5 m) and bottom layers of the water column. The sampling cruises in winter and spring seasons were carried out with the R/V K. Piri Reis on February 2015 and April 2015, respectively. The cruises in summer and autumn seasons were performed with Dokuz Eylül 3 on September 2015 and December 2015, respectively. The samples were collected with a CTD system (SBE 911plus, Sea-Bird Electronics, USA) attached to the multi-rosette sampler. For total organic matter analyses, the samples were directly transferred from Niskin bottles to the HDPE (Nalgene, USA) or PTFE capped glass amber bottles (Thermo Scientific, USA) and stored frozen at -20 °C until the laboratory analyses. For dissolved organic matter and nutrient analyses, the samples were transferred to PP bottles and immediately filtered from 0.7 µm glass fiber filters (Whatman, USA) by vacuum filtration. Then, the filtrates were stored frozen in the HDPE or PTFE capped glass amber bottles until the laboratory analyses. The glass fiber filters were sterilized by keeping at 450 °C for 3 h before use.

#### **2.2 Hydrographic Analyses**

In the scope of hydrographic analyses, physical characteristics of the seawater (temperature, salinity, density and light penetration) were determined at winter and spring seasons with SBE 911plus CTD system (Sea-Bird Electronics, USA) attached to our research vessel. The CTD system is primarily capable of measuring the water pressure, temperature and electrical conductivity, as well as it is possible to measure light penetration, pH and dissolved oxygen levels with the use of additional auxiliary sensors. The sensors are calibrated each year by the producer company. Also, it is possible to calculate other physical parameters like depth, salinity, density, potential temperature, potential density and sound velocity in seawater by the use of software.

In summer and autumn seasons, physical characteristics of seawater (temperature, salinity and density) were measured with a MicroCAT system (Sea-Bird Electronics, USA).

In order to investigate the physical characteristics, contour plots at surface depths, vertical profiles at each station and at a vertical transect were used. By this way, it was possible to investigate the seasonal variations of physical characteristics and stratification depths (thermocline, halocline and pycnocline, etc.).

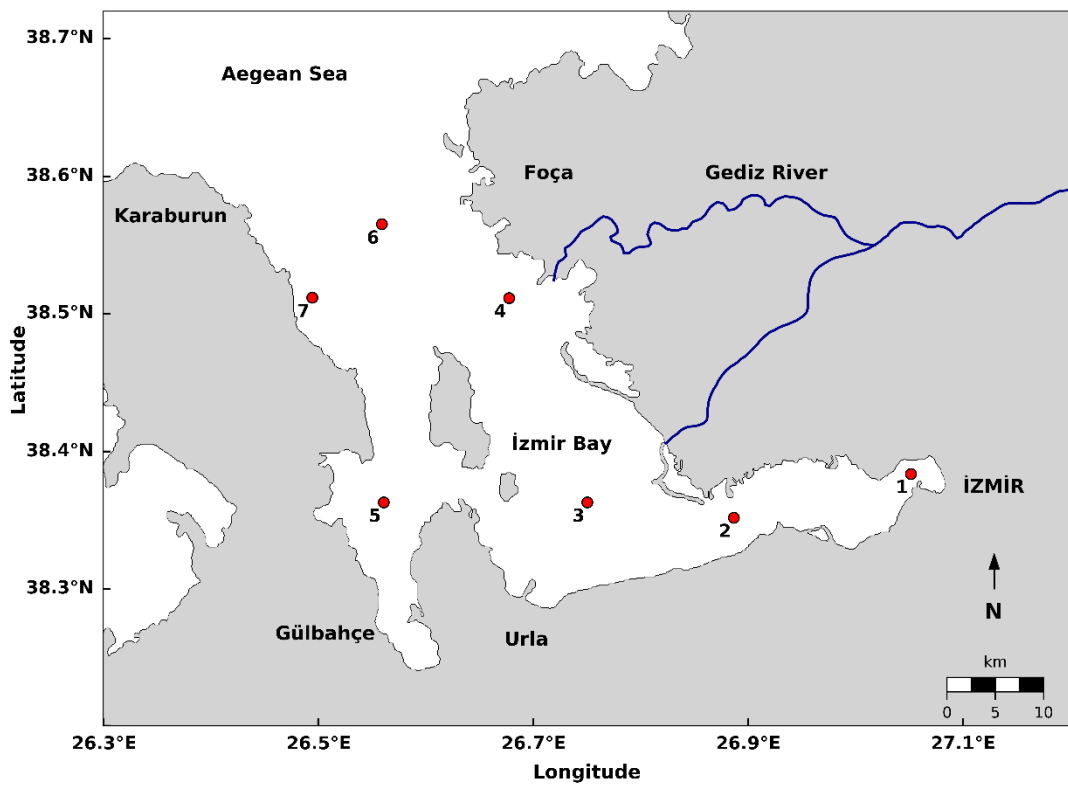


Figure 2.1 The sampling stations in the İzmir Bay

### 2.3 Determination of pH and Dissolved Oxygen

Dissolved oxygen (DO) in seawater was analyzed according to Winkler's titration method (Strickland & Parsons, 1972). pH's of seawater samples were recorded with a portable pH meter just after the sampling.

## 2.4 Analyses of Chlorophylls and Pheopigments

Following the filtration from GF/F filters, saturated MgCO<sub>3</sub> solution was added and the membrane was stored frozen in glass vials at -20 °C and kept in dark. The samples were extracted with 90% acetone solution for 24 h and centrifuged at 5000 rpm for 15 min after extraction. Absorbance of the samples were recorded at 630, 647, 664 and 750 nm on a spectrophotometer. For pheopigment analysis, 30 µL 1N HCl was added to per 1 mL of samples and their absorbances were recorded before and after acidification at 664 and 665 nm, respectively. Pigments concentrations were calculated from below equations (APHA, 1998):

$$Chl - a, \left( \frac{\mu g}{L} \right) = \frac{(11.85 \times (A_{664} - A_{750}) - 1.54 \times (A_{647} - A_{750}) - 0.08 \times (A_{630} - A_{750})) \times V_{ext}}{V_{filt} \times L} \quad (2.1)$$

$$Chl - b, \left( \frac{\mu g}{L} \right) = \frac{(21.03 \times (A_{647} - A_{750}) - 5.43 \times (A_{664} - A_{750}) - 2.66 \times (A_{630} - A_{750})) \times V_{ext}}{V_{filt} \times L} \quad (2.1)$$

$$Chl - c, \left( \frac{\mu g}{L} \right) = \frac{(24.52 \times (A_{630} - A_{750}) - 7.60 \times (A_{647} - A_{750}) - 1.67 \times (A_{664} - A_{750})) \times V_{ext}}{V_{filt} \times L} \quad (2.3)$$

$$Pheophytin, \left( \frac{\mu g}{L} \right) = \frac{26.7 \times (1.7 \times (A_{665} - A_{664})) \times V_{ext}}{V_{filt} \times L} \quad (2.4)$$

where  $A_{630}$ ,  $A_{647}$ ,  $A_{664}$ ,  $A_{665}$  and  $A_{750}$  are absorbances at specified wavelengths,  $V_{ext}$  is extraction volume (mL),  $V_{filt}$  is sample filtration volume (L), and  $L$  is length of light path.

## 2.5 Analyses of Dissolved Nutrients

Following the filtration from GF/F filters, seawater samples were stored in 100 mL polyethylene bottles at -20 °C.

Nutrient analysis methods were checked with certified seawater samples obtained from QUASI-MEME, Plymouth Marine Laboratory (Round 22) for inter-laboratory calibration and comparison. After 10 replicate analyses of these samples, the results

(Mean  $\pm$  Std. Dev.) were as follows (Certified value; Measured value): TNO<sub>x</sub>-N (8.68  $\pm$  0.38; 8.78  $\pm$  0.04), NO<sub>2</sub>-N (0.50  $\pm$  0.04; 0.50  $\pm$  0.02), NH<sub>4</sub>-N (0.84  $\pm$  0.29; 0.74  $\pm$  0.09), oPO<sub>4</sub>-P (0.76  $\pm$  0.05; 0.78  $\pm$  0.008) and total PO<sub>4</sub>-P (0.88  $\pm$  0.08; 1.0  $\pm$  0.07).

### ***2.5.1 Nitrite Nitrogen Analysis***

Under acidic conditions, diazonium compound generated from the reaction of nitrite in water with sulfanilamide forms a red-purple complex with  $\alpha$ -naphthylethylenediamine dihydrochloride. The color intensity of this complex is measured at 540 nm (Grasshoff et al., 1999) using Skalar autoanalyzer.

### ***2.5.2 Nitrate Nitrogen Analysis***

The analysis of both Nitrate and Nitrite (TNO<sub>x</sub> = NO<sub>2</sub><sup>-</sup>+NO<sub>3</sub><sup>-</sup>) depends on hydrazinium reduction method. In the method, nitrate is transformed to nitrite with hydrazinium sulfate. Both reduced and natural nitrite is determined according to nitrite analysis method given at Section 2.5.1 (APHA, 1980; Novane, 1964; Walinga et al., 1989) using Skalar autoanalyzer.

### ***2.5.3 Ammonium Nitrogen Analysis***

In the method, ammonia is chlorinated to monochloroamine by reacting with phenol. After the oxidation reaction, a green colored complex is formed. This reaction is catalyzed by nitroprusside and the need for chlorine is supplied by adding sodium hypochloride. The color intensity of the complex is measured at 630 nm using Skalar autoanalyzer (Grasshoff et al., 1999).

Dissolved inorganic nitrogen (DIN) was found by summing the concentrations of NO<sub>2</sub>, NO<sub>3</sub> and NH<sub>4</sub>.

#### ***2.5.4 Inorganic Phosphate Phosphorus Analysis***

Dissolved inorganic phosphorus (DIP) in samples were determined by the reaction of ammonium molybdate and potassium antimony tartrate in acidic medium. The absorbance of blue colored antimony-phospho-molybdate complex was measured at 880 nm using a spectrophotometer (EPA, 1983; Grasshoff et al., 1999; Strickland & Parsons, 1972).

### **2.6 Analyses of Dissolved Total & Total Nitrogen & Phosphorus**

#### ***2.6.1 Dissolved Total and Total Nitrogen Analysis***

The samples filtered from GF/F filters for dissolved total nitrogen (DTN) analysis were stored at -20 °C. The samples for total nitrogen (TN) analysis were stored frozen without filtration. The nitrogen containing species in samples were transformed to inorganic nitrogen by persulfate oxidation at 110 °C for 30 min. Then, the samples were analyzed according to nitrate analysis method (Section 2.5.2) in autoanalyzer (Grasshoff et al., 1999).

Dissolved organic nitrogen (DON) was calculated by subtracting DIN from DTN. Particulate nitrogen was found by subtracting DTN from TN.

#### ***2.6.2 Dissolved Total and Total Phosphorus Analysis***

The samples for dissolved total phosphorus (DTP) and total phosphorus (TP) analyses were prepared as given at Section 2.6.1. The analyses were performed with spectrophotometric methods according to inorganic phosphate analysis method given at Section 2.5.4 (Grasshoff et al., 1999).

Dissolved organic phosphorus (DOP) was found by subtracting DIP from DTP. Particulate phosphorus (PP) was determined from subtracting DTP from TP.

## **2.7 Analyses of Dissolved & Total Organic Carbon**

### **2.7.1 Dissolved Organic Carbon Analysis**

Dissolved organic carbon (DOC) analyses were performed at an autoanalyzer. Prior to the oxidation step, inorganic carbon was removed by acidification. Persulfate solution was added to the acidified sample and oxidized under UV light. Then, hydroxylamine solution was added, and the sample was subjected to dialysis membrane. The generated carbon dioxide is diffused to slightly buffered phenolphthalein solution along the silicon membrane. The color intensity of the indicator solution was reduced proportionally to pH change. The color intensity is measured at 550 nm (Grasshoff et al., 1999).

### **2.7.2 Total Organic Carbon Analysis**

Prior to the analysis steps given for DOC (Section 2.7.1), inorganic carbon was removed by acidification with sulfuric acid and flushing with high purity nitrogen gas. Then, organic carbon containing compounds were transformed to inorganic forms by chemical oxidation at 120 °C for 30 min with addition of persulfate solution. Following the oxidation, inorganic species were subjected to autoanalyzer and measured as given at DOC analysis by photometric method (Grasshoff et al., 1999). Particulate organic carbon (POC) concentrations were found by subtracting DOC from TOC.

## **2.8 Determination of Eutrophication Level by TRIX and UNTRIX Indexes**

TRIX index was calculated according to below equation (Volleinweider et al., 1998):

$$\text{TRIX} = (\log [\text{Chl-a} \times |100 - \text{DO}\%| \times \text{TN} \times \text{TP}] - (-1.5)) / 1.2 \quad (2.5)$$

In the equation, Chl-a indicates Chlorophyll-a concentration in µg/L unit, DO% indicates dissolved oxygen percent saturation, TN and TP indicates total nitrogen and

total phosphorus concentrations, respectively, in  $\mu\text{g/L}$  units. The constants of 1.5 and 1.2 at the end indicate corrections obtained from data of Adriatic Sea.

Eutrophication risks for the İzmir Bay were evaluated according to below criteria (Table 2.1):

Table 2.1 Eutrophication risk evaluation criteria for TRIX index scales

<b>TRIX Index</b>	<b>Evaluation</b>
$\text{TRIX} < 4$	No eutrophication risk
$4 \leq \text{TRIX} \leq 6$	High eutrophication risk
$\text{TRIX} > 6$	Eutrophic

UNTRIX index was calculated according to below equation (Pettine et al., 2007):

$$\text{UNTRIX} = \log [\text{Chl-a} \times |100 - \text{DO}\%| \times \text{TN} \times \text{TP}] \quad (2.6)$$

Evaluation of trophic status according to UNTRIX index values were performed based on comparison of 100th and 75th percentiles of UNTRIX at reference and sampling stations (Pettine et al., 2007).

## **2.9 Analyses of Carbohydrates**

### **2.9.1 Dissolved Free Carbohydrate Analysis**

In the analysis of dissolved free carbohydrates (MCHO), 1 ml of seawater or hydrolysate or standard solution is transferred into a test tube and 1 ml of potassium ferricyanide solution is added and kept in a boiling water bath for 10 min. Then, 1 ml of ferric chloride and 2 ml of 2,4,6-Tri(2-pyridyl)-s-triazine (TPTZ) solutions are added and mixed thoroughly on a Vortex-mixer. 30 min later, the absorbance is read at 595 nm against distilled water. A reagent blank was also read in purified seawater or Milli-Q water and should be subtracted for sample readings. The unit will be  $\mu\text{mol C L}^{-1}$  (Myklestad et al., 1997).



### ***2.9.2 Dissolved Total Carbohydrate Analysis***

For dissolved total carbohydrate (TDCHO) analysis, 4 mL filtered seawater sample (or standard) and 0.4 mL 1 M HCl were added to 5 mL glass vials. Then, the vials were placed into heater block at 150 °C for 1 h. Following the hydrolysis, the hydrolysates were neutralized with 1 M NaOH and analyzed as given at Section 2.9.1. Dissolved polysaccharide (PCHO) concentrations were calculated by subtracting MCHO from TDCHO.

## **2.10 Analyses of Amino Acids**

### ***2.10.1 Sampling***

Samples of dissolved free amino acids (DFAA) and dissolved total hydrolysable amino acids (TDHAA) were filtered from GF/F filters and transferred to 2 mL amber vials. The particulate samples retained on GF/F filters were used in the particulate hydrolysable amino acids (PHAA) analysis and transferred to 2 mL glass vials. All samples were stored frozen at -20°C.

### ***2.10.2 Hydrolysis***

For analysis of TDHAA, 0.5 mL 12 M HCl and 5 µL 11 mM ascorbic acid were added onto 0.5 mL sample within 2 mL glass vial. For PHAA samples, 1 mL 6M HCl and 5 µL 11mM ascorbic acid were added to 2 mL glass vials containing folded 25 mm GF/F filter. The vials were hydrolyzed at 110 °C for 24 h. Then, 0.5 mL of hydrolysates were transferred to a new vial. pH's of the hydrolysates were adjusted to range of 8.0-9.0 with borate buffer. Hydrolysates were filtered from 0.2 µm nylon syringe filters and stored at -20 °C within new vials until the analyses. During this procedure, glutamine (Gln) and asparagine (Asn) are converted to glutamic acid (Glu) and aspartic acid (Asp), respectively, and reported as the sum of Gln + Glu (Glx) and Asp + Asn (Asx).

### 2.10.3 Principle of Amino Acid Analysis

The enantiomers of the amino acids were analyzed by using HPLC-Fluorescence detection after derivatization (Figure 2.2) with o-phthaldialdehyde (OPA) and N-isobutyryl-L/D-cysteine (IBLC or IBDC, respectively) (Fitznar et al., 1999). By this two-step reaction, the amino acid enantiomers (D-AA, L-AA) were converted into their diastereomers which can be separated on a reversed-phase C<sub>18</sub> column:

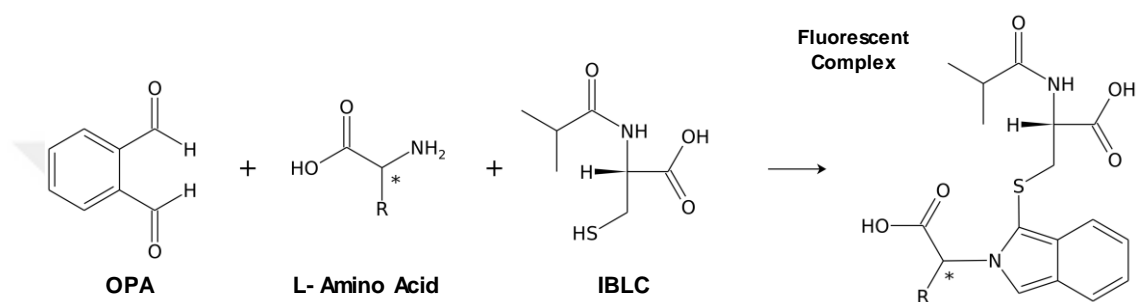
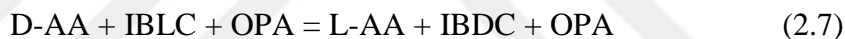
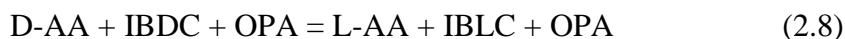


Figure 2.2 The reaction of an L-amino acid with OPA and IBLC to form a stereomeric fluorescent complex



and



This feature could be used for peak identification and resolving coelutions. Each sample is analyzed first with IBLC + OPA and then with IBDC + OPA. The retention times of D- and L-amino acids are inverted in the sequential analyses, but non-chiral amino acids always elute at the same retention time. For blank correction, ultrapure water was derivatized and analyzed using the same procedure of samples.

### 2.10.4 Modifications Applied in the Amino Acid Analysis

Prior to analyses, amino acid determination method in HPLC was modified and optimized. In 2009, Dittmar et al. (2009) proposed a modified version of the original HPLC method of Fitznar et al. (1999). In this thesis, the method proposed by Dittmar et al. (2009) was modified again by changing injection volume, mobile phase

composition, HPLC column, column temperature, gradient elution program, and total analysis time. Also, different columns compared based on their separation power and best column was selected. Chromatograms belong to a 50 nM L-amino acid mix and seawater sample from the İzmir Bay were given at Figure 2.3. The separation power of the method was checked by comparing retention time ( $t_R$ ), retention factor ( $k$ ), peak width ( $w$ ), theoretical plate number ( $N$ ), reduced plate height ( $h$ ), and peak capacity ( $n$ ) (Table 2.2). Separation factors ( $\alpha$ ) and peak resolutions ( $R$ ) were also calculated (Table 2.3).

OPA is dissolved at final concentration of 5 g L<sup>-1</sup> in 0.5 M borate buffer solution (pH 9.5). The IBLC and IBDC are first dissolved in methanol, and then, water is added at a methanol:water ratio of 4:6 to reach final concentration of 5 g L<sup>-1</sup>. For derivatization, 90  $\mu$ L of sample was thoroughly mixed first with 2  $\mu$ L OPA, and then, 2  $\mu$ L IBLC or IBDC reagents within a 150  $\mu$ L micro-insert containing vials. The autosampler should be kept at 4 °C to prevent sample and reagent decay. Injection volume was set as 10  $\mu$ L. Detection limits of all amino acids were  $\leq 1$  nM.

The chromatographic separation was performed on a conventional reversed-phase C18 column with a linear binary solvent gradient between mobile phase A (Table 2.4-2.5): sodium acetate buffer solution (pH 6.0) and mobile phase B: acetonitrile:methanol:water (45:45:10, v/v). The pH of 25 mM sodium acetate buffer was adjusted to 6.0 with 0.1 M HCl. Chromatographic separations were performed on Agilent Eclipse Plus C<sub>18</sub> (4.6 x 150 mm, 3.5  $\mu$ m) analytical column. Flow rate and column temperature were adjusted as 1.1 mL/min and 40 °C, respectively. Total analysis time was 78.01 min. The column was rinsed with 100% mobile phase B after each run. The fluorescence of peaks was detected at 230/330 nm of excitation and 445 nm of emission wavelengths. For identification of peaks, every single HPLC purity standards of amino acids (prepared from powder form) were injected to column. For calibration, an L-amino acid standard mix (No: 79248, Sigma Aldrich) with quantitative NMR (QNMR) certificate was used.

Degradation index (DI) values of amino acids were calculated from below equation (Dauwe et al., 1999):

$$DI = \sum_i \left[ \frac{x - \bar{X}}{s} \cdot PCI_{1_i} \right] \quad (2.9)$$

In this equation,  $x$  indicates mol percentages of amino acids,  $\bar{X}$  indicates mean mol percentage at all seasons and stations,  $s$  indicates standard deviation at all seasons and stations,  $PCI$  indicates factor coefficients of 1st principal component obtained from principal components analysis.

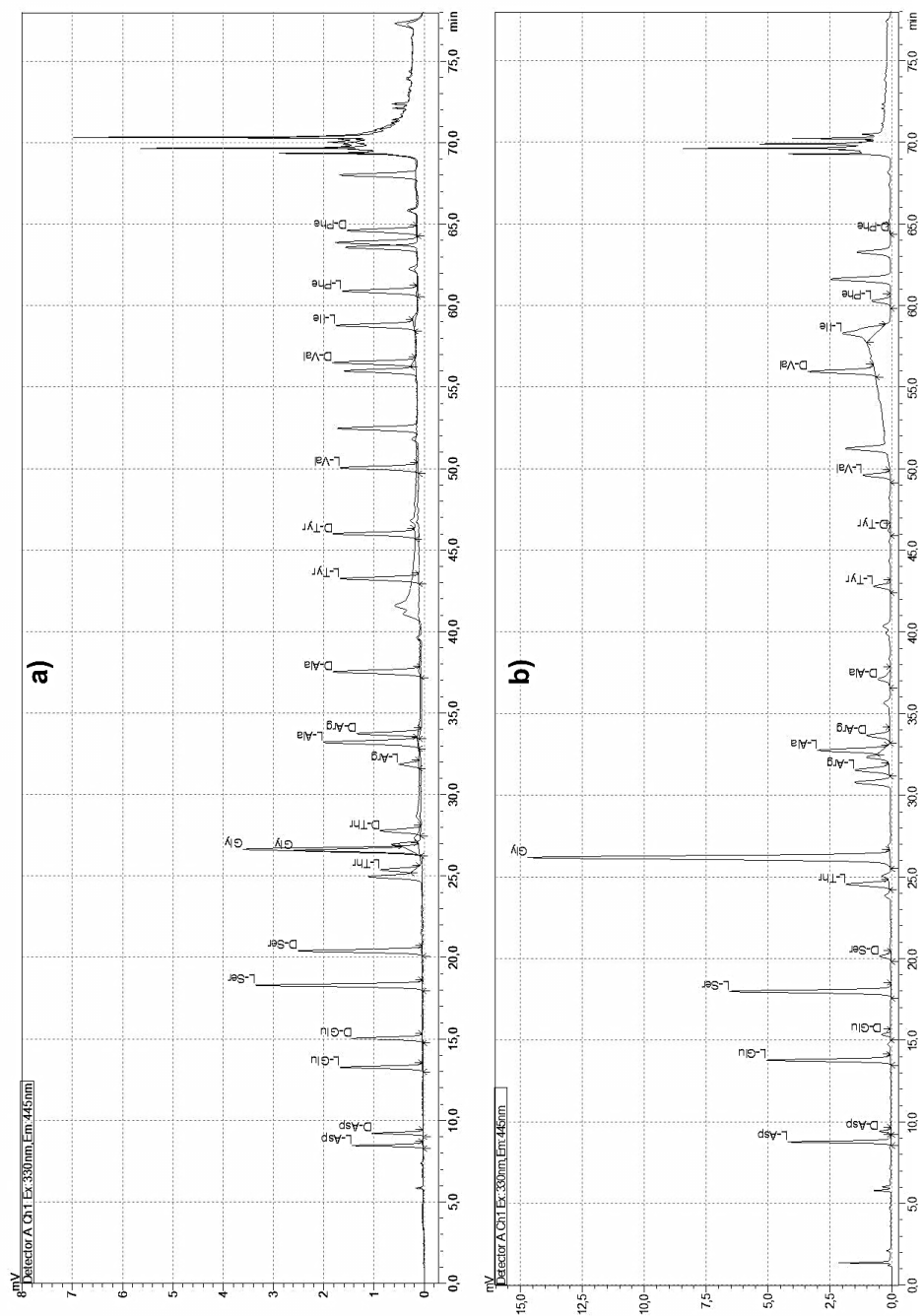


Figure 2.3 Chromatograms belong to D/L-amino acid analysis. a) 50 nM L-amino acid mix analyzed with both IBLC and IBDC methods. b) Sample of dissolved free amino acid analysis from İzmir Bay

Table 2.2 Chromatographic separation parameters for 20 nM D/L-amino acid standards ( $t_R$ : retention time,  $k$ : retention factor,  $w$ : peak width,  $N$ : theoretical plate number,  $h$ : reduced plate height,  $n$ : peak capacity)

<b><i>Peak Name</i></b>	<b><i>t<sub>R</sub> (min)</i></b>	<b><i>k</i></b>	<b><i>w (min)</i></b>	<b><i>N</i></b>	<b><i>h</i></b>	<b><i>n</i></b>
<b>L-Asp</b>	8.5	5.1	0.22	23511	2.1	70
<b>D-Asp</b>	9.2	5.5	0.23	25544	2.0	76
<b>L-Glu</b>	13.3	8.5	0.29	33552	1.5	104
<b>D-Glu</b>	15.0	9.7	0.30	39734	1.3	119
<b>L-Ser</b>	18.3	12.1	0.33	48032	1.0	142
<b>D-Ser</b>	20.4	13.6	0.34	57263	0.9	161
<b>L-Thr</b>	24.7	16.6	0.42	56136	0.9	171
<b>Gly</b>	26.4	17.9	0.43	61738	0.8	183
<b>D-Thr</b>	27.8	18.9	0.42	71453	0.7	201
<b>L-Arg</b>	31.5	21.5	0.37	116597	0.4	267
<b>L-Ala</b>	33.0	22.5	0.42	97545	0.5	248
<b>D-Arg</b>	33.8	23.2	0.38	126072	0.4	284
<b>D-Ala</b>	37.6	25.8	0.42	128503	0.4	296
<b>L-Tyr</b>	42.9	29.6	0.38	208091	0.2	391
<b>D-Tyr</b>	46.1	31.9	0.35	272407	0.2	457
<b>L-Val</b>	49.9	34.6	0.39	261514	0.2	458
<b>D-Val</b>	56.0	39.0	0.39	331586	0.2	532
<b>L-Ile</b>	58.6	40.9	0.41	328449	0.2	536
<b>L-Phe</b>	60.6	42.3	0.40	367478	0.1	572

Table 2.3 Separation factors ( $a$ ) and peak resolutions ( $R$ ) for 20 nM D/L-amino acid standards  
(Criteria:  $a \geq 1.05$ ,  $R \geq 1.5$ )

<b><i>Adjacent Peaks</i></b>	<b><i>a</i></b>	<b><i>R</i></b>
<b>L-Asp/D-Asp</b>	1.09	2.8
<b>D-Asp/L-Glu</b>	1.53	15.9
<b>L-Glu/D-Glu</b>	1.14	5.7
<b>D-Glu/L-Ser</b>	1.25	10.6
<b>L-Ser/D-Ser</b>	1.12	6.2
<b>D-Ser/L-Thr</b>	1.23	11.3
<b>L-Thr/Gly</b>	1.07	4.0
<b>Gly/D-Thr</b>	1.06	3.3
<b>D-Thr/L-Arg</b>	1.14	9.4
<b>L-Arg/L-Ala</b>	1.05	3.7
<b>L-Ala/D-Arg</b>	1.03	2.2
<b>D-Arg/D-Ala</b>	1.12	9.3
<b>D-Ala/L-Tyr</b>	1.15	13.4
<b>L-Tyr/D-Tyr</b>	1.08	8.7
<b>D-Tyr/L-Val</b>	1.09	10.2
<b>L-Val/D-Val</b>	1.13	15.8
<b>D-Val/L-Ile</b>	1.05	6.5
<b>L-Ile/L-Phe</b>	1.04	5.0

Table 2.4 Modules of HPLC system used in amino acid analysis

<b>HPLC Modules</b>	<b>Model</b>
System Controller Unit	CBM-20Alite
Pump	LC-20AT
Autosampler	SIL-30AC
Column Oven	CTO-10ASvp
Fluorescent Detector	RF-20A

Table 2.5 Gradient elution program for Mobile Phase B

<b>Retention Time</b>	<b>Mobile Phase B (%)</b>
0.00	2.0
2.00	8.0
20.00	16.0
23.00	16.5
35.00	22.1
67.00	39.5
68.00	100
75.00	100
76.00	2.0
78.01	2.0

## 2.11 Statistical Analyses

R Statistical Computing Software, v3.3.2 (R Core Team, 2017) was used in statistical analyses. In all statistical tests, significance level was  $\alpha=0.05$ . Seasonal and spatial changes of chemical parameters were evaluated with One Way or Two-Way ANOVA tests. Correlations between chemical parameters were tested with Pearson correlation or Spearman's rank correlation tests. Linear relationships between chemical parameters were investigated with linear regression analyses. Data was further analyzed with factor analysis or principal component analysis tests. K-means clustering method was used for grouping standardized principal component loadings.



## **CHAPTER THREE**

### **RESULTS**

#### **3.1 Results of Hydrographic Analyses**

Physical characteristics of the seawater were continuously profiled with temperature, conductivity, pressure and light transmission sensors. The results of seasonal CTD measurements at each station were given as vertical profiles from Figure 3.1 to 3.4. In winter, spring and autumn seasons, temperature was not fluctuated with depth and therefore, there were no stratifications in the water column (Figure 3.1). However, in summer, the thermoclines were clearly seen especially at outer bay stations. Temperature was higher in summer from surface to mid-depths. Similar to temperature profiles, salinities at the sampling stations were not changed dramatically with depth (Figure 3.2). There were remarkable fluctuations of salinity at all stations in summer season. Salinity values were also higher in summer compared to other seasons. Conductivity did not change vertically in winter and spring seasons, but there were clear vertical deviations in summer season (Figure 3.3). Conductivity was obviously higher in summer season. Similarly, potential density did not fluctuate in winter, spring and autumn seasons (Figure 3.4). In summer, there were remarkable changes in potential density especially at outer bay stations. Potential density was lower compared to other seasons in summer season.

The physical characteristics of seawater from inner to outer bay stations were also investigated with vertical transect plots at five adjacent stations in Figure 3.5 (Stations 1-4 and 6). Vertical variation of temperature at outer to inner bay stations was close to homogeneity in winter, spring and autumn seasons especially for outer bay stations (Figure 3.6). In summer, there were strong stratifications at outer bay stations that was also confirmed by vertical profile plots resembling the presence of thermoclines. Similar observations in vertical salinity and density transect plots were also supported the presence of strong stratification at summer season (Figure 3.7-3.8).

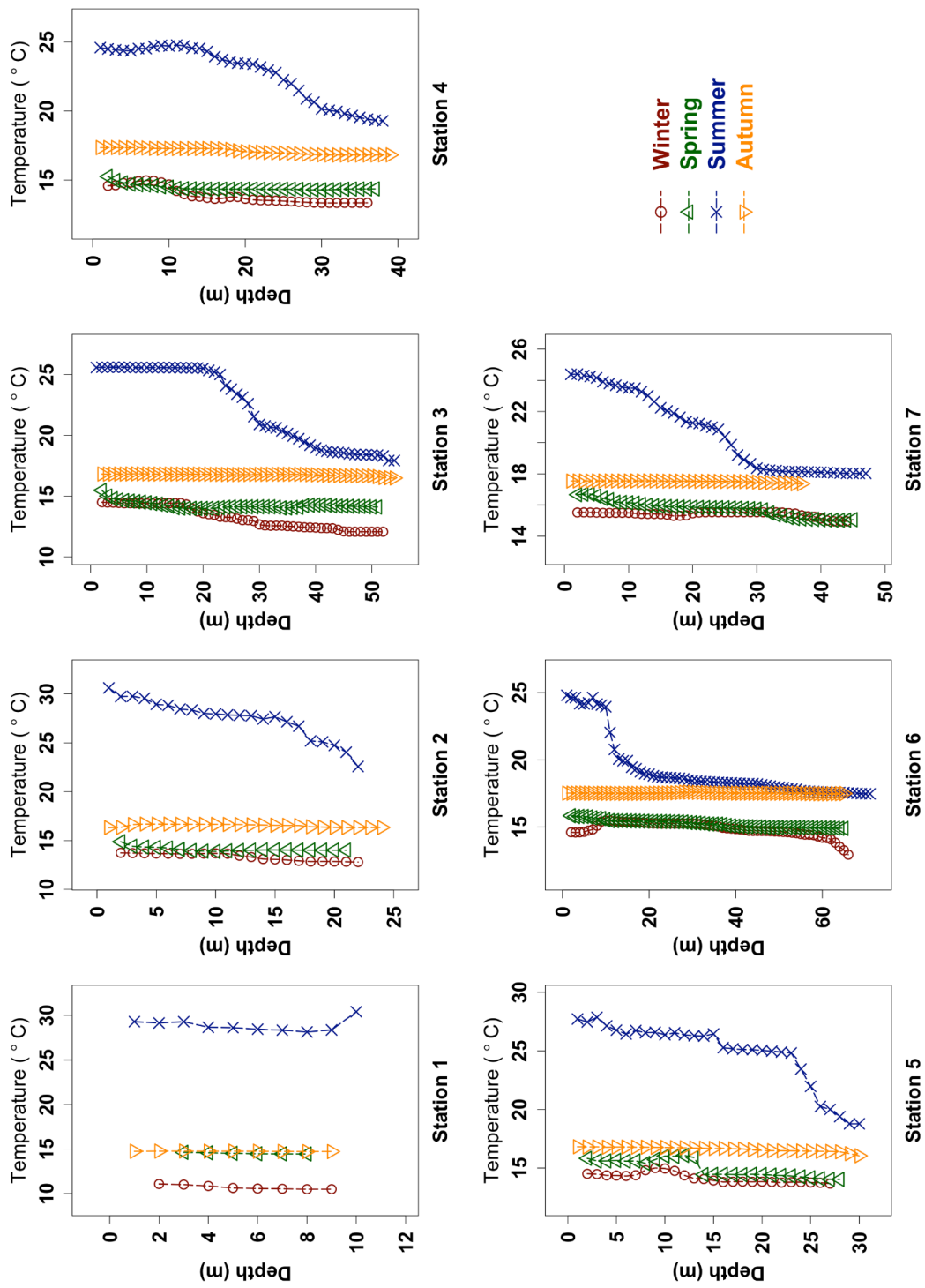


Figure 3.1 Depth profiles of temperature at the sampling stations

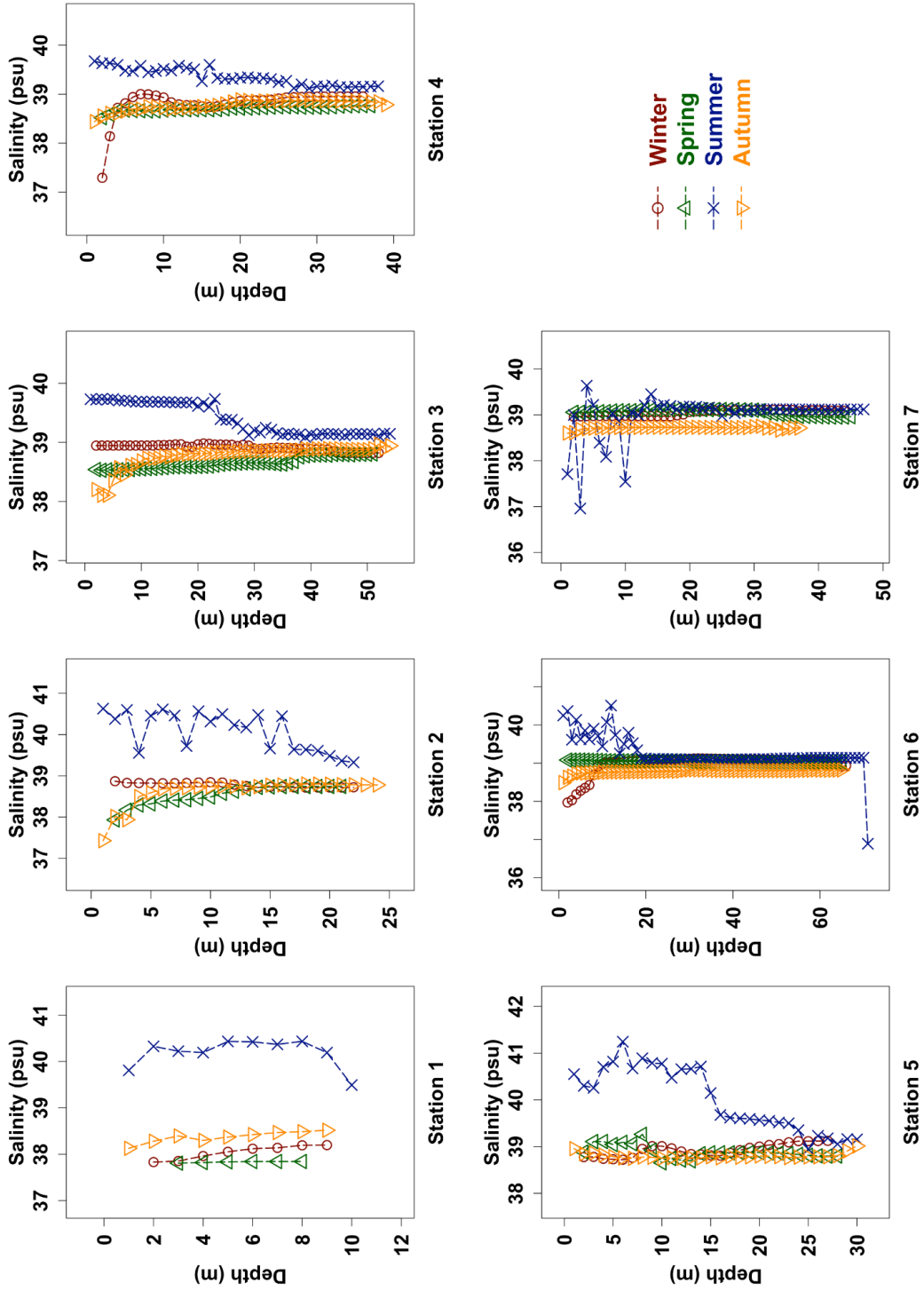


Figure 3.2 Depth profiles of salinity at the sampling stations

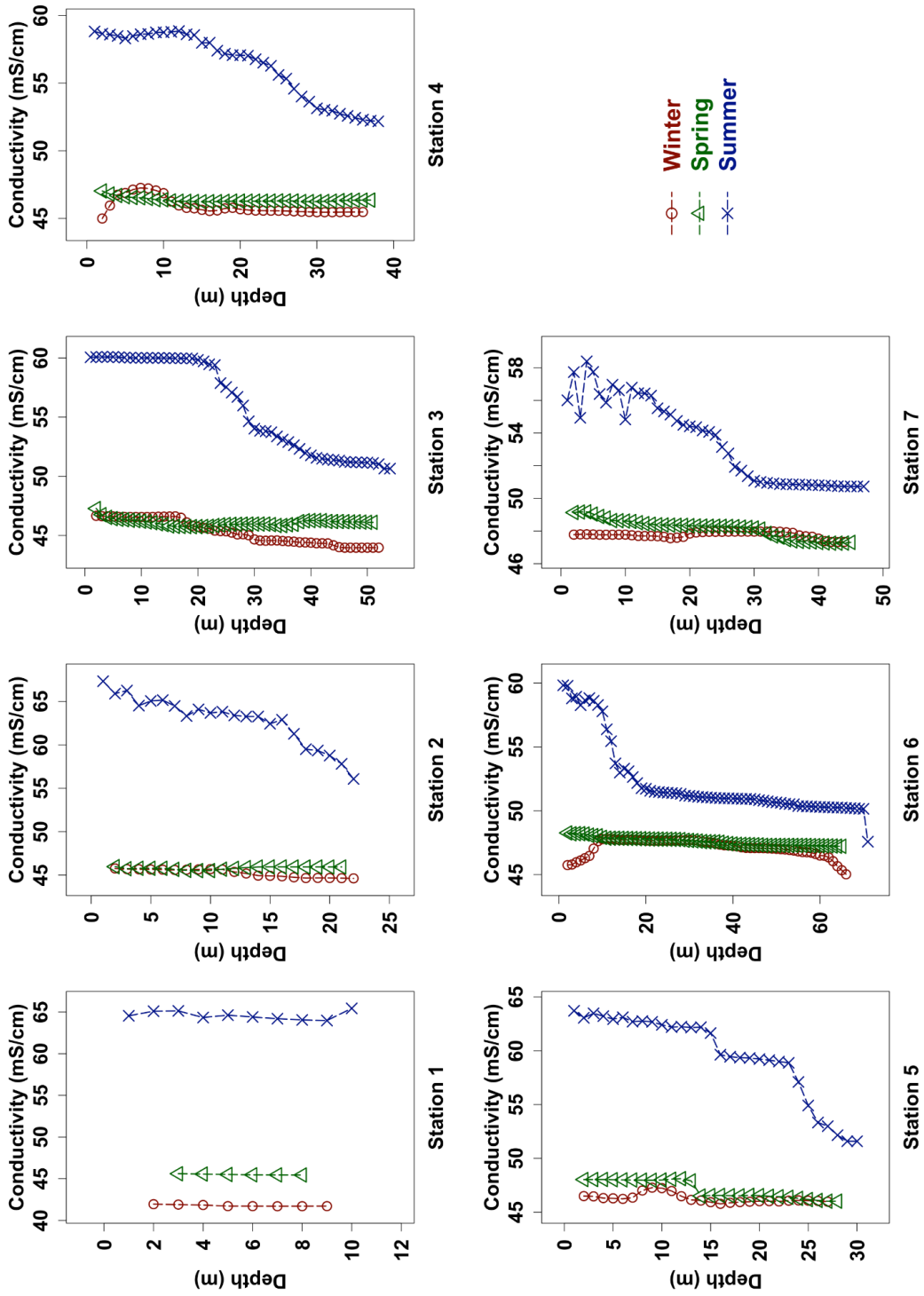


Figure 3.3 Depth profiles of conductivity at the sampling stations

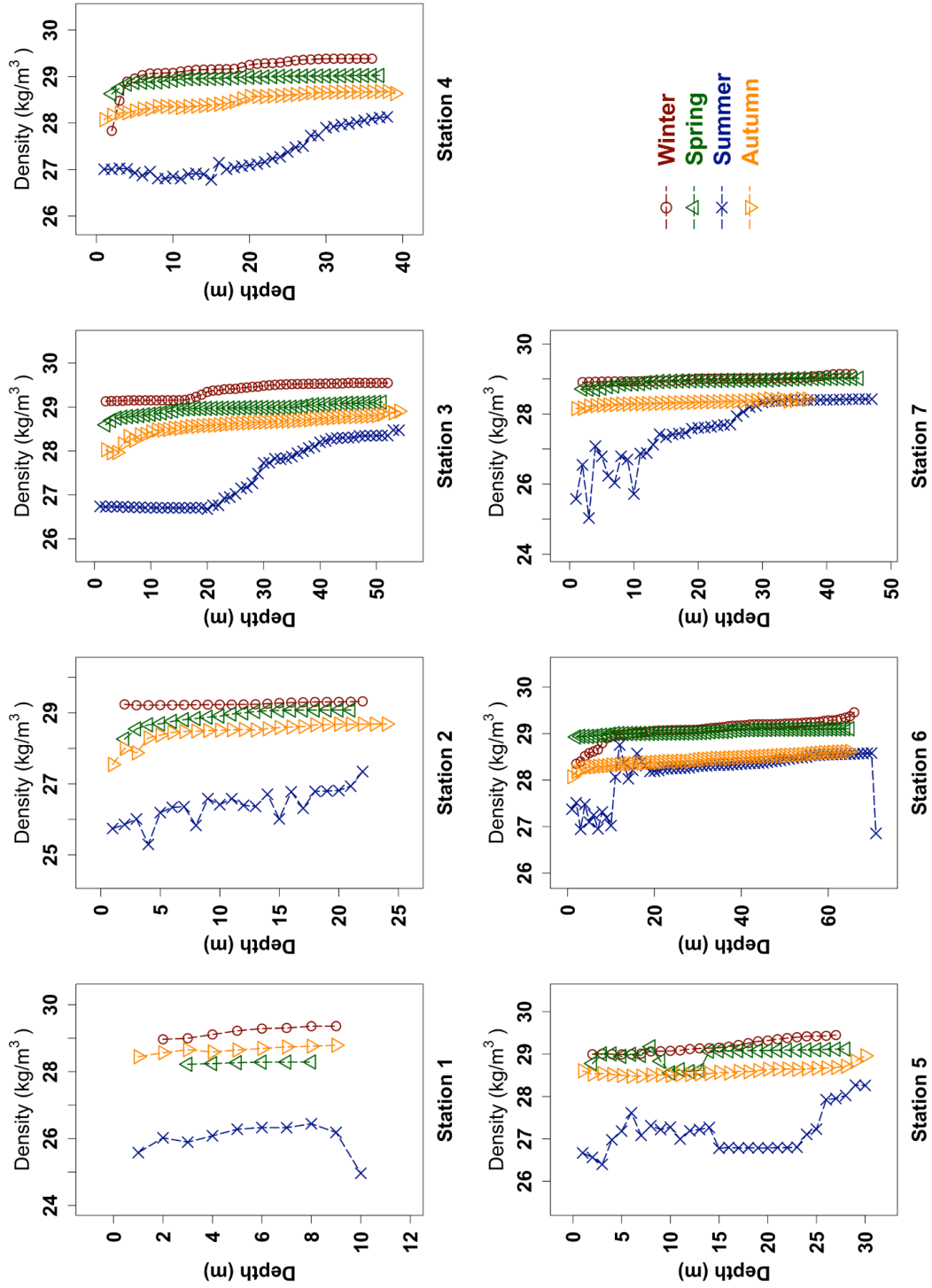


Figure 3.4 Depth profiles of potential density at the sampling stations

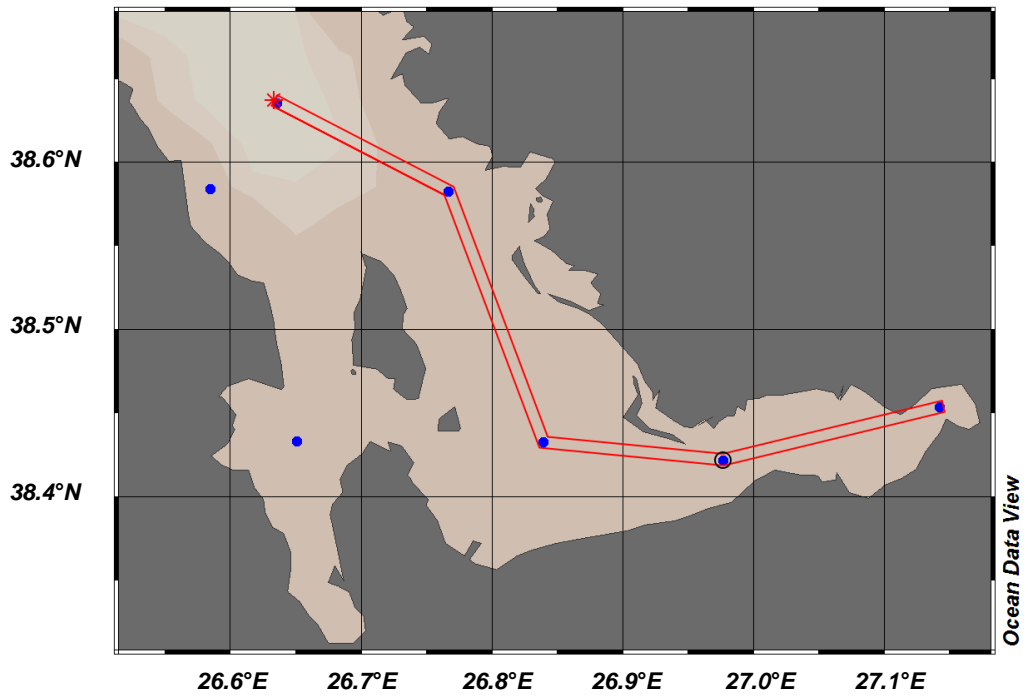


Figure 3.5 The map showing the path of vertical contour maps of seawater temperature, salinity and density at five adjacent stations

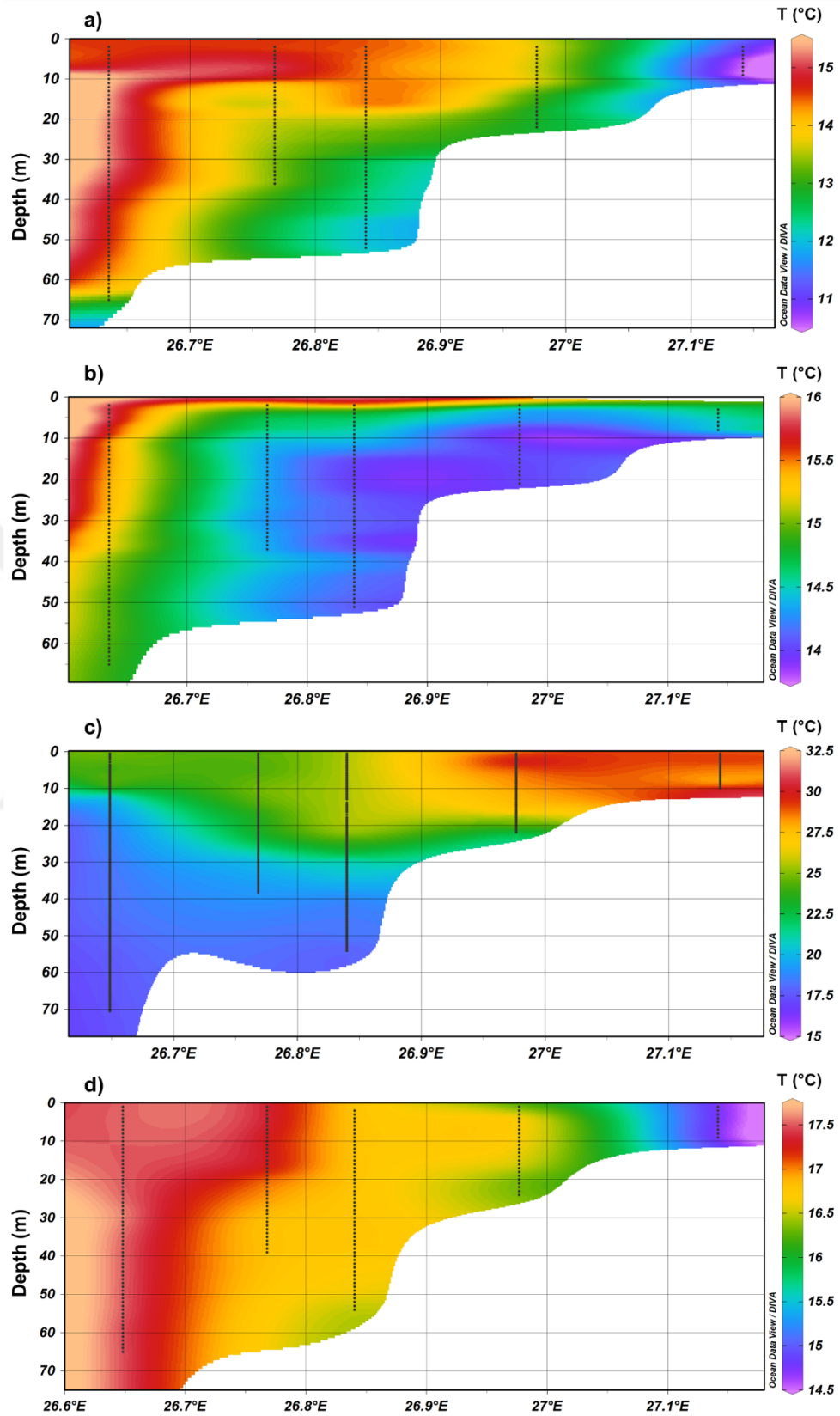


Figure 3.6 Vertical transect profiling maps of temperature for five stations at a) winter, b) spring, c) summer, and d) autumn seasons

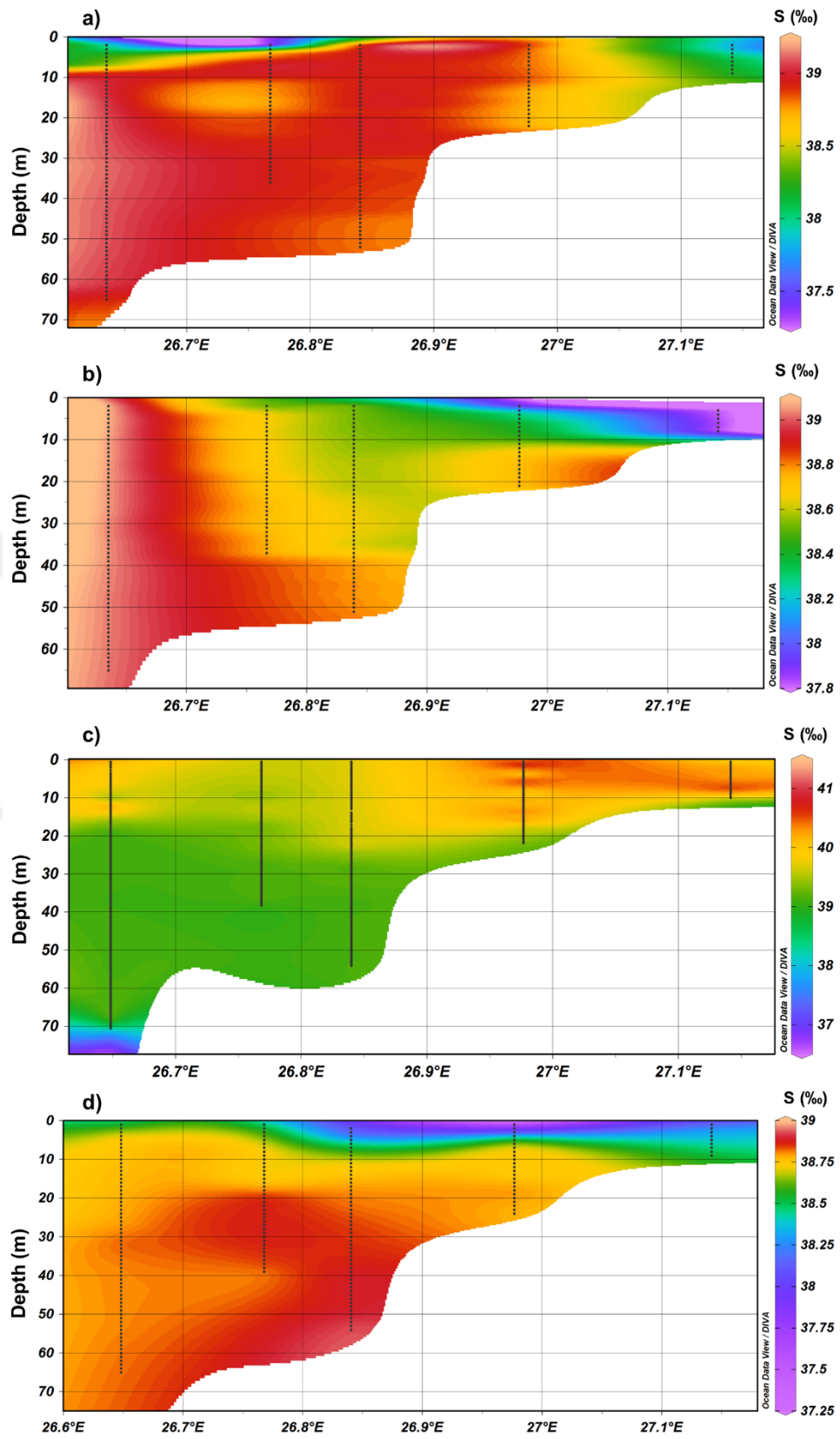


Figure 3.7 Vertical transect profiling maps of salinity for five stations at a) winter, b) spring, c) summer, and d) autumn seasons



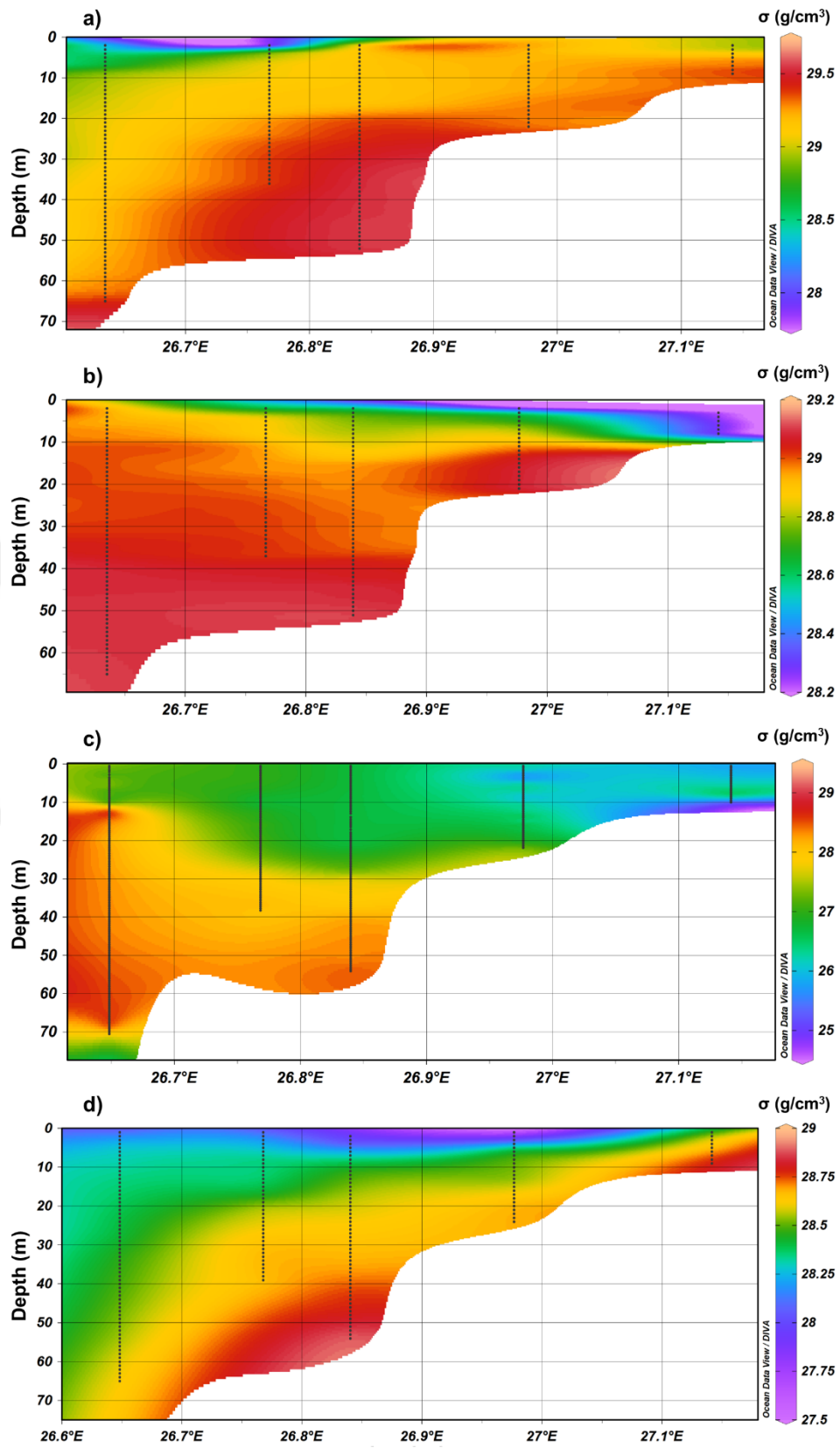


Figure 3.8 Vertical transect profiling maps of seawater densities for five stations at a) winter, b) spring, c) summer, and d) autumn seasons

### 3.2 Results of pH, Dissolved Oxygen, Chlorophyll and Pheopigment Analyses

Seawater pH in the bay was changed from 7.91 to 8.37 throughout all seasons (Figure 3.9). Maximum pH was observed at surface of Station 2 in summer and minimum values were recorded at all depths of Station 1 (7.91, 7.93, and 7.93, respectively) in autumn. In other seasons and stations, pH was fluctuated between 8.1 and 8.3.

DO levels were found between 5.04 and 9.69 mg/L throughout all seasons (Figure 3.10-3.13). Both maximum and minimum DO levels were observed at Station 1 in winter and autumn seasons, respectively. Seasonal DO levels were decreased in the order of winter, spring, summer and autumn. Highest fluctuations in DO levels were observed at inner bay stations, whereas variations between stations were much smaller at outer bay stations.

Chl-a levels were found between 0.11 and 25.4  $\mu\text{g/L}$  at all seasons (Figure 3.10-3.13). Maximum Chl-a levels were observed at surface of Station 1 in summer. Chl-a levels in Station 1 were greatly higher in winter, spring and summer seasons compared to other stations. Chl-a levels at outer bay stations were lower than 3  $\mu\text{g/L}$  and mostly fluctuated below 0.1-1.0  $\mu\text{g/L}$ . Similar to Chl-a, Chl-b and Chl-c levels at inner bay stations were higher compared to outer bay stations. Maximum Chl-b and Chl-c concentrations were observed at Station 1. Pheophytin concentrations were found very low throughout the bay. Highest pheophytin concentrations were observed at Station 1 and 2 in summer season. Pheophytin concentrations were increased from spring to summer and decreased at autumn and winter seasons.

Seasonal covariation of pH, oxygen saturation ( $\text{O}_2\%$ ) and Chl-a at surface depths of stations were shown in Figure 3.14-3.17. These three parameters changed in parallel to each other almost in all stations.

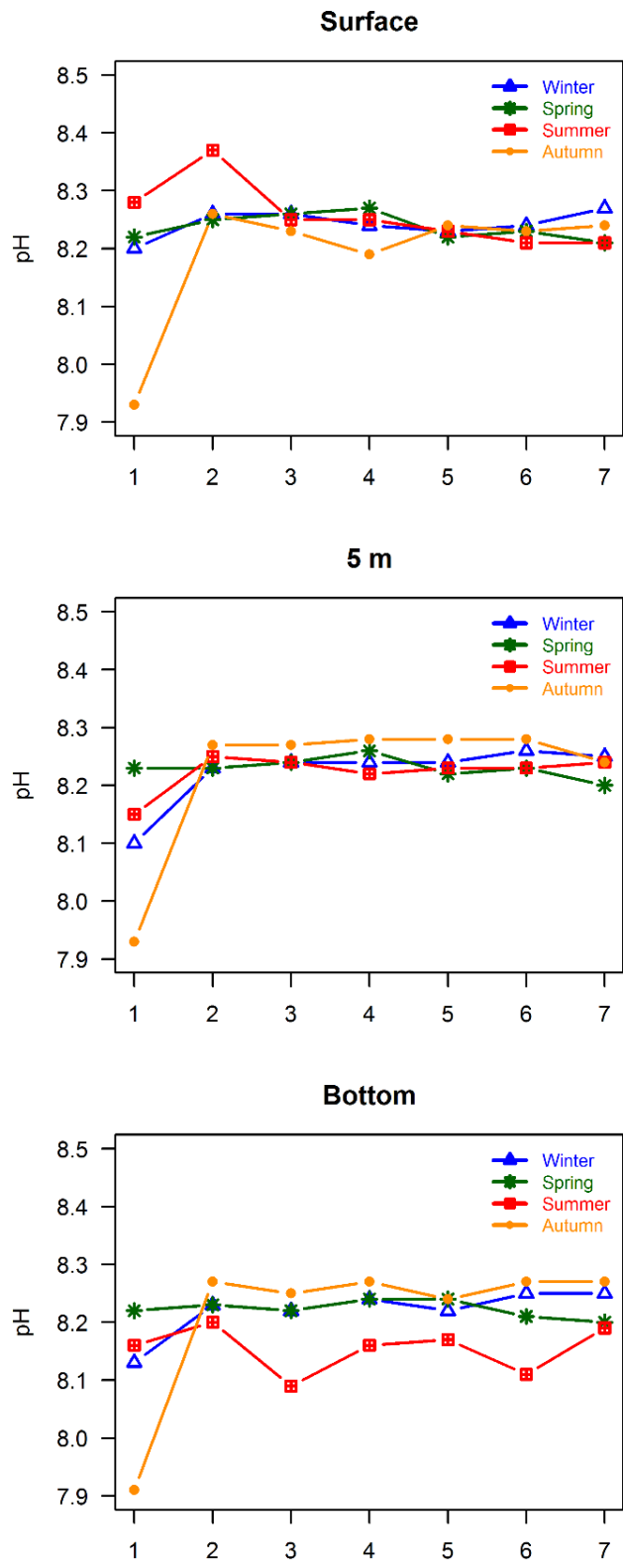


Figure 3.9 Seasonal pH profiles of seawater at sampling stations

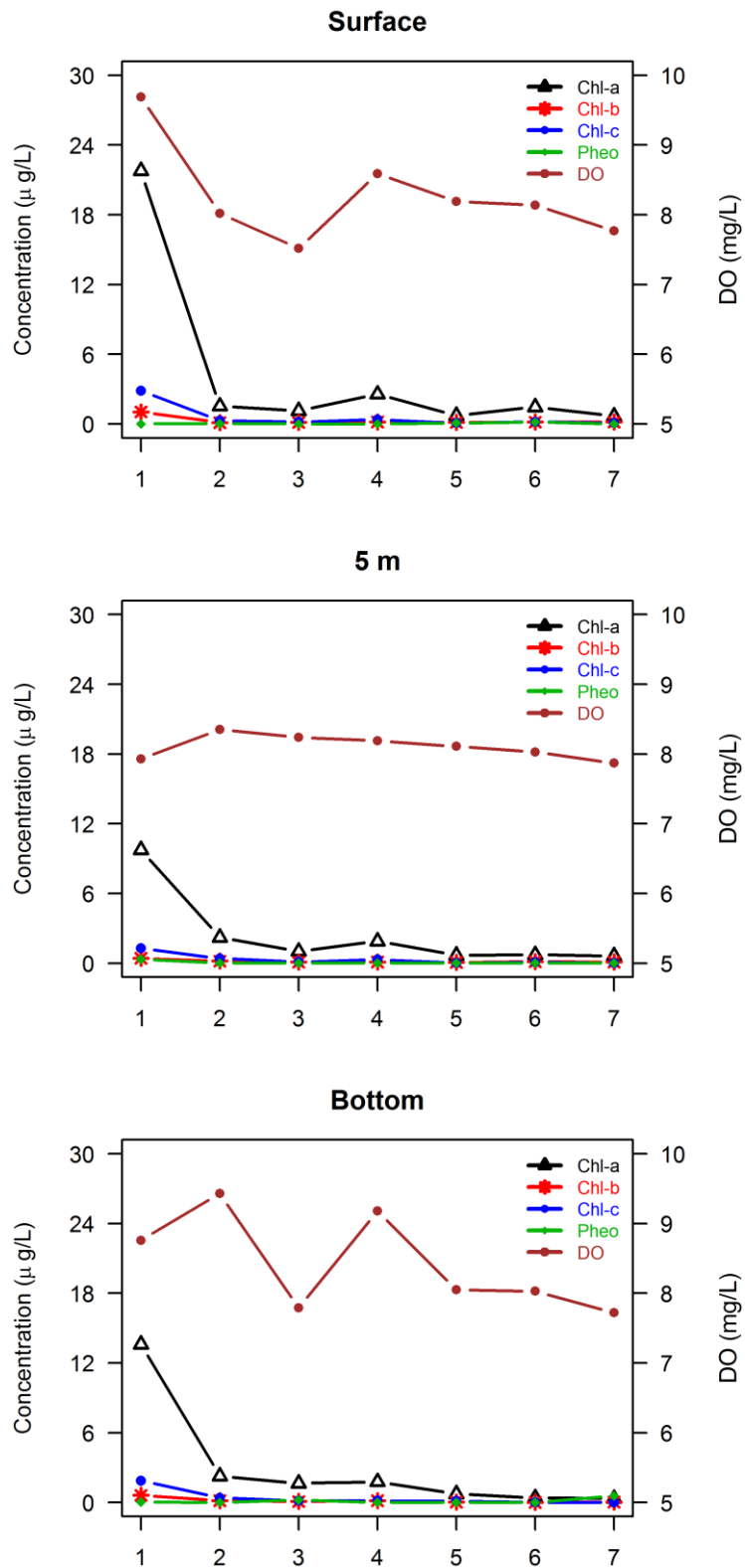


Figure 3.10 Chl-a, Chl-b, Chl-c, Pheophytin and DO profiles of seawater at sampling stations in winter

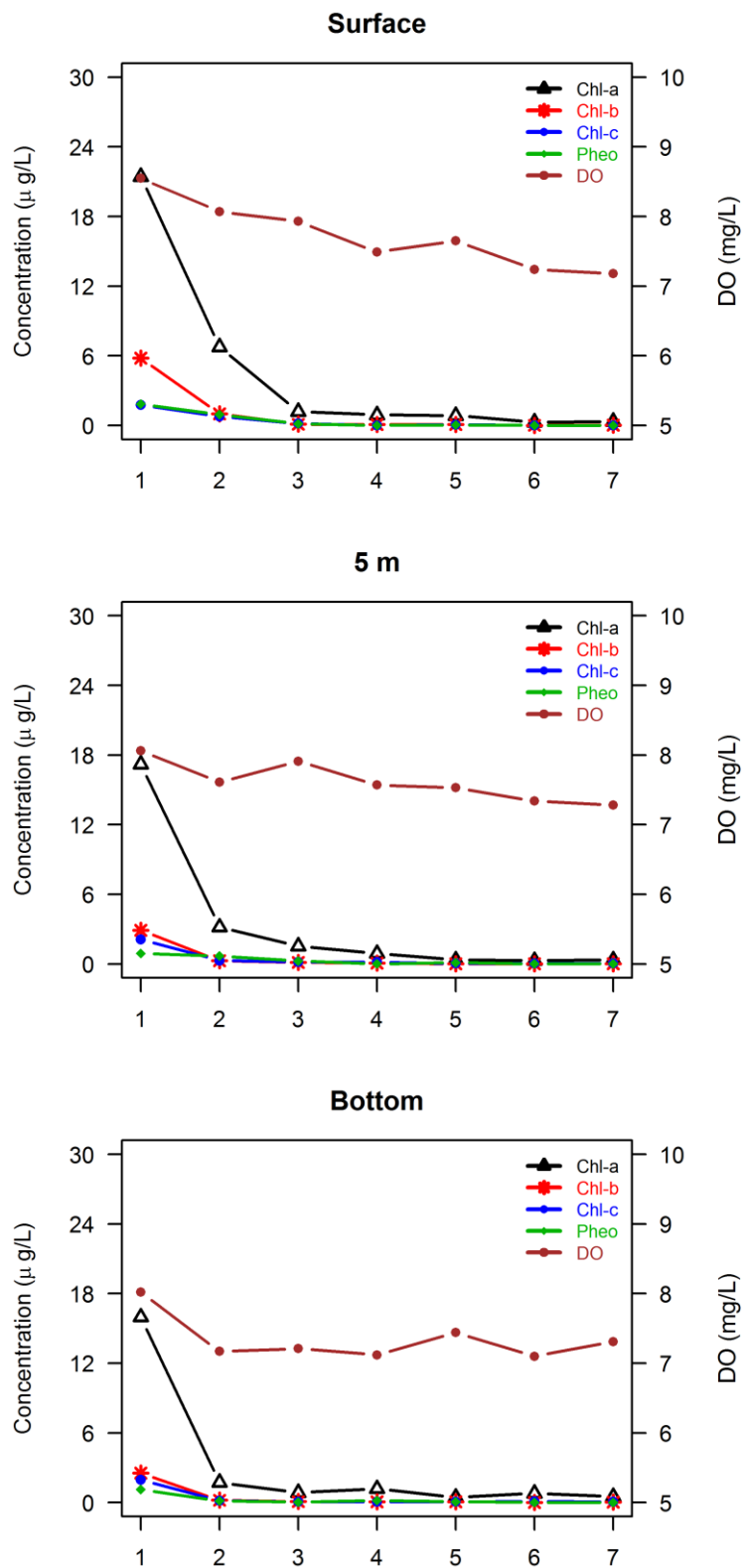


Figure 3.11 Chl-a, Chl-b, Chl-c, Pheophytin and DO profiles of seawater at sampling stations in spring

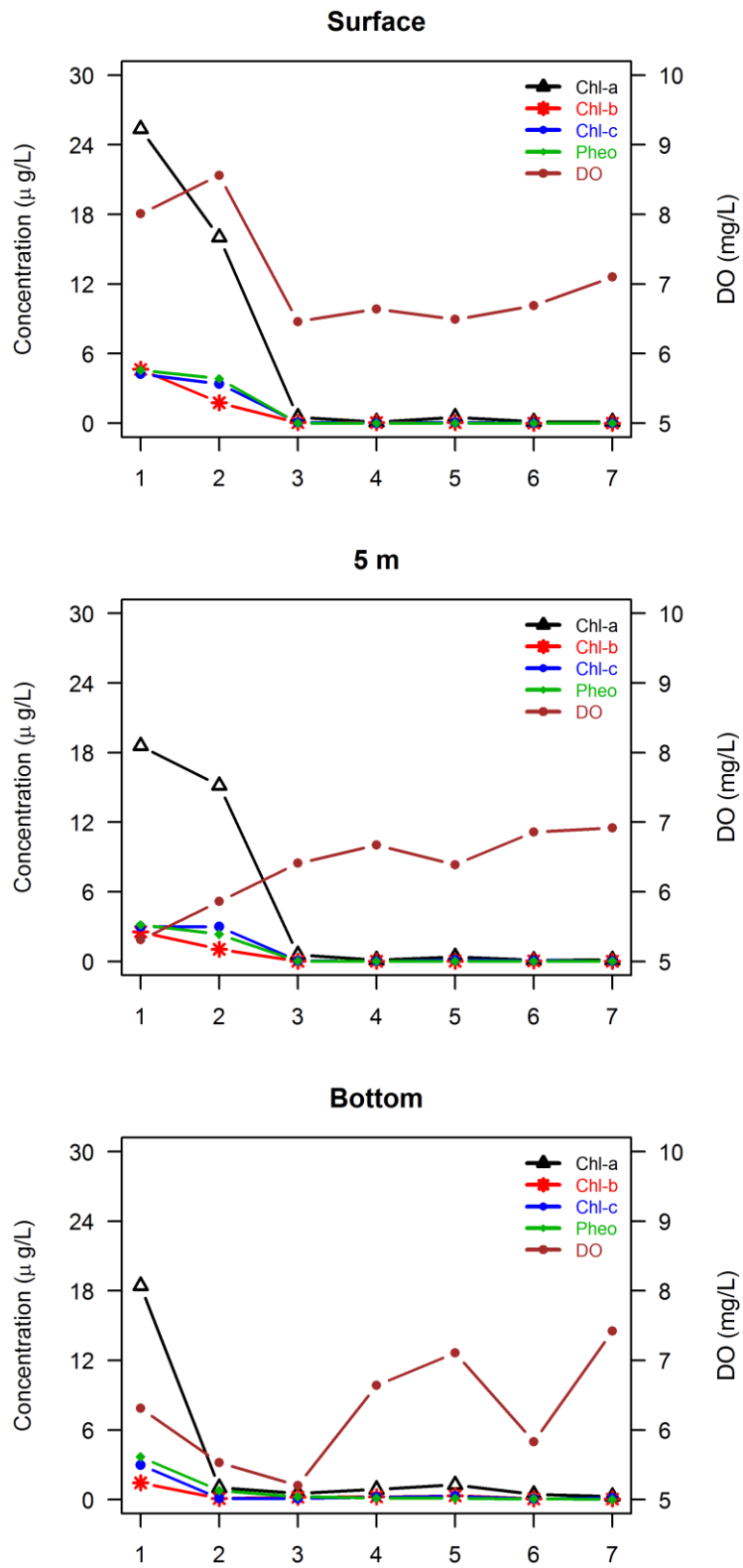


Figure 3.12 Chl-a, Chl-b, Chl-c, Pheophytin and DO profiles of seawater at sampling stations in summer

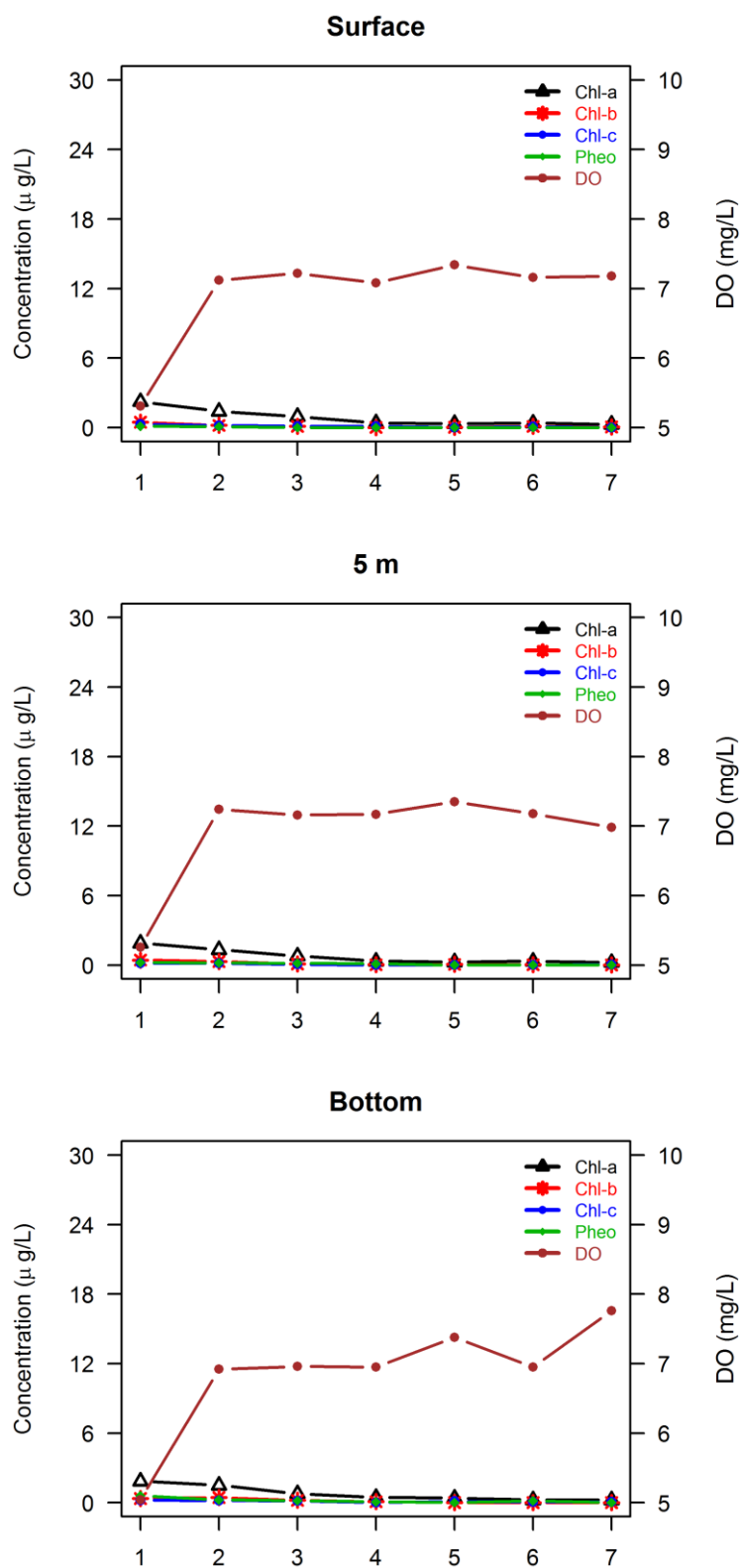


Figure 3.13 Chl-a, Chl-b, Chl-c, Pheophytin and DO profiles of seawater at sampling stations in autumn

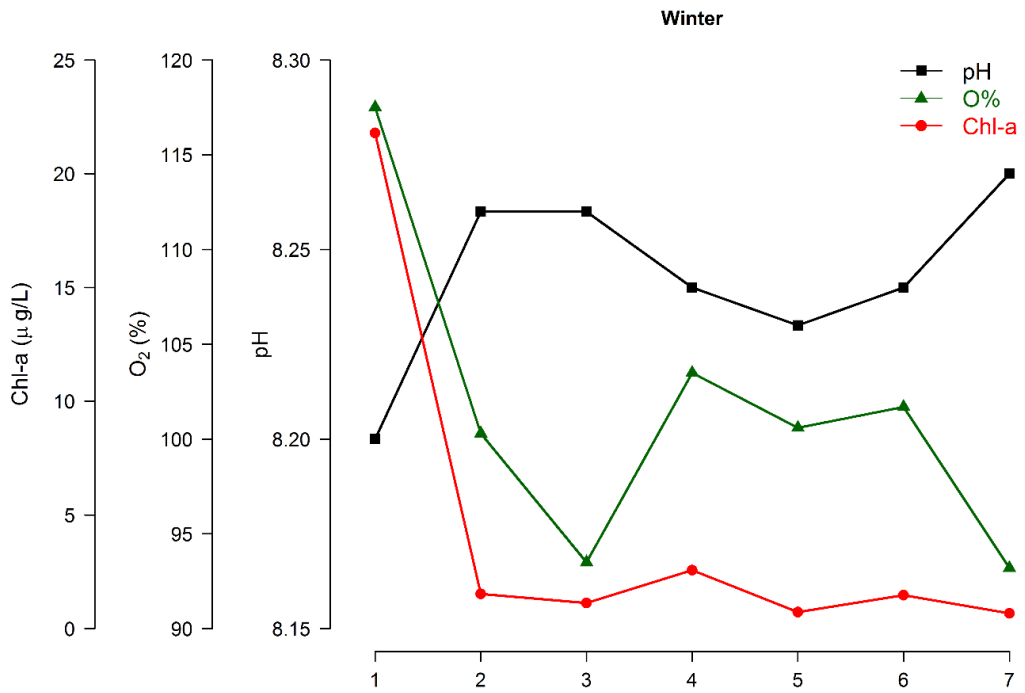


Figure 3.14 pH, O<sub>2</sub>% and Chl-a profiles of seawater at surface waters in winter

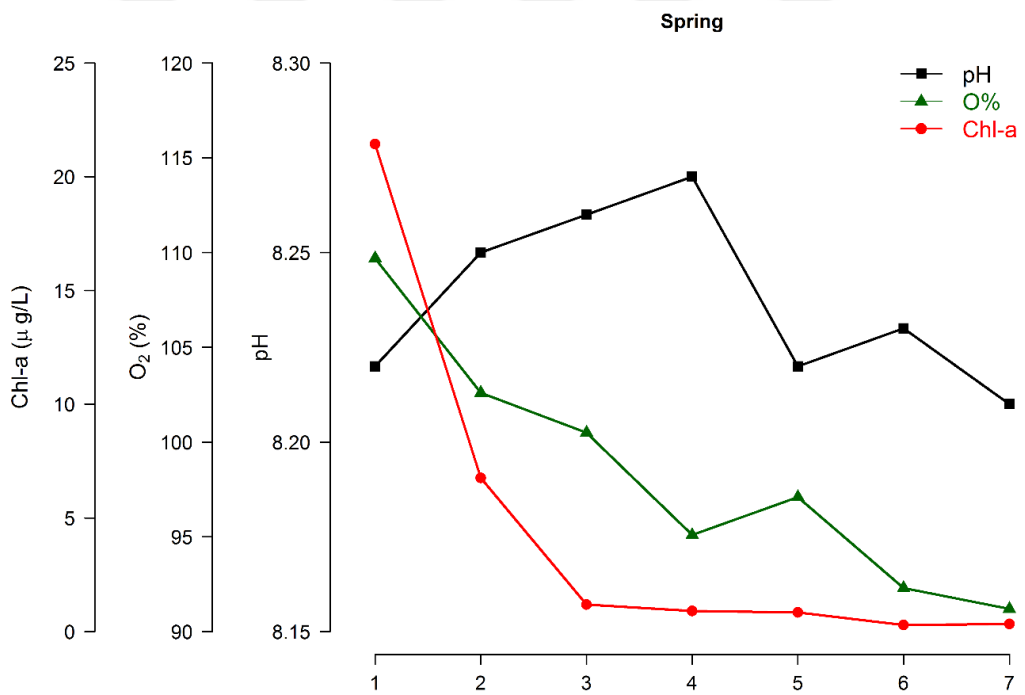


Figure 3.15 pH, O<sub>2</sub>% and Chl-a profiles of seawater at surface waters in spring



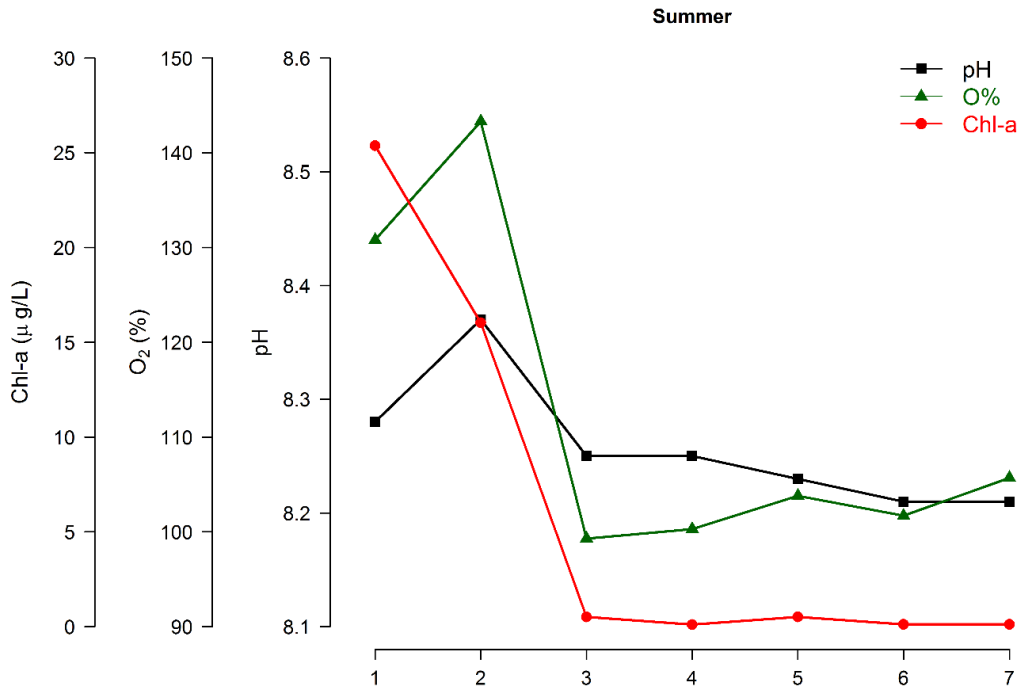


Figure 3.16 pH, O<sub>2</sub>% and Chl-a profiles of seawater at surface waters in summer

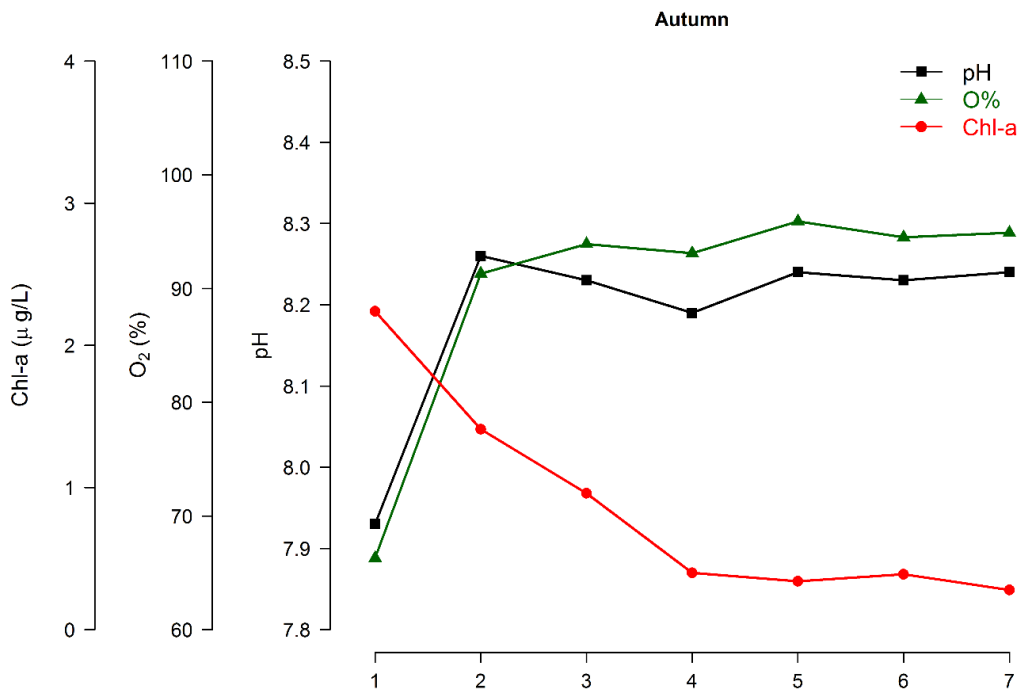


Figure 3.17 pH, O<sub>2</sub>% and Chl-a profiles of seawater at surface waters in autumn

### 3.3 Results of Dissolved Nutrient Analyses

NO<sub>2</sub> concentrations in the bay were between 0.01-3.87 μM in all seasons (Figures 3.18-3.21). Maximum NO<sub>2</sub> concentration was observed at bottom of Station 1 in autumn. In contrast, NO<sub>2</sub> levels were equal to or below detection limit (0.01 μM) in most stations. Among all stations, highest NO<sub>2</sub> levels were observed at Station 1 except for bottom depth of summer season in which highest NO<sub>2</sub> level was detected at Station 3.

NO<sub>3</sub> concentrations in the bay were between 0.03-6.76 μM throughout all seasons (Figures 3.18-3.21). Maximum NO<sub>3</sub> concentration was observed at bottom of Station 1 in autumn. Among all stations, highest NO<sub>3</sub> levels were observed at Station 1 except for bottom depth of summer season in which highest NO<sub>3</sub> level was detected at Station 3.

TNO<sub>x</sub> concentrations in the bay were between 0.10-10.63 μM at all seasons (Figures 3.18-3.21). Maximum TNO<sub>x</sub> concentration was observed at bottom of Station 1 in autumn. Among all stations, highest TNO<sub>x</sub> levels were observed at Station 1 except for bottom depth of summer season in which highest TNO<sub>x</sub> level was detected at Station 3.

NH<sub>4</sub> concentrations in the bay were between 0.10-22.62 μM in all seasons (Figures 3.18-3.21). Maximum NH<sub>4</sub> concentration was observed at bottom of Station 1 in autumn. Highest NH<sub>4</sub> levels were generally observed at Station 1 in most seasons.

DIN concentrations in the bay were between 0.2-33.3 μM at all seasons (Figures 3.22-3.25). Maximum DIN concentration was determined at bottom of Station 1 in autumn. In autumn, DIN concentrations at all depths of Station 1 were found higher compared to other stations.

DON concentrations in the bay were between 0.3-13.7 μM in all seasons (Figures 3.22-3.25). Maximum DON concentrations were found at Station 1 in autumn. DON

concentrations were generally low and highest values were detected at Station 1 almost in all seasons.

DTN concentrations in the bay were between 0.5-45.0  $\mu\text{M}$  throughout all seasons (Figures 3.22-3.25). Maximum DTN concentration was determined at surface of Station 1 in autumn. In autumn, DTN concentrations at all depths of Station 1 were found higher compared to other stations.

PN concentrations in the bay were between 0.1-22.9  $\mu\text{M}$  in all seasons (Figures 3.22-3.25). Maximum PN concentration was determined at surface of Station 2 in summer. In general, PN concentrations at all depths of Station 1 were found higher compared to other stations.

TN concentrations in the bay were between 1.6-58.7  $\mu\text{M}$  in all seasons (Figures 3.22-3.25). Maximum TN concentration was determined at surface of Station 1 in autumn. In general, TN concentrations at all depths of Station 1 were found higher compared to other stations.

DIP concentrations in the bay were between 0.01-3.21  $\mu\text{M}$  in all seasons (Figures 3.26-3.29). Maximum DIP concentration was observed at bottom of Station 1 in summer. Among all stations, highest DIP levels were observed at Station 1 in summer and autumn seasons.

DOP concentrations in the bay were between 0.10-0.65  $\mu\text{M}$  in all seasons (Figures 3.26-3.29). Maximum DOP concentration was observed at surface of Station 2 in summer. Among all stations, highest DOP levels were observed at middle-inner bay stations in summer season.

DTP concentrations in the bay were between 0.16-3.78  $\mu\text{M}$  in all seasons (Figures 3.26-3.29). Maximum DTP concentration was observed at bottom of Station 1 in summer. Among all stations, highest DTP levels were observed at middle-inner bay stations especially in summer and autumn seasons.

PP concentrations in the bay were observed between 0.02-1.46  $\mu\text{M}$  in all seasons (Figures 3.26-3.29). Maximum PP concentration was observed at 5 m of Station 2 in summer. Among all stations, highest PP levels were observed at middle-inner bay stations especially in summer and autumn seasons.

TP concentrations in the bay were observed between 0.24-4.90  $\mu\text{M}$  in all seasons (Figures 3.26-3.29). Maximum TP concentration was observed at bottom of Station 1 in summer. Among all stations, highest TP levels were observed at middle-inner bay stations especially in summer and autumn seasons.



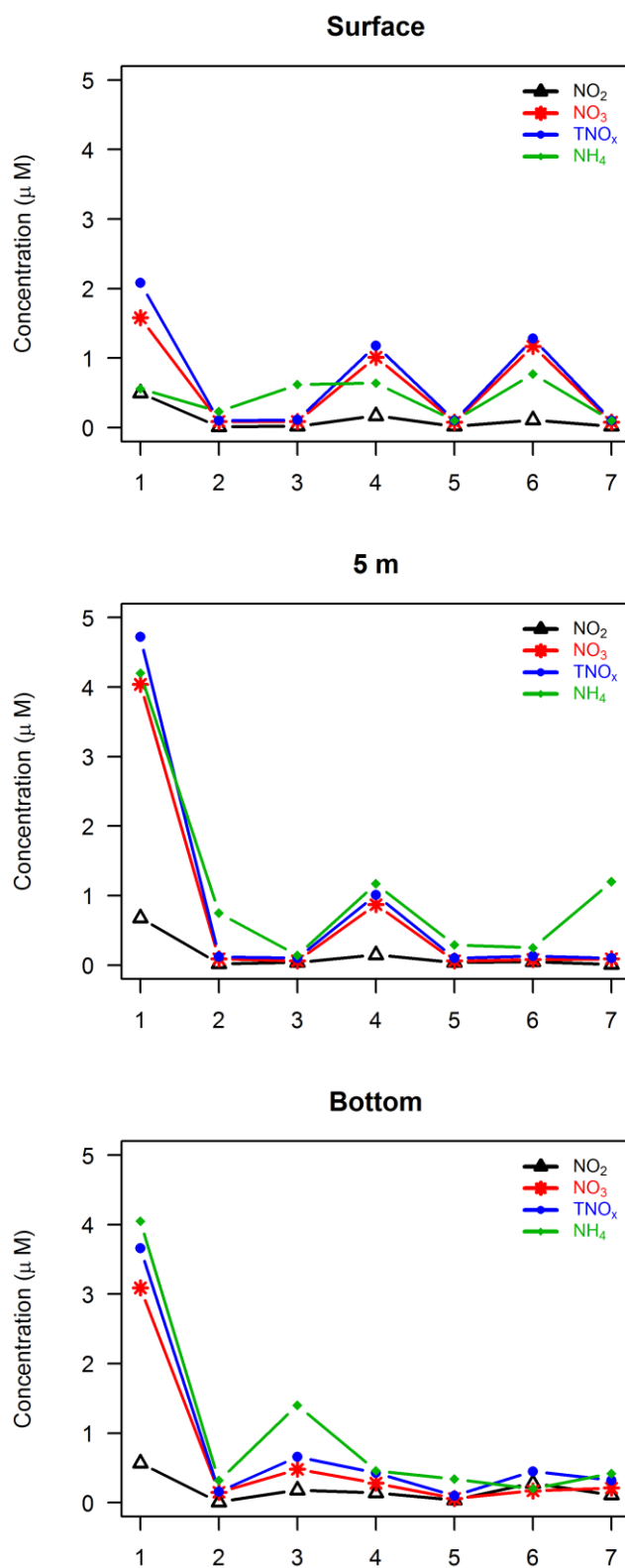


Figure 3.18 NO<sub>2</sub>, NO<sub>3</sub>, TNO<sub>x</sub> and NH<sub>4</sub> profiles of seawater at sampling stations in winter

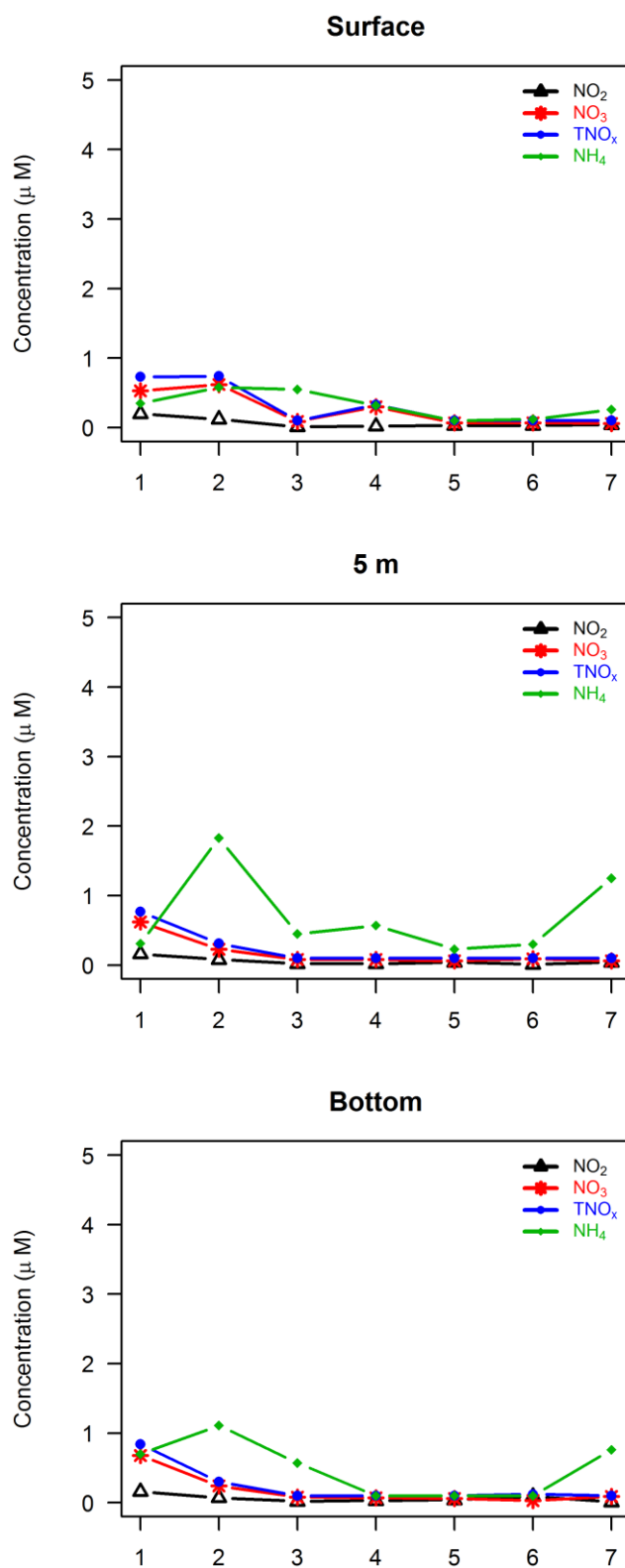


Figure 3.19 NO<sub>2</sub>, NO<sub>3</sub>, TNO<sub>x</sub> and NH<sub>4</sub> profiles of seawater at sampling stations in spring

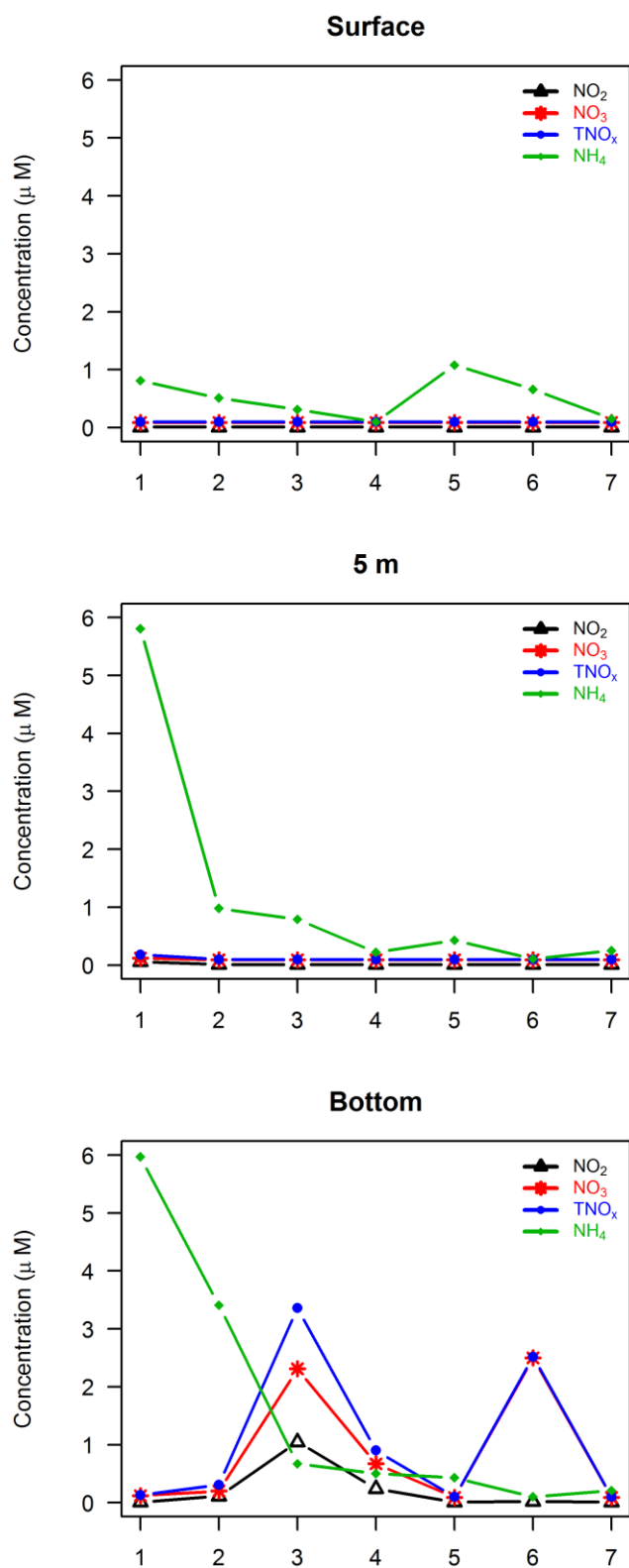


Figure 3.20  $\text{NO}_2$ ,  $\text{NO}_3$ ,  $\text{TNO}_x$  and  $\text{NH}_4$  profiles of seawater at sampling stations in summer

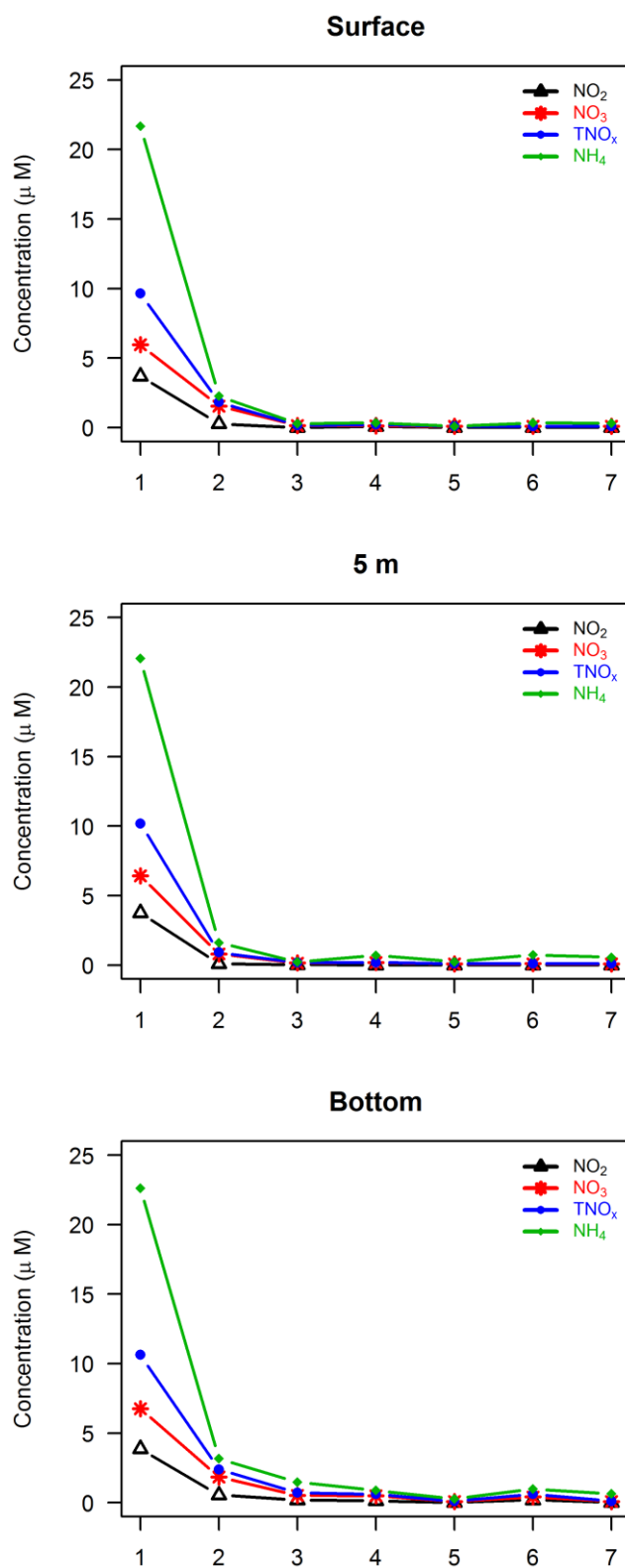


Figure 3.21 NO<sub>2</sub>, NO<sub>3</sub>, TNO<sub>x</sub> and NH<sub>4</sub> profiles of seawater at sampling stations in autumn



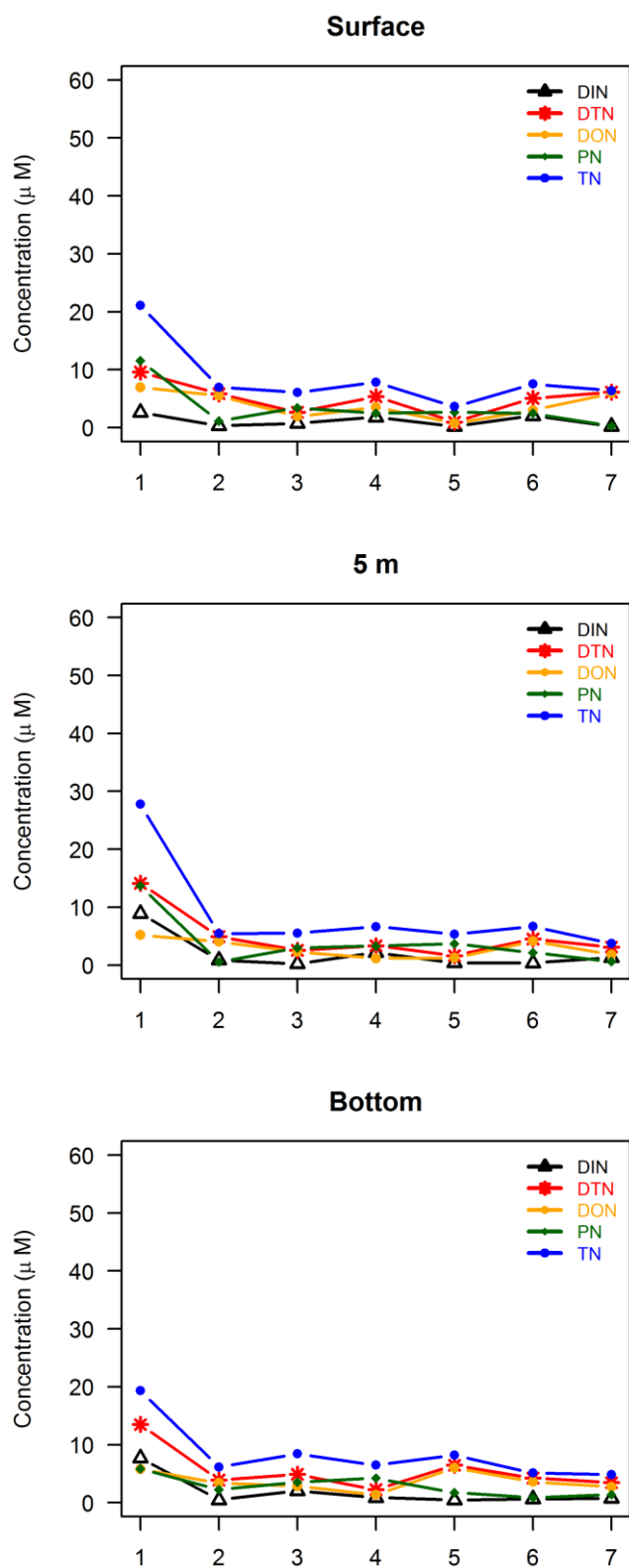


Figure 3.22 DIN, DTN, DON, PN and TN profiles of seawater at sampling stations in winter

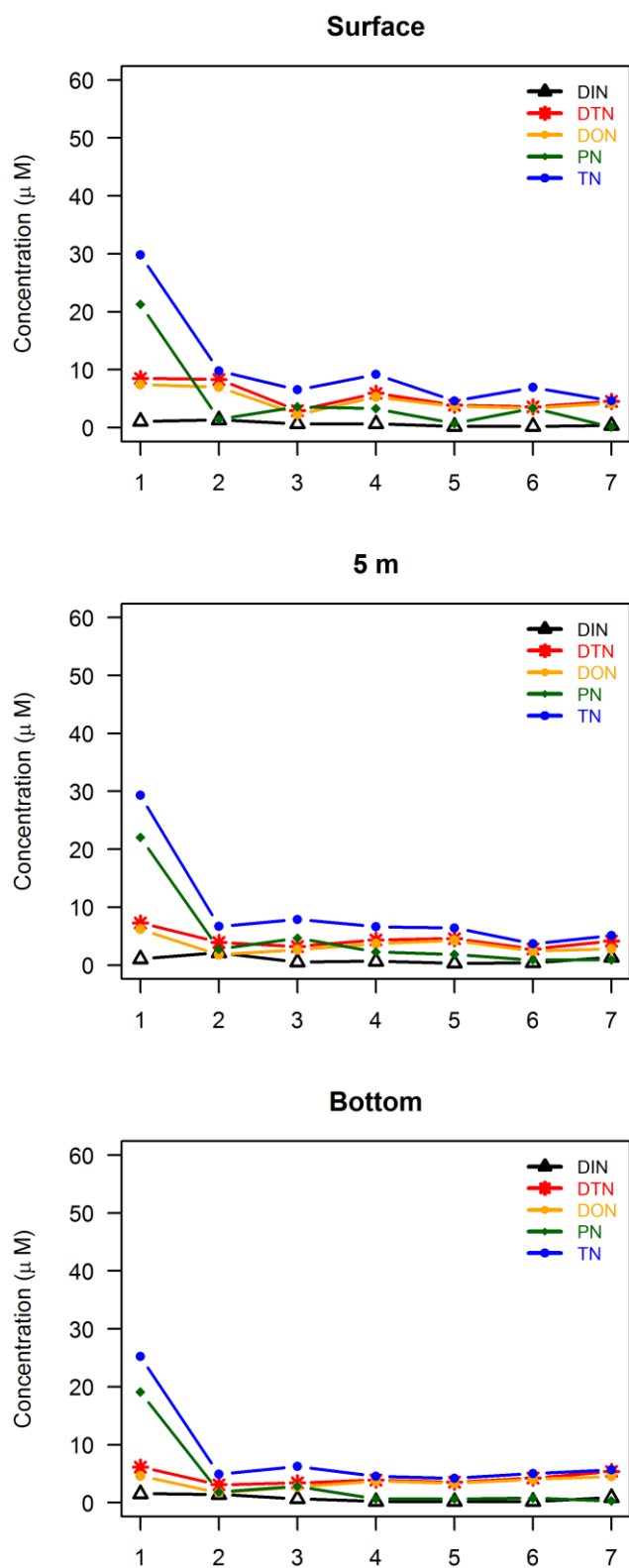


Figure 3.23 DIN, DTN, DON, PN and TN profiles of seawater at sampling stations in spring

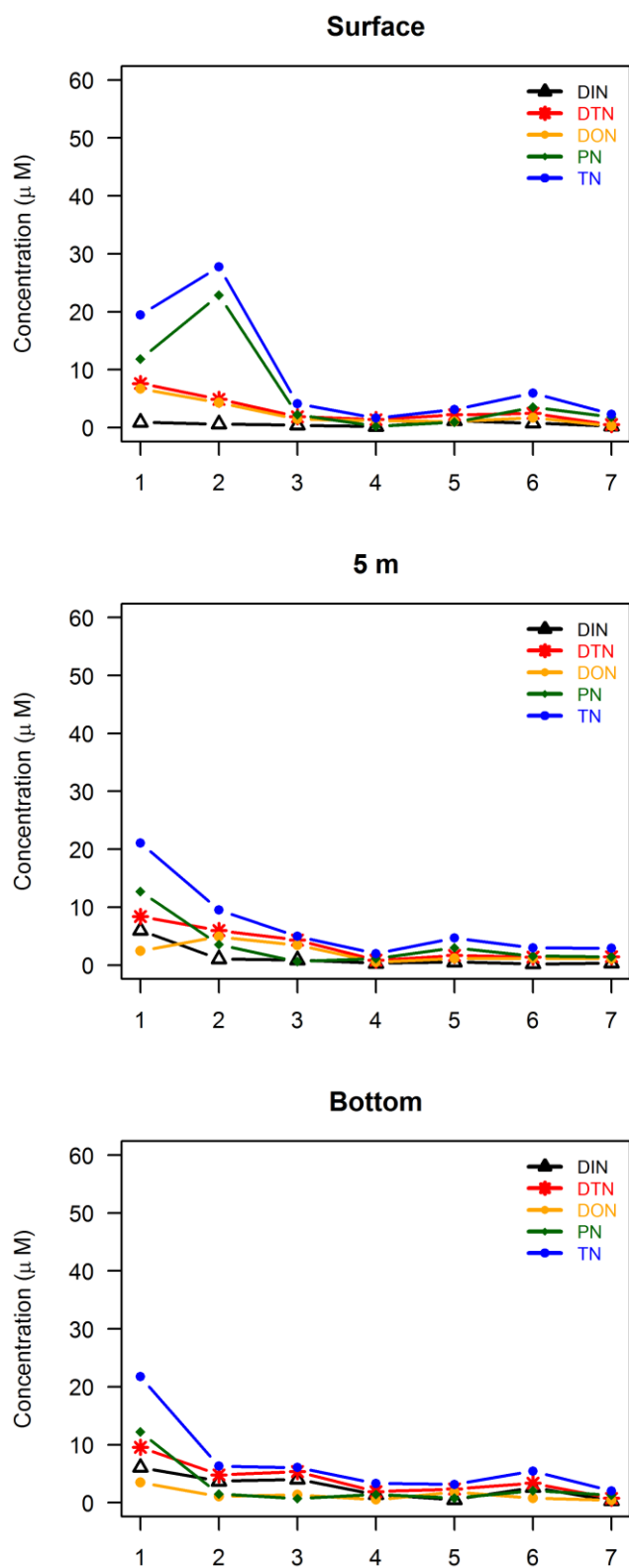


Figure 3.24 DIN, DTN, DON, PN and TN profiles of seawater at sampling stations in summer

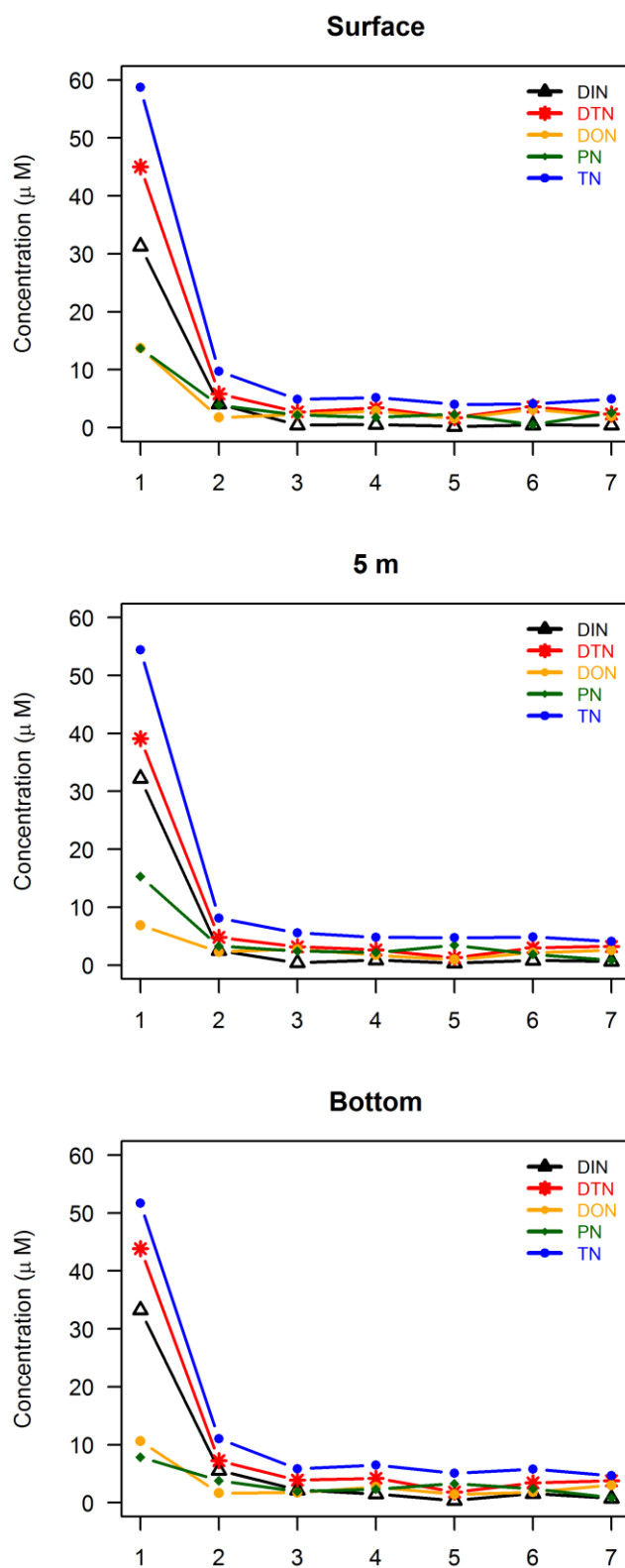


Figure 3.25 DIN, DTN, DON, PN and TN profiles of seawater at sampling stations in autumn

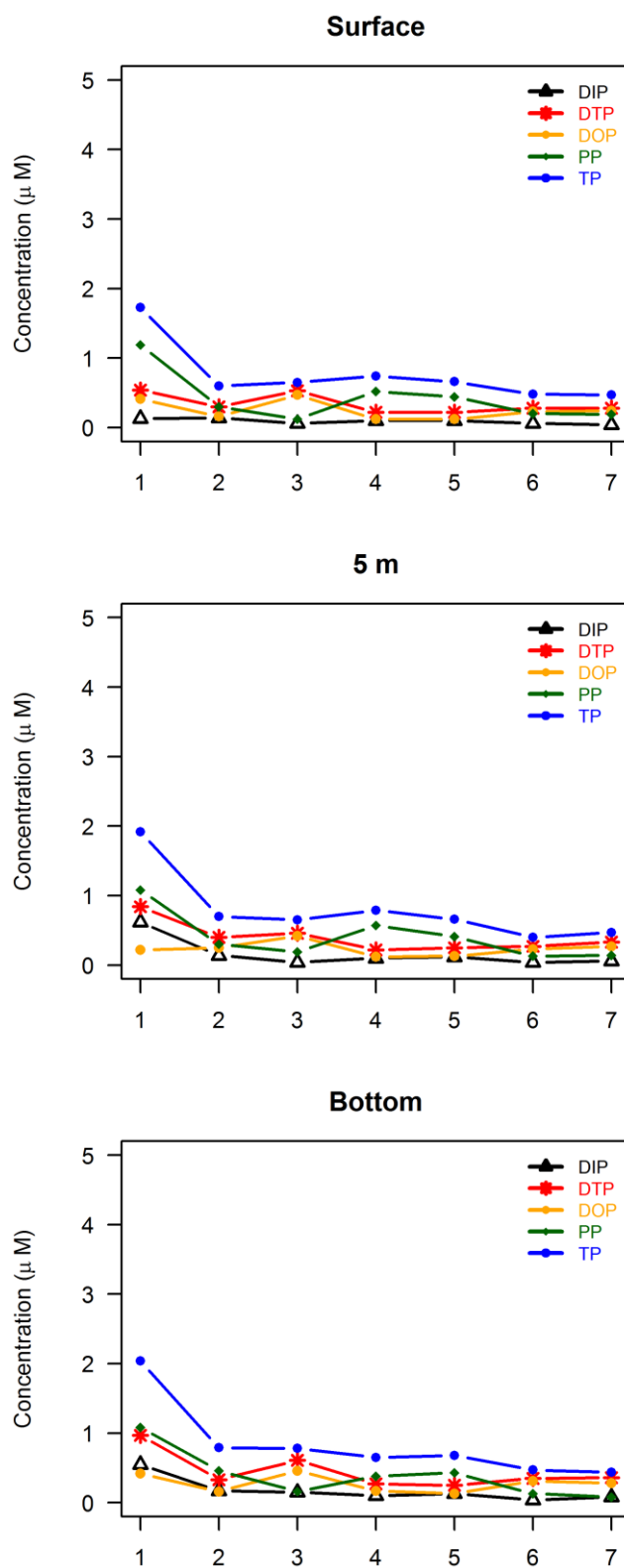


Figure 3.26 DIP, DOP, DTP, PP and TP profiles of seawater at sampling stations in winter

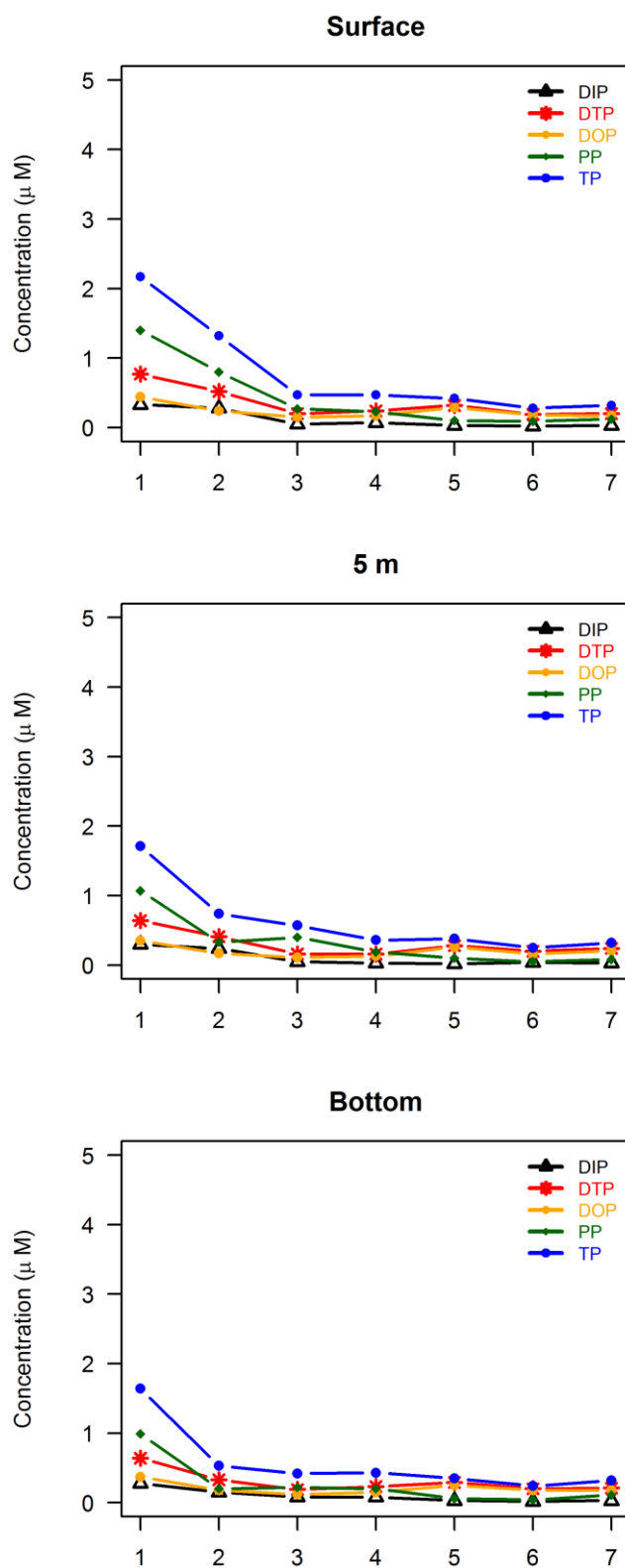


Figure 3.27 DIP, DOP, DTP, PP and TP profiles of seawater at sampling stations in spring

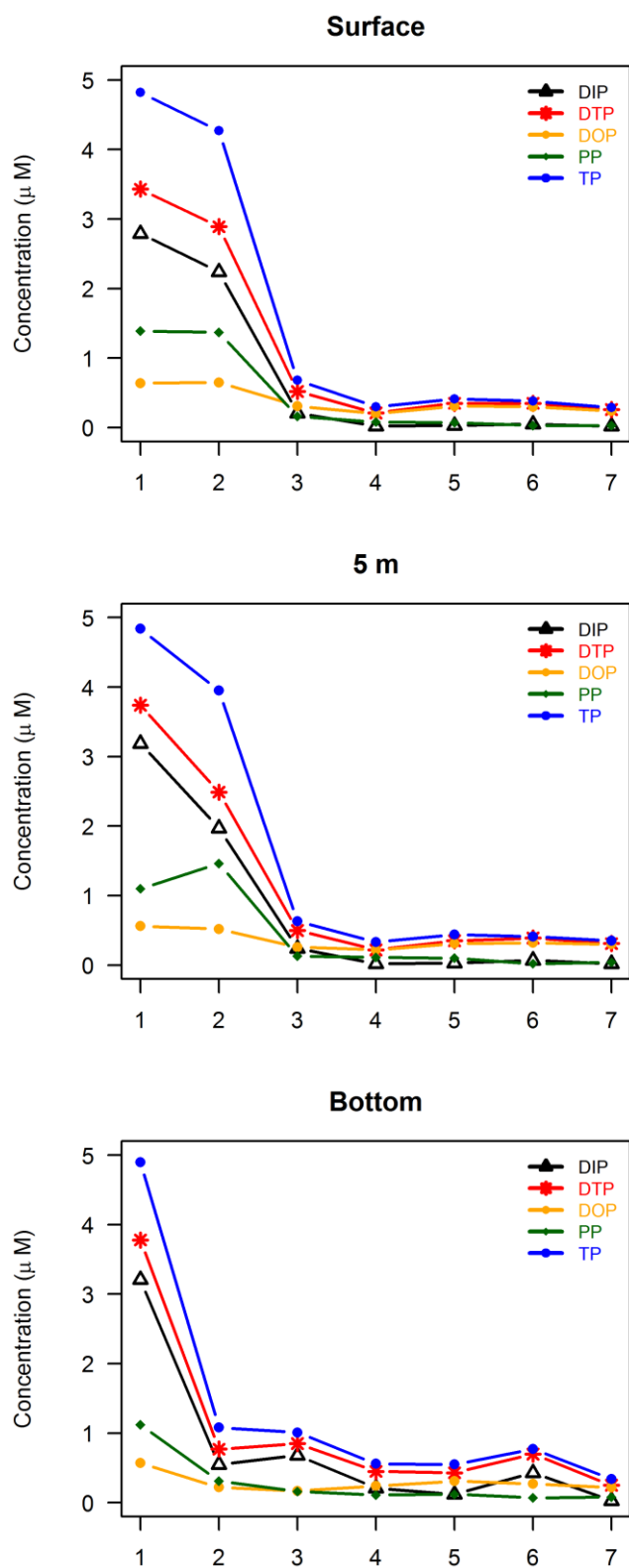


Figure 3.28 DIP, DOP, DTP, PP and TP profiles of seawater at sampling stations in summer

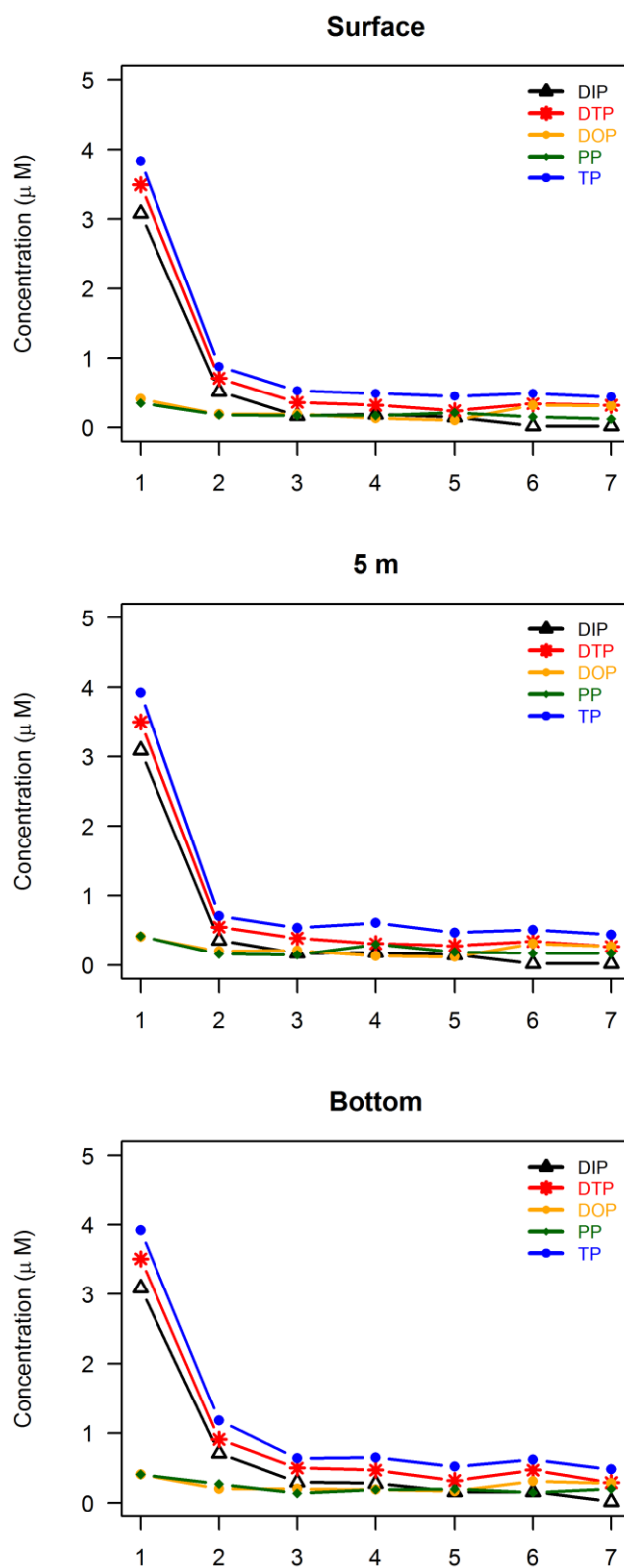


Figure 3.29 DIP, DOP, DTP, PP and TP profiles of seawater at sampling stations in autumn



### **3.4 Results of Dissolved & Total Organic Carbon Analyses**

DOC concentrations in the bay were determined between 32.2–244  $\mu\text{M}$  in all seasons (Figures 3.30-3.33). Maximum DOC concentration was observed at surface of Station 1 in summer. DOC concentrations increased from winter to spring and maximum levels were observed at summer, then decreased slightly at autumn. Highest DOC levels were observed at surface depths and did not change clearly with depth. Among all stations, highest DOC levels were observed at Station 1 in summer and autumn.

POC concentrations in the bay were found between 10-285  $\mu\text{M}$  throughout all seasons (Figures 3.30-3.33). Maximum POC concentration was observed at bottom of Station 1 in summer. POC levels did not change obviously with depth. Among all stations, highest POC levels were observed at Station 1 and 2 in spring and summer.

TOC concentrations in the bay were observed between 37–493  $\mu\text{M}$  at all seasons (Figures 3.30-3.33). Maximum TOC concentration was observed at bottom of Station 1 in summer. TOC levels did not change with depth. Among all stations, highest TOC levels were observed at Station 1 and 2 in spring and summer.

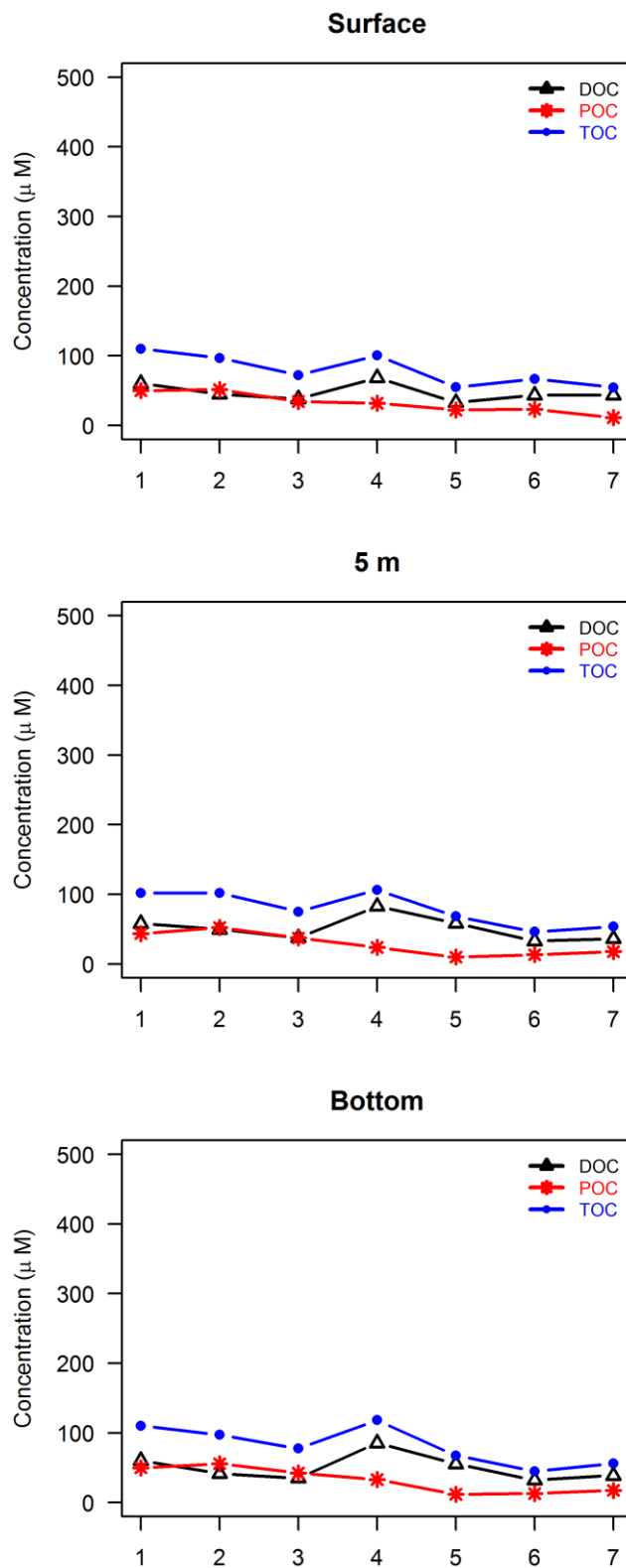


Figure 3.30 DOC, POC and TOC profiles of seawater at sampling stations in winter

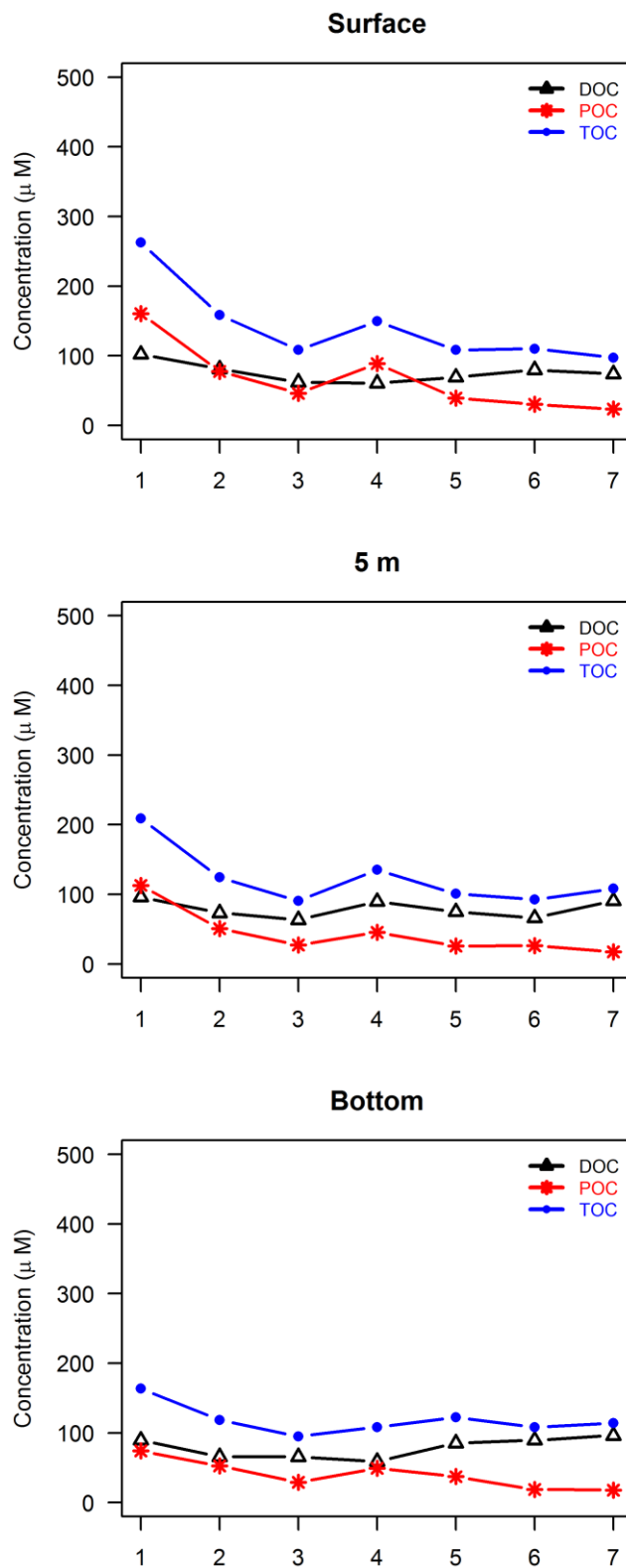


Figure 3.31 DOC, POC and TOC profiles of seawater at sampling stations in spring

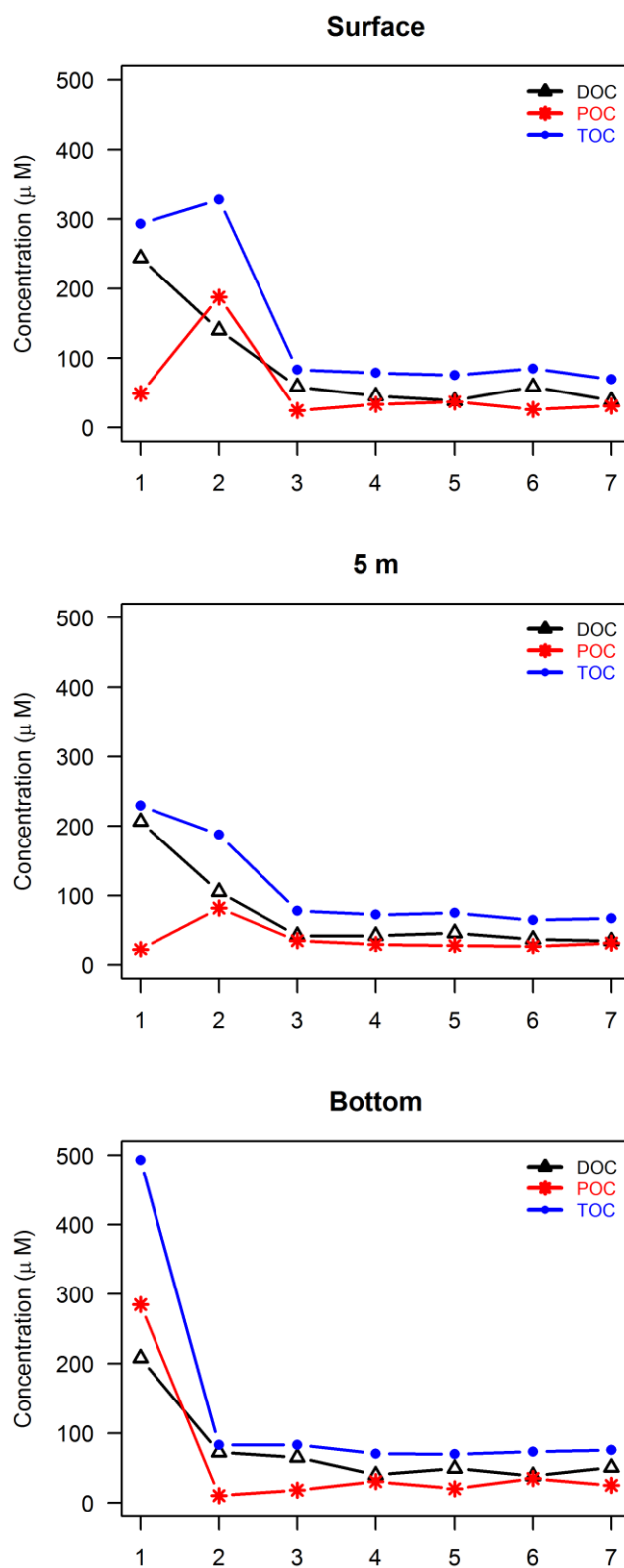


Figure 3.32 DOC, POC and TOC profiles of seawater at sampling stations in summer

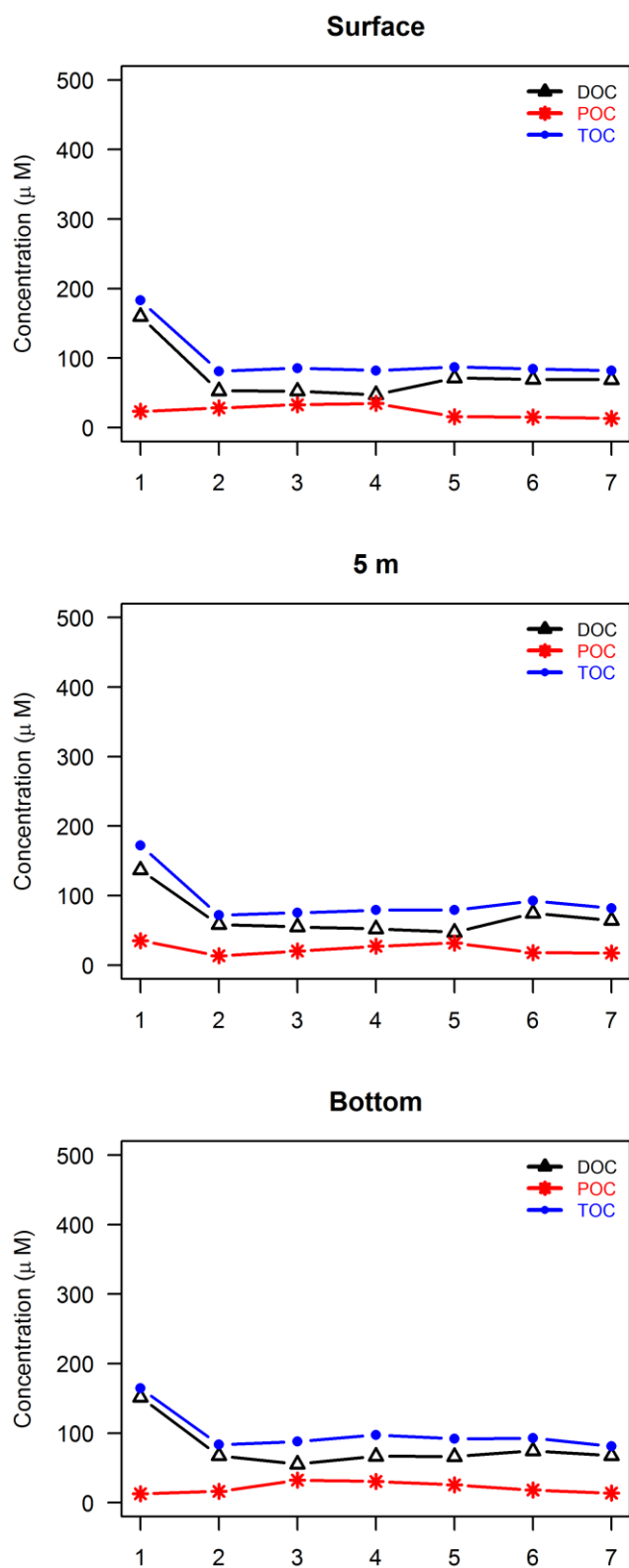


Figure 3.33 DOC, POC and TOC profiles of seawater at sampling stations in autumn

### **3.5 Results of Eutrophication Level Determination by TRIX and UNTRIX Indexes**

TRIX values were ranged between 1.21 and 6.75 throughout the bay (Figures 3.34-3.35). In middle-inner bay, TRIX values were between 2.55 and 6.75, whereas in outer bay, TRIX values were observed between 1.21 and 4.98. According to TRIX limit values for coastal waters in Turkey (Table 2.1), mean and median TRIX values at middle-inner bays were below eutrophication limit of 6 at winter, spring and autumn seasons. However, in summer, mean and median TRIX values at middle-inner bays were higher than 6. In outer bay, mean and median TRIX values at all seasons were below high eutrophication risk limit of 4.

UNTRIX values were found between -0.04 and 6.60 throughout the bay (Figures 3.34-3.35). In middle-inner bay, UNTRIX values were between 1.57 and 6.60, whereas in outer bay, UNTRIX values were observed between -0.04 and 4.47. According to UNTRIX limit values, mean UNTRIX values at middle-inner bays were found within high quality limits at all seasons. Median UNTRIX values were only found within good quality limit in summer season. In outer bay, both mean and median UNTRIX values were determined within high quality limits at all seasons.

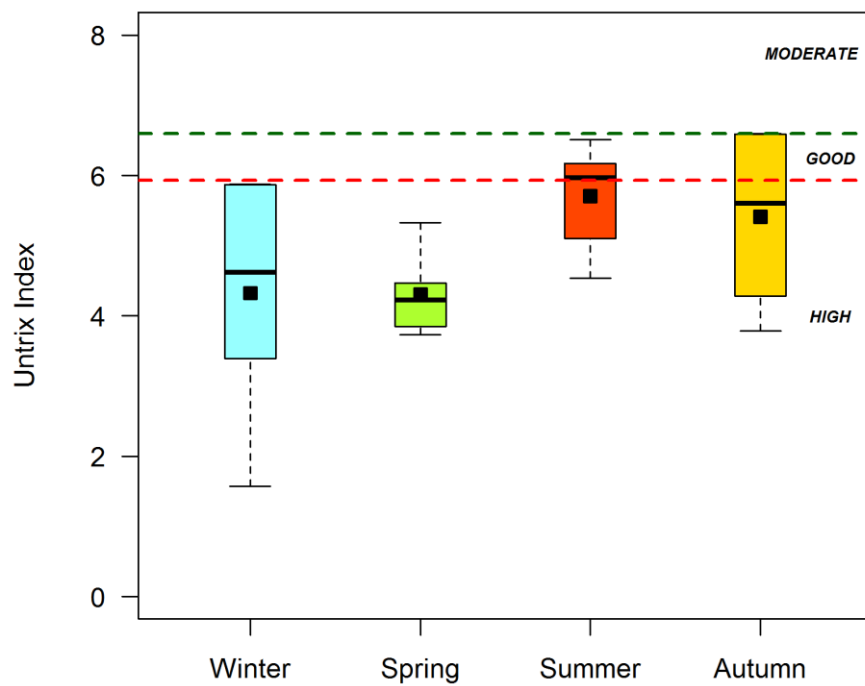
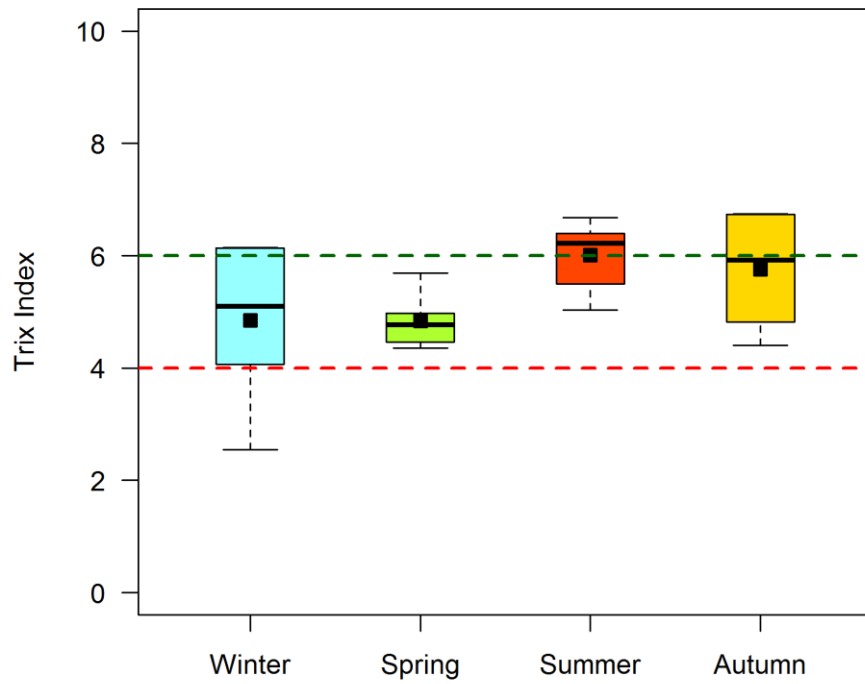


Figure 3.34 Seasonal TRIX and UNTRIX profiles at Middle-Inner Parts of the İzmir Bay

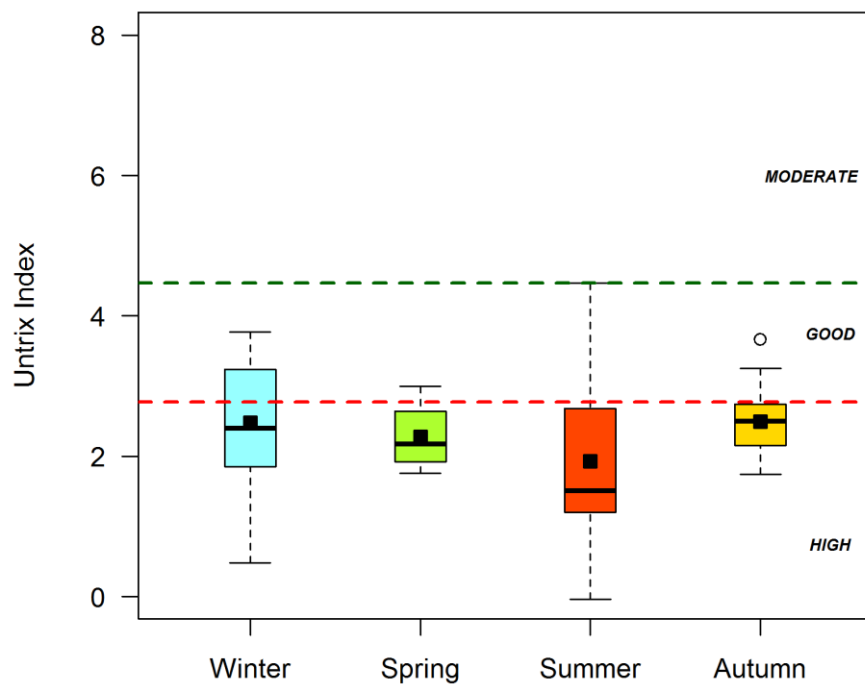
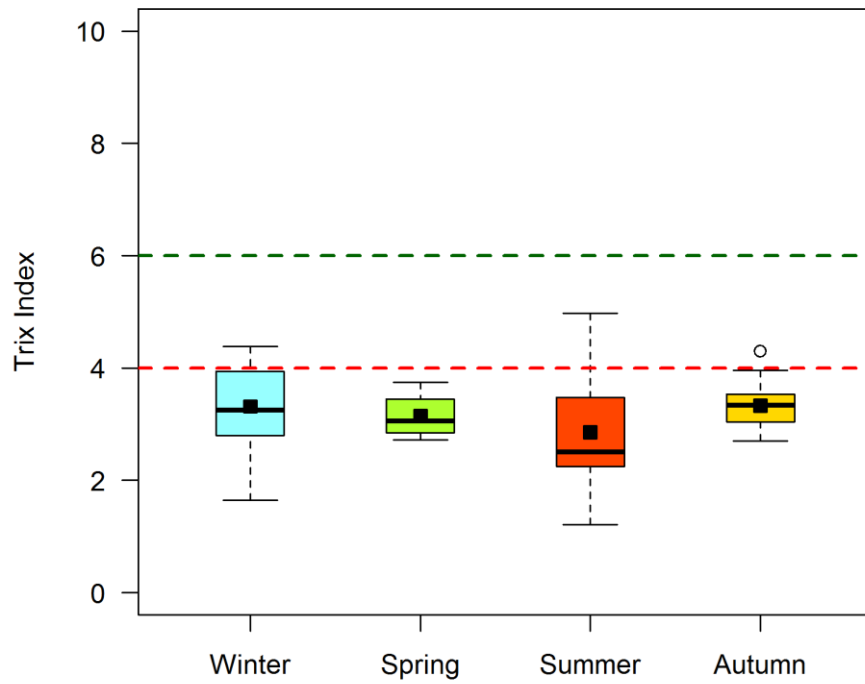


Figure 3.35 Seasonal TRIX and UNTRIX profiles at Outer Part of the İzmir Bay



### 3.6 Elemental C/N/P Ratios

Seasonal variations of dissolved, dissolved total and total (dissolved+particulate) N/P ratios are given at Table 3.1. Dissolved inorganic N/P (DIN/DIP) ratios changed between 2-10 at middle-inner and 11-15 at outer bay stations. Dissolved total N/P (DTN/DTP) ratios ranged between 3-15 at middle-inner and 5-19 at outer bay stations. Highest ratios for dissolved and dissolved total N/P ratios observed at winter for middle-inner bays and at spring for outer bay. Total N/P (TN/TP) ratios changed between 5-12 at middle-inner and 8-16 at outer bay stations. Highest ratios for total N/P ratios observed at spring throughout the bay. Lowest ratios were determined at summer for all N/P forms.

Seasonal variations of C/N/P ratios in dissolved and particulate matter are given at Table 3.2. DOC/DON/DOP ratios ranged between 214/21/1-334/18/1 at middle-inner bay and 182/5/1-439/20/1 at outer bay. Highest DOC/DOP ratios observed at spring season throughout the bay. DON/DOP ratios found between 7-21 at middle-inner bay and 5-20 at outer bay. Highest DON/DOP ratios determined at winter for middle-inner and at spring for outer bay. Particulate POC/PP ratios ranged between 81-134 at middle-inner bay and 117-502 at outer bay. Highest POC/PP ratios at particulate matter for middle-inner bays found at spring and lowest POC/PP ratios observed at autumn. Highest POC/PP ratios for outer bay observed at summer and lowest POC/PP ratios determined at winter. PN/PP ratios for particulate matter changed between 6-25 at middle-inner bay and 11-29 at outer bay.

Table 3.1 Seasonal variations of dissolved, dissolved total and total N/P ratios

<b>Season</b>	<b>Bay Area</b>	<b>N/P</b>	<b>N/P</b>	<b>N/P</b>
		<b>(DIN/DIP)</b>	<b>(DTN/DTP)</b>	<b>(TN/TP)</b>
<b>Winter</b>	Middle-Inner	10	15	11
	Outer	12	13	11
<b>Spring</b>	Middle-Inner	6	11	12
	Outer	15	19	16
<b>Summer</b>	Middle-Inner	2	3	5
	Outer	11	5	8
<b>Autumn</b>	Middle-Inner	9	10	12
	Outer	13	9	10

Table 3.2 Seasonal variations of C/N/P ratios in dissolved and particulate matter

<b>Season</b>	<b>Bay Area</b>	<b>C/N/P</b>	<b>C/N/P</b>
		<b>(DOC/DON/DOP)</b>	<b>(POC/PN/PP)</b>
<b>Winter</b>	Mid-Inner	214 / 21 / 1	99 / 6 / 1
	Outer	268 / 14 / 1	117 / 11 / 1
<b>Spring</b>	Mid-Inner	313 / 16 / 1	134 / 12 / 1
	Outer	439 / 20 / 1	292 / 13 / 1
<b>Summer</b>	Mid-Inner	312 / 7 / 1	89 / 9 / 1
	Outer	182 / 5 / 1	502 / 29 / 1
<b>Autumn</b>	Mid-Inner	334 / 18 / 1	81 / 25 / 1
	Outer	324 / 11 / 1	132 / 12 / 1

## 3.7 Results of Carbohydrate Analyses

### 3.7.1 Seasonal Variations

Seasonal and vertical salinity, Chl-a, DOC, MCHO, TDCHO and PCHO levels were given in Table 3.3. According to One Way ANOVA test results, there were no significant vertical changes for salinity, Chl-a, DOC, MCHO, TDCHO and PCHO ( $p < 0.05$ ). Seawater salinity was found between 36.9–40.8 ‰ in all seasons. Salinity was remarkably higher in summer at middle-inner and outer bays ( $p < 0.05$ , Table 3.4). Salinity was nearly constant with increasing depth.

MCHO levels were found between 0.7–8.3  $\mu\text{M}$  (1.3–8.3  $\mu\text{M}$  for middle-inner bay, 0.7–5.6  $\mu\text{M}$  for outer bay) and maximum MCHO levels were observed in spring. MCHO levels were increased from winter to spring and decreased to minimum levels in autumn. Seasonal changes of MCHO levels were significant at middle-inner and outer bays ( $p < 0.05$ , Table 3.4).

PCHO levels were found between 0.7–19.5  $\mu\text{M}$  (0.7–19.5  $\mu\text{M}$  for middle-inner bay, 1.8–10.8  $\mu\text{M}$  for outer bay). PCHO levels were decreased from winter to autumn and highest PCHO concentrations were observed at surface waters. Seasonal variations of PCHO levels were significant at middle-inner and outer bays ( $p < 0.05$ , Table 3.4).

TDCHO concentrations were ranged between 2.6–14.4  $\mu\text{M}$  and 3.6–24.6  $\mu\text{M}$  at outer and middle-inner bays, respectively. Similar to PCHO, TDCHO levels were decreased from winter to autumn. Seasonal changes of TDCHO levels were significant at middle-inner and outer bays ( $p < 0.05$ , Table 3.4).

Seasonal and vertical MCHO/TDCHO, PCHO/TDCHO, MCHO/DOC, PCHO/DOC, TDCHO/DOC and PCHO/MCHO ratios were given in Table 3.5. MCHO/DOC, PCHO/DOC and TDCHO/DOC ratios showed significant decreasing trends from winter to summer-autumn seasons ( $p < 0.05$ ). Maximum MCHO/DOC ratio was found as 11% at outer bay. Maximum PCHO/DOC (34%) and TDCHO/DOC

(42%) ratios were observed at middle-inner bays. TDCHO/DOC ratios for middle-inner and outer bays were in the range of 2.5-42.3% ( $\bar{x}$ =15.6,  $s^2$ =129.2) and 4.4-37.1% ( $\bar{x}$ =13.1,  $s^2$ =72.9), respectively. MCHO/TDCHO ratios were increased from winter to autumn, especially at middle-inner bays, and MCHO comprised up to 85% of TDCHO in autumn. MCHO/TDCHO ratios observed between 21-42% in winter, spring and summer. PCHO/TDCHO ratios were lower at middle-inner bays compared to outer bay in autumn. PCHO/MCHO ratio was significantly lower at autumn compared to other seasons at middle-inner bays ( $p < 0.05$ , Table 3.4). PCHO/MCHO ratios did not change significantly at outer bay ( $p < 0.05$ ).

Table 3.3 Seasonal variations of MCHO, PCHO and TDCHO in the water column of the İzmir Bay (n=7 for each range)

Season/Depth	MCHO ( $\mu$ M)	PCHO ( $\mu$ M)	TDCHO ( $\mu$ M)
<i>Winter</i>			
Surface	2.6–6.2	5.2–15.3	8.1–21.5
Subsurface	2.1–5.1	5.2–19.5	7.9–24.6
Bottom	1.5–5.6	6.1–13.0	8.6–18.6
<i>Spring</i>			
Surface	2.2–7.0	5.0–12.6	7.3–19.5
Subsurface	2.1–8.3	4.7–11.5	6.9–19.8
Bottom	1.9–4.8	4.5–12.8	6.5–17.6
<i>Summer</i>			
Surface	0.7–5.4	2.4–13.3	3.4–18.7
Subsurface	0.7–5.4	1.9–8.9	3.0–14.3
Bottom	0.7–4.9	1.8–9.2	2.6–14.2
<i>Autumn</i>			
Surface	1.0–2.7	1.3–3.0	3.2–4.2
Subsurface	0.7–3.4	0.7–2.8	2.8–4.0
Bottom	0.7–3.6	0.7–3.7	3.5–4.8

Table 3.4 Results of One Way ANOVA tests for seasonal changes of salinity, Chl-a, DOC, MCHO, TDCHO and PCHO (Values represent Mean±SD; n=6 for inner bay; n=15 for outer bay; p<0.05)

	<i>Winter</i>	<i>Spring</i>	<i>Summer</i>	<i>Autumn</i>
<b><u>Middle-Inner Bays</u></b>				
Salinity (‰)	38.4±0.4 <sup>b</sup>	38.0±0.4 <sup>b</sup>	40.0±0.6 <sup>a</sup>	38.3±0.5 <sup>b</sup>
Chl-a (µg/L)	8.5±8.1 <sup>ab</sup>	11.0±8.2 <sup>ab</sup>	15.8±8.1 <sup>a</sup>	1.7±0.4 <sup>b</sup>
DOC (µM)	52.5±8.2 <sup>c</sup>	84.7±13.8 <sup>bc</sup>	163.0±67.1 <sup>a</sup>	104.5±50.0 <sup>b</sup>
MCHO (µM)	4.5±1.2 <sup>ab</sup>	5.1±2.3 <sup>a</sup>	4.0±1.6 <sup>ab</sup>	2.5±0.9 <sup>b</sup>
PCHO (µM)	12.4±4.4 <sup>a</sup>	10.4±2.3 <sup>a</sup>	8.6±3.1 <sup>a</sup>	1.7±1.0 <sup>b</sup>
TDCHO (µM)	17.0±5.4 <sup>a</sup>	15.4±4.3 <sup>a</sup>	12.6±4.5 <sup>a</sup>	4.0±0.4 <sup>b</sup>
MCHO/DOC (%)	8.6±1.2 <sup>a</sup>	5.8±1.8 <sup>b</sup>	2.4±0.4 <sup>c</sup>	2.5±0.5 <sup>c</sup>
PCHO/DOC (%)	23.4±6.0 <sup>a</sup>	12.2±1.2 <sup>b</sup>	5.5±1.0 <sup>c</sup>	2.2±1.9 <sup>c</sup>
TDCHO/DOC (%)	31.9±6.6 <sup>a</sup>	17.9±2.4 <sup>b</sup>	7.9±1.2 <sup>c</sup>	4.8±2.2 <sup>c</sup>
MCHO/TDCHO (%)	27.4±4.4 <sup>a</sup>	31.7±6.7 <sup>b</sup>	30.9±4.9 <sup>b</sup>	60.3±21.0 <sup>b</sup>
PCHO/TDCHO (%)	72.6±4.4 <sup>a</sup>	68.3±6.7 <sup>a</sup>	69.1±4.9 <sup>a</sup>	39.7±21.0 <sup>b</sup>
PCHO/MCHO	2.7±0.6 <sup>a</sup>	2.3±0.7 <sup>a</sup>	2.3±0.6 <sup>a</sup>	0.9±0.7 <sup>b</sup>
<b><u>Outer Bay</u></b>				
Salinity (‰)	38.7±0.5 <sup>b</sup>	38.9±0.3 <sup>b</sup>	39.3±1.0 <sup>a</sup>	38.7±0.3 <sup>b</sup>
Chl-a (µg/L)	1.1±0.7 <sup>a</sup>	0.7±0.4 <sup>b</sup>	0.4±0.3 <sup>b</sup>	0.4±0.2 <sup>b</sup>
DOC (µM)	48.1±18.0 <sup>c</sup>	75.1±12.6 <sup>a</sup>	46.0±9.0 <sup>c</sup>	62.3±9.6 <sup>b</sup>
MCHO (µM)	2.9±0.6 <sup>a</sup>	3.2±1.2 <sup>a</sup>	0.9±0.2 <sup>b</sup>	1.2±0.4 <sup>b</sup>
PCHO (µM)	7.5±1.5 <sup>a</sup>	7.0±2.1 <sup>a</sup>	2.7±0.7 <sup>b</sup>	2.6±0.6 <sup>b</sup>
TDCHO (µM)	10.4±1.7 <sup>a</sup>	10.2±2.7 <sup>a</sup>	3.6±0.8 <sup>b</sup>	3.8±0.5 <sup>b</sup>
MCHO/DOC (%)	6.6±1.9 <sup>a</sup>	4.4±2.0 <sup>b</sup>	2.0±0.5 <sup>c</sup>	2.0±0.8 <sup>c</sup>
PCHO/DOC (%)	17.5±6.8 <sup>a</sup>	9.7±3.6 <sup>b</sup>	6.0±1.5 <sup>c</sup>	4.3±0.6 <sup>c</sup>
TDCHO/DOC (%)	24.1±8.2 <sup>a</sup>	14.1±5.0 <sup>b</sup>	8.0±1.8 <sup>c</sup>	6.3±1.2 <sup>c</sup>
MCHO/TDCHO (%)	28.7±6.1 <sup>ab</sup>	31.2±7.2 <sup>ab</sup>	25.3±5.1 <sup>b</sup>	31.6±7.3 <sup>a</sup>
PCHO/TDCHO (%)	71.3±6.1 <sup>ab</sup>	68.8±7.2 <sup>ab</sup>	74.7±5.1 <sup>a</sup>	68.4±7.3 <sup>b</sup>
PCHO/MCHO	2.7±1.0	2.4±1.0	3.1±0.8	2.4±0.9

Table 3.5 Seasonal variations for MCHO/TDCHO, PCHO/TDCHO, MCHO/DOC, PCHO/DOC and TDCHO/DOC ratios in the water column of İzmir Bay (n=7)

Season/Depth	MCHO/TDCHO(%)			PCHO/TDCHO(%)			MCHO/DOC(%)			PCHO/DOC(%)			TDCHO/DOC(%)		
	Outer Bay	Middle- Inner Bay	Outer Bay	Middle- Inner Bay	Outer Bay	Middle- Inner Bay	Outer Bay	Middle- Inner Bay	Outer Bay	Middle- Inner Bay	Outer Bay	Middle- Inner Bay	Outer Bay	Middle- Inner Bay	
<b>Winter</b>															
Surface	23-39	26-29	61-77	71-74	5-11	7-10	8-26	20-26	12-37	27-36					
Subsurface	23-39	21-33	61-77	67-79	4-9	8-9	6-25	16-34	10-33	23-42					
Bottom	15-33	26-30	67-85	70-74	4-8	8-9	9-28	22-24	13-32	31-32					
<b>Spring</b>															
Surface	20-39	34-36	61-80	64-66	3-9	6-7	6-14	12.0-12.3	9-23	18-19					
Subsurface	18-41	28-42	59-82	58-72	3-9	4-9	6-14	11-12	10-23	15-21					
Bottom	26-39	24-27	61-74	73-76	2-5	4-5	5-15	12-14	7-20	15-20					
<b>Summer</b>															
Surface	17-32	28.8-28.9	68-83	71.1-71.2	1-3	2-3	4-7	6-7	6-9	8-9					
Subsurface	19-35	31-38	65-81	62-69	2-3	2.6-2.9	6-10	4-7	8-13	7-9					
Bottom	24-29	24-35	71-76	65-76	1-2	1.7-2.4	4-7	4-6	5-9	6.8-7.2					
<b>Autumn</b>															
Surface	25-42	46-67	58-75	33-54	2-4	2-3	3.7-5.0	0.8-3.7	6-9	3-7					
Subsurface	24-41	46-83	59-76	17-54	1-3	2.5-2.9	3.3-4.8	0.5-3.3	4-8	3-6					
Bottom	19-38	35-85	63-81	15-65	1-3	2.4-2.5	3.8-5.3	0.4-4.7	5-8	3-7					

### 3.7.2 Spatial Distribution

Spatial and vertical distributions of MCHO, PCHO, TDCHO and DOC were given in Figures 3.36-3.39. Carbohydrate concentrations did not change significantly with depth. In summer, all carbohydrate species at stations 1 and 2 (especially at surface and subsurface) were remarkably higher than outer bay stations. Also, MCHO, PCHO and TDCHO levels at station 1 were higher than other stations at all seasons, except for autumn.

### 3.7.3 Correlation Analysis

Correlations between MCHO, TDCHO, DOC, Chl-a, and salinity were investigated with Spearman's rank correlation test (Table 3.6). MCHO and TDCHO were positively correlated in all seasons ( $p < 0.05$ ) and a strong positive correlation was observed in summer ( $\rho = 0.822$ ,  $p < 0.001$ ). DOC was positively correlated with MCHO and Chl-a in winter and summer ( $p < 0.01$ ). Also, there was a strong positive correlation between DOC and TDCHO in summer ( $\rho = 0.798$ ,  $p < 0.001$ ). Chl-a and MCHO were positively correlated in all seasons ( $p < 0.01$ ). Chl-a was positively correlated with TDCHO in spring and summer ( $p < 0.01$ ). Also, there were strong negative correlations between salinity and other variables (MCHO, TDCHO and Chl-a) in spring ( $p < 0.001$ ).

As shown in Fig. 3.40, strong linear relationships observed between PCHO and TDCHO/DOC ratio at both parts of the bay (middle-inner bays:  $R^2 = 0.621$ ,  $p < 0.001$ , outer bay:  $R^2 = 0.684$ ,  $p < 0.001$ ). Linear relationships with low goodness of fit ( $R^2$ ) were also observed between MCHO and TDCHO/DOC ratio in middle-inner ( $R^2 = 0.196$ ,  $p < 0.05$ ) and outer ( $R^2 = 0.390$ ,  $p < 0.001$ ) bays, respectively. The ratio of TDCHO/DOC was linearly related to Chl-a at outer bay with low goodness of fit ( $R^2 = 0.089$ ,  $p < 0.05$ ). However, linear relationship between Chl-a and TDCHO/DOC ratio was not significant at middle-inner bays ( $R^2 = 0.029$ ,  $p = 0.426$ ).

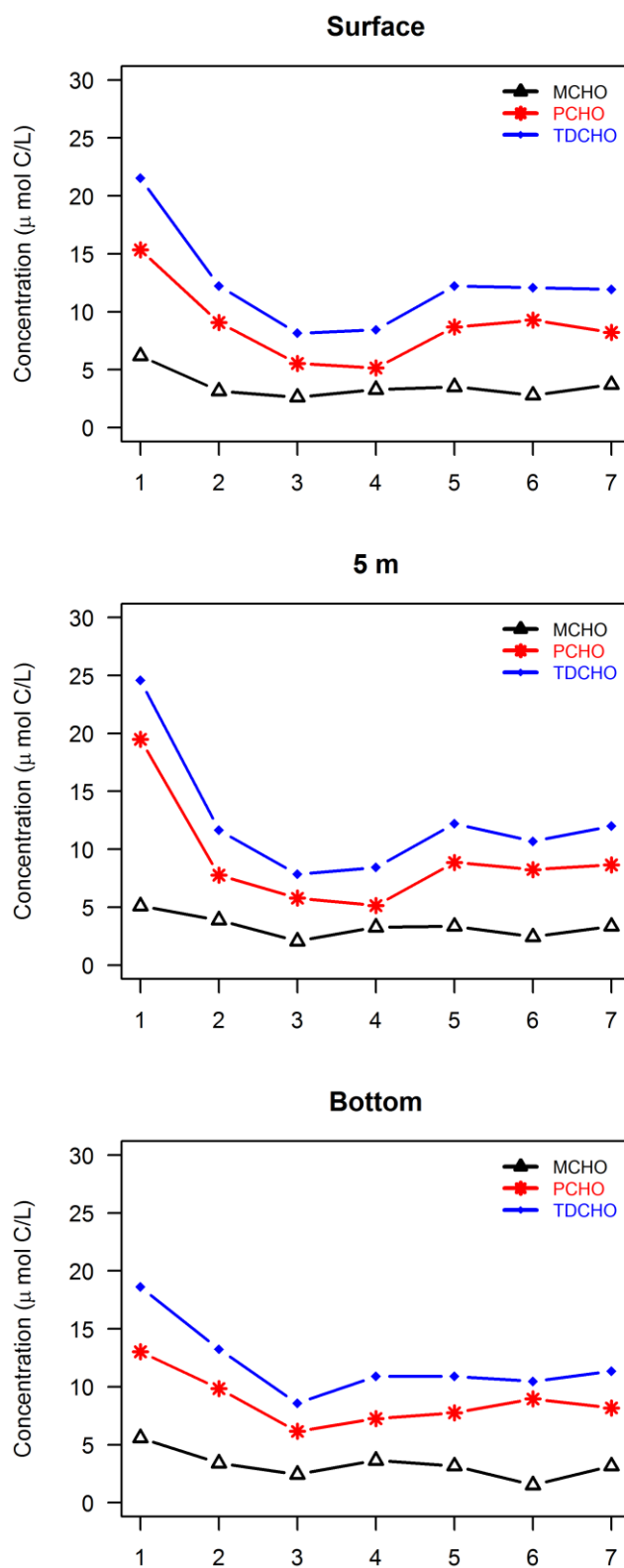


Figure 3.36 MCHO, PCHO and TDCHO profiles of seawater in winter



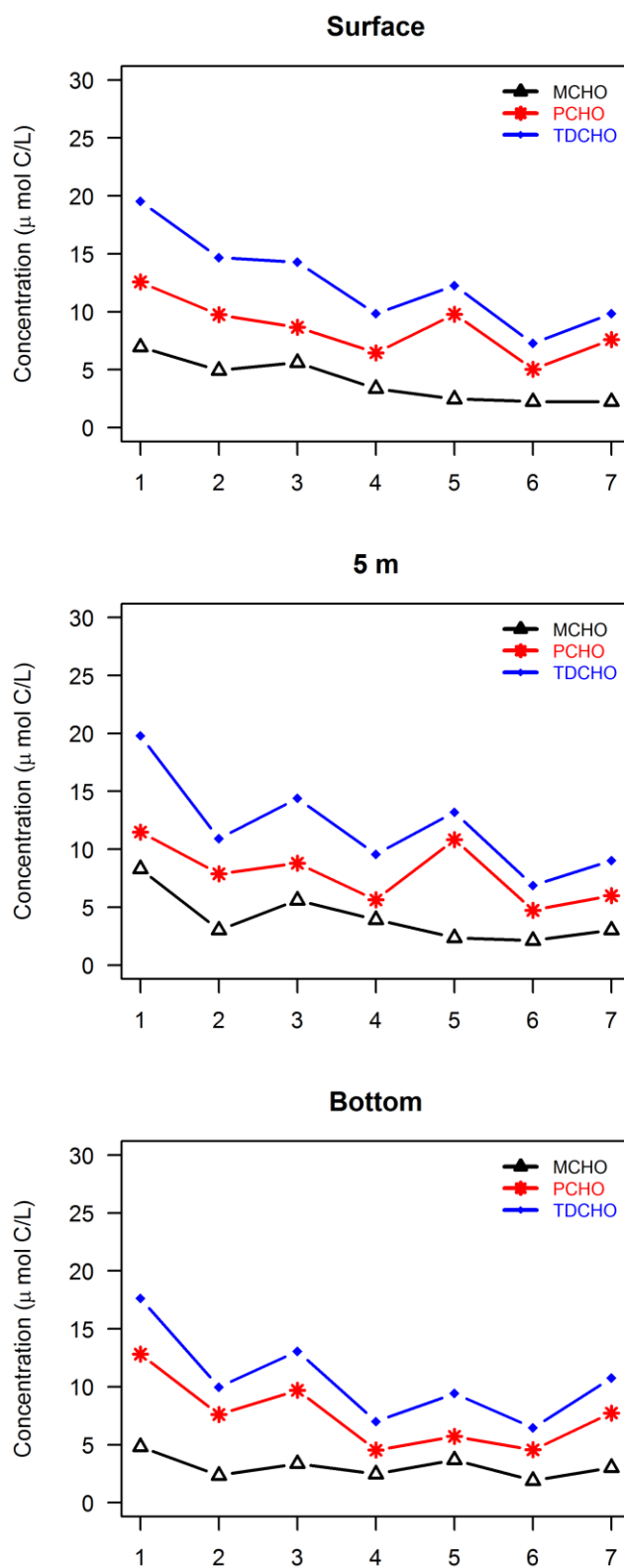


Figure 3.37 MCHO, PCHO and TDCHO profiles of seawater in spring

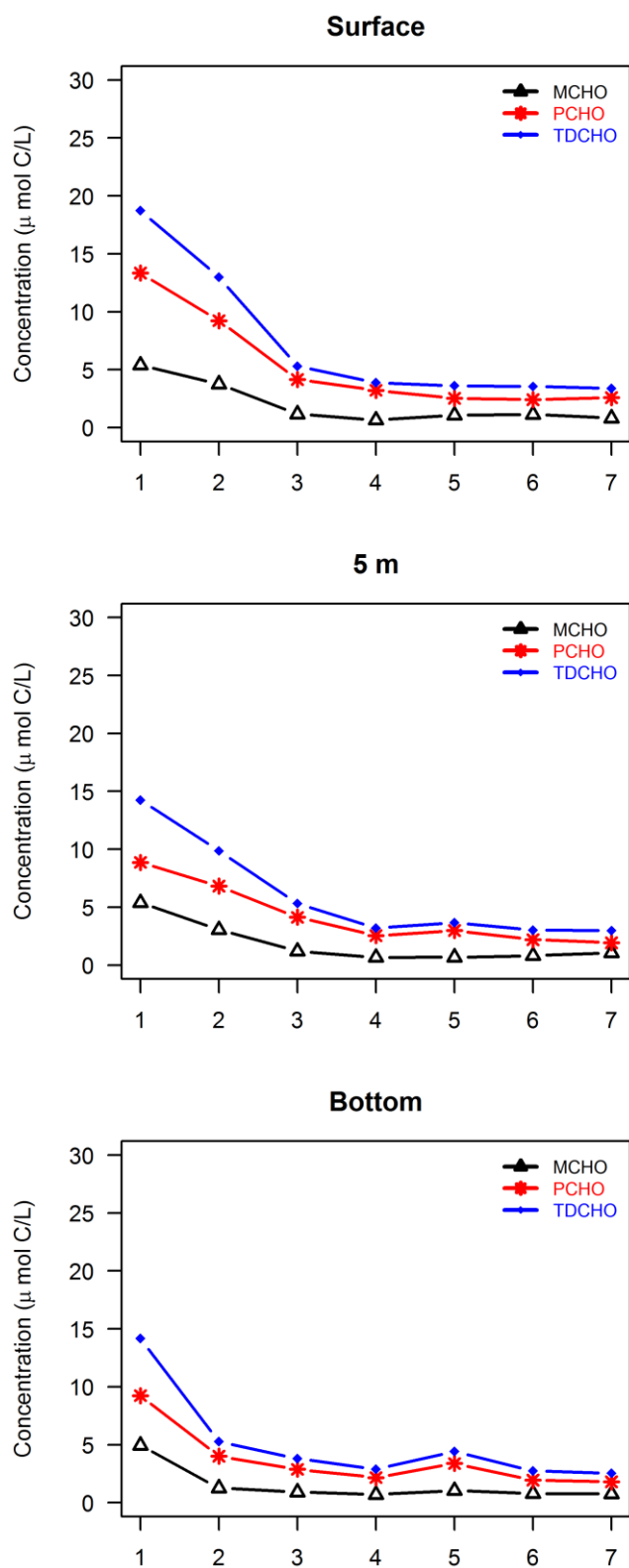


Figure 3.38 MCHO, PCHO and TDCHO profiles of seawater in summer

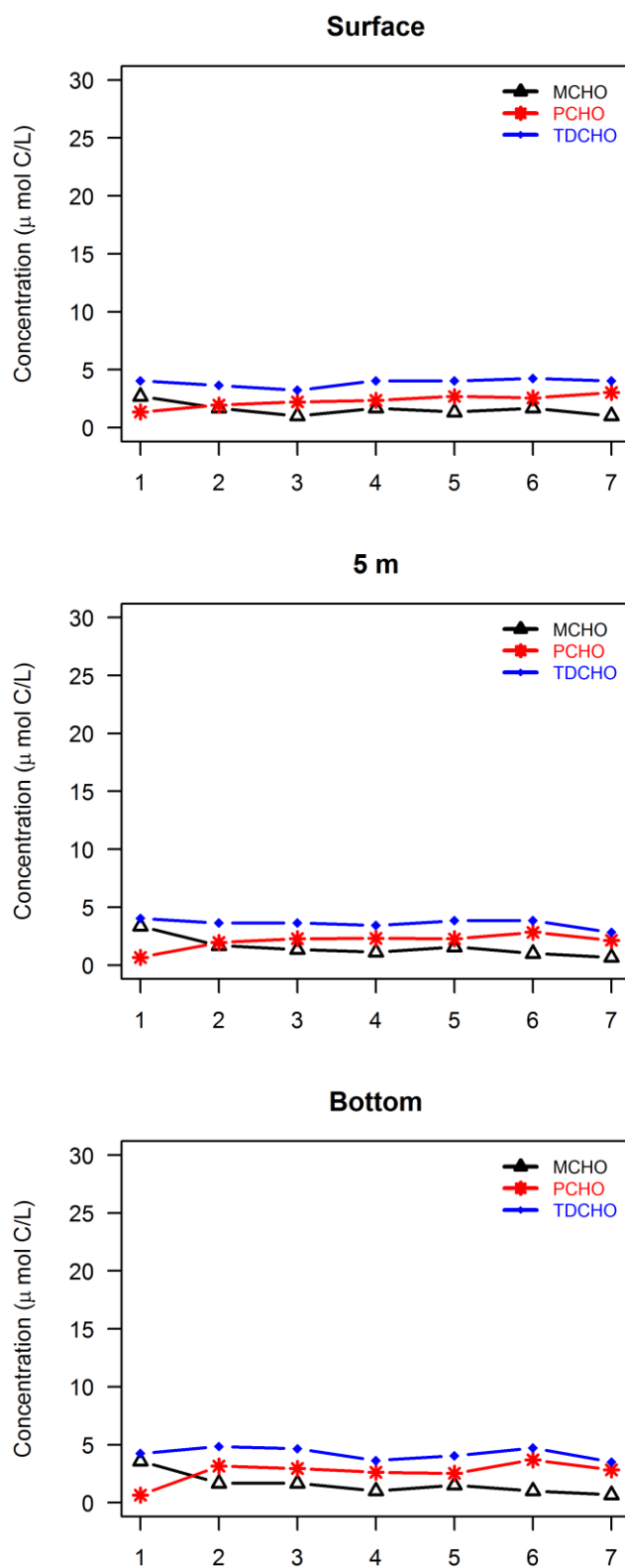


Figure 3.39 MCHO, PCHO and TDCHO profiles of seawater in autumn

Table 3.6 Correlations between MCHO, PCHO, TDCHO, DOC, Chl-a and salinity (n=21 for all tests,  $\rho$  is the Spearman's rank correlation coefficient, p is the significance level, \* means significance level of 0.05, \*\* means significance level of 0.01, \*\*\* means significance level of 0.001)

	PCHO		TDCHO		DOC		Chl-a		Salinity		
	$\rho$	p	$\rho$	p	$\rho$	p	$\rho$	p	$\rho$	p	
MCHO	winter	0.391	0.079	0.683	<0.001***	0.613	0.003**	0.578	0.006**	-0.285	0.211
	spring	0.588	0.005**	0.752	<0.001***	0.203	0.376	0.697	<0.001***	-0.815	<0.001***
	summer	0.754	<0.001***	0.822	<0.001***	0.661	0.001**	0.722	<0.001***	0.400	0.072
	autumn	-0.467	0.033*	0.533	0.013*	0.173	0.453	0.793	<0.001***	-0.328	0.147
PCHO	winter			0.900	<0.001***	-0.021	0.929	0.181	0.430	-0.380	0.089
	spring			0.951	<0.001***	0.219	0.340	0.507	0.019*	-0.595	0.004**
	summer			0.981	<0.001***	0.777	<0.001**	0.745	<0.001***	0.516	0.017*
	autumn			0.392	0.079	0.061	0.794	-0.552	0.010*	0.640	0.002**
TDCHO	winter					0.214	0.350	0.303	0.181	-0.343	0.127
	spring					0.165	0.475	0.660	0.001**	-0.743	<0.001***
	summer					0.798	<0.001**	0.749	<0.001***	0.546	0.010*
	autumn					0.487	0.025*	0.241	0.293	0.256	0.263
DOC	winter							0.643	0.002**	-0.270	0.237
	spring							0.050	0.830	-0.049	0.831
	summer							0.742	<0.001***	0.357	0.111
	autumn							0.159	0.492	0.019	0.936
Chl-a	winter									-0.670	<0.001***
	spring									-0.950	<0.001***
	summer									0.246	0.282
	autumn									-0.503	0.020*

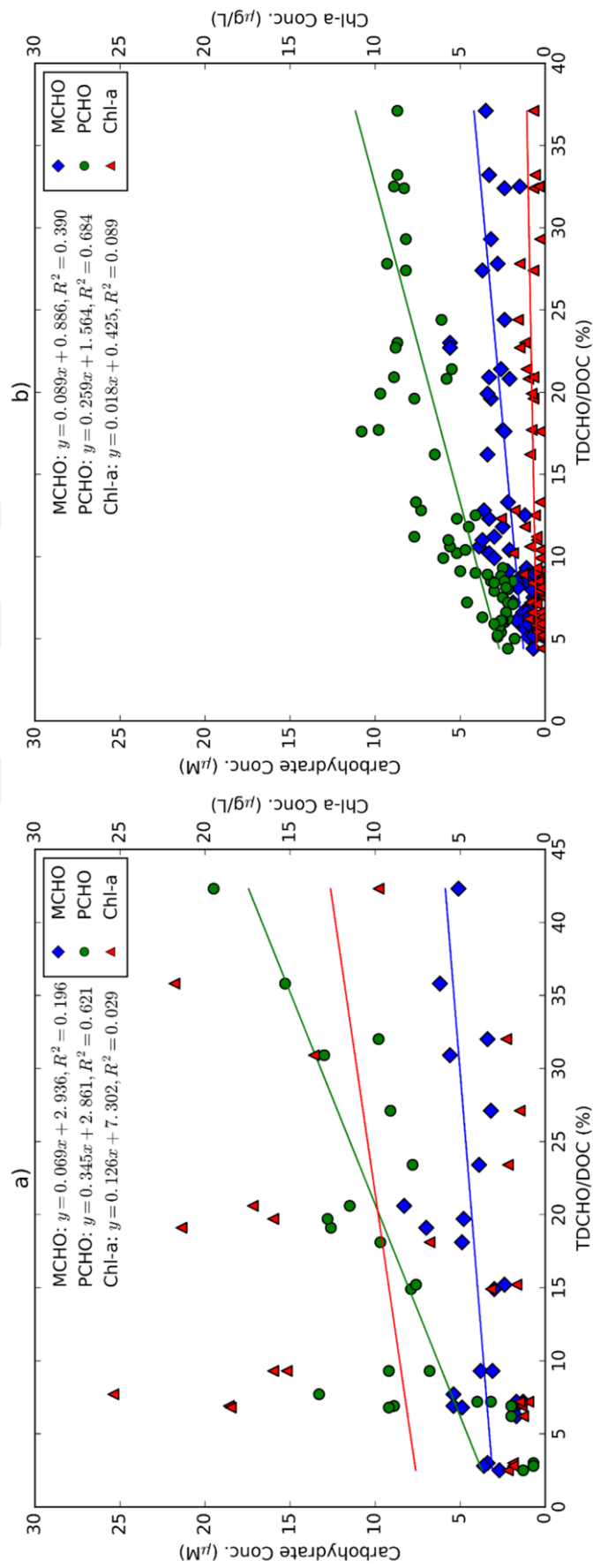


Figure 3.40 Linear relationships between MCHO, PCHO, Chl-a, and TDCHO/DOC (%) for a) middle-inner bay and b) outer bay

### ***3.7.4 Factor Analysis of Dissolved Carbohydrates***

According to factor analysis between salinity, Chl-a, DOC, MCHO and TDCHO (Figure 3.41a), two factors were extracted, and the factors were statistically sufficient to model the variations in the data of middle-inner bays. Factor 1 and 2 sufficiently explained 68% and 32% of the variability in the data, respectively. While the MCHO, TDCHO, DOC and Chl-a were explained by factor 1, salinity and also DOC identified by factor 2 for middle-inner bays. Factor analysis showed that variability of the data could be explained by at least 2 factors at outer bay (Figure 3.41b). Factor 1 and 2 were accounted for 83% and 17% of the variability in the data, respectively. DOC, MCHO, TDCHO and Chl-a were explained by factor 1. Salinity and Chl-a were explained by factor 2 at outer bay.

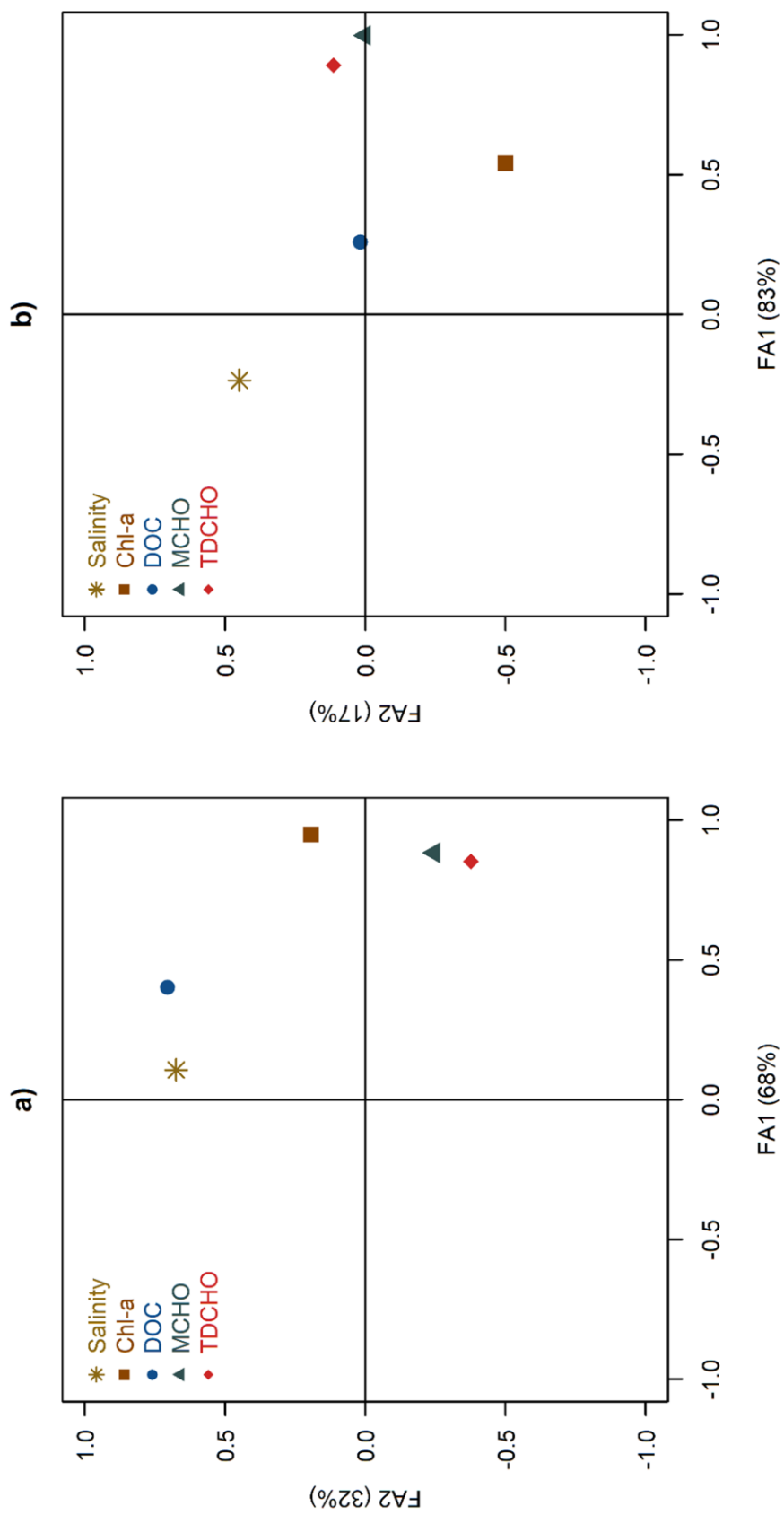


Figure 3.41 Biplots of factor loadings indicating the explained proportions of variances for salinity, Chl-a, DOC, MCHO, and TDCHO in the bay: a) middle-inner bay, b) outer bay

### 3.8 Results of Amino Acid Analyses

Seasonal variations of mean molecular DFAA concentrations among stations are given at Figure 3.42. Highest mean DFAA concentrations (>30 nM) observed at spring and summer at station 1 and 6, respectively. Mean DFAA concentrations at summer and winter were higher than other seasons. Seasonal variations of DFAA mol percentages are given at Figure 3.43. Highest mean mol percentages were found for L-Glu, L-Ser, Gly and D-Arg. While means of L-Glu, L-Arg and D-Arg especially were higher at spring and autumn, mol percentages of L-Ser and Gly were higher at winter and summer. Although there were some minor variations, mean concentrations of L-Asp, L-Thr and L-Ala were almost stable in all seasons.

Seasonal changes of  $\Sigma$ DFAA concentrations among stations are given at Figure 3.44. Highest  $\Sigma$ DFAA concentrations (>450 nM) were observed at spring and summer at station 1 and 6, respectively.  $\Sigma$ DFAA concentrations at summer and autumn were higher than other seasons except for station 1. Seasonal changes of DFAA concentrations with depth are given at Figure 3.45. DFAA concentrations decreased in the order of surface, 5 m and bottom except for autumn in middle-inner bays. In autumn, DFAA levels decreased in the order of 5 m, bottom and surface. However, in the outer bay, DFAA levels were lower than the levels at 5m except for winter.

In winter, DFAA concentrations were observed in the ranges of n.d.-66.6, n.d.-27.4 and n.d.-33.3 nM at surface, 5 m and bottom, respectively. Highest concentrations found for L-Ser at 5 m and for L-Glu at surface and bottom. At spring, DFAA concentrations were in the ranges of n.d.-188, n.d.-125 and n.d.-113 nM at surface, 5 m and bottom, respectively. Highest DFAA concentrations found for Gly at all depths. DFAA concentrations were determined in the ranges of n.d.-371, n.d.-173 and n.d.-99.3 nM at summer. Highest DFAA concentrations were found for L-Ser at all depths. DFAA concentrations were in the ranges of n.d.-42.2, n.d.-182 and n.d.-101 nM at autumn. Highest concentrations were found for Gly at surface and for L-Ser at 5 m bottom.



According to principal component analysis applied between DFAAs, 2 principal components were statistically sufficient enough to model experimental data ( $p < 0.05$ , Figure 3.46). The first component was able to explain 48% and the second component was able to explain 23% of the variance. First component explained 68% of the data, whereas the second component explained 32% of the data. While L-Arg and D-Ser were poorly explained by 1<sup>st</sup> component, Gly, D-Arg, D-Ser, D-Thr and L-Asp poorly explained by 2<sup>nd</sup> component.

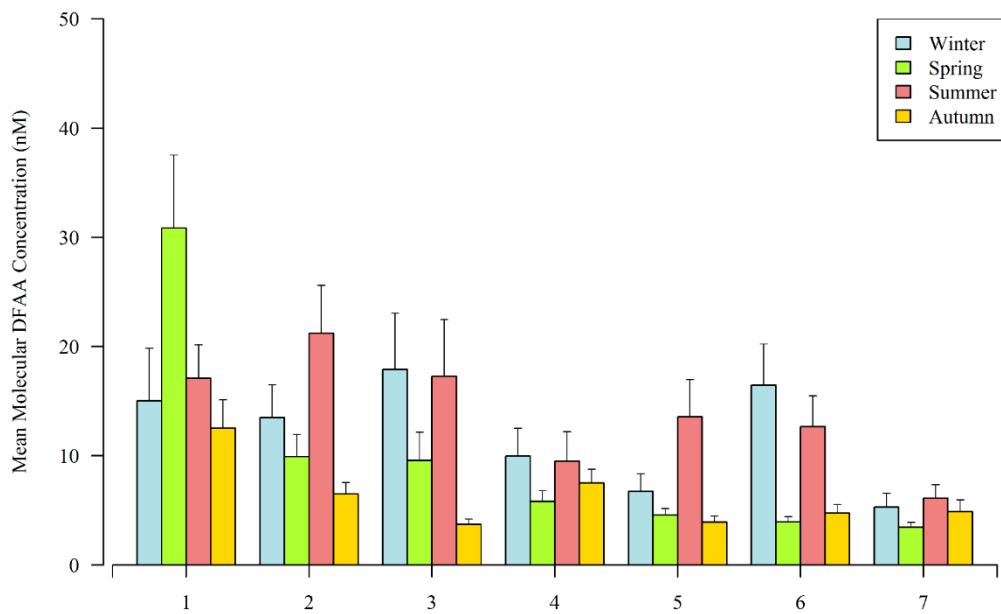


Figure 3.42 Seasonal and spatial variations of mean molecular DFAA concentrations at all sampling depths in the İzmir Bay

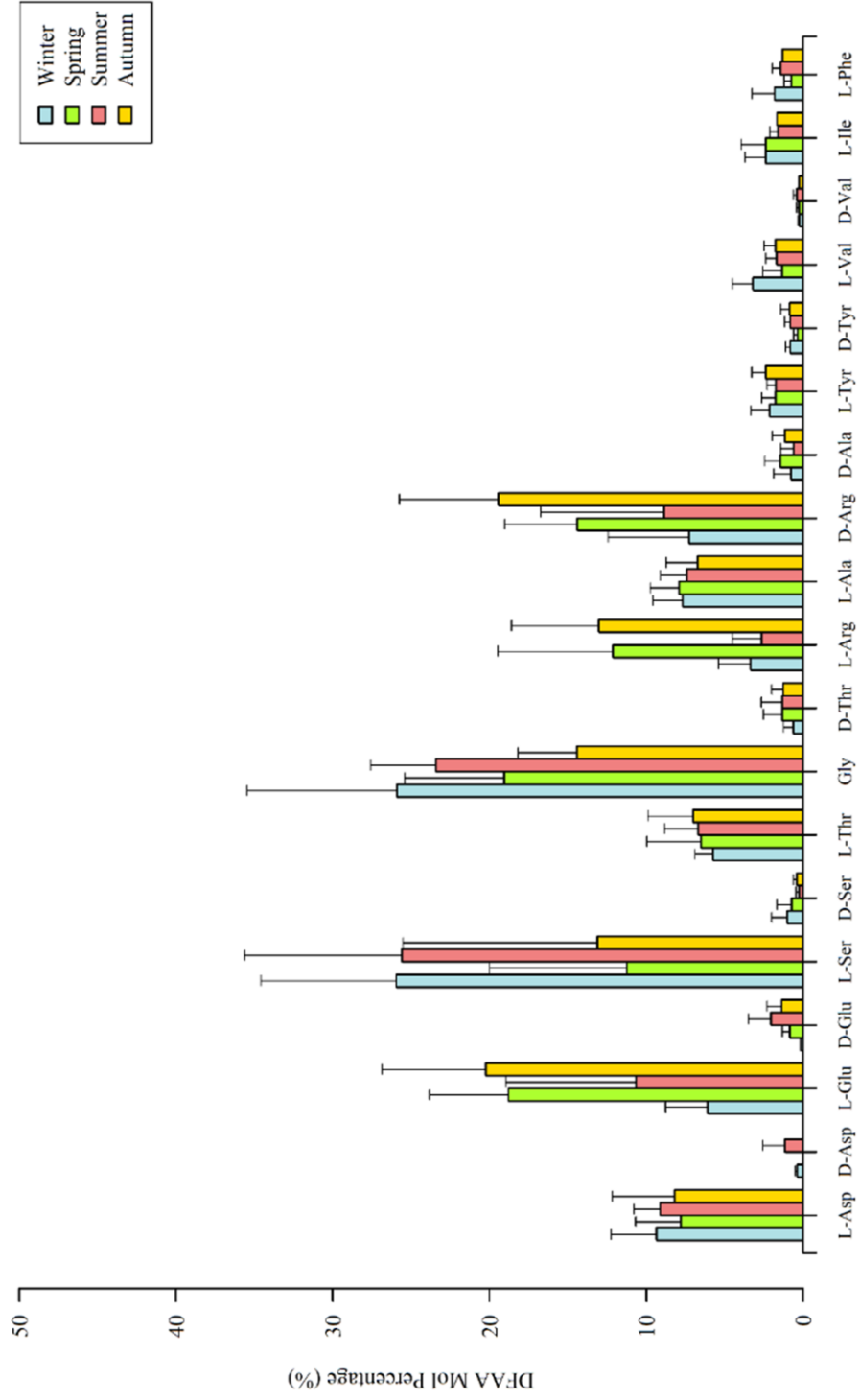


Figure 3.43 Seasonal variations of DFAA mol percentages at all depths and stations in Izmir Bay

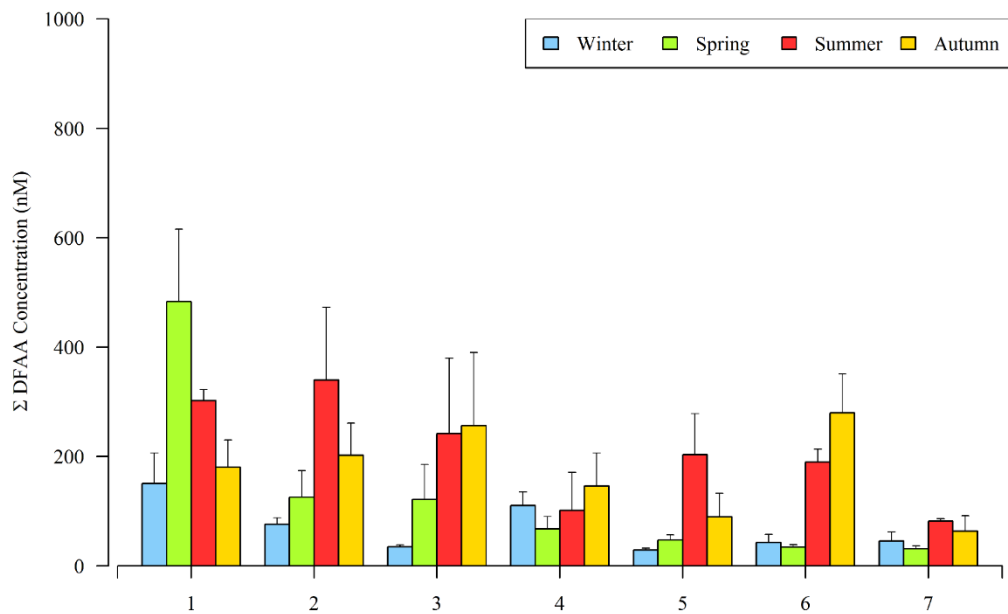


Figure 3.44 Seasonal and spatial variations of total DFAA concentrations at the İzmir Bay

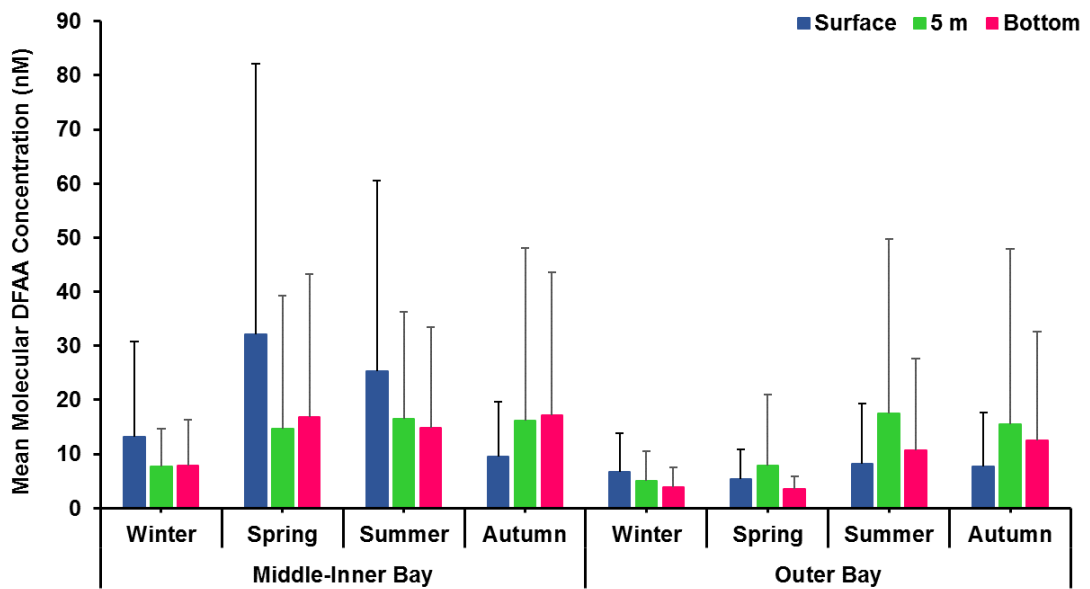


Figure 3.45 Seasonal variations of DFAA concentrations with depth at the İzmir Bay. Data are represented as Mean±SD

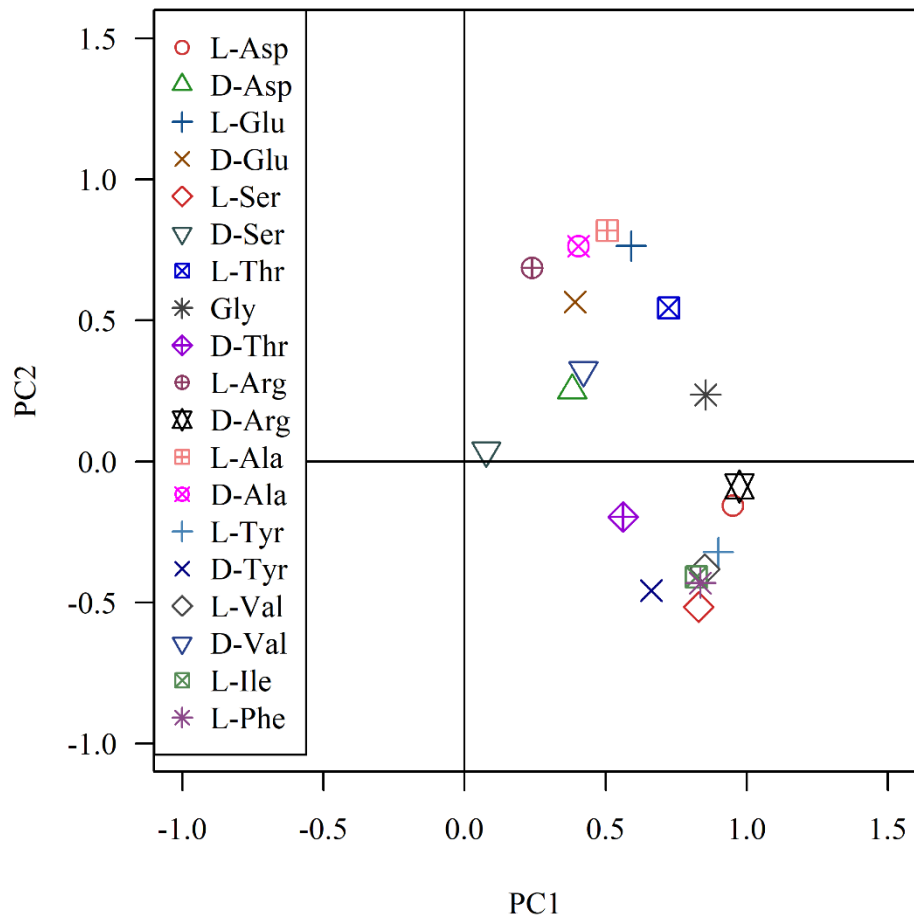


Figure 3.46 Biplot of PCA loadings for DFAA

Seasonal variations of mean molecular TDHAA concentrations among stations are given at Figure 3.47. Highest mean TDHAA concentrations (>80 nM) were observed in spring at station 1. In winter, mean TDHAA concentrations at stations 3, 4 and 6 were higher than other seasons. Seasonal variations of TDHAA mol percentages are given at Figure 3.48. Highest mean mol percentages were found for Gly at all seasons. Mol percentages of L-Asx, L-Glu and L-Ser were also higher than other amino acids. Among TDHAA mol percentages, seasonal changes were not clear.

Seasonal changes of  $\sum$ TDHAA concentrations among stations are given at Figure 3.49. Highest  $\sum$ TDHAA concentrations (>1500 nM) observed in spring at station 1. In autumn,  $\sum$ TDHAA concentrations at stations 3, 4, 6 and 7 were higher than other seasons. Seasonal changes of TDHAA concentrations with depth are given at Figure 3.50. In winter, spring and autumn, TDHAA concentrations did not change obviously, but, in summer, TDHAA levels decreased from surface to bottom.

In winter, TDHAA concentrations were observed in the ranges of 0.7-272, 0.6-238 and 0.5-250 nM at surface, 5 m and bottom, respectively. Highest concentrations were found for Gly at all depths. At spring, TDHAA concentrations were in the ranges of n.d.-372, n.d.-309 and n.d.-369 nM at surface, 5 m and bottom, respectively. Highest TDHAA concentrations were found for L-Asx at bottom and for Gly at surface and 5 m. TDHAA concentrations were in the ranges of n.d.-480, n.d.-382 and n.d.-232 nM at summer. Highest TDHAA concentrations were found for Gly at all depths. TDHAA concentrations were observed in the ranges of 1.2-376, 0.8-356 and 1.1-267 nM at autumn. Highest concentrations found for Gly at all depths.

According to principal component analysis applied between TDHAAs, 2 principal components were statistically sufficient enough to model experimental data ( $p < 0.05$ , Figure 3.51). The first component was able to explain 72% and the second component was able to explain 11% of the variance. First component explained 86% of the data, whereas the second component explained 14% of the data. While D-Tyr and D-Val were poorly explained by 1<sup>st</sup> component, L-Asx, L-Glx, D-Thr, L-Arg, L-Ala, D-Ala, L-Tyr, L-Val, L-Ile and L-Phe poorly explained by 2<sup>nd</sup> component.

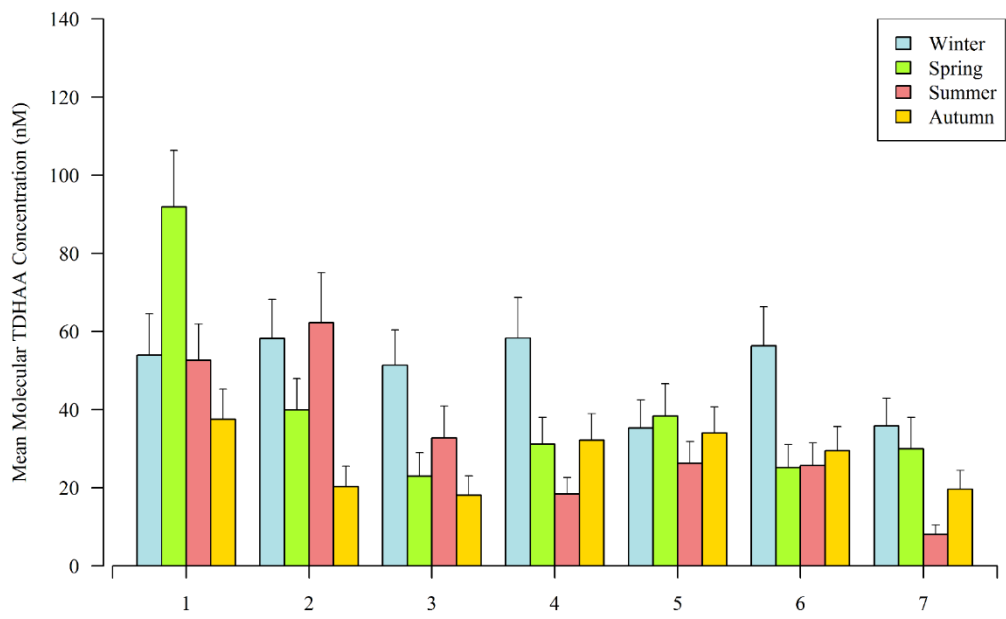


Figure 3.47 Seasonal and spatial variations of mean molecular TDHAA concentrations at all sampling depths in the İzmir Bay

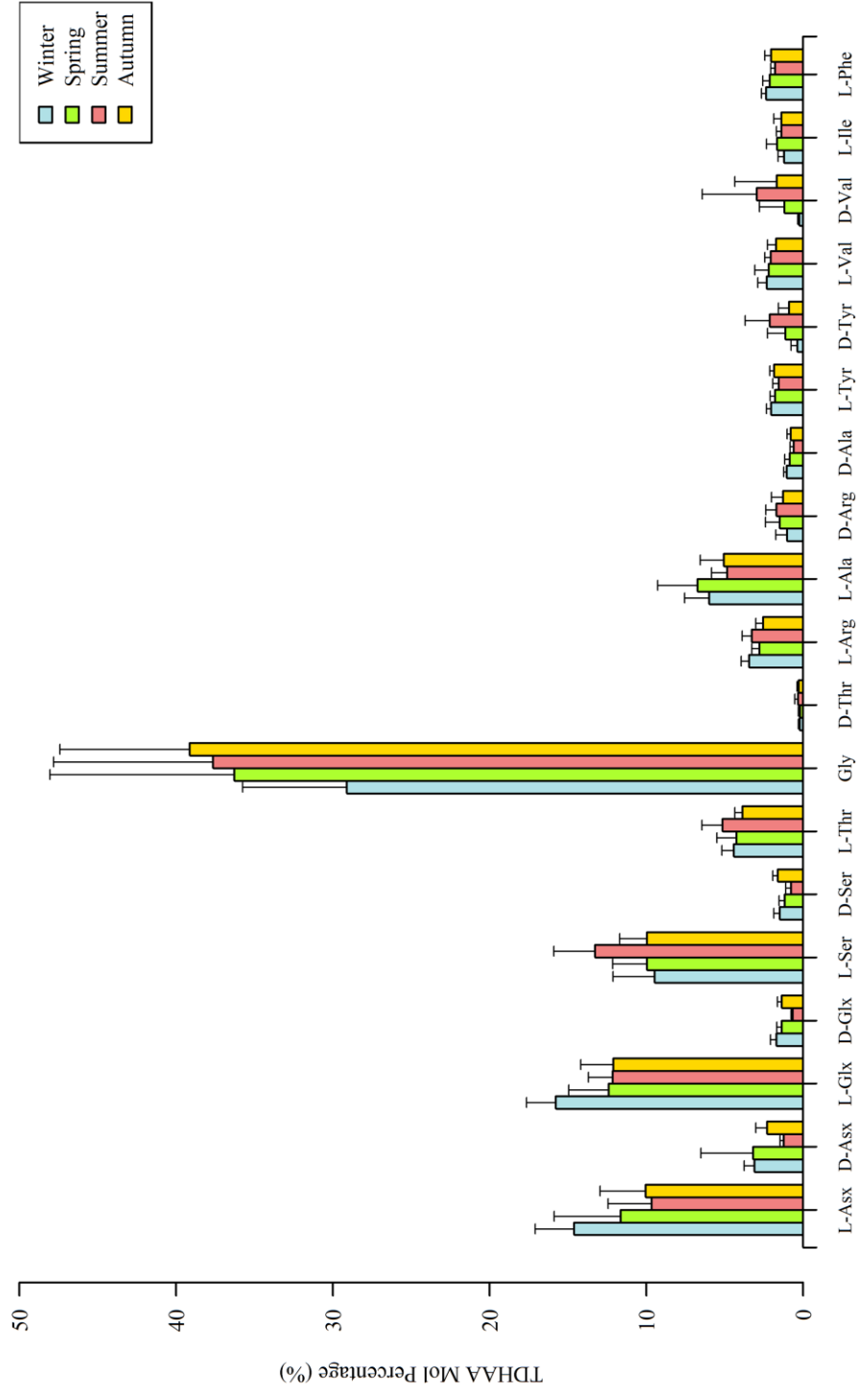


Figure 3.48 Seasonal variations of TDHAA mol percentages at İzmir Bay

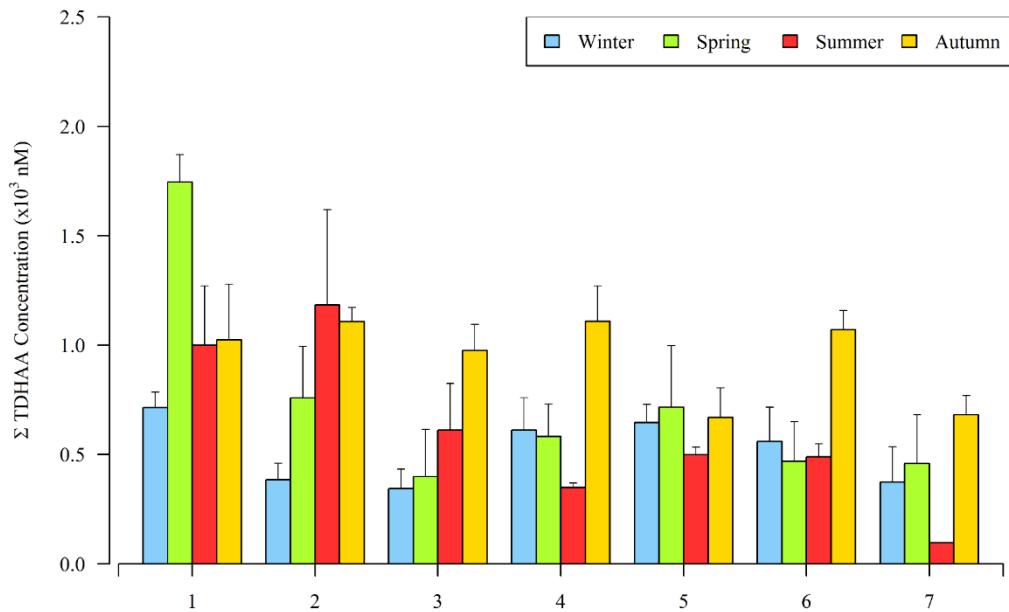


Figure 3.49 Seasonal and spatial variations of total TDHAA concentrations at the İzmir Bay

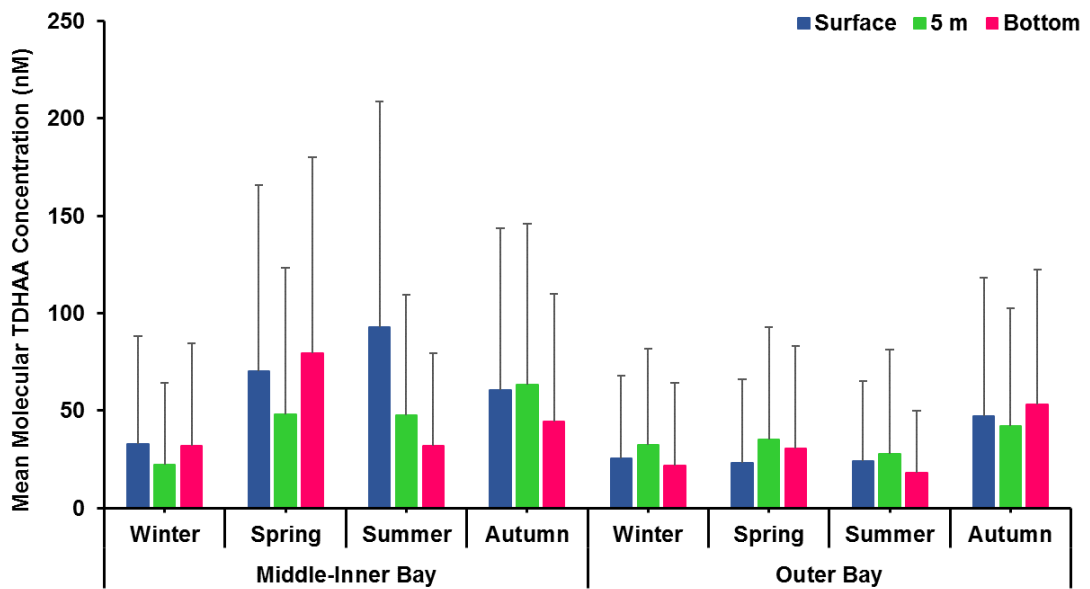


Figure 3.50 Seasonal variations of TDHAA concentrations with depth at the İzmir Bay. Data are represented as Mean±SD



### Principal Components

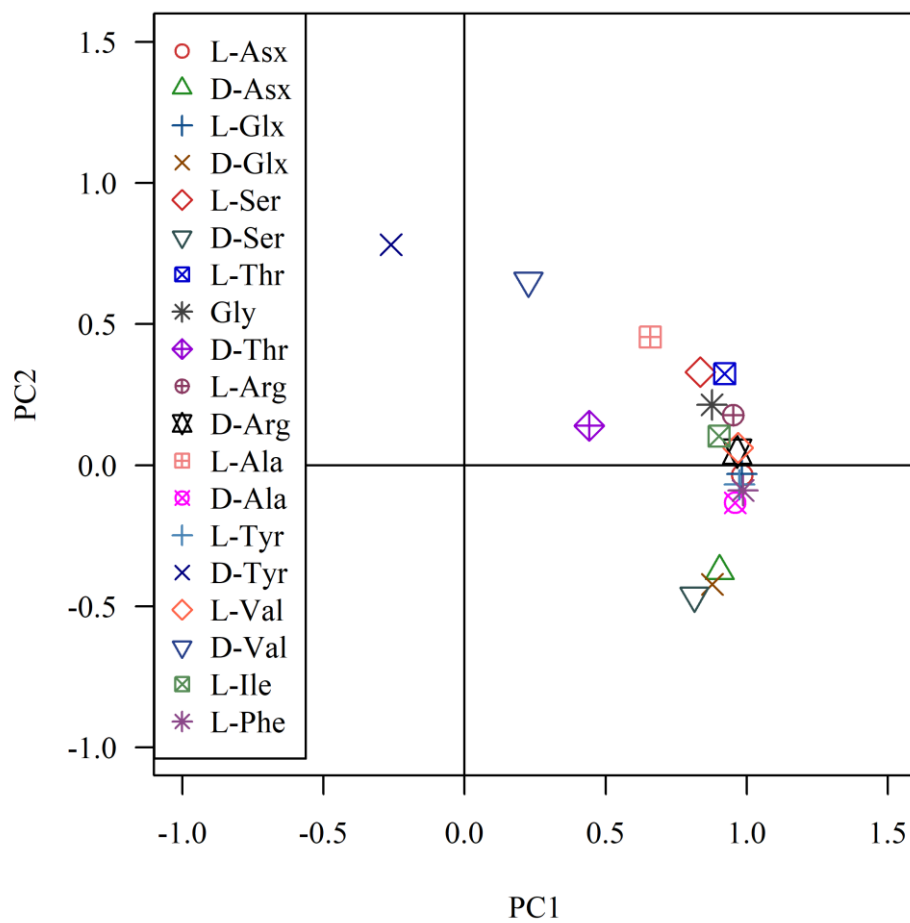


Figure 3.51 Biplot of PCA loadings for TDHAA

Seasonal variations of mean molecular PHAA concentrations among stations are given at Figure 3.52. Highest mean PHAA concentrations ( $>1.75$  nM) were observed in spring and summer at station 1. Mean PHAA concentrations at station 1 were higher than other stations. For station 2, mean PHAA concentrations in summer were higher than other seasons. Seasonal mean PHAA concentrations at outer bay stations did not change remarkably. Seasonal variations of PHAA mol percentages are given at Figure 3.53. Highest mean mol percentages were found for Gly at winter and summer seasons. Mol percentages of L-Glx, L-Thr, Gly, L-Arg and L-Ala were also higher than other amino acids. Among PHAA mol percentages, seasonal changes were not clear.

Seasonal changes of  $\Sigma$ PHAA concentrations among stations are given at Figure 3.54. Highest  $\Sigma$ PHAA concentrations ( $>45$  nM) were observed in summer at station 1. For station 1,  $\Sigma$ PHAA concentrations were remarkably higher in spring and summer than other seasons. In summer,  $\Sigma$ PHAA concentrations at station 2 were also higher than other seasons. Outer bay stations did not show remarkable seasonal changes. Seasonal changes of PHAA concentrations with depth are given at Figure 3.55. In winter, spring and summer, PHAA levels decreased from surface to bottom and in autumn, PHAA levels did not clearly change.

In winter, PHAA concentrations were observed in the ranges of n.d.-5.0, n.d.-2.1 and n.d.-2.1 nM at surface, 5 m and bottom, respectively. Highest concentrations were found for L-Glx at all depths. At spring, PHAA concentrations were in the ranges of n.d.-7.6, n.d.-4.7 and n.d.-3.8 nM at surface, 5 m and bottom, respectively. Highest PHAA concentrations were found for Gly at bottom and for L-Glx at surface and 5 m. PHAA concentrations were in the ranges of n.d.-8.0, n.d.-5.4 and n.d.-5.2 nM at summer. Highest PHAA concentrations were found for Gly at all depths. PHAA concentrations were observed in the ranges of n.d.-3.0, n.d.-3.1 and n.d.-3.3 nM at autumn. Highest concentrations were found for L-Glx at all depths.

According to principal component analysis applied between PHAAs, 2 principal components were statistically sufficient enough to model experimental data ( $p < 0.05$ ,

Figure 3.56). The first component was able to explain 85% and the second component was able to explain 7% of the variance. First component explained 92% of the data, whereas the second component explained 8% of the data. While D-Ser and D-Val were poorly explained by 1<sup>st</sup> component, only D-Ser and D-Val were explained by 2<sup>nd</sup> component.

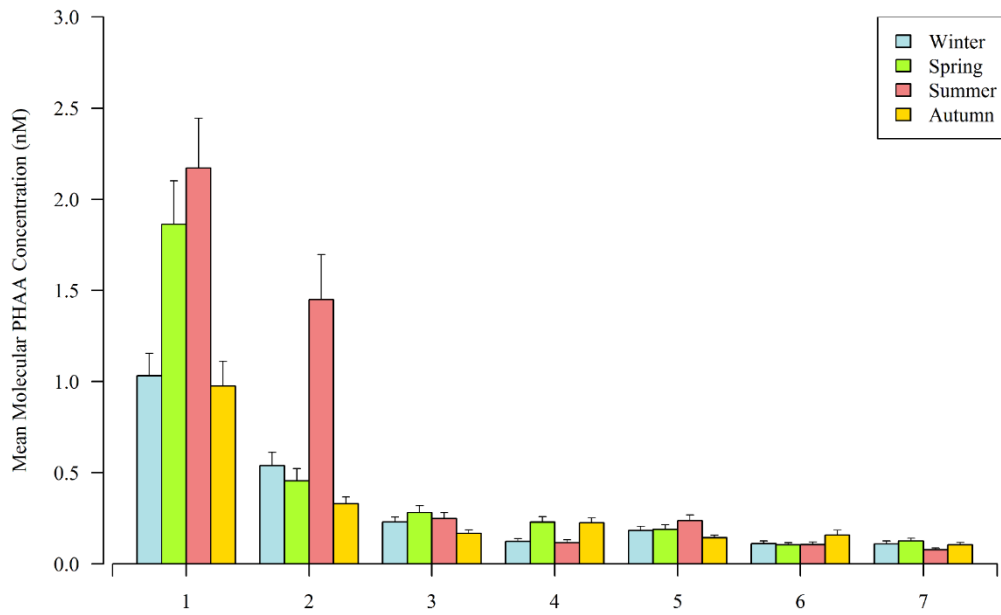


Figure 3.52 Seasonal and spatial variations of mean molecular PHAA concentrations at all sampling depths in the İzmir Bay

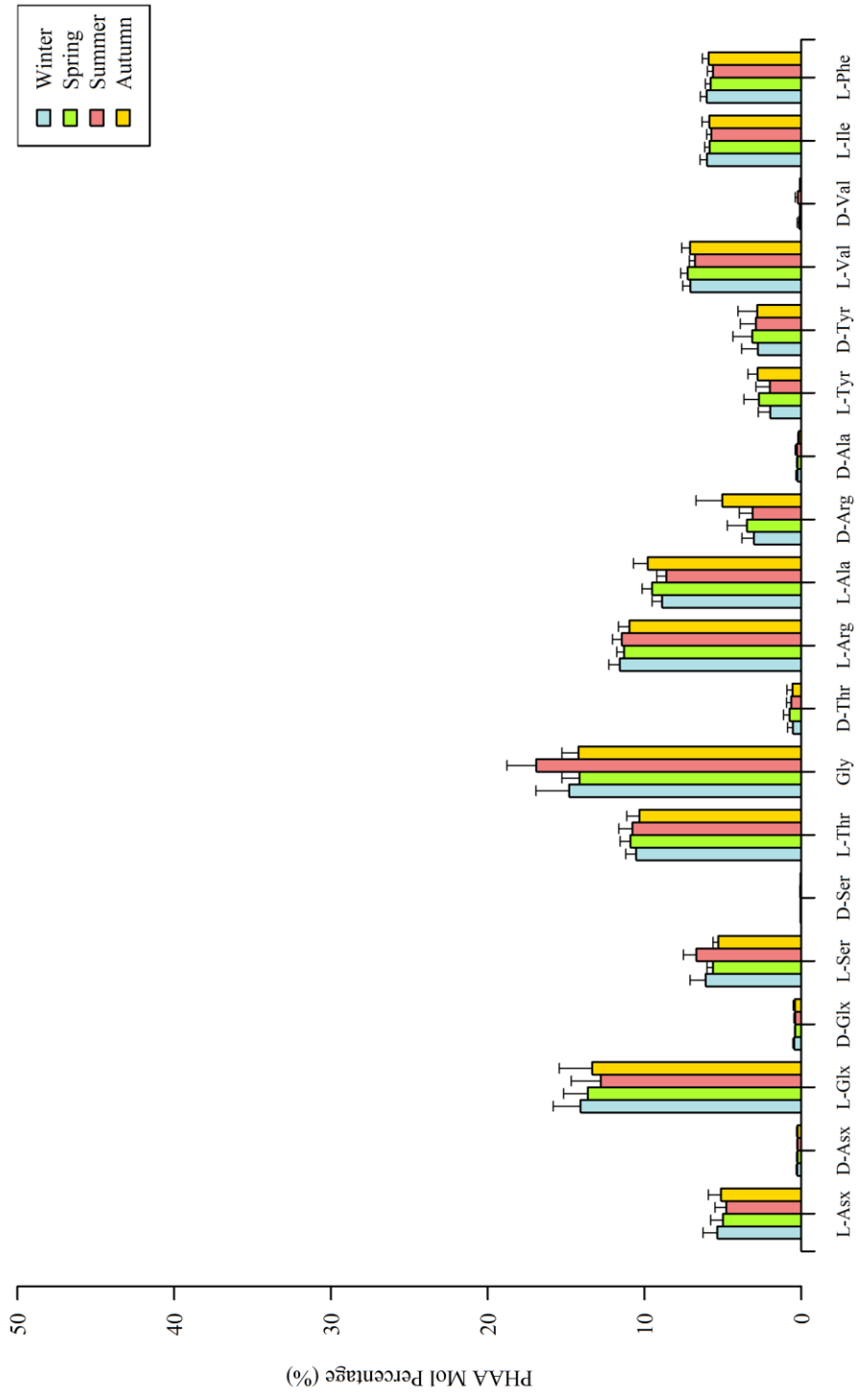


Figure 3.53 Seasonal variations of PHAA mol percentages at İzmir Bay

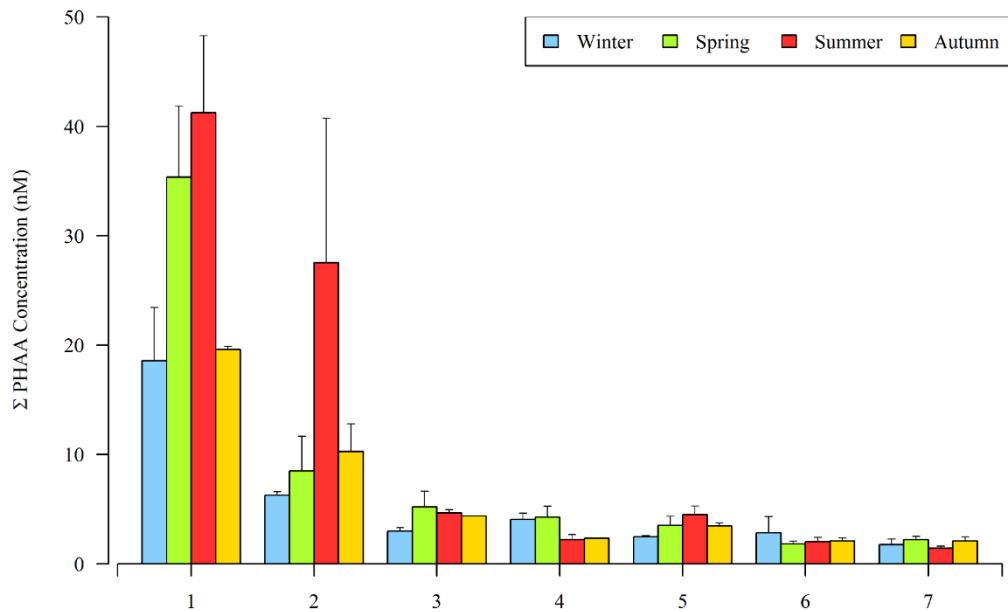


Figure 3.54 Seasonal and spatial variations of total PHAA concentrations at the İzmir Bay

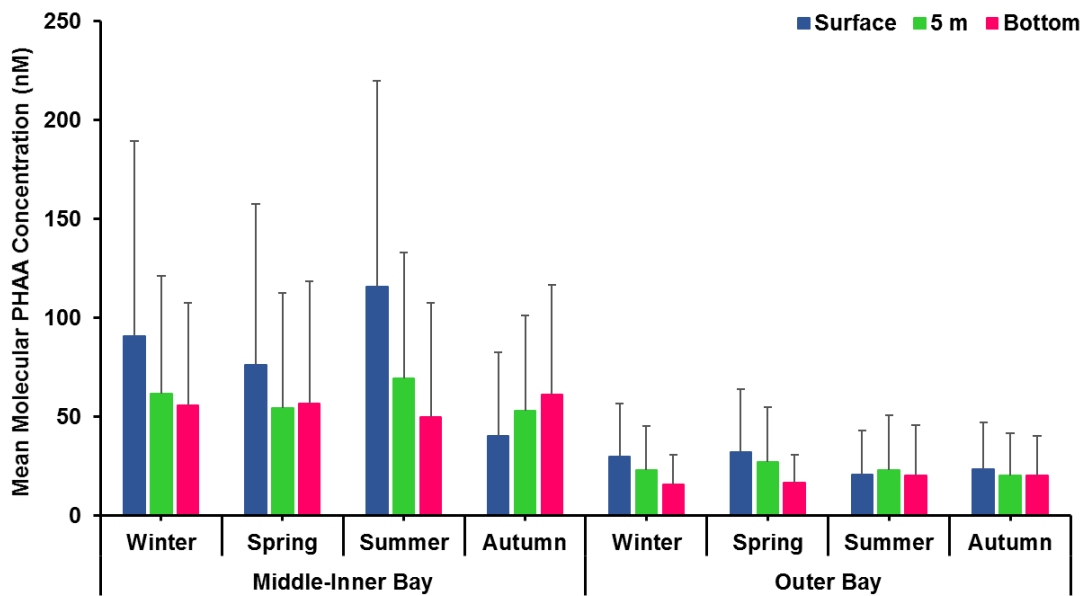


Figure 3.55 Seasonal variations of PHAA concentrations with depth at the İzmir Bay. Data are represented as Mean±SD

### Principal Components

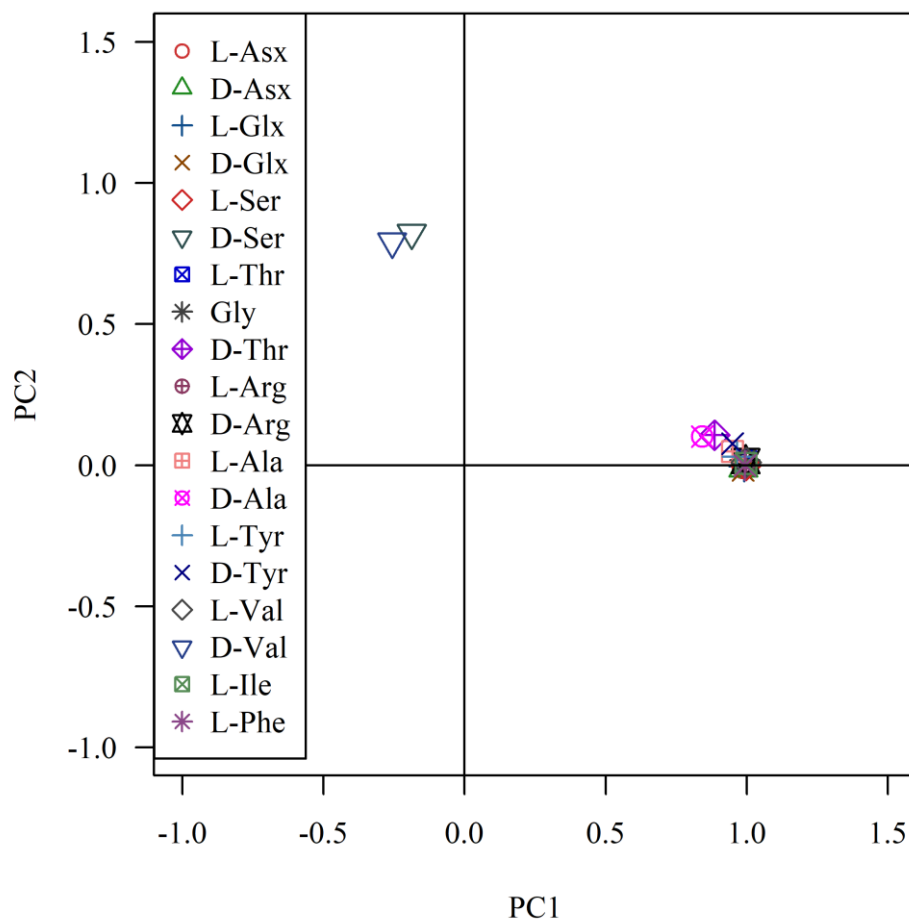


Figure 3.56 Biplot of PCA loadings for PHAA

### 3.9 D/L Ratios and Degradation Index Results for Amino Acid Analyses

Seasonal variations of D/L-ratios of Asp, Glu, Ser and Ala in the forms of DFAA, TDHAA and PHAA are given at Figure 3.57. Concentrations L-forms were proportionally higher than D-forms in all amino acid types. Ranges of D/L-ratios were 0.002-0.668, 0.007-4.486 and 0.004-3.329 for DFAA, TDHAA and PHAA forms, respectively. Highest fluctuations (distance between highest and lowest ratios) were observed in winter and spring seasons in DFAA form, however, fluctuations were lower in other forms. Lowest ratios for DFAA were observed in Ser at summer and autumn seasons. TDHAA ratios were lowest at summer season for Glx and Ser. Also, lowest PHAA ratios were found for Ser in all seasons. For PHAA form, seasonal D/L-ratios for amino acids did not change remarkably and ratios decreased in the order of Asx, Glx, Ala and Ser.

Seasonal variations of degradation index values for DFAA, TDHAA and PHAA forms of amino acids are given at Figure 3.58. DI values of DFAA forms were generally greater than 0 at all depths. In TDHAA forms, both positive and negative DI values were observed, and autumn values were higher than other seasons. For PHAA forms, DI values distributed near 0 or below and highest values were found in autumn season.

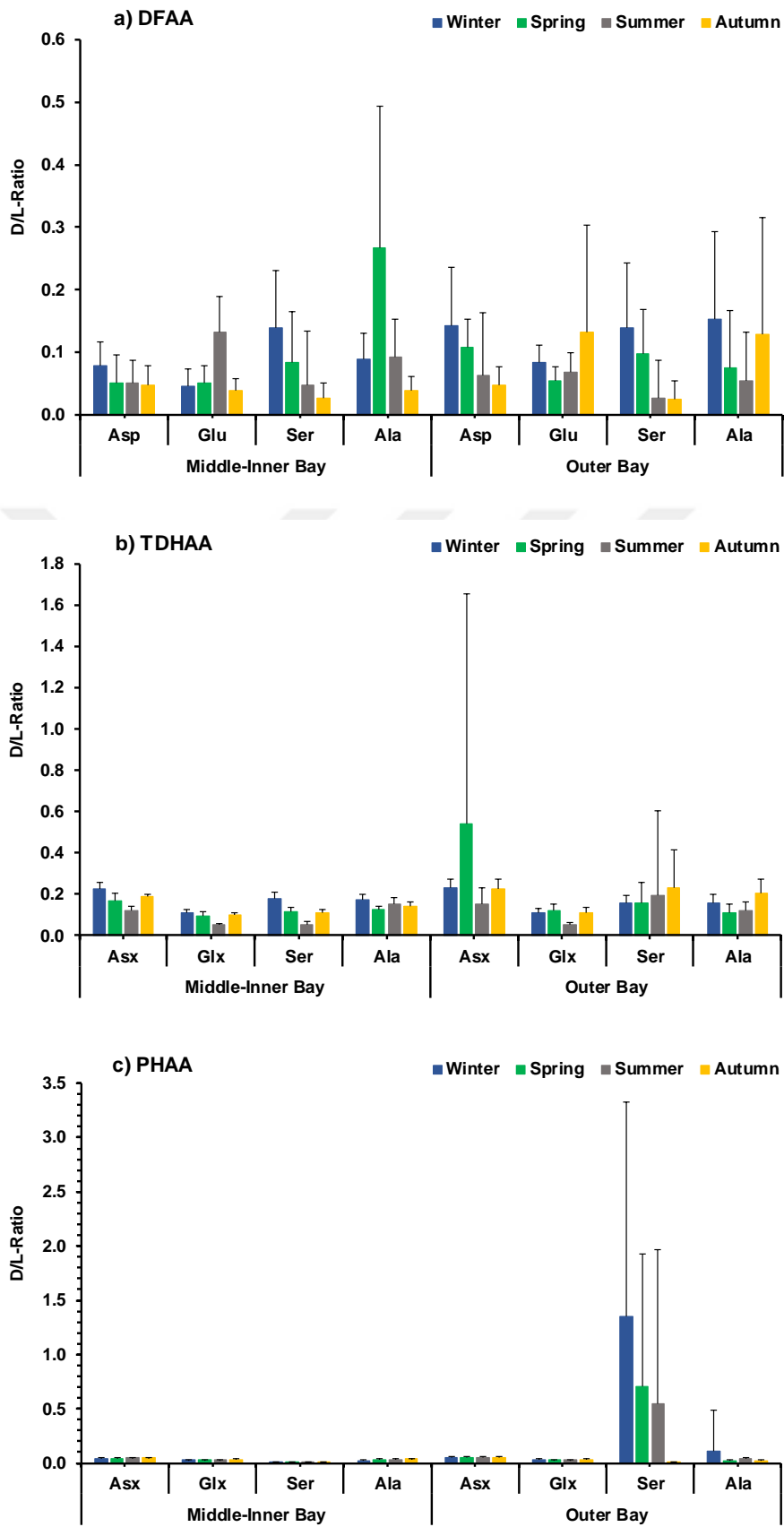


Figure 3.57 Seasonal D/L-Ratios of Asp, Glu, Ser and Ala at all depths and stations (Mean±SD)



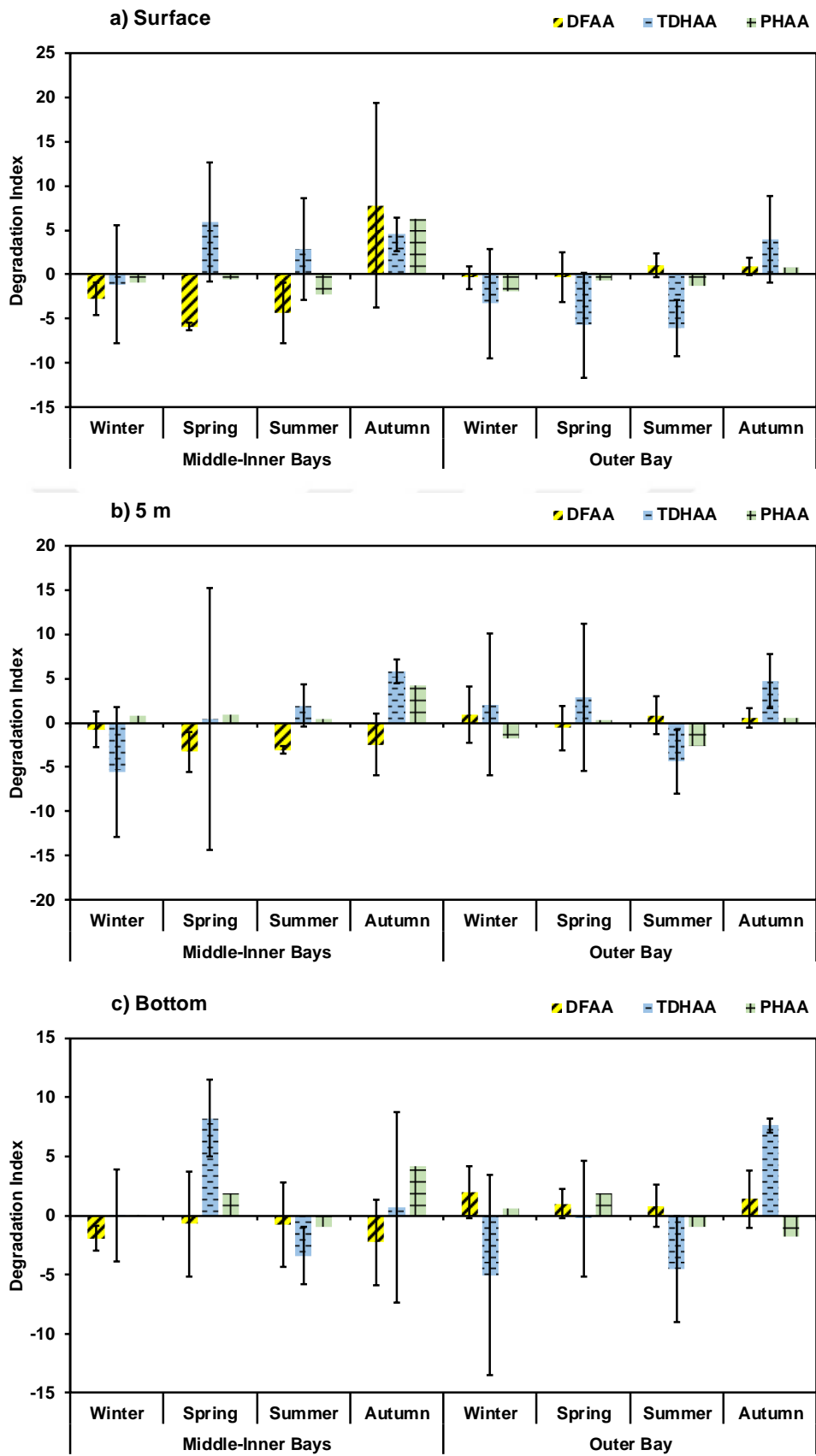


Figure 3.58 Seasonal variations of Degradation Index values (Mean±SD)

### 3.10 Molecular Composition of Dissolved Organic Carbon, Nitrogen and Total Phosphorus

Distributions of MCHO, PCHO, DFAA and DCAA in DOC pool at middle-inner and outer bays are given in Figure 3.59. MCHO and PCHO ratios decreased from winter to autumn both at middle-inner and outer bays. DFAA ratios were maximum in spring and in summer at middle-inner and outer bays, respectively. Highest DCAA ratios were observed in autumn at middle-inner and outer bays. On the other hand, DCAA ratios decreased from winter to summer in outer bay. Ratios of undefined components within DOC increased from winter to autumn at outer bay.

Distributions of DFAA and DCAA in DON pool at middle-inner and outer bays are given in Figure 3.60. DFAA ratios increased from winter to summer and decreased in autumn at middle-inner and outer bays. Lowest DCAA ratios (1.7%) were observed in winter at middle-inner bays. DCAA ratio increased to over 30% in spring, summer and autumn seasons at middle-inner bays. DCAA ratios at outer bay were found between 0.2-77%. Minimum ratios were observed in spring and highest ratios were found in summer. Ratios of undefined components within DON decreased from winter to spring and did not changed remarkably from spring to autumn. At outer bay, ratios of other fractions were lower in summer and autumn compared to winter and spring.

Distributions of DIP, DOP and PP in TP pool at middle-inner and outer bays are given in Figure 3.61. DIP ratios increased from winter-spring to summer-autumn at middle-inner and outer bays. Highest DIP ratios (68%) were observed in autumn at middle-inner bays. DOP and PP ratios decreased from winter-spring to summer-autumn at middle-inner bays. At outer bay, DOP ratios increased from winter to summer and decreased in autumn. On the contrary, PP ratios decreased from winter to summer and increased in autumn at outer bay.



Figure 3.59 Seasonal variations of identified DOC components: a) Inner bay, b) Outer bay

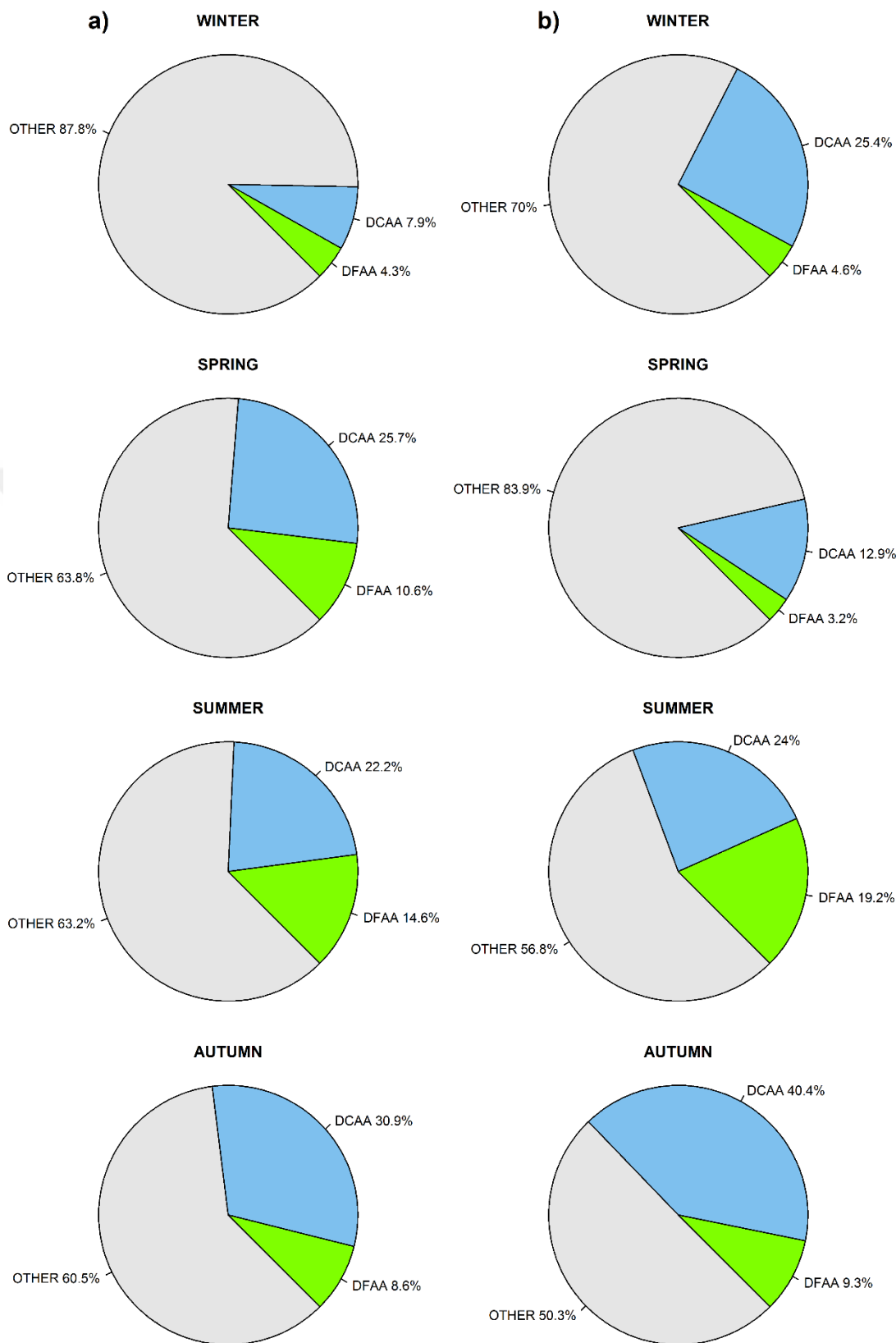


Figure 3.60 Seasonal variations of identified DON components: a) Inner bay, b) Outer bay

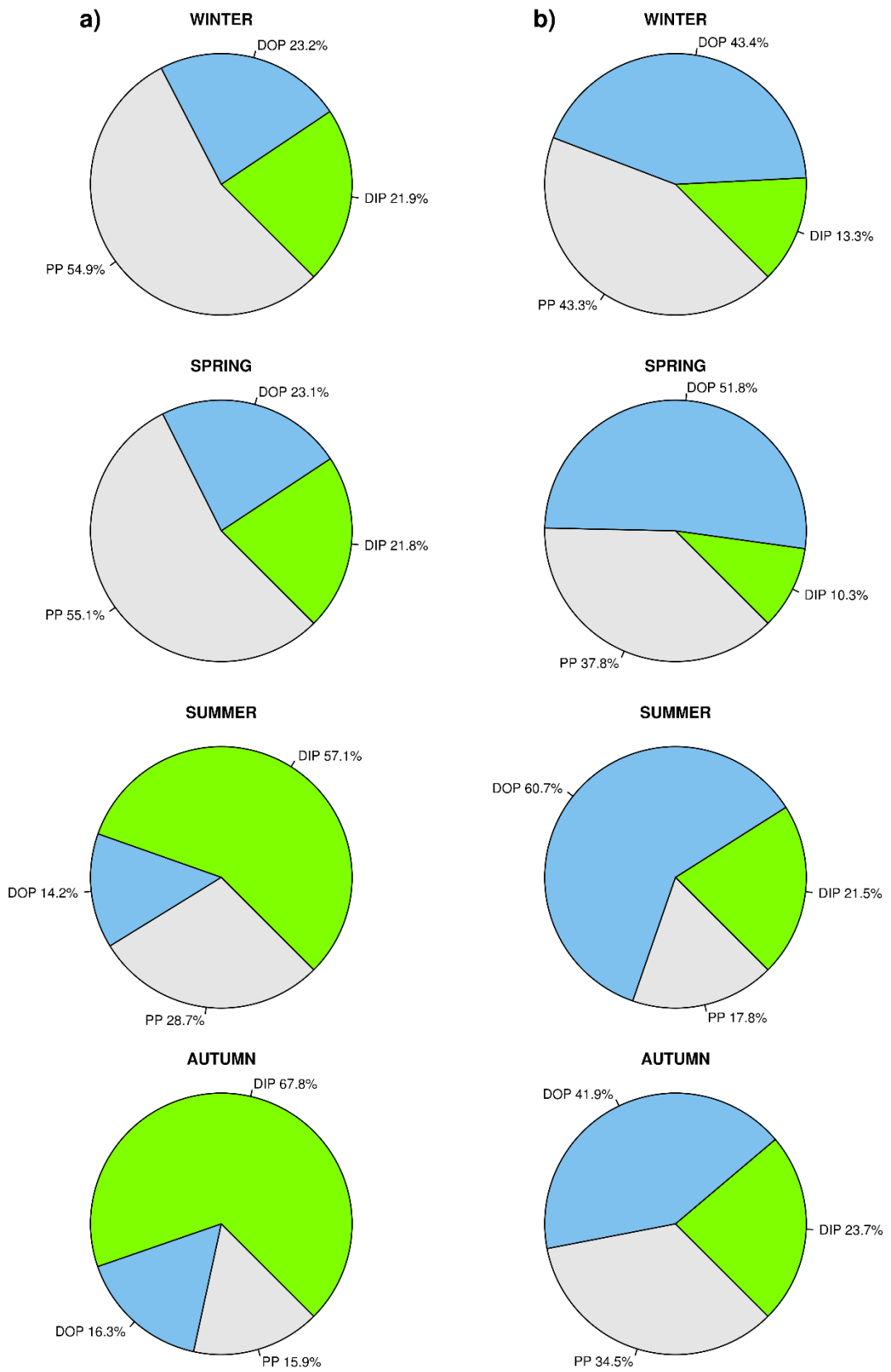


Figure 3.61 Seasonal variations of identified TP components: a) Inner bay, b) Outer bay

### 3.11 Statistical Analyses and Plots

Correlations, ANOVA results and PCA analysis results were given in this section. According to Figure 3.62, DOP, PP, PN, MCHO, TDCHO, PCHO and  $\Sigma$ PHAA were highly correlated with Chl-a at Middle-Inner Bays. From Figure 3.63, it could be seen that PP, TN, TRIX, MCHO and  $\Sigma$ PHAA were highly correlated with Chl-a at Outer Bay. o-PO<sub>4</sub>, DOP, TP, TN and DOC were highly correlated with TRIX at Middle-Inner Bays (Figure 3.64). Chl-a, o-PO<sub>4</sub>, TP and DIN were highly correlated with TRIX at Outer Bay (Figure 3.65).

Linear relationships between bulk chemical components of seawater and differences in levels of these components at Middle-Inner and Outer Bays were investigated with scatter plots and linear regression analysis. Scatter and linear regression plots were given at Figures 3.66-3.79.

Box-plots representing seasonal and spatial differences were given in Figures 3.80-3.114. These plots were used in this study as complementary tools for assessment of Two-Way ANOVA analysis results. Two-Way ANOVA results were given in Table 3.7. According to Two-ANOVA analysis, there were statistically significant changes in concentrations of bulk chemical components in terms of season and location.

Results of PCA components analysis on bulk chemical components were given in Figures 3.115-3.116 and Table 3.8-3.9. For Middle-Inner Bay, 3 principal components were enough to model data. Variances explained by principal components were 43%, 22% and 13% for PC1, PC2 and PC3, respectively. Explained percent of data by principal components were 55%, 29% and 16% for PC1, PC2 and PC3, respectively. For Outer Bay, 4 principal components were enough to model data. Variances explained by principal components were 17%, 11% and 9% for PC1, PC2 and PC3, respectively. Explained percent of data by principal components were 27%, 17% and 14% for PC1, PC2 and PC3, respectively.

According to K-means clustering analysis of principal component loadings (Table 3.10) among bulk chemical parameters, DFAA, TDHAA and PHAA were found in the same group with dissolved carbohydrates (MCHO, TDCHO, PCHO), PP, PN and Chl-a at Middle-Inner Bays. For Outer Bay, only PHAA was in the same group with dissolved carbohydrates (MCHO, TDCHO, PCHO), PP, PN and Chl-a. DFAA and TDHAA were found in different groups at Outer Bay.



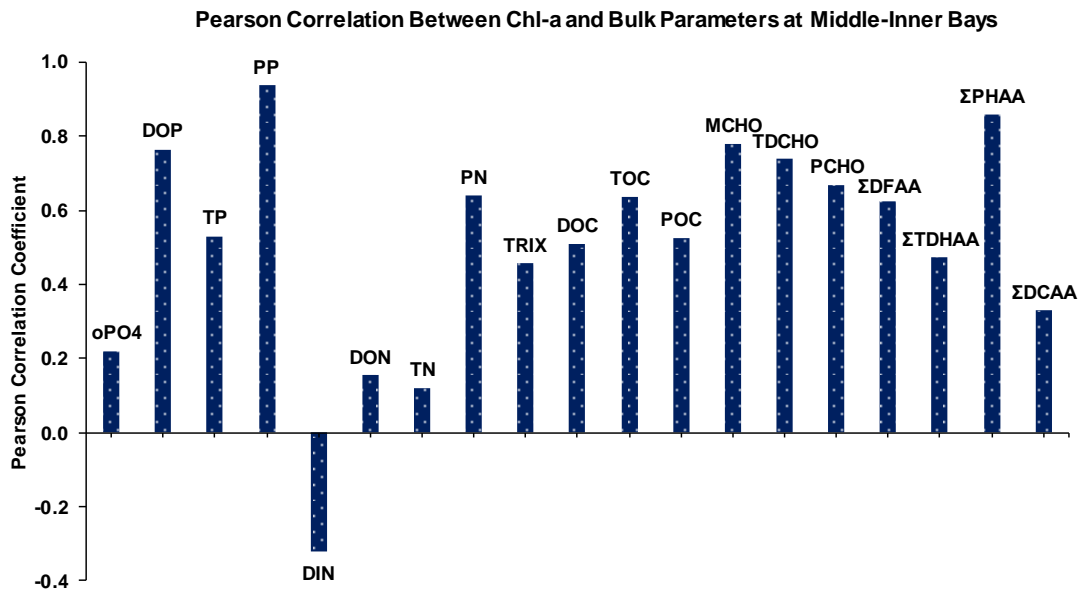


Figure 3.62 Pearson correlation coefficient results between Chl-a and bulk chemical parameters at Middle-Inner Bays

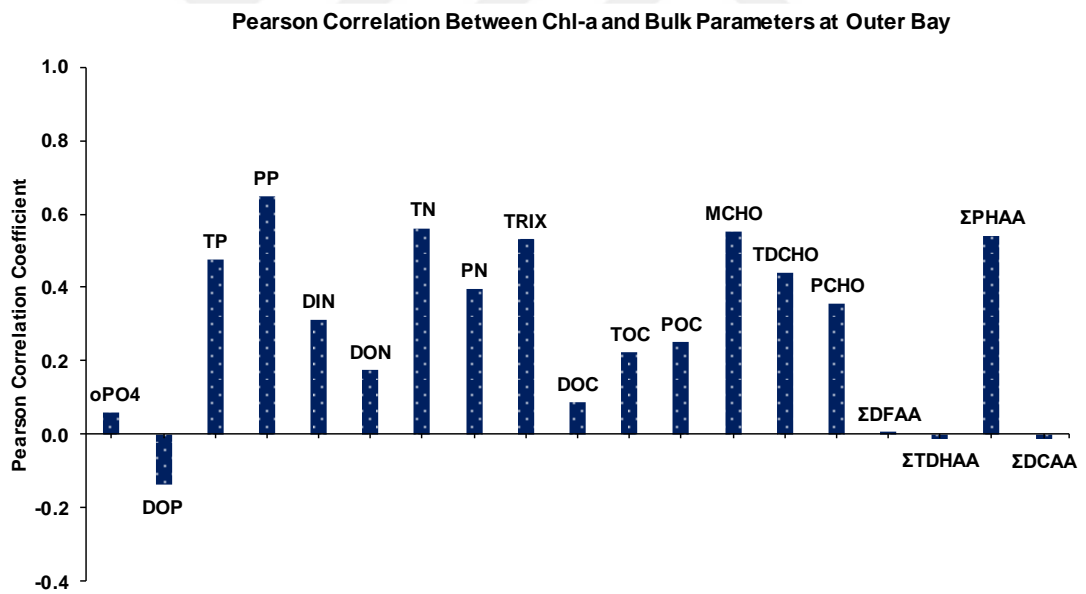


Figure 3.63 Pearson correlation coefficient results between Chl-a and bulk chemical parameters at Outer Bay



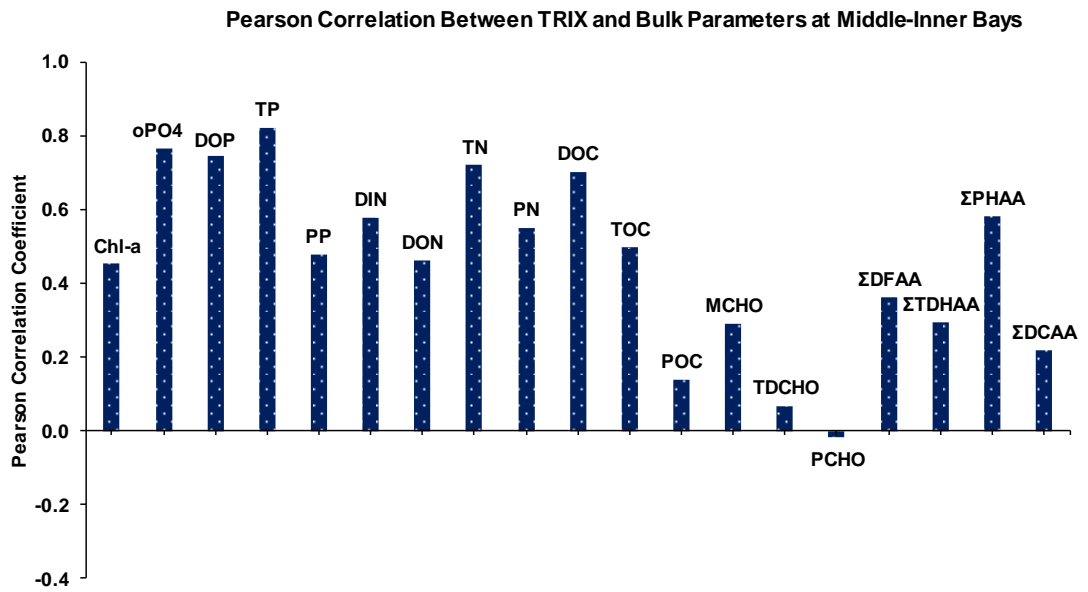


Figure 3.64 Pearson correlation coefficient results between TRIX and bulk chemical parameters at Middle-Inner Bays

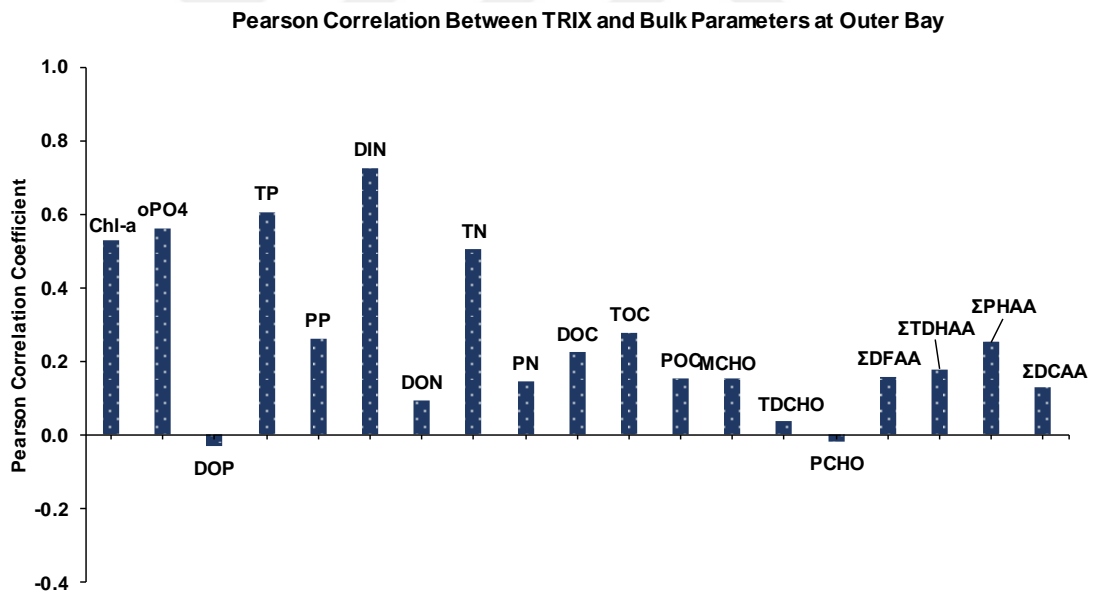


Figure 3.65 Pearson correlation coefficient results between TRIX and bulk chemical parameters at Outer Bay

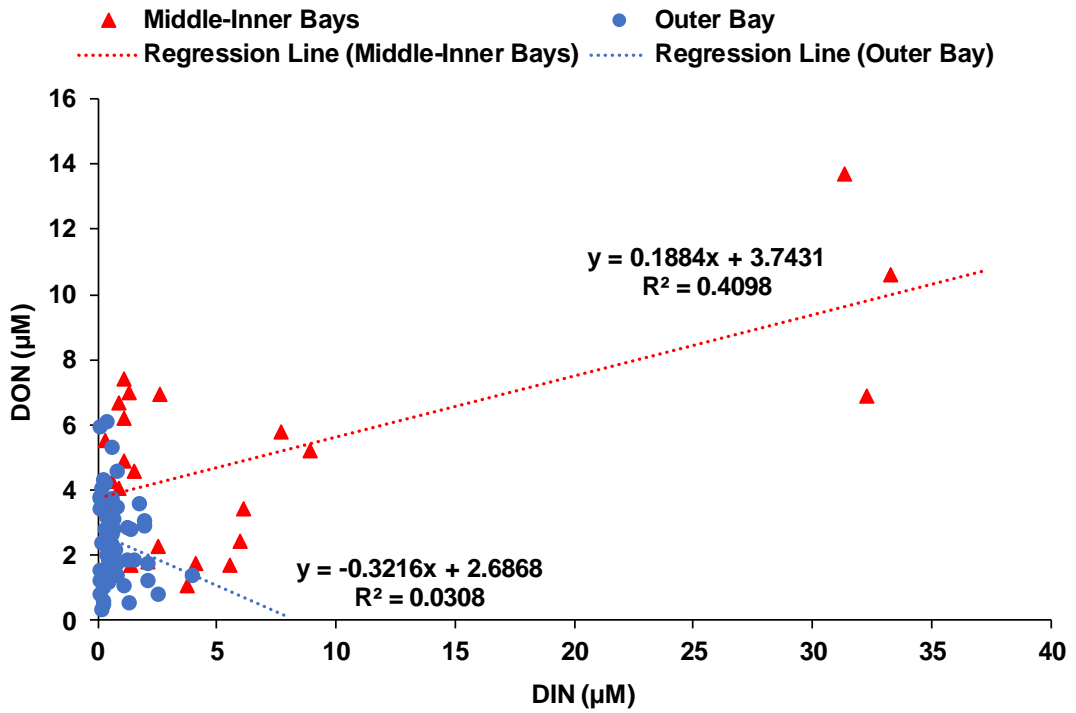


Figure 3.66 Linearity between DIN and DON at Middle-Inner and Outer Bays

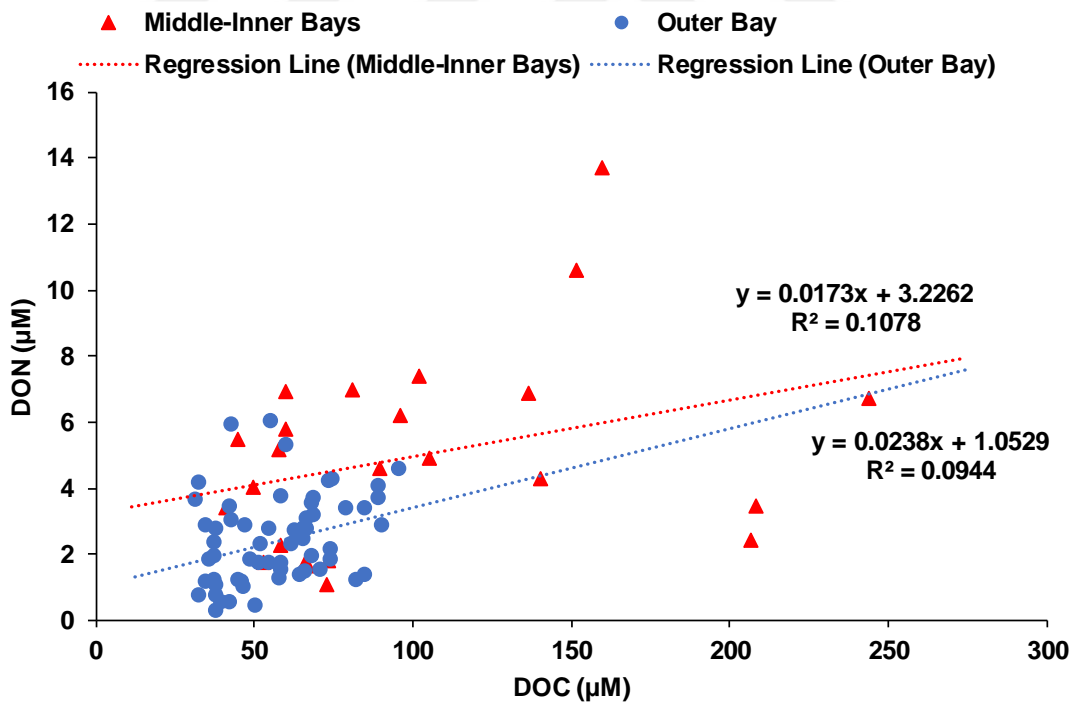


Figure 3.67 Linearity between DOC and DON at Middle-Inner and Outer Bays





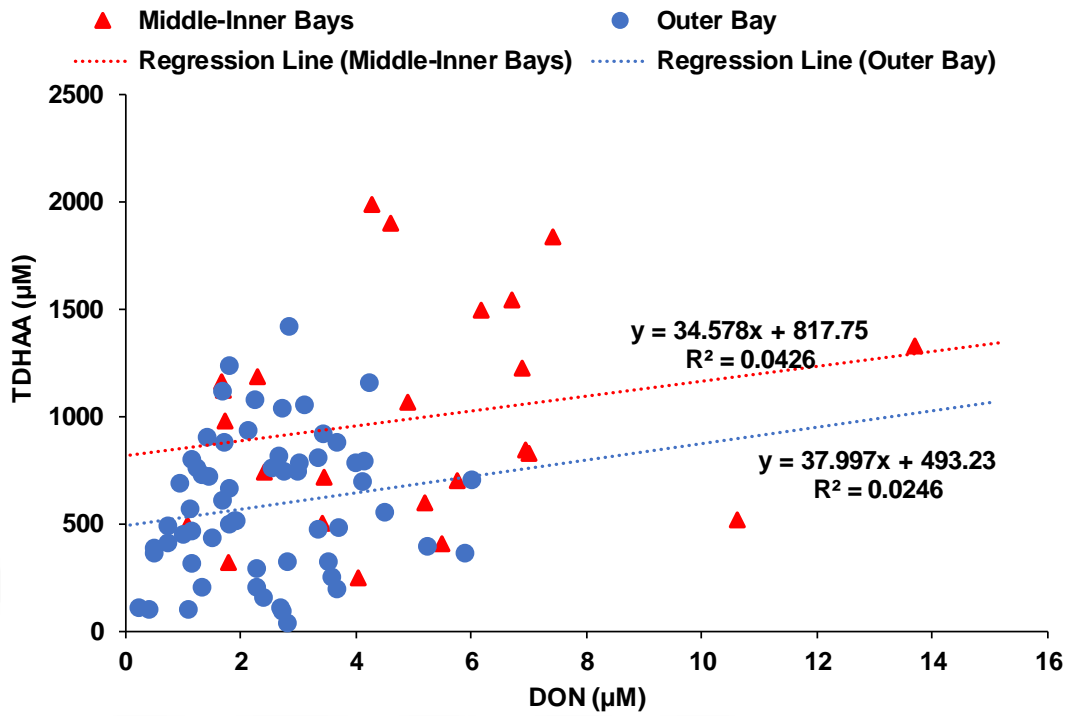


Figure 3.72 Linearity between DON and TDHAA at Middle-Inner and Outer Bays

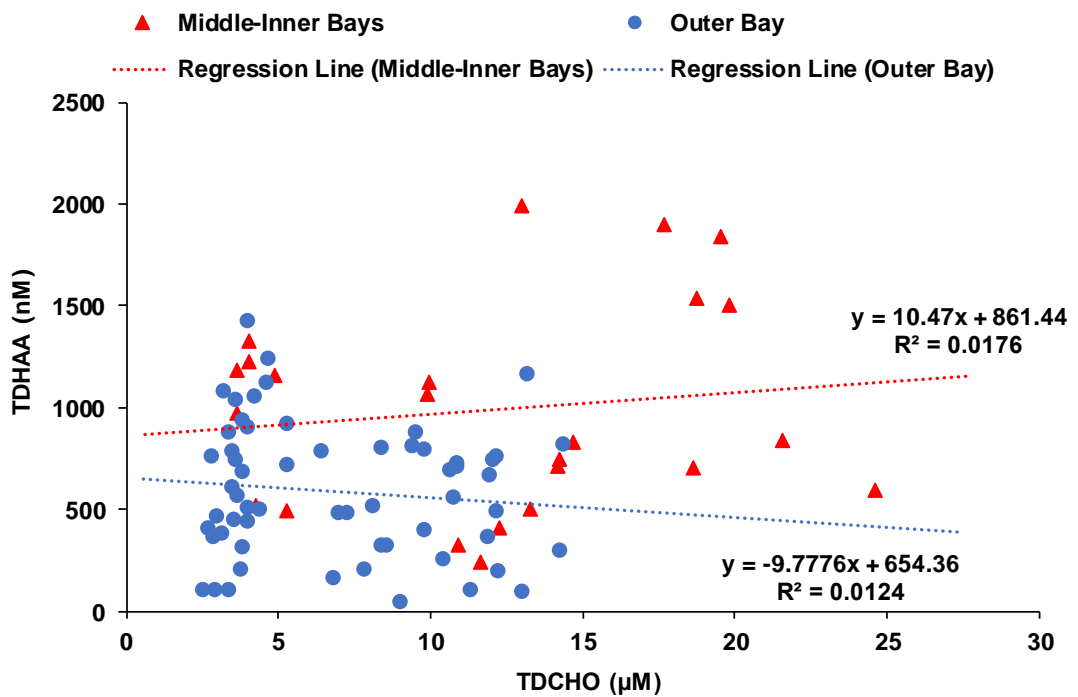


Figure 3.73 Linearity between TDCHO and TDHAA at Middle-Inner and Outer Bays

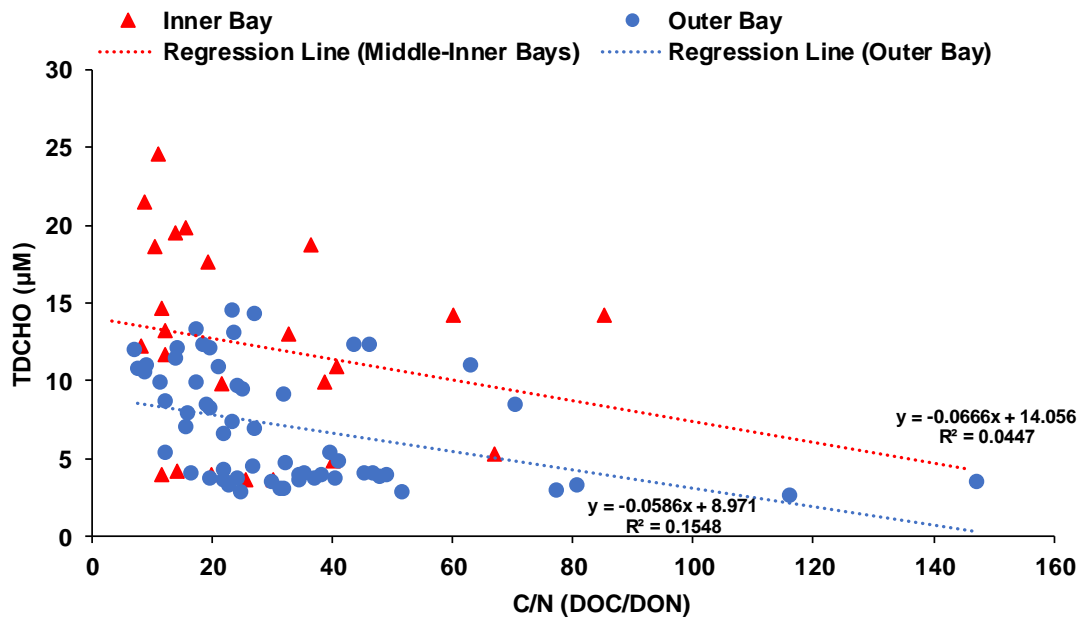


Figure 3.74 Linearity between C/N (DOC/DON) and TDCHO at Middle-Inner and Outer Bays

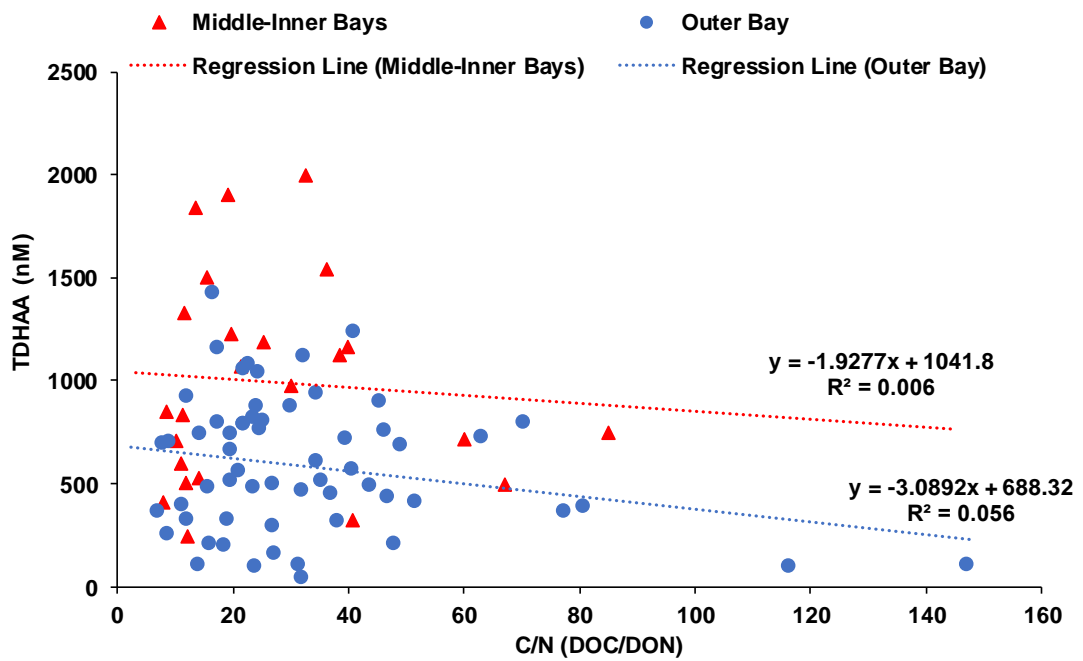


Figure 3.75 Linearity between C/N (DOC/DON) and TDHAA at Middle-Inner and Outer Bays

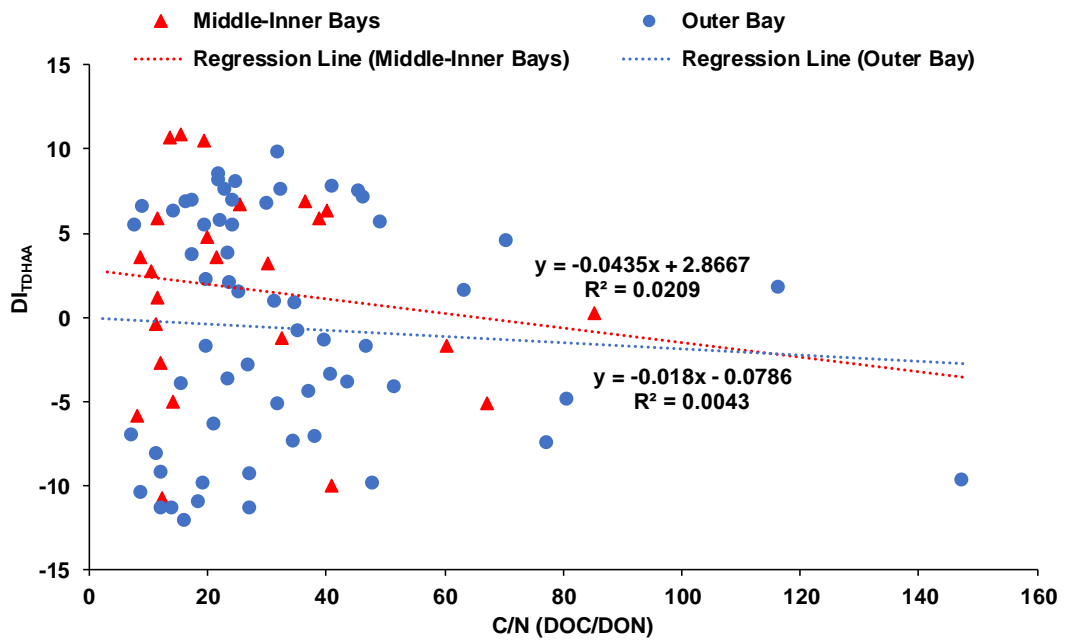


Figure 3.76 Linearity between C/N (DOC/DON) and  $DI_{TDHAA}$  at Middle-Inner and Outer Bays

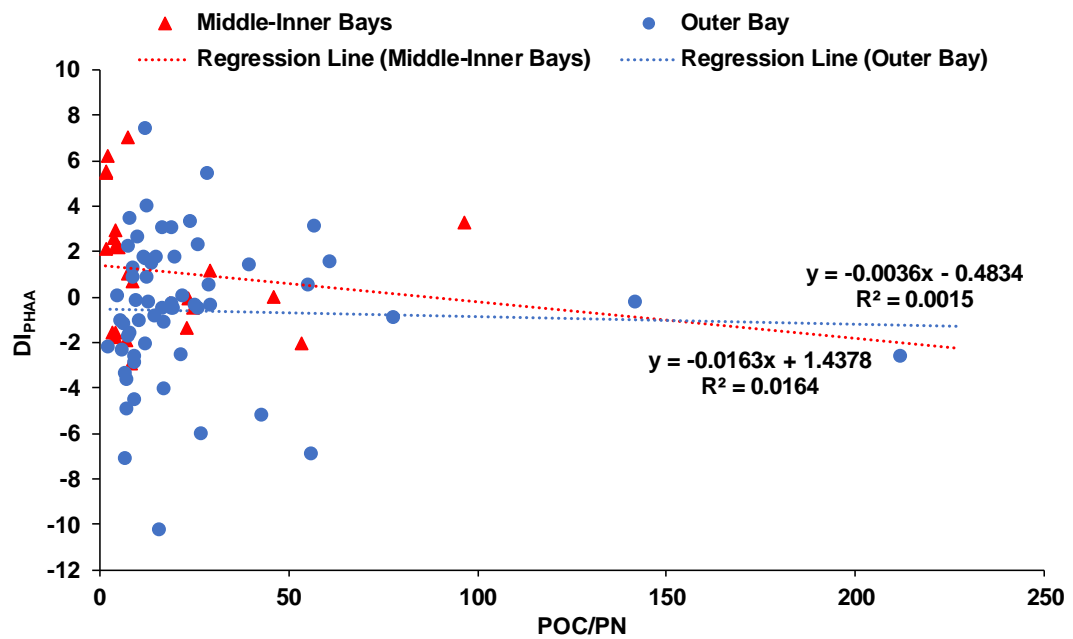


Figure 3.77 Linearity between POC/PN and  $DI_{PHAA}$  at Middle-Inner and Outer Bays

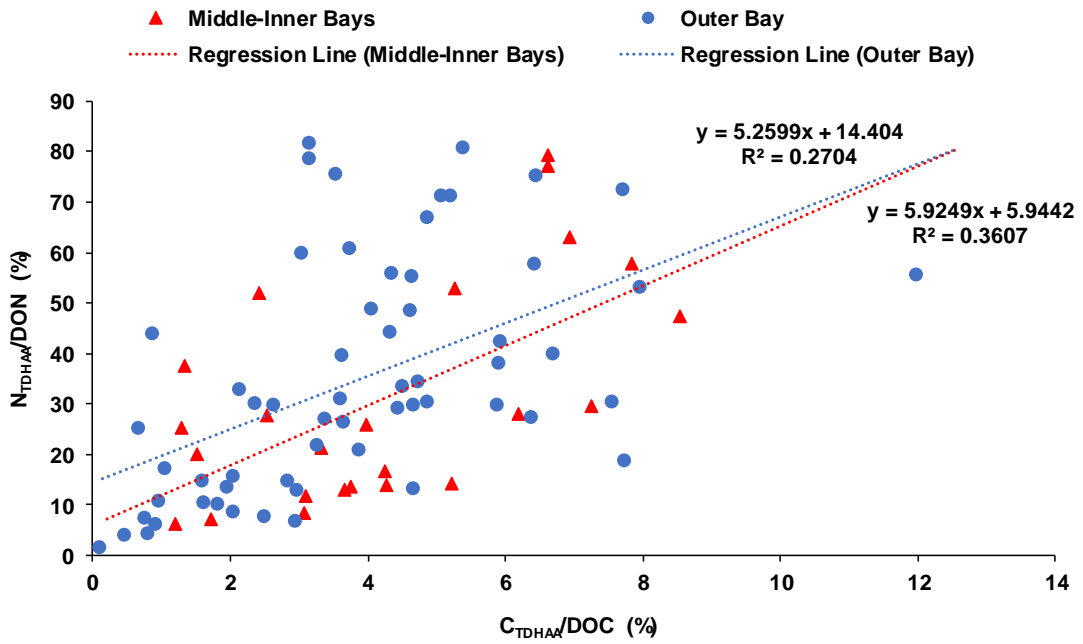


Figure 3.78 Linearity between  $C_{TDHAA}/DOC$  and  $N_{TDHAA}/DON$  at Middle-Inner and Outer Bays

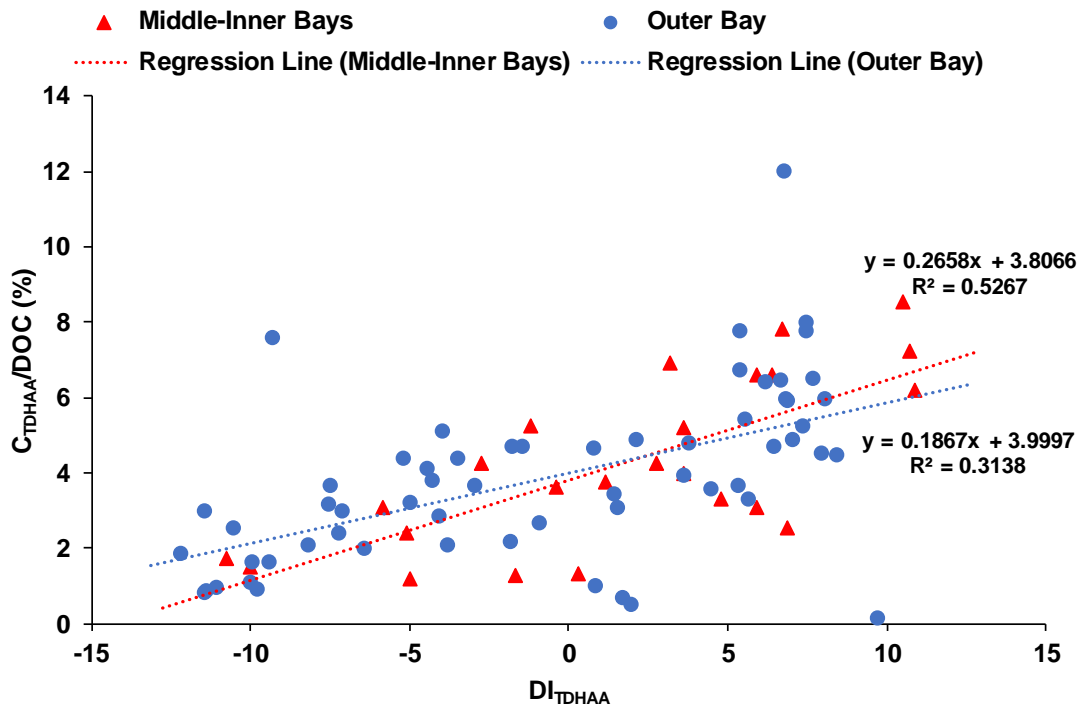


Figure 3.79 Linearity between  $DI_{TDHAA}$  and  $C_{TDHAA}/DOC$  at Middle-Inner and Outer Bays



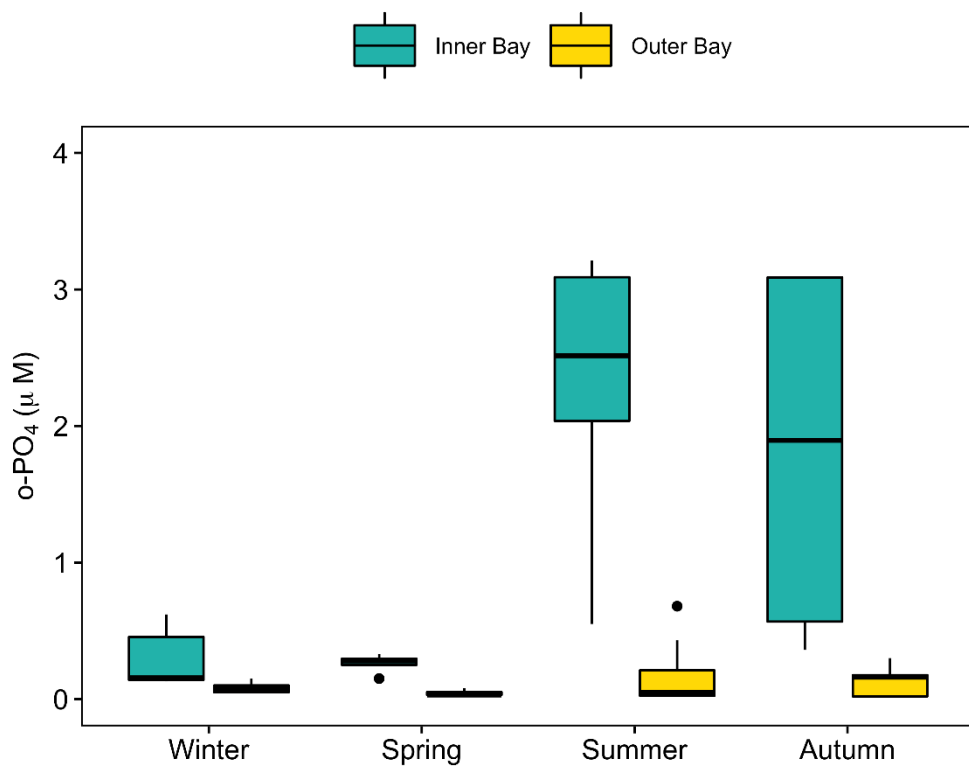


Figure 3.80 Seasonal and spatial variations of o-PO<sub>4</sub>

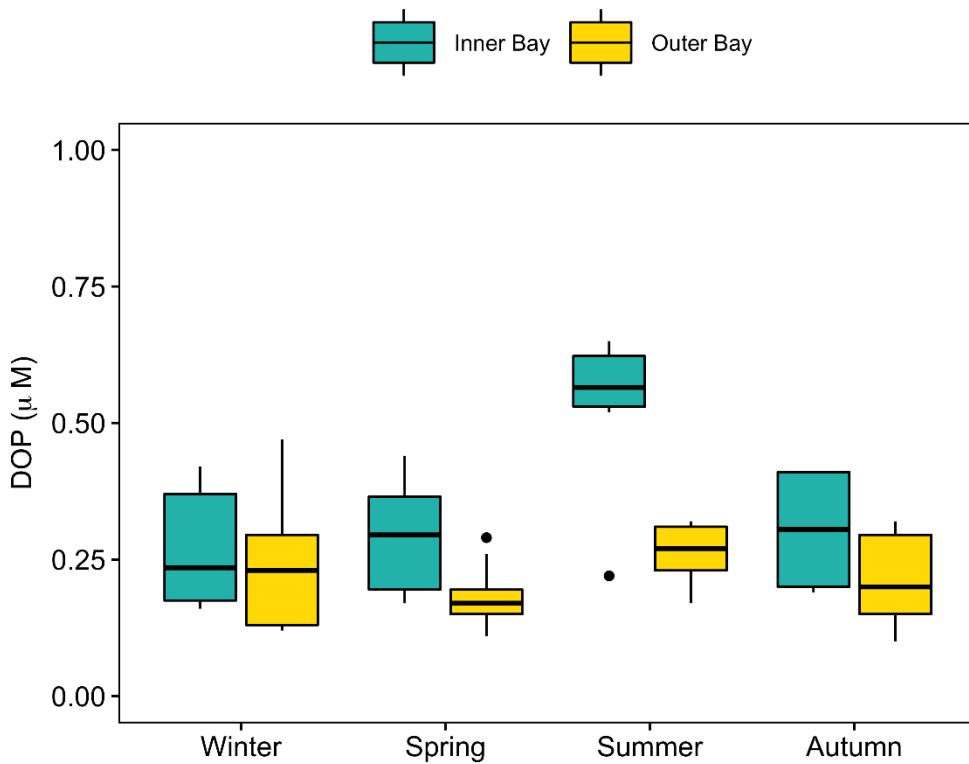


Figure 3.81 Seasonal and spatial variations of DOP

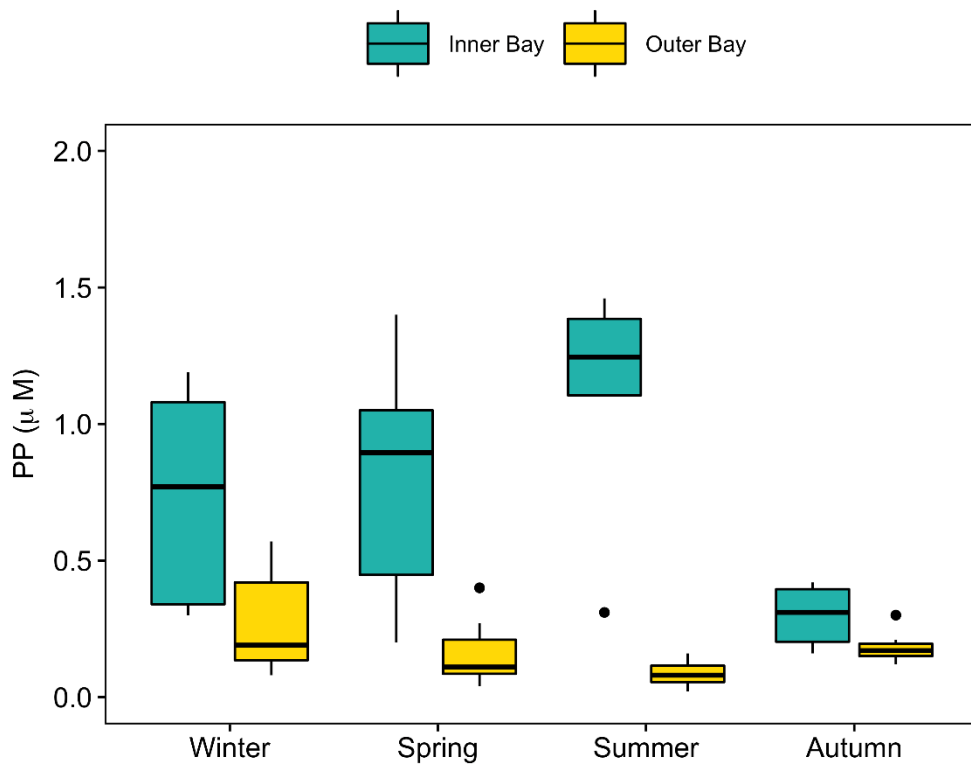


Figure 3.82 Seasonal and spatial variations of PP

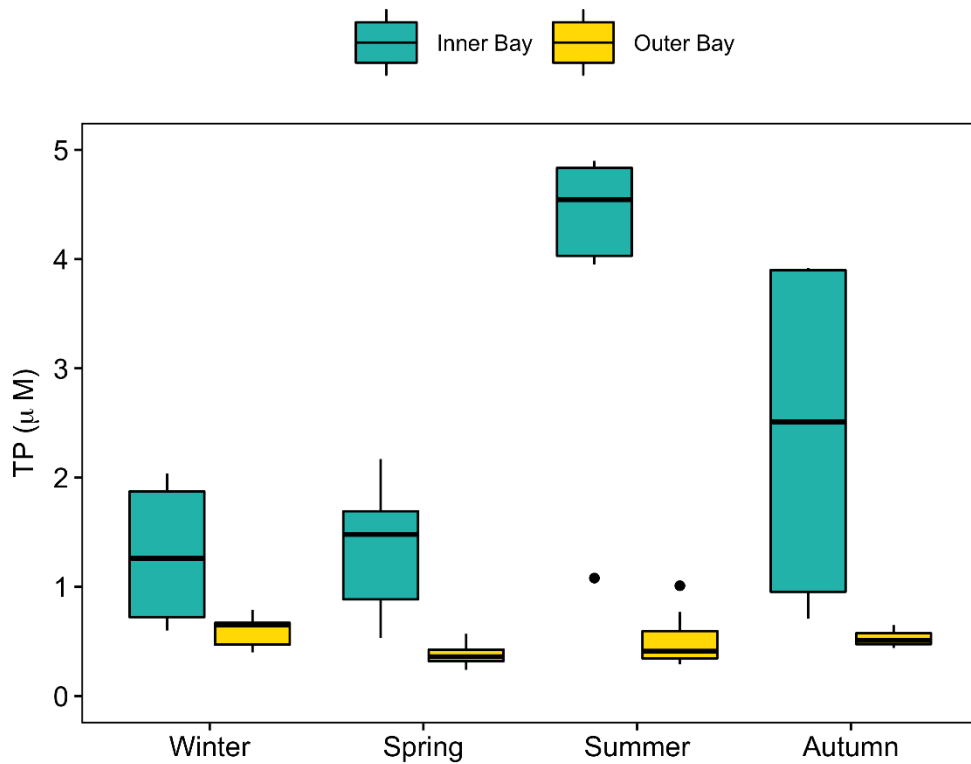


Figure 3.83 Seasonal and spatial variations of TP

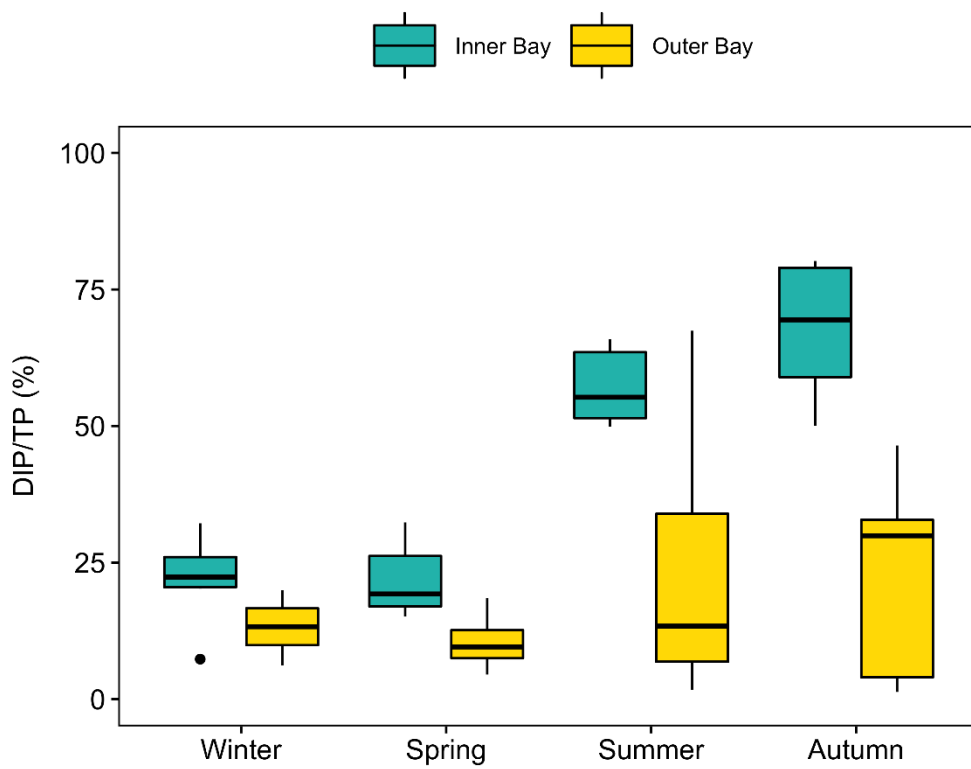


Figure 3.84 Seasonal and spatial variations of DIP/TP

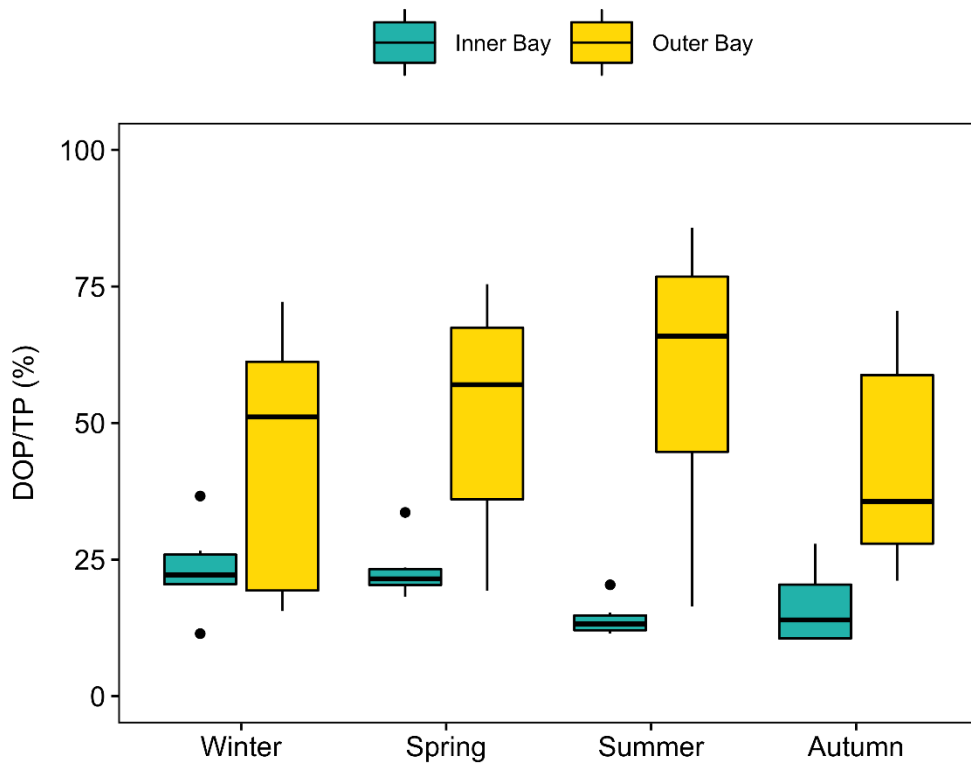


Figure 3.85 Seasonal and spatial variations of DOP/TP

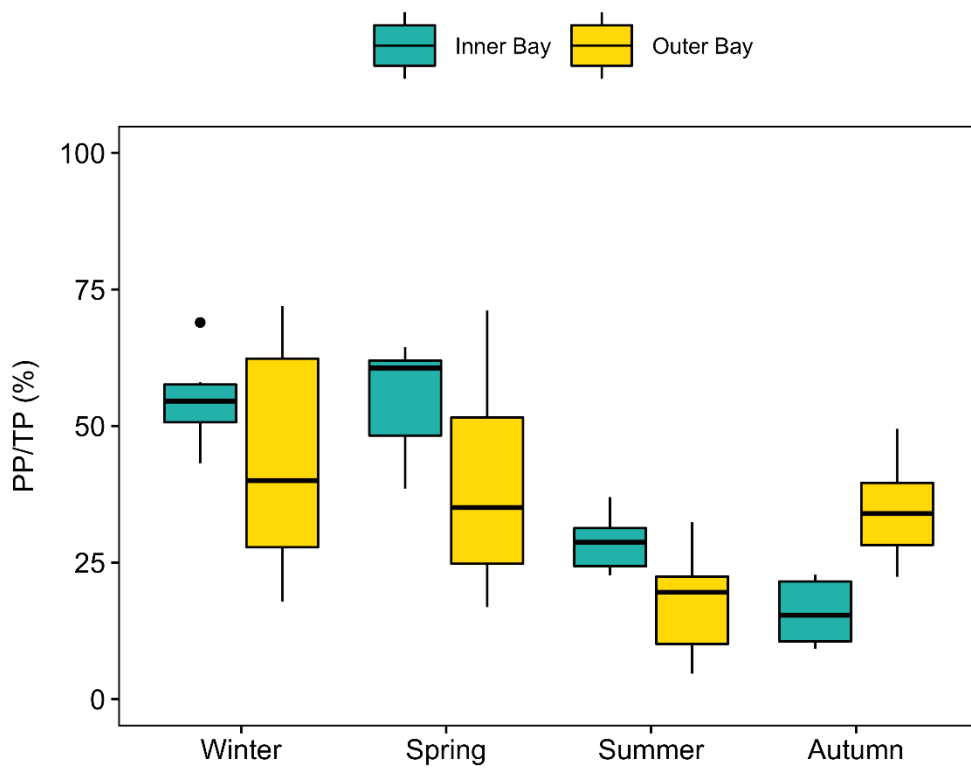


Figure 3.86 Seasonal and spatial variations of PP/TP

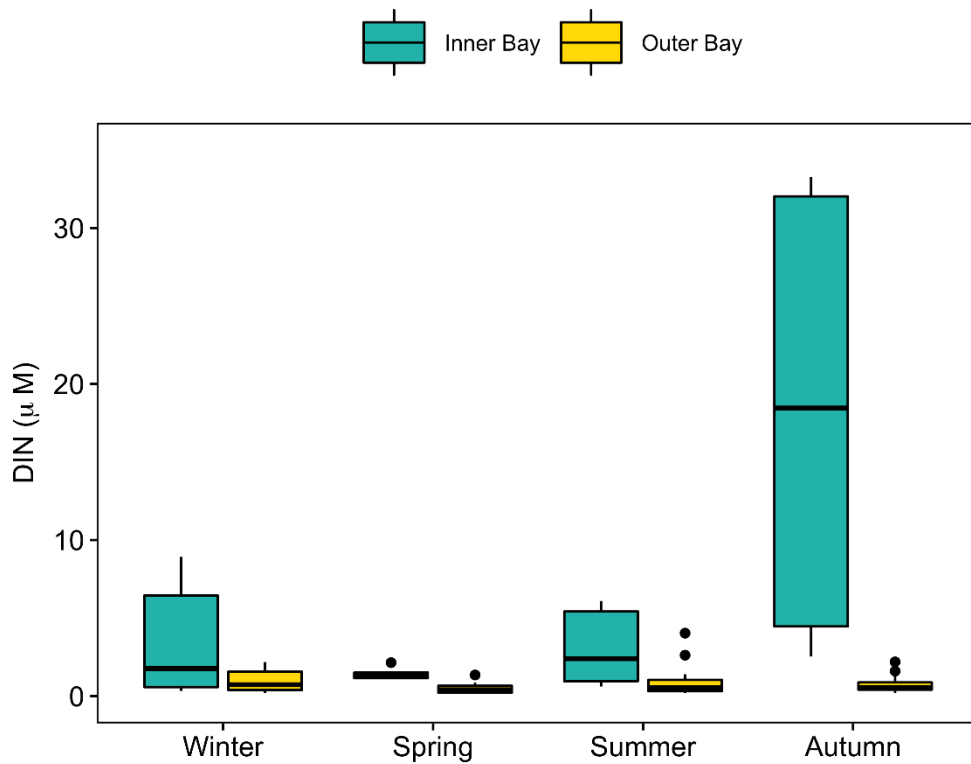


Figure 3.87 Seasonal and spatial variations of DIN

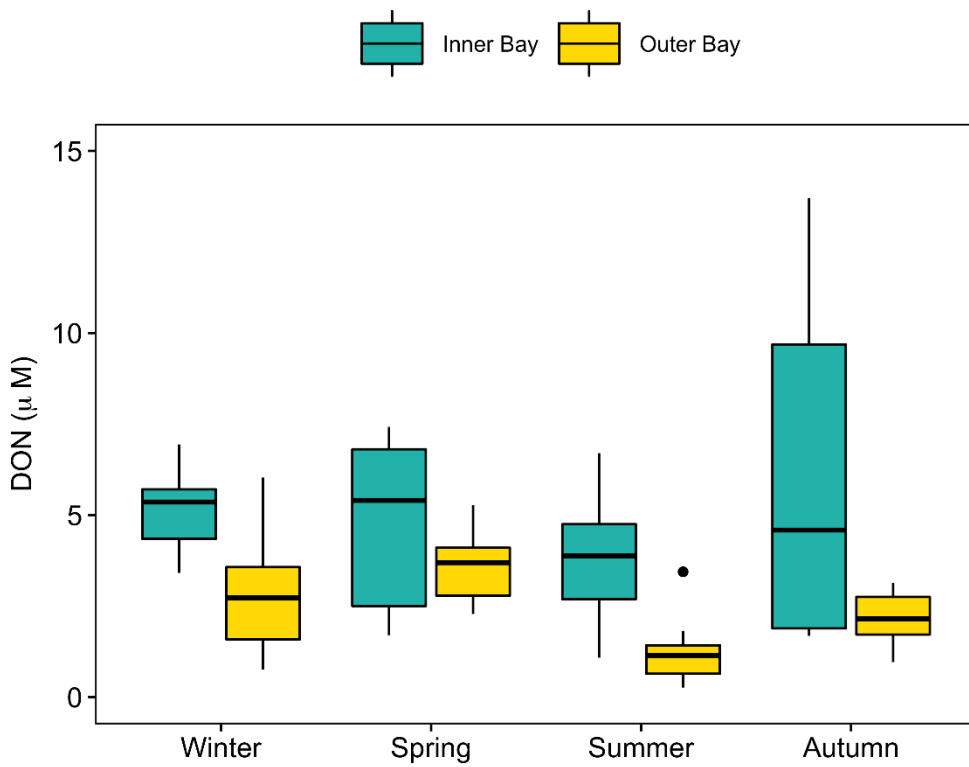


Figure 3.88 Seasonal and spatial variations of DON

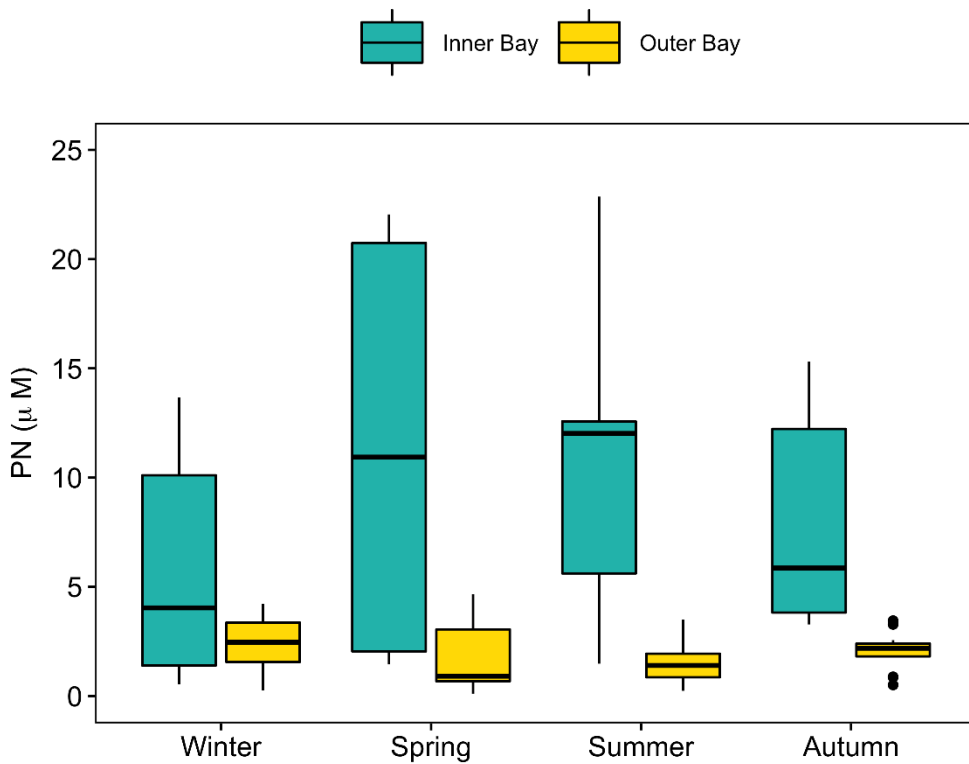


Figure 3.89 Seasonal and spatial variations of PN

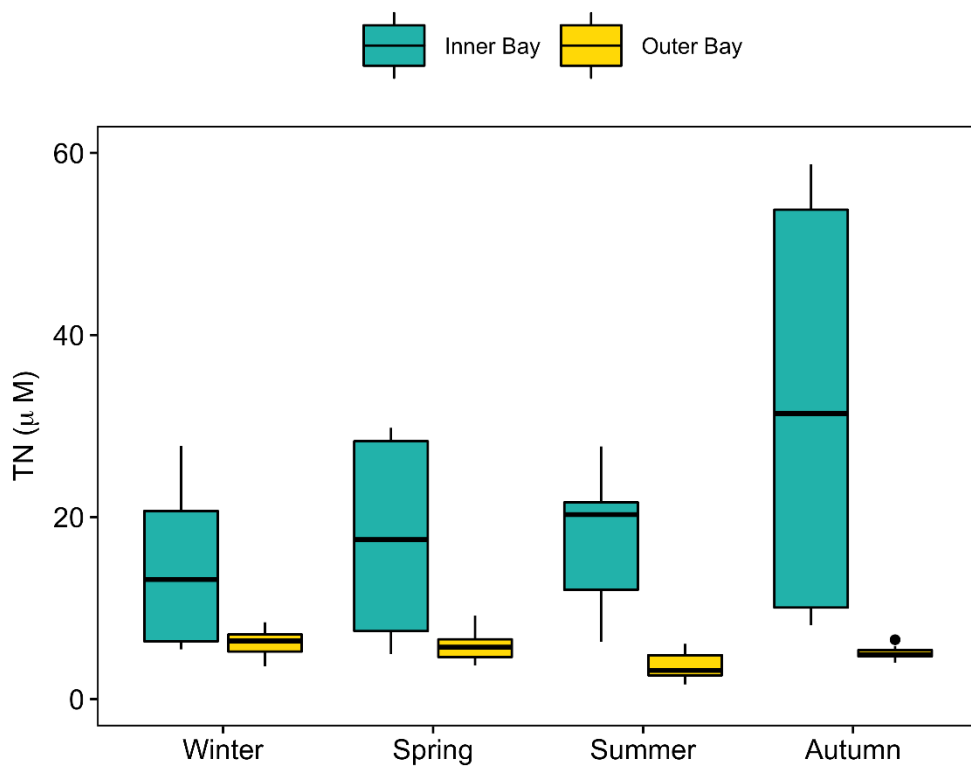


Figure 3.90 Seasonal and spatial variations of TN

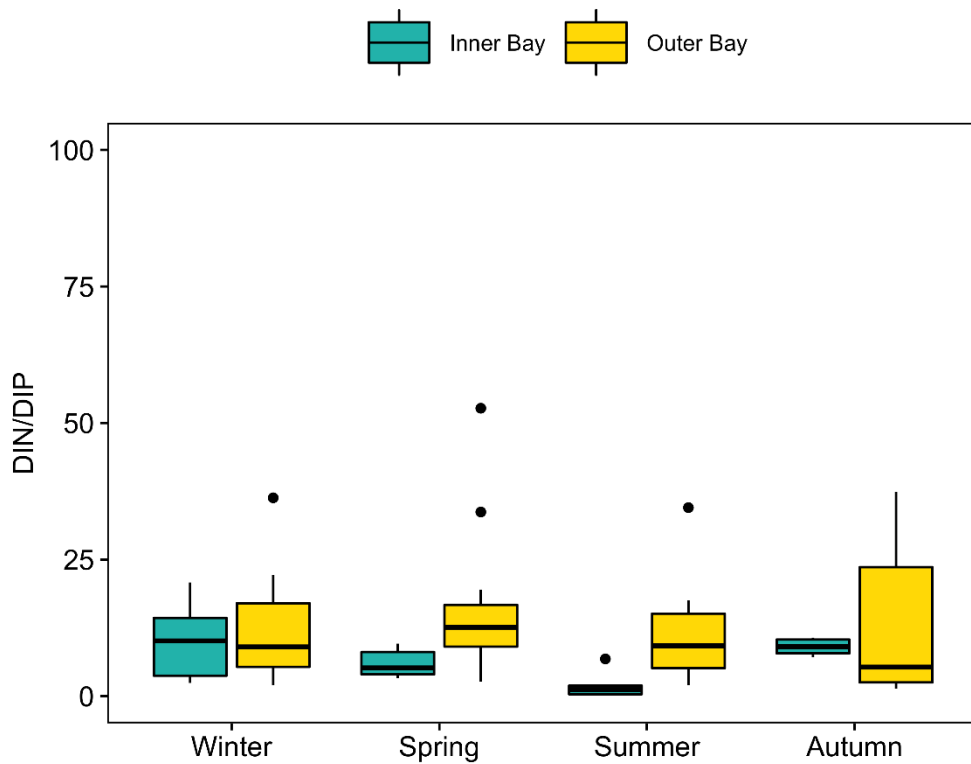


Figure 3.91 Seasonal and spatial variations of DIN/DIP

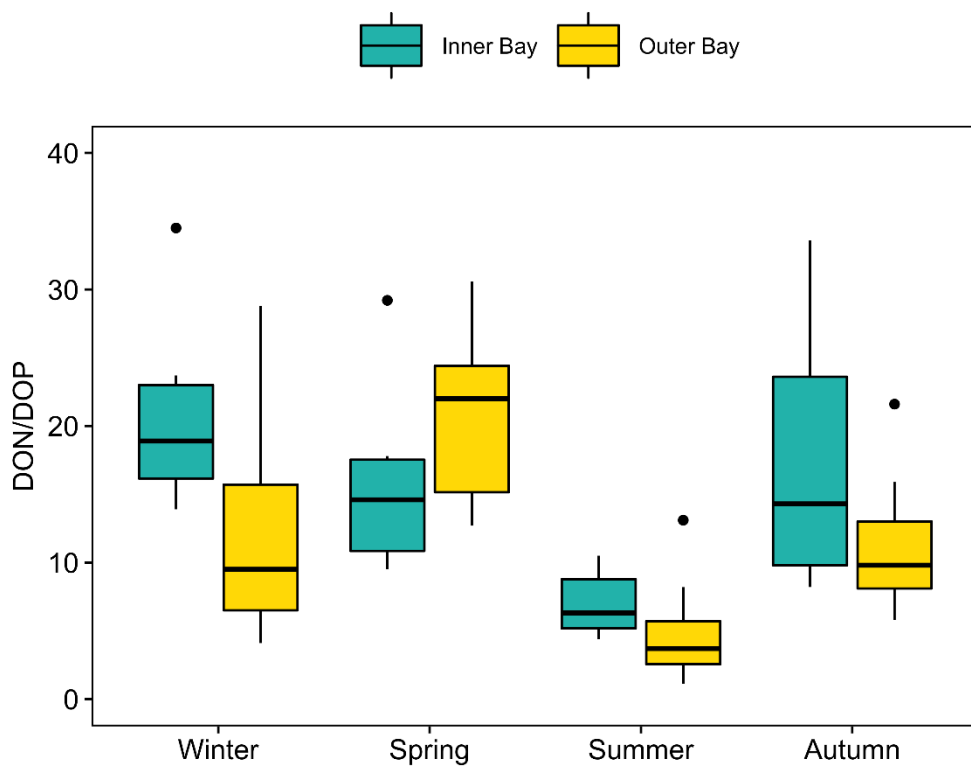


Figure 3.92 Seasonal and spatial variations of DON/DOP

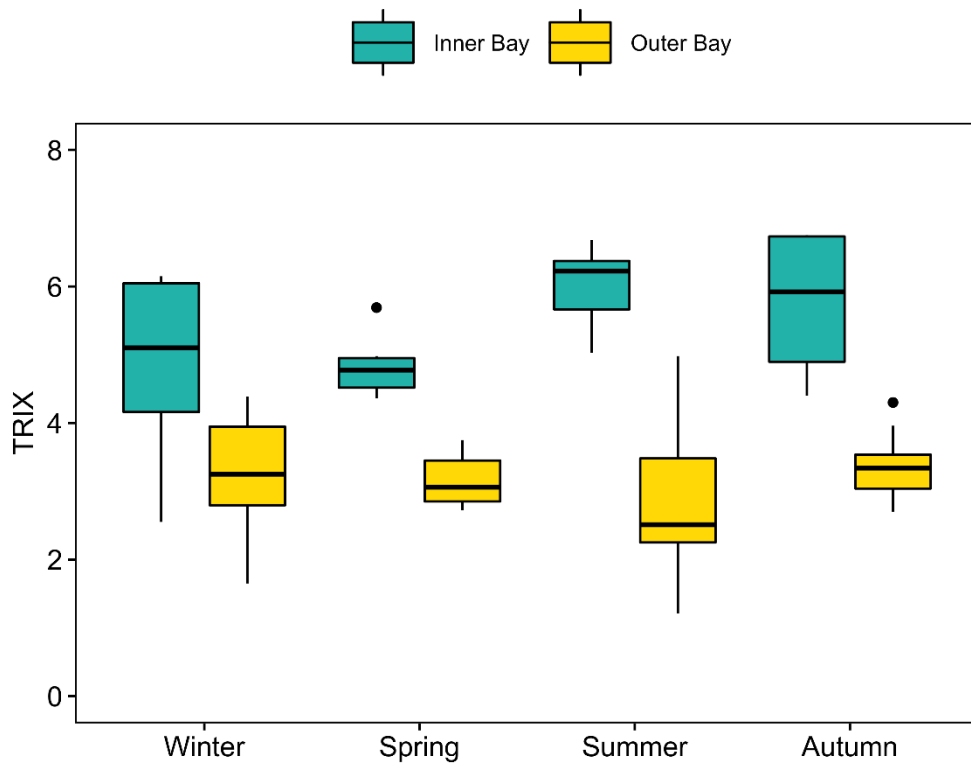


Figure 3.93 Seasonal and spatial variations of TRIX

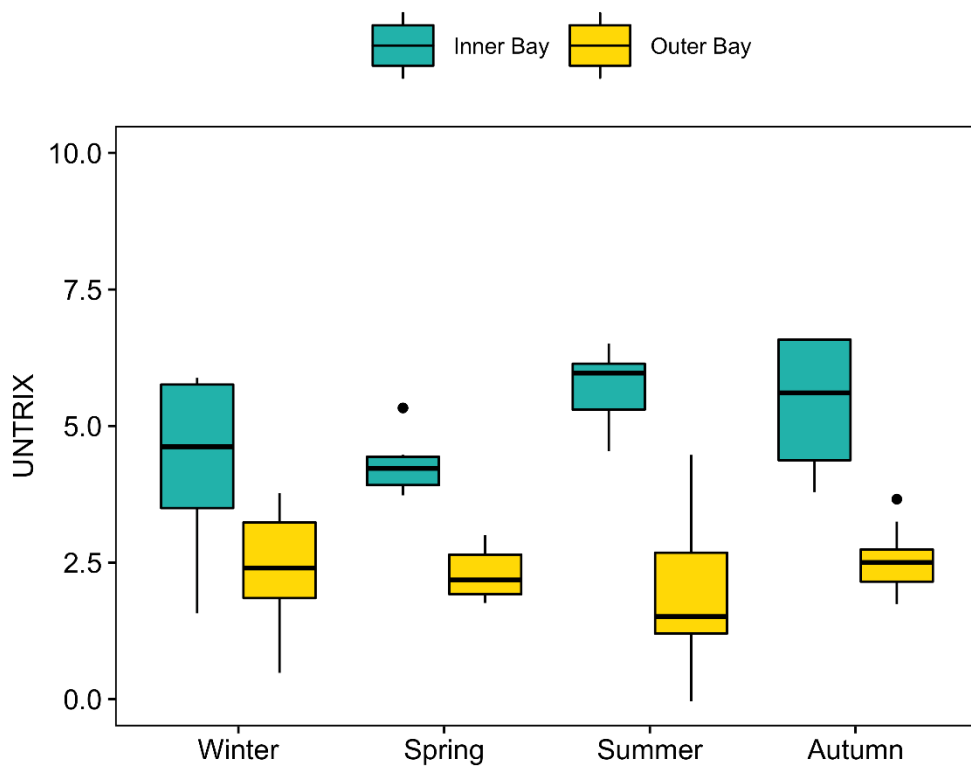


Figure 3.94 Seasonal and spatial variations of UNTRIX

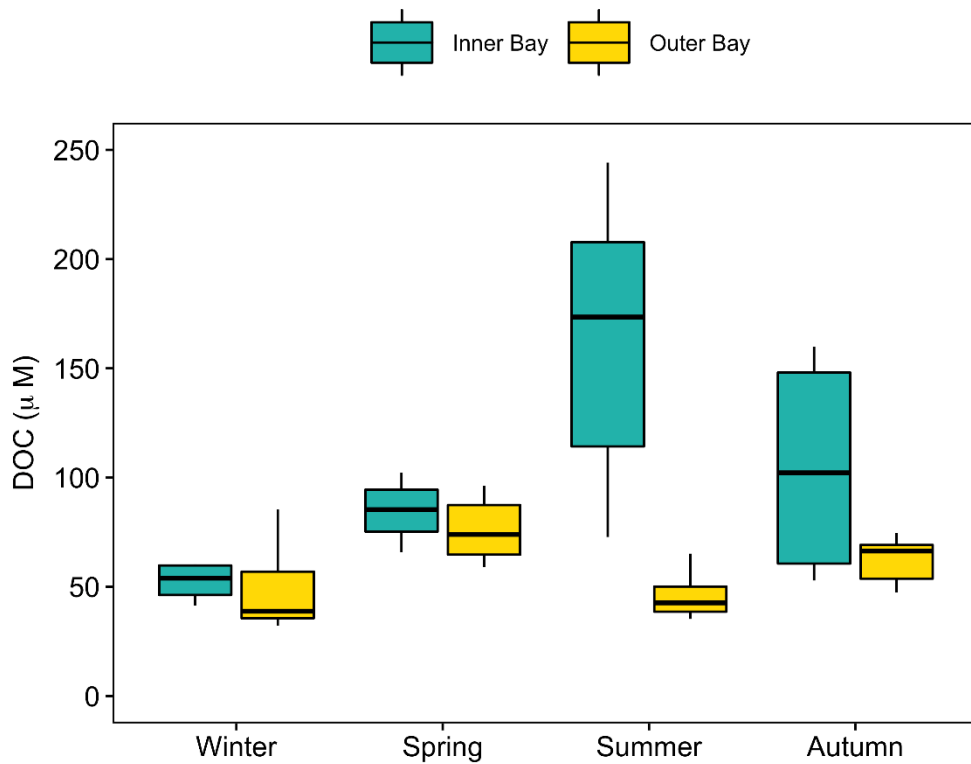


Figure 3.95 Seasonal and spatial variations of DOC



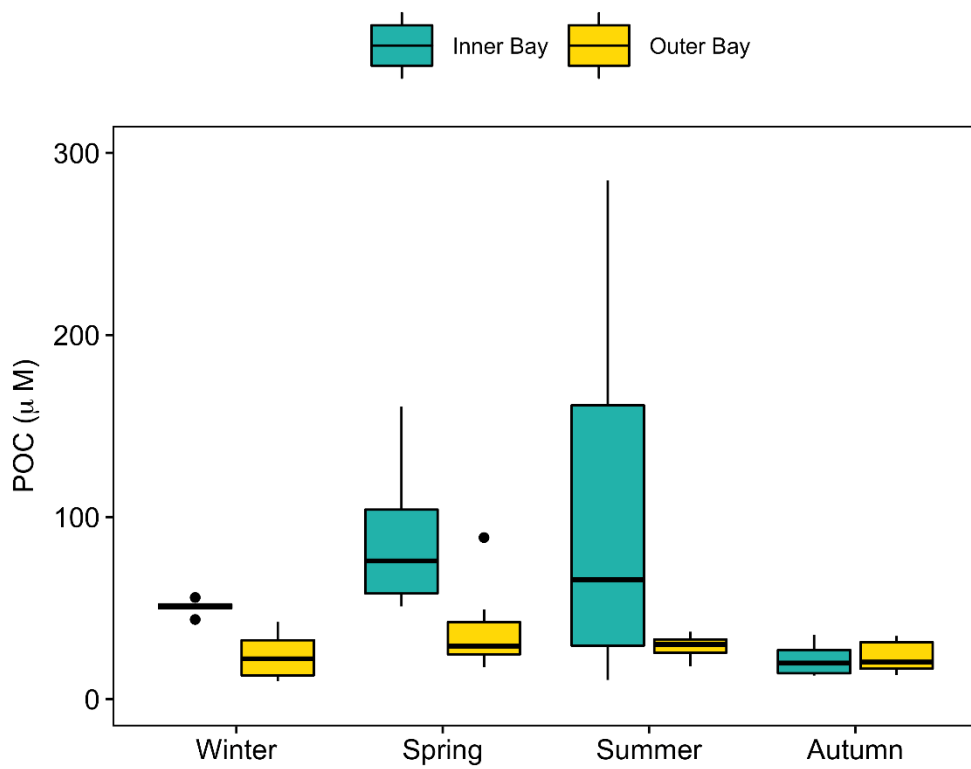


Figure 3.96 Seasonal and spatial variations of POC

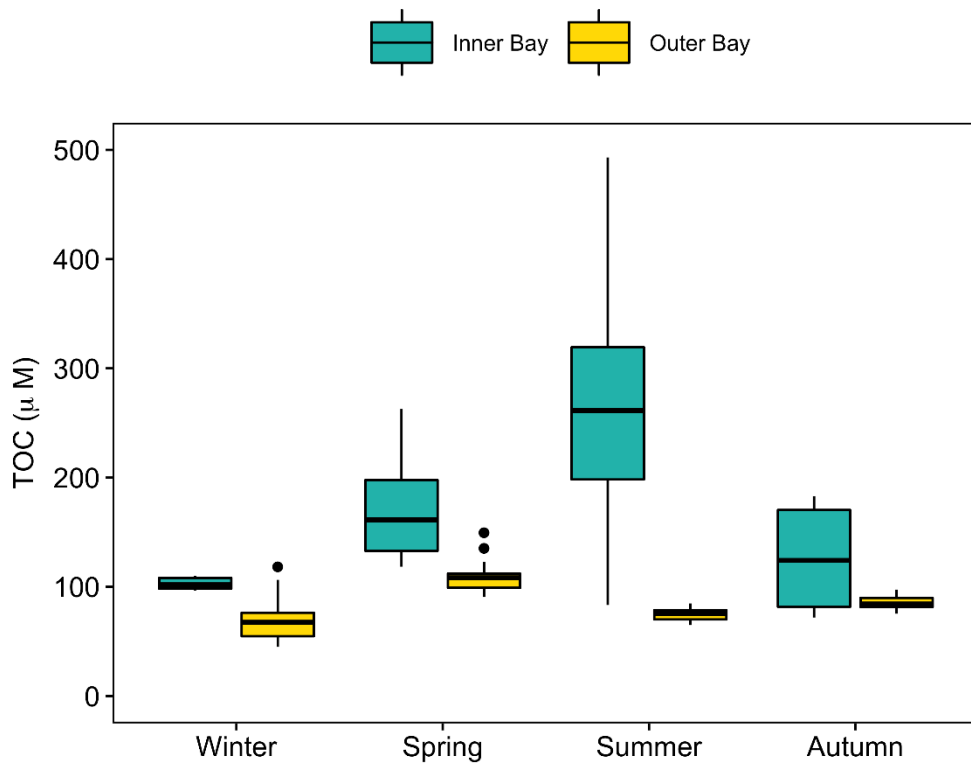


Figure 3.97 Seasonal and spatial variations of TOC

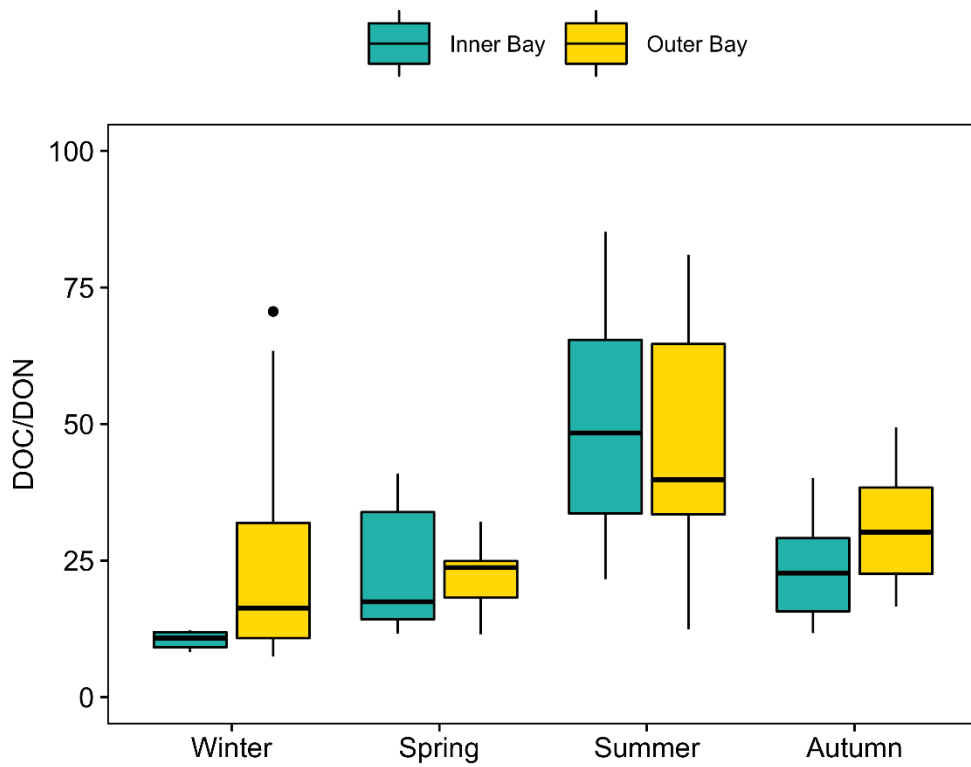


Figure 3.98 Seasonal and spatial variations of DOC/DON

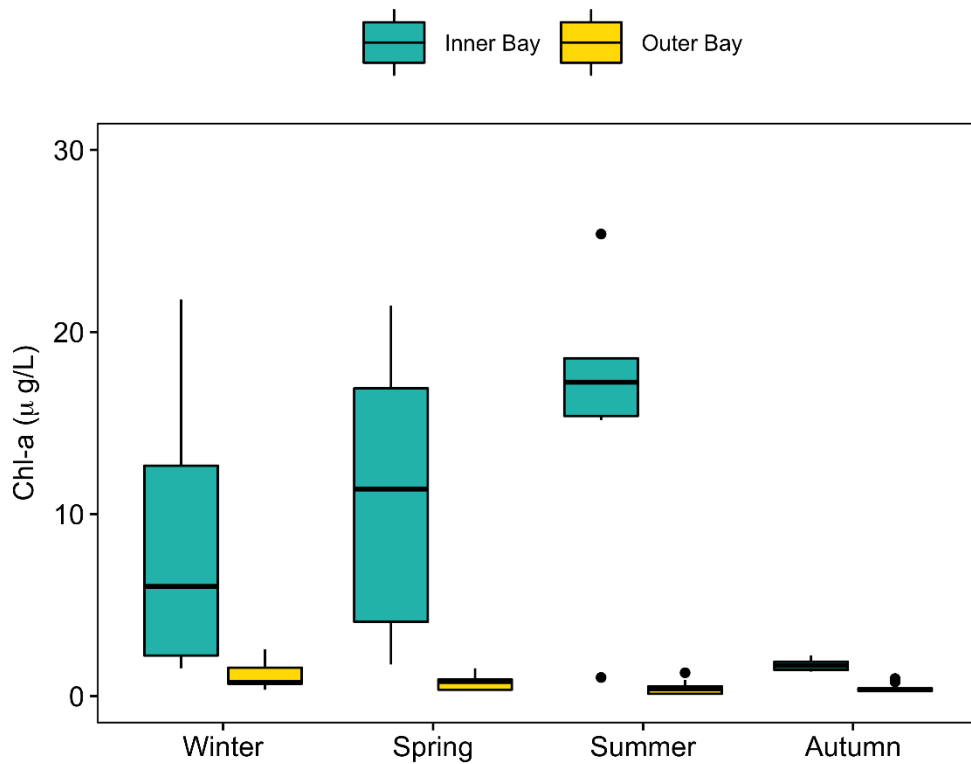


Figure 3.99 Seasonal and spatial variations of Chl-a

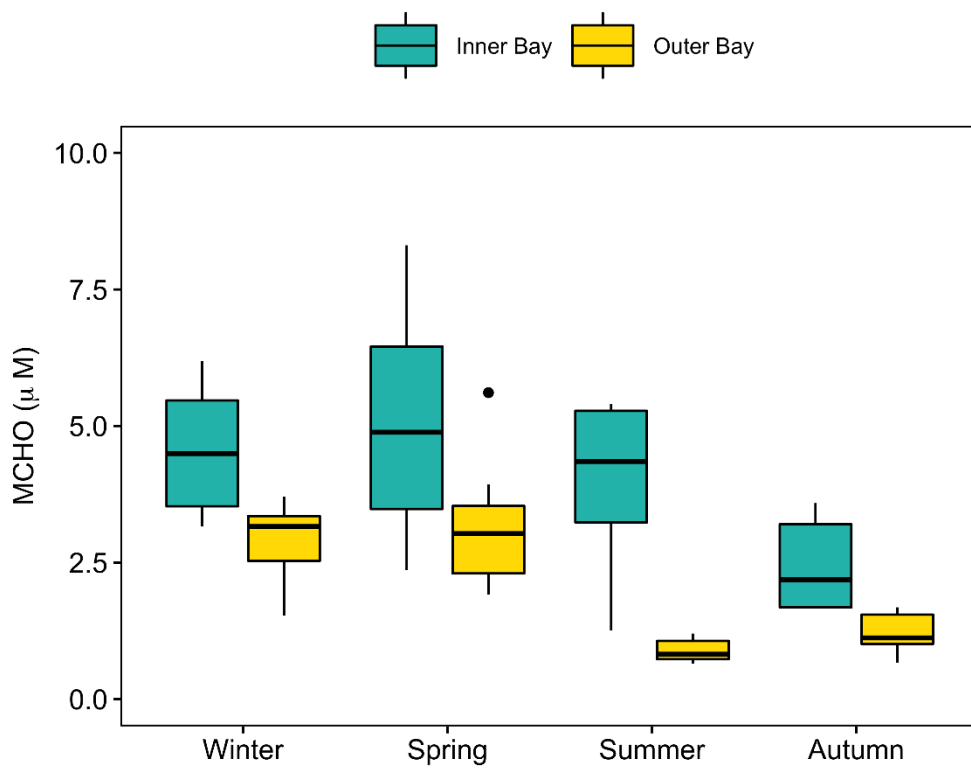


Figure 3.100 Seasonal and spatial variations of MCHO

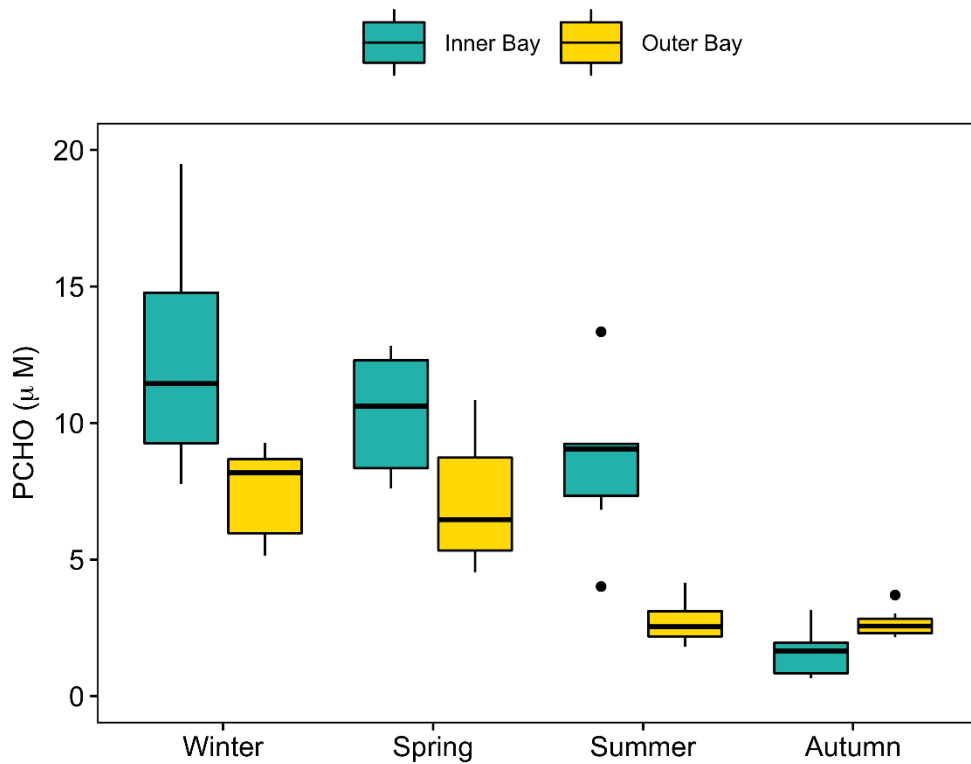


Figure 3.101 Seasonal and spatial variations of PCHO

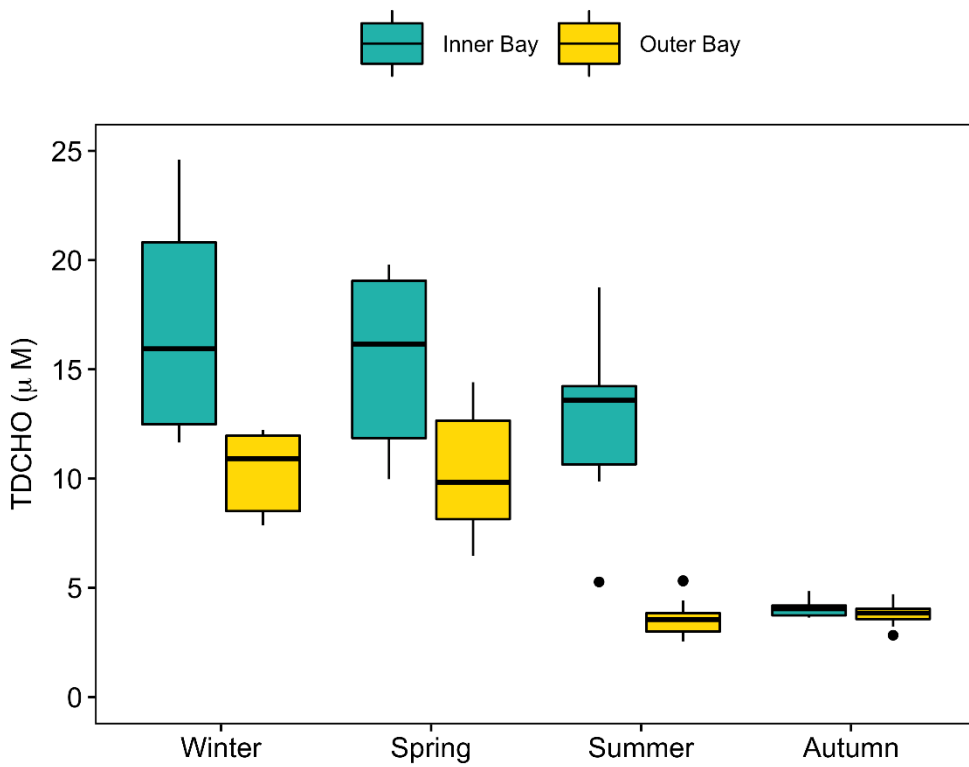


Figure 3.102 Seasonal and spatial variations of TDCHO

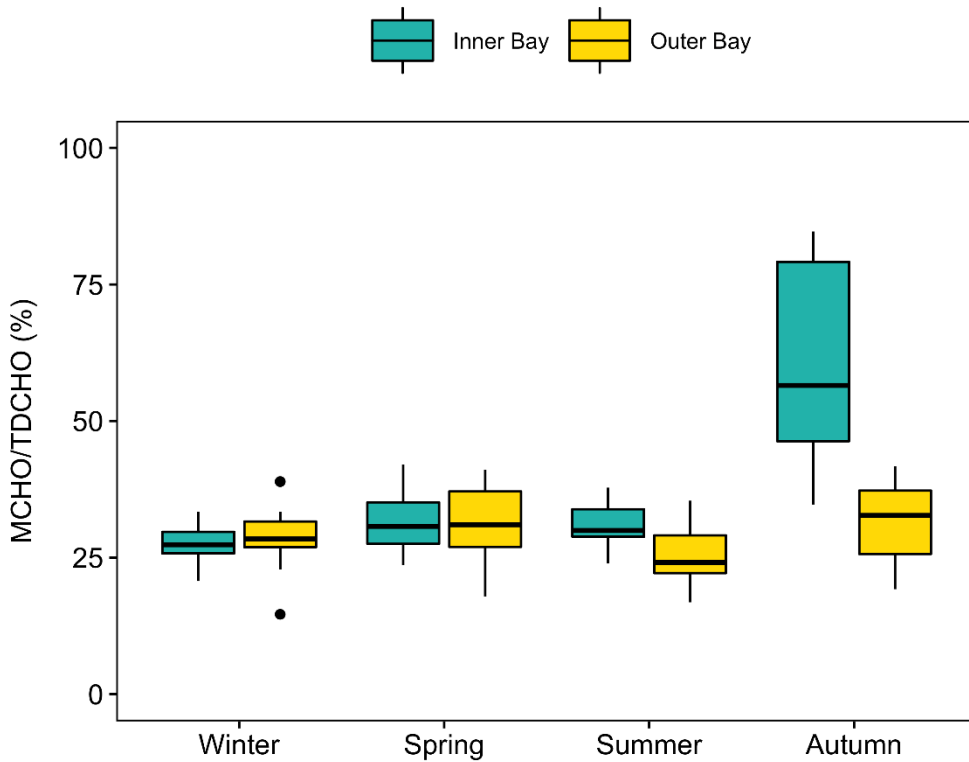


Figure 3.103 Seasonal and spatial variations of MCHO/TDCHO

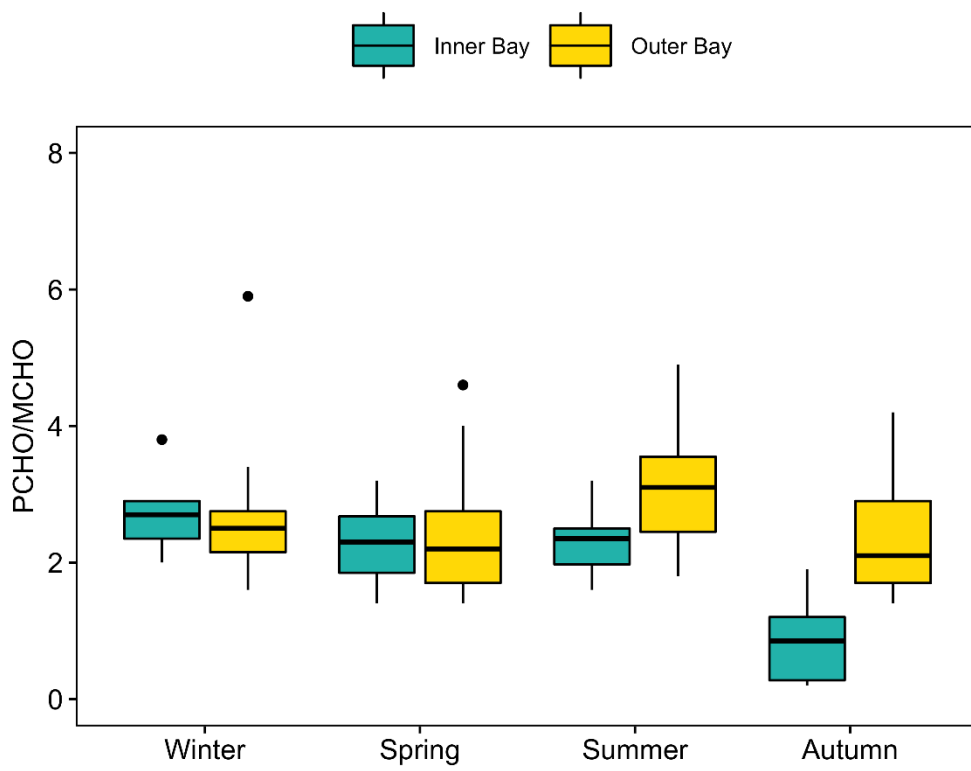


Figure 3.104 Seasonal and spatial variations of PCHO/MCHO

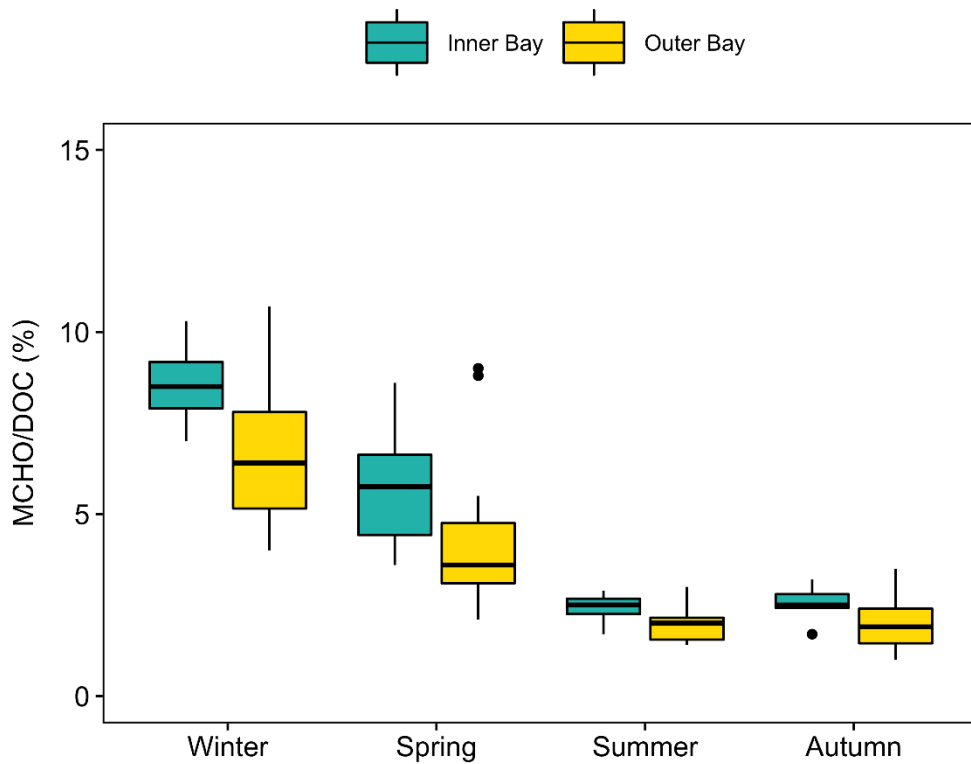


Figure 3.105 Seasonal and spatial variations of MCHO/DOC

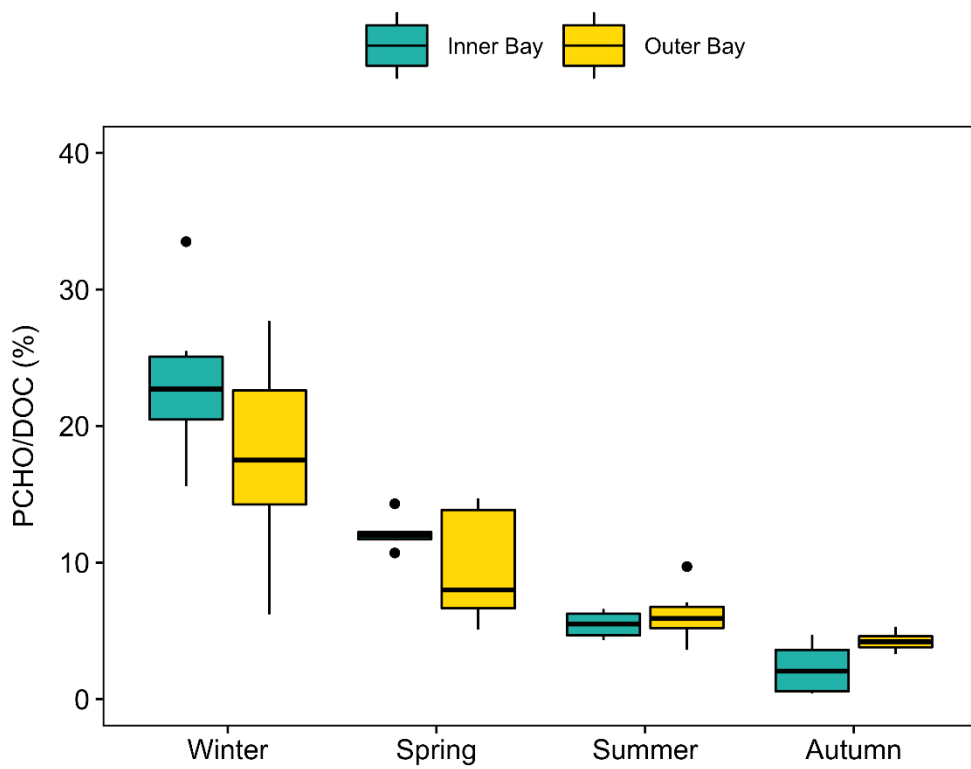


Figure 3.106 Seasonal and spatial variations of PCHO/DOC

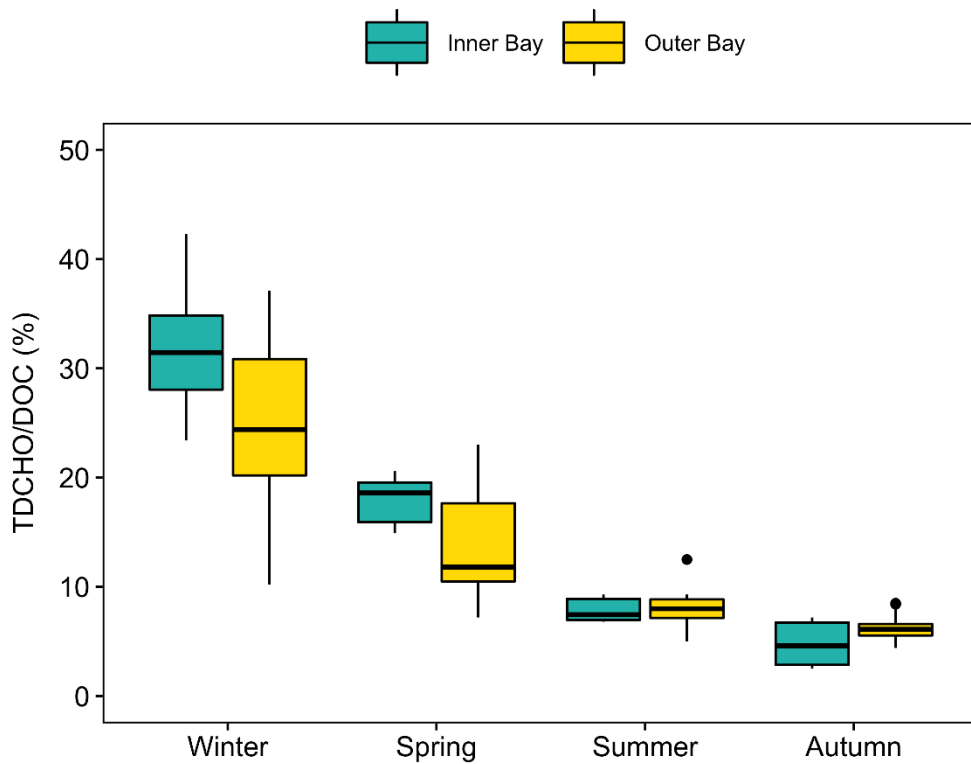


Figure 3.107 Seasonal and spatial variations of TDCHO/DOC

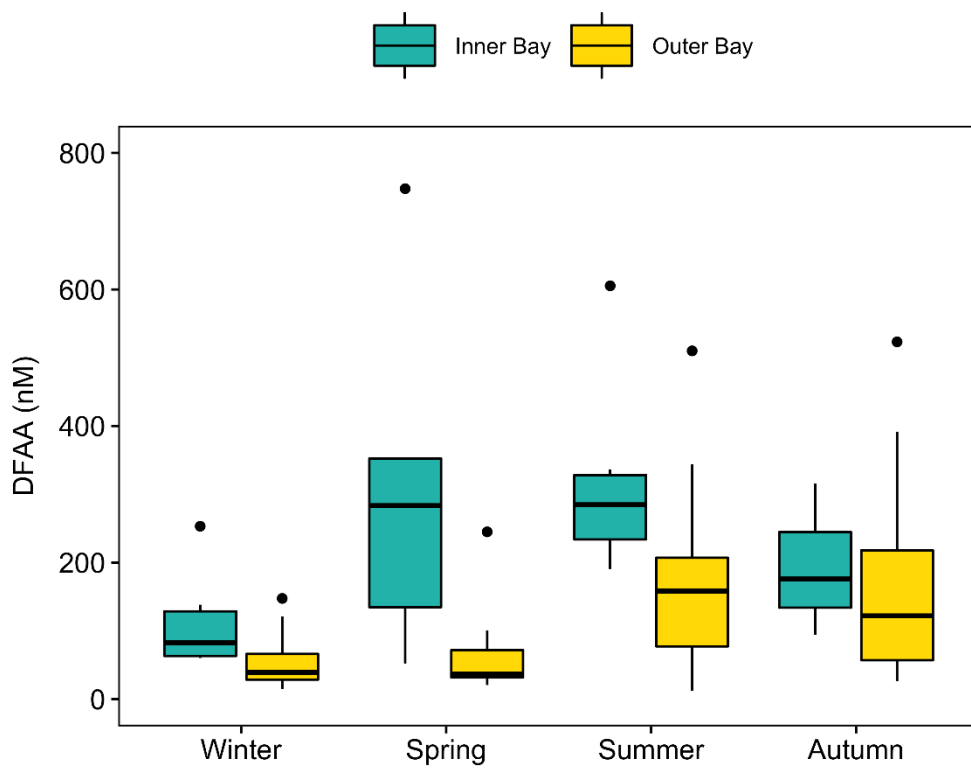


Figure 3.108 Seasonal and spatial variations of DFAA

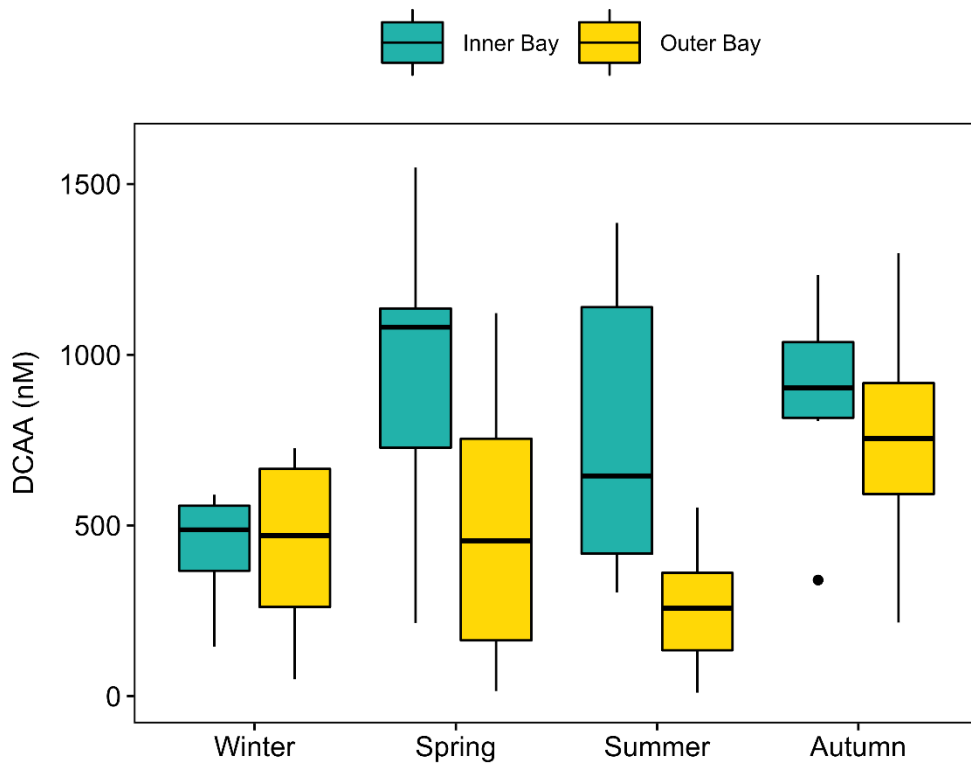


Figure 3.109 Seasonal and spatial variations of DCAA

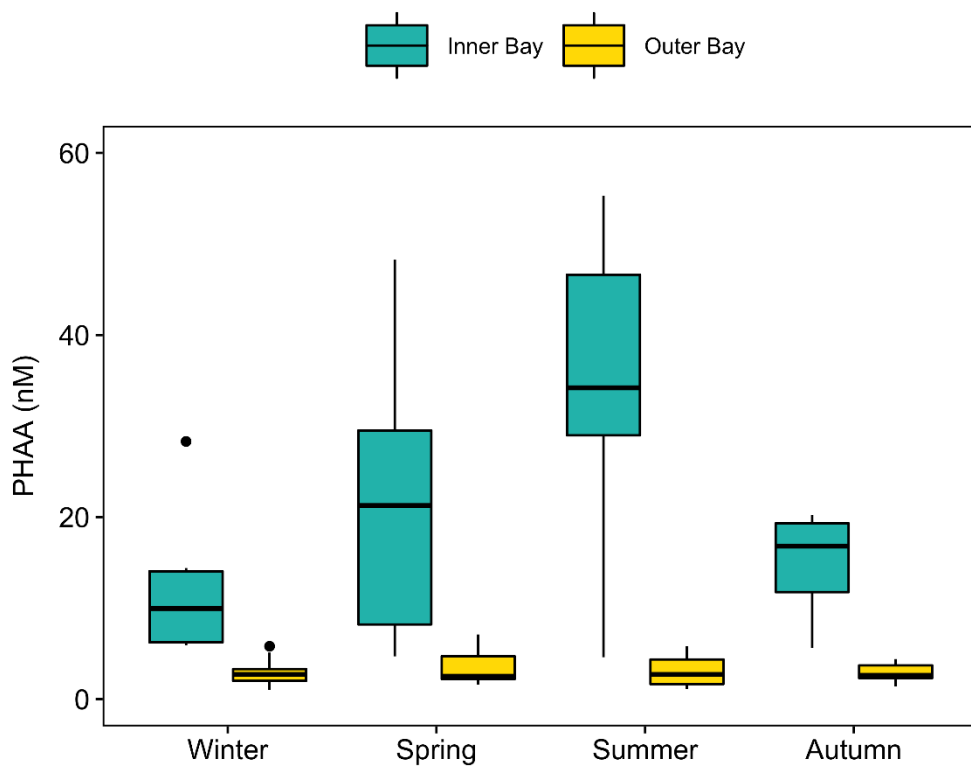


Figure 3.110 Seasonal and spatial variations of PHAA

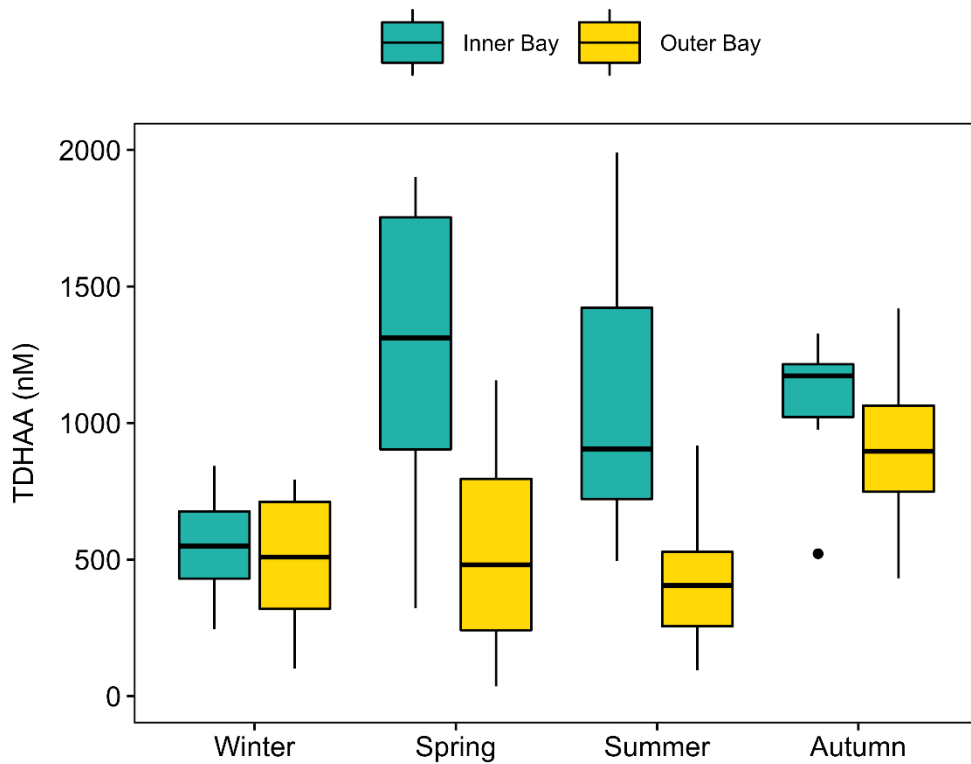


Figure 3.111 Seasonal and spatial variations of TDHAA



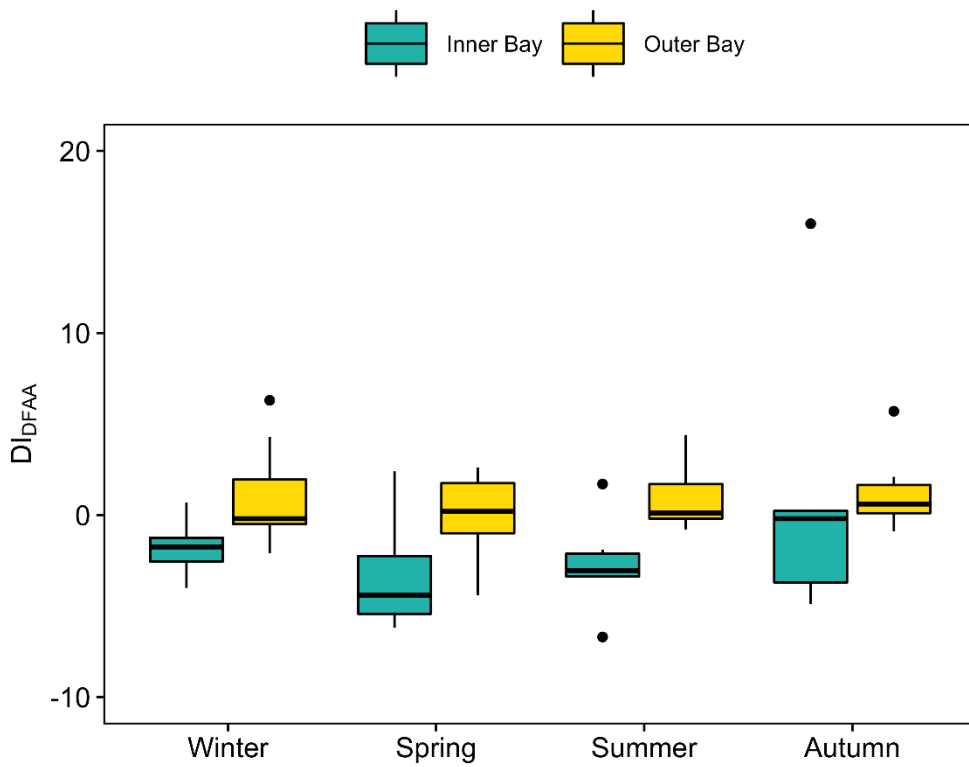


Figure 3.112 Seasonal and spatial variations of  $DI_{DFAA}$

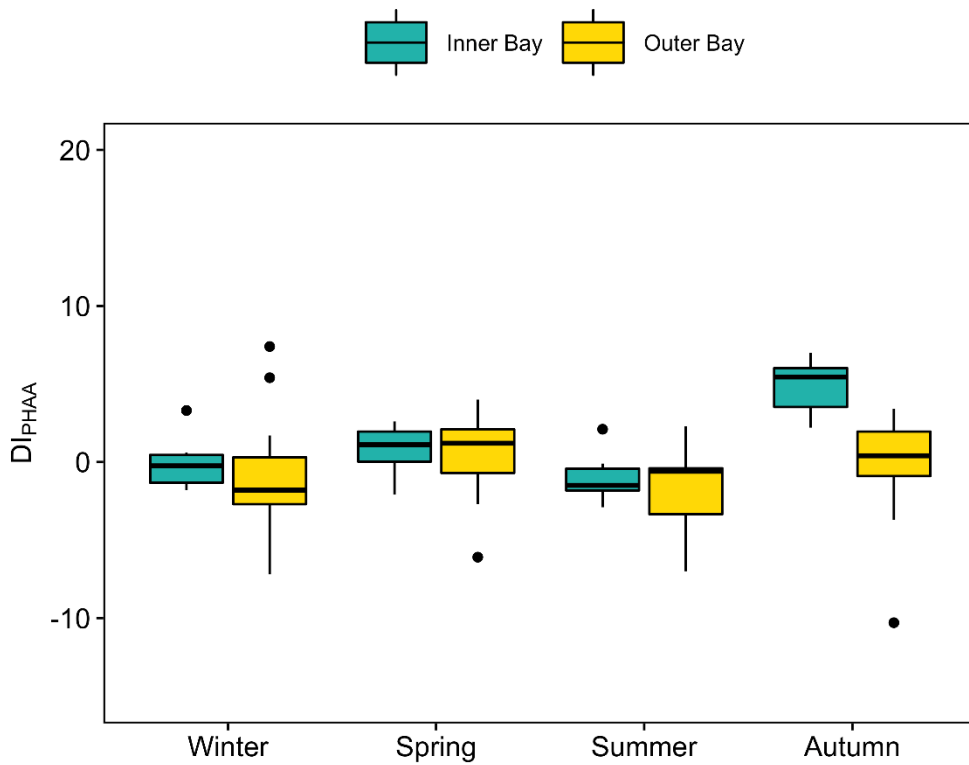


Figure 3.113 Seasonal and spatial variations of  $DI_{PHAA}$

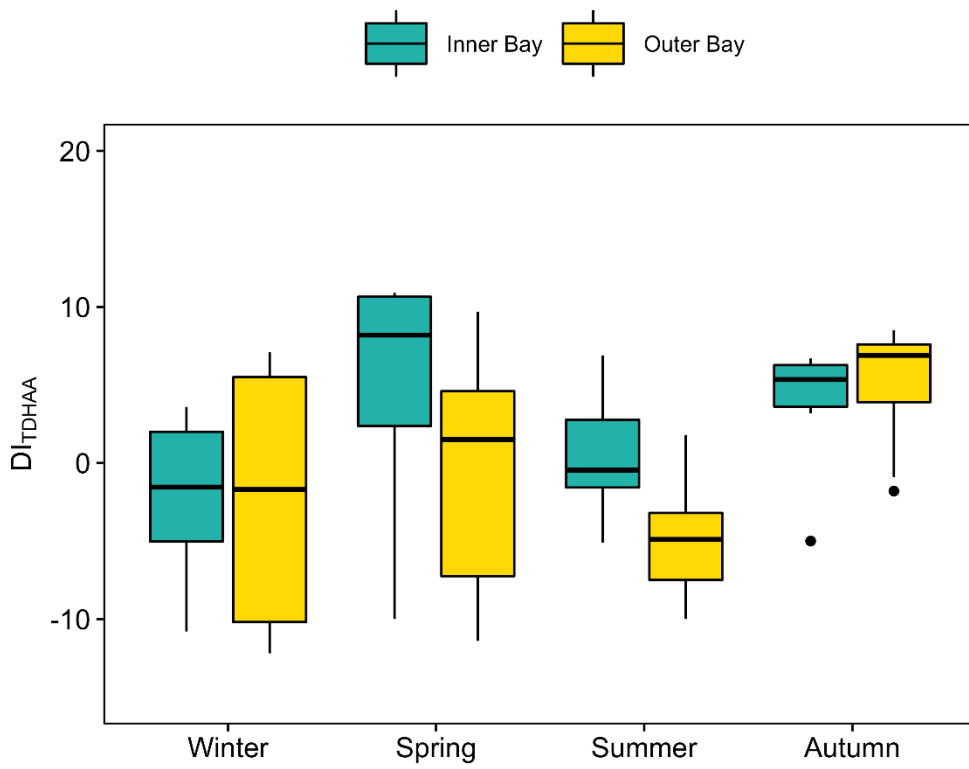


Figure 3.114 Seasonal and spatial variations of  $DI_{TDHAA}$

Table 3.7 Two-Way ANOVA results (Season and location vs. bulk parameters, Win: Winter, Spr: Spring, Sum: Summer, Aut: Autumn, Out: Outer Bay, MidIn: Middle-Inner Bays)

	Two-Way ANOVA (Seasons + Location)			Contrast 1: Seasons						Contrast 2: Location
	Season	Location	Season: Location	Spr-Win	Sum-Win	Aut-Win	Sum-Spr	Aut-Spr	Aut-Sum	Out-MidIn
<b>DO</b>	<0.001	0.911	<0.001	0.106	<0.001	<0.001	0.001	<0.001	0.554	0.038
<b>Chl-a</b>	0.006	<0.001	<0.001	0.629	0.005	0.009	0.119	<0.001	<0.001	<0.001
<b>DIP</b>	<0.001	<0.001	<0.001	1.000	<0.001	<0.001	<0.001	<0.001	0.212	0.343
<b>DOP</b>	<0.001	<0.001	0.004	0.979	<0.001	0.930	<0.001	0.997	<0.001	0.614
<b>TP</b>	<0.001	<0.001	<0.001	0.999	<0.001	0.014	<0.001	0.021	<0.001	0.023
<b>DIN</b>	<0.001	<0.001	<0.001	0.830	0.998	<0.001	0.906	<0.001	<0.001	0.214
<b>DON</b>	0.006	<0.001	0.190	0.986	0.583	0.775	0.789	0.567	0.125	0.010
<b>TN</b>	0.165	<0.001	0.004	0.898	0.896	<0.001	1.000	0.010	0.010	0.031
<b>DOC</b>	<0.001	<0.001	<0.001	0.112	<0.001	0.002	<0.001	0.500	<0.001	0.710
<b>POC</b>	0.008	<0.001	0.003	0.172	0.016	0.389	0.754	0.003	<0.001	0.072
<b>TOC</b>	<0.001	<0.001	<0.001	0.028	<0.001	0.783	<0.001	0.234	<0.001	0.121
<b>TRIX</b>	0.452	<0.001	0.018	1.000	0.073	0.223	0.068	0.213	0.950	<0.001
<b>MCHO</b>	<0.001	<0.001	0.053	0.813	0.744	0.003	0.239	<0.001	0.052	0.002
<b>TDCHO</b>	<0.001	<0.001	<0.001	0.717	0.019	<0.001	0.219	<0.001	<0.001	<0.001
<b>DFAA</b>	0.002	<0.001	0.037	0.034	0.018	0.666	0.995	0.360	0.245	0.294
<b>TDHAA</b>	<0.001	<0.001	0.004	0.002	0.028	0.040	0.833	0.761	0.999	0.791
<b>PHAA</b>	0.018	<0.001	<0.001	0.092	<0.001	0.923	0.014	0.310	<0.001	0.006

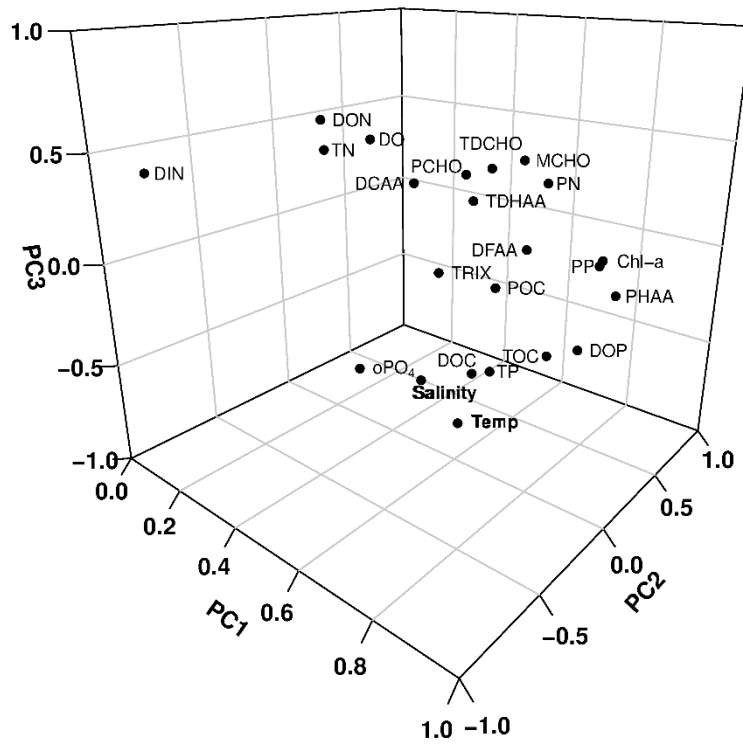


Figure 3.115 PCA results for bulk parameters at Middle-Inner Bays

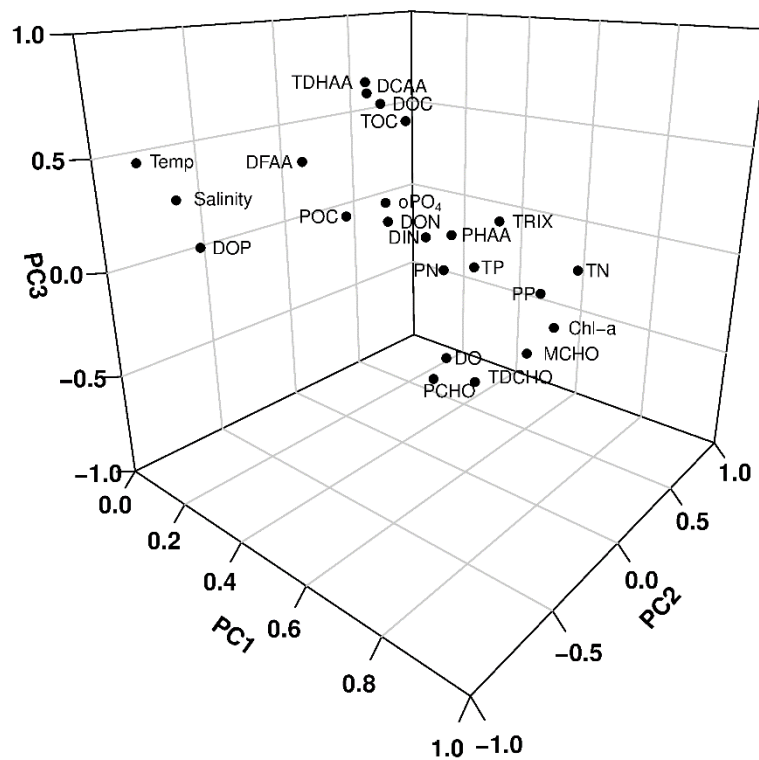


Figure 3.116 PCA results for bulk parameters at Outer Bay

Table 3.8 PCA results of bulk parameters at Middle-Inner and Outer Bays (PC: Principal Component represents standardized loadings based on correlation matrix)

	Middle-Inner Bays			Outer Bay			
	PC1	PC2	PC3	PC1	PC2	PC3	PC4
<b>Temp</b>	0.64	-0.07	-0.74	-0.79	0.12	0.05	0.39
<b>Salinity</b>	0.44	0.12	-0.73	-0.41	-0.10	-0.02	0.40
<b>DO</b>	-0.07	0.86	0.24	0.71	-0.41	-0.18	-0.1
<b>Chl-a</b>	0.83	0.46	0.00	0.74	0.27	-0.27	0.21
<b>oPO<sub>4</sub></b>	0.64	-0.71	-0.20	-0.04	0.84	-0.10	-0.19
<b>DOP</b>	0.94	-0.13	-0.15	-0.39	0.00	-0.32	0.01
<b>TP</b>	0.85	-0.44	-0.17	0.32	0.79	-0.33	-0.18
<b>PP</b>	0.83	0.43	-0.02	0.71	0.22	-0.10	-0.07
<b>DIN</b>	0.10	-0.86	0.42	0.16	0.76	-0.21	-0.18
<b>DON</b>	0.37	-0.36	0.64	0.52	-0.33	0.28	-0.14
<b>TN</b>	0.51	-0.59	0.59	0.80	0.24	0.04	0.06
<b>PN</b>	0.80	0.08	0.42	0.43	0.25	-0.14	0.36
<b>TRIX</b>	0.73	-0.44	0.16	0.43	0.70	0.00	-0.11
<b>DOC</b>	0.80	-0.41	-0.23	0.37	-0.05	0.69	0.07
<b>TOC</b>	0.85	-0.04	-0.27	0.41	0.03	0.61	0.50
<b>POC</b>	0.60	0.32	-0.21	0.17	0.12	0.06	0.74
<b>MCHO</b>	0.60	0.50	0.38	0.85	-0.29	-0.11	0.13
<b>TDCHO</b>	0.42	0.77	0.23	0.78	-0.43	-0.22	-0.02
<b>PCHO</b>	0.32	0.81	0.16	0.70	-0.47	-0.25	-0.08
<b>DFAA</b>	0.71	0.21	0.06	-0.21	0.50	0.16	0.22
<b>TDHAA</b>	0.61	0.09	0.28	0.16	0.30	0.71	-0.28
<b>PHAA</b>	0.95	0.13	0.00	0.42	0.34	0.01	0.56
<b>DCAA</b>	0.47	0.02	0.32	0.24	0.13	0.69	-0.38

Table 3.9 Proportional and cumulative variances explained by each Principal Component

	Middle-Inner Bays			Outer Bay			
	<i>PC1</i>	<i>PC2</i>	<i>PC3</i>	<i>PC1</i>	<i>PC2</i>	<i>PC3</i>	<i>PC4</i>
<b>SS loadings</b>	9.93	5.15	2.95	6.37	3.92	2.45	2.04
<b>Proportion var (%)</b>	43	22	13	28	17	11	9
<b>Cumulative var (%)</b>	43	66	78	28	45	55	64
<b>Proportion explained (%)</b>	55	29	16	43	27	17	14
<b>Cumulative proportion (%)</b>	55	84	100	43	7	86	100

Table 3.10 K-Means Clustering results of PCA loadings for bulk parameters at Middle-Inner and Outer Bays

	Middle-Inner Bays	Outer Bay
<b>Temp</b>	2	2
<b>Salinity</b>	2	2
<b>DO</b>	3	4
<b>Chl-a</b>	3	4
<b>oPO<sub>4</sub></b>	2	1
<b>DOP</b>	2	2
<b>TP</b>	2	1
<b>PP</b>	3	4
<b>DIN</b>	1	1
<b>DON</b>	1	4
<b>TN</b>	1	4
<b>PN</b>	3	4
<b>TRIX</b>	1	1
<b>DOC</b>	2	3
<b>TOC</b>	2	3
<b>POC</b>	3	2
<b>MCHO</b>	3	4
<b>TDCHO</b>	3	4
<b>PCHO</b>	3	4
<b>DFAA</b>	3	2
<b>TDHAA</b>	3	3
<b>PHAA</b>	3	4
<b>DCAA</b>	3	3

## CHAPTER FOUR

### DISCUSSION AND CONCLUSION

Hydrography of the İzmir Bay is influenced from several factors such as freshwater inputs that carry anthropogenic loads to the bay, atmospheric transport of low molecular weight molecules, exchange of water between the Aegean Sea and the bay, topography of the bay, the sea level changes, movement of waters directed by wind-driven circulation and winter convection. Under the influences of these factors, the İzmir Bay could be divided into three parts as outer, middle and inner bays since each part have different water mass characteristics. While inner bay water has been anthropogenically polluted, outer bay water is influenced from Gediz River and Aegean Sea, the upwelling water at Gülbahçe Bay, and the water mass located at salt production area (Sayin, 2003). The third water mass at middle bay connects outer bay to inner bay. In previous studies, remarkable differences have been reported for DOC, Chl-a, dissolved inorganic nitrogen (DIN), and dissolved inorganic phosphorus (DIP) levels at outer and middle-inner bay stations (Kontas et al., 2004; Kucuksezgin et al., 2005; Ozkan & Buyukisik, 2012; Ozkan et al., 2008a, 2008b; Sunlu et al., 2012). Also, eutrophication has been reported for inner part of the İzmir Bay (Kontas et al., 2004). On the contrary, outer bay has oligotrophic character. Compared to previous studies, similar trends at middle-inner and outer bays were also observed in this study. Nutrinet, DOC and Chl-a concentrations were higher in middle-inner bays (Table 4.1).

In Izmir, a wastewater treatment plant has been activated in 2001 to process wastewater generated from domestic and industrial use. The effectiveness of this treatment plant has been investigated in previous studies by comparing nutrient, Chl-a and DOC profiles before and after the establishment of this plant (Kontas et al., 2004). In Table 4.1, nutrient, Chl-a and DOC profiles of 1996-1998, 2000, 2001, 2002 and 2003 have been given with the results of this study (2015). It should be noted that sampling stations in this study are the same stations that have been used in previous studies. Only difference is the number of stations. It can be seen from the Table 3.7 that mean values of  $\text{o-PO}_4\text{-P}$ ,  $\text{TNO}_x\text{-N}$ ,  $\text{NH}_4\text{-N}$  and  $\text{TNO}_x/\text{PO}_4$  at Middle-Inner and Outer Bays did not change obviously. However, remarkable differences in Chl-a,

DOC, POC and PP concentrations were observed among Middle-Inner and Outer Bays. In this study, Chl-a has been observed with means of 9.3 at Middle-Inner Bays and 0.66 at Outer Bay. However, mean Chl-a concentrations were in the ranges of 1.2-4.6 and 0.15-0.48 at Middle-Inner and Outer Bays, respectively, from 1996 to 2003. Similarly, POC and PP concentrations increased at Middle-Inner and Outer Bays compared to 2000-2001. In this study, DOC concentrations were observed in the range of  $101.2 \pm 57.1$  at Middle-Inner Bays and  $57.9 \pm 17.2$  at Outer Bay. In previous studies at 2000-2001, DOC concentrations were observed in the ranges of  $89.5 \pm 37.9$  at Middle-Inner Bays and  $60.6 \pm 16.9$  at Outer Bay. According to these results, DOC concentrations slightly increased at Middle-Inner Bays and slightly decreased at Outer Bay from 2000-2001 to 2015.

Seasonal nutrient concentrations ranged between  $\text{o-PO}_4\text{-P}$ : 0.02-3.21  $\mu\text{M}$ ,  $\text{NH}_4\text{-N}$ : 0.10-22.62  $\mu\text{M}$ ,  $\text{NO}_2\text{-N}$ : 0.01-3.87  $\mu\text{M}$ ,  $\text{NO}_3\text{-N}$ : 0.03-6.76  $\mu\text{M}$ , whereas  $\text{O}_2\%$  and Chl-a were found between 63-143% and 0.11-25.4  $\mu\text{g/L}$ , respectively.  $\text{O}_2\%$  and Chl-a concentrations were higher at middle-inner bays. Dissolved nitrogen concentrations were found remarkably higher at middle-inner bays and highest levels observed at station 1, especially for  $\text{NH}_4\text{-N}$  in summer and autumn.  $\text{o-PO}_4$  levels were only higher in summer and autumn at middle-inner bays. In autumn, low  $\text{O}_2\%$  and Chl-a as well as high  $\text{NH}_4\text{-N}$  levels at station 1 might be a result of organic matter decomposition. TRIX index ranged between 1.21-6.75 at all seasons and stations. According to TRIX, high eutrophication risks were observed at winter-spring and eutrophication was observed in summer-autumn at Middle-Inner Bays. There were no eutrophication risks at outer bay. Dissolved inorganic N/P (DIN/DIP) ratios changed between 2-10 at middle-inner and 11-15 at outer bay stations. Dissolved total N/P (DTN/DTP) ratios ranged between 3-15 at middle-inner and 5-19 at outer bay stations. Total N/P (TN/TP) ratios changed between 5-12 at middle-inner and 8-16 at outer bay stations. In conclusion, nutrient levels and TRIX index indicated that the İzmir Bay has high eutrophic potential to eutrophic state at middle-inner parts and there is no eutrophication risk at outer part. N/P ratios were relatively high at outer bay and nitrogen is the limiting element for middle-inner parts of the İzmir Bay. This might be explained by inadequate capacity of wastewater plant for the removal of phosphate.



C/N/P ratios in dissolved and particulate matter showed seasonal variations at Middle-Inner and Outer Bays. In dissolved matter, C ratios were found over Redfield ratio (C/N/P: 106/16/1) in all seasons and N ratios were found close to Redfield ratio except for summer. In particulate matter, C ratios were generally below Redfield ratio in middle-inner bays. However, C ratios of particulate matter were found higher than Redfield ratio in outer bay. N ratios in particulate fraction were generally below Redfield ratio except for outer bay at summer and middle-inner bays at autumn. Lower C ratio at particulate and higher C ratio at dissolved matter in middle-inner bays indicated that particulate matter might have been transformed into dissolved form by a degradation process. Also, phytoplankton can produce C-rich DOM under nutrient (N and/or P) depleted conditions (Carlson & Hansell, 2015; Carlson et al., 1998; Conan et al., 2007; Hopkinson & Vallino, 2005; Wetz & Wheeler, 2007; Sambrotto et al., 1993). In outer bay, variances between C/N/P ratios of dissolved and particulate matter were lower and always above Redfield ratio. Therefore, particulate and dissolved fractions might be in equilibrium for outer bay.

In the literature, it has been reported that PCHO levels changed on a seasonal basis and high PCHO values were observed in winter and summer (Myklestad & Børsheim, 2007). Nutrient transport from seabed to the surface waters might also support phytoplankton activity in winter following the breakdown of stratification at water column (Scoullou et al., 2006). In some studies, higher dissolved carbohydrate levels have been reported in spring and summer than in winter and autumn (He et al., 2015; Hung et al., 2009; Myklestad & Børsheim, 2007). However, high carbohydrate levels have also been reported in winter (Lee et al., 2017). In this study, maximum MCHO levels were found in spring. Highest PCHO and TDCHO levels observed in winter and spring.

Seasonal changes of PCHO and TDCHO showed similar trends with Chl-a levels. According to Table 3.6, PCHO and TDCHO were highly correlated with Chl-a levels at spring and summer. Also, PCHO, TDCHO and Chl-a concentrations decreased in autumn. These results indicated that PCHO and TDCHO levels might be influenced from biological processes especially at spring, summer and autumn. Similar significant

correlations between carbohydrate and Chl-a concentrations were reported in the literature (Hung et al., 2001; Hung et al., 2003; Khodse et al., 2007). However, carbohydrate concentrations are also influenced from other factors like bacterial utilization and grazing activities (Hopkinson et al., 2002; Guo et al., 2004; Strom et al., 1997; Wang et al., 2006). In winter, PCHO and TDCHO levels might be affected from rain run-offs, weathering and terrestrial inputs (He et al., 2015; Shin et al., 2003; Wang et al., 2003). DOC and carbohydrate levels (MCHO, PCHO and TDCHO) were found higher in middle-inner bays, under the influence of anthropogenic inputs, compared to outer bay.

Vertical variations of Chl-a, DOC and dissolved carbohydrate concentrations were not significant in this study ( $p < 0.05$ ). This might be resulted from shallow water depths in the İzmir Bay. Depths of stations at middle-inner and outer bays range between 9-22 m and 27-66 m, respectively. In the literature, significant vertical variations in Chl-a, DOC and dissolved carbohydrate concentrations were observed between upper water column (euphotic zone) and deep waters where light penetration is very low (Hung et al., 2003; Lin & Guo, 2015; Wang et al., 2006).

The ratio of MCHO/TDCHO increased from winter to autumn, especially at middle-inner bays, and similar results were reported in the literature (He et al., 2015; Lin & Guo, 2015; Wang et al., 2006). The ratios of MCHO/DOC and TDCHO/DOC decreased from winter to autumn and similar ratios were also observed in the literature (He et al., 2015; Lin & Guo, 2015; Myklestad & Børsheim, 2007; Wang et al., 2006). Increasing MCHO/TDCHO and decreasing TDCHO/DOC ratios indicated production of significant MCHO fraction or breaking down of significant PCHO fraction from winter to autumn in the bay. A similar case was also reported by Wang et al. (2006).

Table 4.1 Nutrient, chlorophyll and organic matter concentrations in the İzmir Bay

	<i>Period</i>	<i>Middle-Inner Bays</i>	<i>Outer Bay</i>	<i>Reference</i>
<b>o-PO<sub>4</sub>-P (μM)</b>	1996-1998	0.83±0.06	0.060±0.001	Kontas et al., 2004
	2000	1.30±0.13	0.050±0.003	Kontas et al., 2004
	2001	0.95±0.19	0.040±0.002	Kontas et al., 2004
	2002	1.20±0.20	0.050±0.005	Kontas et al., 2004
	2003	1.60±0.26	0.050±0.004	Kontas et al., 2004
	2015	1.20±1.20	0.100±0.110	This Study
<b>TNO<sub>x</sub>-N (μM)</b>	1996-1998	2.60±0.25	0.48±0.01	Kontas et al., 2004
	2000	2.50±0.40	0.44±0.02	Kontas et al., 2004
	2001	3.10±0.91	0.40±0.02	Kontas et al., 2004
	2002	1.70±0.35	0.48±0.03	Kontas et al., 2004
	2003	1.90±0.62	0.46±0.04	Kontas et al., 2004
	2015	2.10±3.30	0.32±0.57	This Study
<b>NH<sub>4</sub>-N (μM)</b>	1996-1998	2.50±0.18	0.30±0.02	Kontas et al., 2004
	2000	3.40±0.67	0.21±0.01	Kontas et al., 2004
	2001	5.80±2.80	0.32±0.02	Kontas et al., 2004
	2002	1.50±0.29	0.23±0.01	Kontas et al., 2004
	2003	0.89±0.14	0.22±0.02	Kontas et al., 2004
	2015	4.40±7.10	0.47±0.35	This Study
<b>TNO<sub>x</sub>/PO<sub>4</sub></b>	1996-1998	6.70±0.40	9.80±0.13	Kontas et al., 2004
	2000	2.20±0.21	8.30±0.27	Kontas et al., 2004
	2001	3.70±0.55	11.00±0.37	Kontas et al., 2004
	2002	2.60±0.48	11.00±0.32	Kontas et al., 2004
	2003	3.80±1.20	11.00±0.40	Kontas et al., 2004
	2015	2.80±3.50	3.80±3.50	This Study
<b>Chl-a (μg/L)</b>	1996-1998	4.60±0.49	0.48±0.03	Kontas et al., 2004
	2000	4.30±0.63	0.34±0.02	Kontas et al., 2004
	2001	2.20±0.45	0.24±0.02	Kontas et al., 2004
	2002	1.20±0.19	0.15±0.01	Kontas et al., 2004
	2003	1.30±0.17	0.22±0.03	Kontas et al., 2004
	2015	9.30±8.40	0.66±0.50	This Study
<b>DOC (μM)</b>	2000-2001	89.5±37.9	60.6±16.9	Kucuksezgin et al., 2005
	2015	101.2±57.1	57.9±17.2	This Study
<b>POC (μM)</b>	2000-2001	61.6±56.7	8.30±3.90	Kucuksezgin et al., 2005
	2015	66.6±63.8	27.4±12.3	This Study
<b>PP (μM)</b>	2000-2001	0.47±0.41	0.06±0.04	Kucuksezgin et al., 2005
	2015	0.74±0.47	0.17±0.12	This Study

Carbohydrate concentrations in bulk DOC pool (i.e., TDCHO/DOC ratio) were used as a tool to investigate the degradation and diagenetic status of bulk DOM and its conversion rate in aquatic environments (Hung et al., 2009; Kaiser & Benner, 2009; Khodse et al., 2010; Lin & Guo, 2015; Skoog & Benner, 1997). Lin & Guo (2015) have reported TDCHO/DOC ratios in the ranges of 11-71% and 14-52% at surface waters of shelf and basin parts of Gulf of Mexico, respectively. Similar TDCHO/DOC ratios (2.5-42.3% at middle-inner and 4.4-37.1% at outer bays) were found in the present study. According to Figure 3.40, TDCHO/DOC ratios distributed at wide ranges and it might be related to the presence of newly forming and degrading fractions of DOM in the bay. Higher carbohydrate fractions were observed in freshly produced DOM and lower TDCHO/DOC ratios were found during the degradation process of DOM (Lin & Guo, 2015; Opsahl & Benner, 1999).

According to results of factor analyses, Chl-a and dissolved carbohydrate species (MCHO and TDCHO) were explained by the same factor and phytoplankton activities could have an important role on the dissolved carbohydrate concentrations in the the İzmir Bay.

Table 4.2 Comparison of DOC, MCHO and TDCHO levels of the İzmir Bay with different parts of the world

<b>Location</b>	<b>DOC (<math>\mu\text{M}</math>)</b>	<b>MCHO (<math>\mu\text{M}</math>)</b>	<b>TDCHO (<math>\mu\text{M}</math>)</b>	<b>Reference</b>
Atlantic and Pacific Oceans	47–119	2.4–6.2	7–33	Pakulski & Benner, 1994
Black Sea	148–270	–	12–20	Cauwet et al., 2002
Northern Adriatic Sea	–	5–54	5–95	Ahel et al., 2005
Beaufort Sea	30–202	–	0.6–1.3	Panagiotopoulos et al., 2014
Bengal Bay	–	0.9–2.9	4.5–7.9	Bhosle et al., 1998
Trieste Gulf	108–200	2–13	11–126	Terzić et al., 1998
San Francisco Bay	52–172	0.2–1.3	1–4	Murrell & Hollibaugh, 2000
Gulf of Mexico	205	–	28.8	Hung & Santschi, 2001
Galveston Bay	300–363	–	27.1–83.3	Hung & Santschi, 2001
South Yellow Sea	89–208	2.3–11.1	7.5–23.4	Chen et al., 2016a
İzmir Bay	32–244	0.7–8.3	2.6–24.6	This study

DOC, MCHO and TDCHO levels determined in this study were similar to levels reported from other bays and gulfs (Table 4.2). DOC concentrations in the present study were very close to DOC levels observed at Beaufort Sea (Panagiotopoulos et al., 2014), Black Sea (Cauwet et al., 2002) and Gulf of Mexico (Hung & Santschi, 2001). Also, DOC levels at Galveston Bay (Hung & Santschi, 2001) were greatly higher than the DOC levels in this study. MCHO levels in this study were only lower than those reported from Northern Adriatic (Ahel et al., 2005). Maximum MCHO concentration in this study was higher than the maximum levels in Atlantic and Pacific Oceans, Beaufort Sea, Trieste Gulf, San Francisco Bay and Gulf of Mexico (Hung & Santschi, 2001; Murrell & Hollibaugh, 2000; Pakulski & Benner, 1994; Panagiotopoulos et al., 2014; Terzić et al., 1998). TDCHO levels in this study were close to the TDCHO levels at Black Sea, Bengal Bay, Gulf of Mexico and San Francisco Bay (Bhosle et al., 1998; Cauwet et al., 2002; Hung & Santschi, 2001; Murrell & Hollibaugh, 2000). On the other hand, maximum TDCHO levels at Northern Adriatic and Trieste Gulf were much higher than the TDCHO levels in this study (Ahel et al., 2005; Terzić et al., 1998).

Mean DFAA concentrations in summer and winter were found higher than other seasons in all stations. Mean TDHAA concentrations in summer and autumn were higher than other seasons in all stations. Highest mean PHAA concentrations (>1.75 nM) were observed in spring and summer at Middle-Inner Bays.

Highest mean mol percentages in DFAA were found for L-Glu, L-Ser, Gly and D-Arg. Highest mean mol percentages in TDHAA were found for Gly, L-Asx, L-Glx and L-Ser. Highest mean mol percentages in PHAA were found for Gly at winter and summer seasons. Mol percentages of L-Glx, L-Thr, Gly, L-Arg and L-Ala in PHAA were also higher than other amino acids. According to these results, most abundant amino acids in DFAA, TDHAA or PHAA pools were L-Asp, L-Glu, L-Ser, Gly and L-Ala and this finding is similar to previous studies in coastal waters (Chen et al., 2013; Chen et al., 2016a; Cowie & Hedges, 1992, 1996; Meon & Kirchman, 2001; Yang et al., 2009).

Table 4.3 Comparison of organic and inorganic chemical concentrations in the İzmir Bay with different parts of the world

	Middle- Inner Bay (This Study)	Outer Bay (This Study)	Laptev Sea (Kattner et al., 1999)	Eastern Arctic Ocean (Dittmar et al., 2001)	Mississippi River Plume (Bianchi et al., 2014)	South Yellow Sea (Chen et al., 2016a)	South Yellow Sea (Chen et al., 2016b)
<b>Chl-a (µg/L)</b>	9.3 ± 8.4	0.7 ± 0.5	–	–	4.4 ± 4.5	0.84 ± 0.84	3.27 (0.40–6.89)
<b>o-PO<sub>4</sub>-P (µM)</b>	1.20 ± 1.20	0.10 ± 0.10	0.73 ± 0.04	0.51 ± 0.06	–	–	–
<b>DIN (µM)</b>	6.5 ± 10.2	0.8 ± 0.7	8.1 ± 0.8	3.0 ± 0.8	–	–	8.6 (1.7–14)
<b>DON (µM)</b>	5.0 ± 3.0	2.4 ± 1.3	4.5 ± 0.3	6.2 ± 0.4	–	–	13.9 (6.4–24.8)
<b>DOC (µM)</b>	101 ± 57	58 ± 17	82 ± 8	125 ± 8	459 ± 137	135 ± 32	102 (64–144)
<b>POC (µM)</b>	66.6 ± 63.8	27.4 ± 12.3	–	–	16.8 ± 8.6	–	–
<b>MCHO (µM)</b>	4.0 ± 1.8	2.1 ± 1.2	–	–	–	6.7 ± 2.4	–
<b>TDCHO (µM)</b>	12.3 ± 6.4	7.0 ± 3.7	–	–	–	14.7 ± 4.5	–
<b>DFAA (µM)</b>	0.23 ± 0.17	0.11 ± 0.11	–	–	–	0.72 ± 0.26	–
<b>TDHAA (µM)</b>	0.99 ± 0.50	0.59 ± 0.32	0.32 ± 0.02	0.52 ± 0.05	0.52 ± 0.05	1.91 ± 0.28	0.7 (0.5–0.9)
<b>PHAA (µM)</b>	0.21 ± 0.15	0.03 ± 0.01	0.04 ± 0.02	0.17 ± 0.13	0.17 ± 0.13	–	–

Highest  $\Sigma$ DFAA concentrations (>450 nM) were observed at spring and summer at station 1 and 6, respectively. Highest  $\Sigma$ TDHAA concentrations (>1500 nM) were observed in spring at station 1. In winter, spring and autumn, TDHAA concentrations did not change obviously, but, in summer, TDHAA levels decreased from surface to bottom. Highest  $\Sigma$ PHAA concentrations (>45 nM) were observed in summer at station 1. For station 1,  $\Sigma$ PHAA concentrations were remarkably higher in spring and summer than other seasons.

Concentrations L-forms were proportionally higher than D-forms in all amino acid types. Highest fluctuations (distance between highest and lowest ratios) were observed in winter and spring seasons in DFAA form. TDHAA ratios were lowest at summer season for Glx and Ser. For PHAA form, seasonal D/L-ratios for amino acids did not change remarkably and the ratios decreased in the order of Asx, Glx, Ala and Ser.

DFAA, TDHAA and PHAA levels determined in this study were compared with DFAA, TDHAA and PHAA levels reported from other bays and gulfs (Table 4.3). DFAA concentrations in the İzmir Bay were lower than the levels found at the South Yellow Sea (Chen et al., 2016). TDHAA concentrations especially at Middle-Inner Parts of the İzmir Bay were higher than the levels at the Laptev Sea (Kattner et al., 1999), Eastern Arctic Ocean (Dittmar et al., 2001), and Mississippi River Plume at Gulf of Mexico (Bianchi et al., 2014). On the other hand, TDHAA concentrations at Middle-Inner and Outer Parts of the İzmir Bay were in the same range or below the range of TDHAA concentrations observed at South Yellow Sea (Chen et al., 2016a, 2016b). PHAA concentrations at Middle-Inner Parts of the İzmir Bay were in the range of PHAA concentrations observed from Eastern Arctic Ocean (Dittmar et al., 2001) and Mississippi River Plume at Gulf of Mexico (Bianchi et al., 2014). Similarly, PHAA concentrations at Outer Part of the İzmir Bay were in the range of PHAA concentrations observed from the Laptev Sea (Kattner et al., 1999).

DI values were first used and proposed by Dauwe et al. (1999). DI is calculated based on data from fresh plankton, sinking particles and sediments. It provides information on organic matter movement from water column (produced by fresh

plankton) to sediments. In this path, amino acids are believed to be influenced from degradation processes (Chen et al., 2016a). Based on experimental studies, DI values are observed between +1 (phytoplankton, bacteria) and -1.5 (highly degraded sediments) (Chen et al., 2016a). This index is also used for assessment of early diagenetic status of DOM (Amon et al., 2001; Chen et al., 2016a; Davis et al., 2009; Kaiser & Benner, 2009; Yamashita & Tanoue, 2003).  $DI_{DFAA}$  values were generally greater than 0 at all depths and distributed at a narrow range. In  $DI_{TDHAA}$  form, both positive and negative DI values observed at a wide range and autumn values were higher than other seasons. For  $DI_{PHAA}$ , the values distributed near 0 or below at a narrow range and highest values determined at autumn season. According to these results, DFAA fraction indicates freshly produced matter is more abundant in DOM, PHAA fraction reflects DOM is at equilibrium and TDHAA fraction consists both freshly produced and highly-altered DOM.

In dissolved organic matter pool, carbohydrates and amino acids are two of the labile fractions and these fractions can provide information on sources and diagenetic status of organic matter (Chen et al., 2016a; Cowie & Hedges, 1992; Dauwe & Middelburg, 1998). In general, higher  $C_{TDCHO}/DOC$  and  $C_{TDHAA}/DOC$  ratios are found in freshly produced DOM compared to degraded DOM and these ratios are decreased with diagenesis process (Chen et al., 2016a). In the present study, MCHO and PCHO ratios in DOC decreased from winter to autumn both at middle-inner and outer bays. DFAA ratios in DOC were found maximum in spring and in summer at middle-inner and outer bays, respectively. Highest DCAA ratios in DOC were observed in autumn at middle-inner and outer bays. On the other hand, DCAA ratios in DOC decreased from winter to summer at outer bay. According to the results, DOC was enriched with more freshly produced matter especially in winter and spring and degradation processes were more abundant in summer and autumn.

DFAA ratios in DON increased from winter to summer and decreased in autumn at middle-inner and outer bays. DCAA ratios in DON increased over 30% in spring, summer and autumn seasons at middle-inner bays. DCAA ratios in DON at outer bay were found between 0.2-77%.



According to K-means clustering analysis of principal component loadings among bulk chemical parameters, DFAA, TDHAA and PHAA were found in the same group with dissolved carbohydrates (MCHO, TDCHO, PCHO), PP, PN and Chl-a at Middle-Inner Bays. For Outer Bay, only PHAA was in the same group with dissolved carbohydrates (MCHO, TDCHO, PCHO), PP, PN and Chl-a. DFAA and TDHAA were found in different groups at Outer Bay.

In this thesis, seasonal variations and distributions of nutrients, Chl-a, DOC, dissolved carbohydrates and amino acids were studied in the İzmir Bay. According to the results, DOC and Chl-a levels were higher at middle-inner bays compared to outer bay in summer and autumn. Highest MCHO levels were found in spring and decreased from summer to autumn. Maximum PCHO and TDCHO levels were observed in winter and decreased from winter to autumn. Increasing MCHO/TDCHO and decreasing TDCHO/DOC ratios indicated production of significant MCHO fraction or breaking down of significant PCHO fraction from winter to autumn. TDCHO/DOC ratio distributed at a wide range that might be linked with the presence of newly forming and degrading fractions of DOM. According to results of factor analysis, Chl-a and dissolved carbohydrate species (MCHO and TDCHO) were explained in the same factor group and phytoplankton activities could have an important role on the dissolved carbohydrate concentrations in the İzmir Bay. DFAA, TDHAA and PHAA levels were found higher at Middle-Inner Bays. DFAA, TDHAA and PHAA levels were observed highest in spring and summer. DFAA, TDHAA and PHAA were highly correlated and found in the same group with dissolved carbohydrates (MCHO, TDCHO, PCHO), PP, PN and Chl-a at Middle-Inner Bays. According to DI results, DFAA fraction indicated that freshly produced matter was more abundant in DOM. PHAA fraction reflected DOM was at equilibrium and TDHAA fraction consisted both freshly produced and highly-altered DOM. According to  $C_{TDCHO}/DOC$  and  $C_{TDHAA}/DOC$  ratios, DOC was enriched with more freshly produced matter especially in winter and spring, and degradation processes were more abundant in summer and autumn. TRIX values were higher in Middle-Inner Bays and this part of the bay was found within eutrophication risk level. N/P ratios were relatively high at outer bay and nitrogen is the limiting element for the İzmir Bay. This might be explained by

inadequate capacity of wastewater plant for the removal of phosphate. C/N/P ratios of dissolved and particulate organic matters indicated that particulate organic matter might have been transformed into dissolved form by a degradation process in middle-inner bays. Dissolved and total nutrients, DOC, TOC, Chl-a, dissolved carbohydrates and amino acid levels increased from outer to middle-inner bay due to anthropogenic and terrestrial inputs. As indicators of biological and physical processes in seawater, seasonal and vertical variations of nutrients, DOC, Chl-a, dissolved carbohydrates and amino acids were useful in investigation of organic matter distribution.



## REFERENCES

- Ahel, M., Tepic, N., Terzic, S. (2005). Spatial and temporal variability of carbohydrates in the northern Adriatic—a possible link to mucilage events. *Science of the Total Environment*, 353, 139-150.
- Aksu, A. E., & Piper, D. J. W. (1983). Progradation of the late quaternary Gediz delta, Turkey. *Marine Geology*, 54, 1-25.
- Aksu, A. E., Yatar, D., Uslu, O. (1998). Assessment of marine pollution in İzmir Bay: heavy metal and organic compound concentrations in surficial sediments. *Translations and Journal of Engineering and Environmental Science*, 22, 387-415.
- Allredge, A. L., Passow, U., Logan, B. E. (1993). The abundance and significance of a class of large, transparent organic particles in the ocean. *Deep Sea Research Part I: Oceanographic Research Papers*, 40 (6), 1131-1140.
- Amon, R. M. W., & Benner, R. (2003). Combined neutral sugars as indicators of the diagenetic state of dissolved organic matter in the Arctic Ocean. *Deep Sea Research Part I: Oceanographic Research Papers*, 50 (1), 151-169.
- Amon, R. M. W., Fitznar, H. P., Benner, R. (2001). Linkages among the bioreactivity, chemical composition, and diagenetic state of marine dissolved organic matter. *Limnology and Oceanography*, 46, 287-297.
- APHA, (1980). *Standard methods for the examination of water and wastewater* (15th ed.). Washington: American Public Health Association.
- APHA, (1998). Chlorophyll. In L. S. Clesceri, A. E. Greenberg, A. D. Eaton, (Eds.). *Standard Methods for the Examination of Water and Wastewater* (20th ed.) (10200 H). Baltimore: United Book Press.

- Baldi, F., Minacci, A., Saliot, A., Mejanelle, L., Mozetic, P., Turk, V., et al. (1997). Cell lysis and release of particulate polysaccharides in extensive marine mucilage assessed by lipid biomarkers and molecular probes. *Marine Ecology Progress Series*, 153, 45-57.
- Balkaş, T. I., & Juhasz, F. (1993). *Case study of the Bay of İzmir*. Mediterranean Action Plan-MED POL, MAP Technical Report Series No:72, Unep Athens, 1–28.
- Bauer, J. E. & Bianchi, T. S., (2011). Dissolved organic carbon cycling and transformation. In E. Wolanski, D. McLusky (Eds.). *Treatise on Estuarine and Coastal Science* (Vol 5). Italy: Academic Press.
- Benner, R. (2002). Chemical Composition and Reactivity. In D. A. Hansell, C. A. Carlson, (Eds.). *Biogeochemistry of Marine Dissolved Organic Matter* (1st ed.) (59-90). Florida: Academic Press.
- Benner, R., & Opsahl, S. (2001). Molecular indicators of the sources and transformations of dissolved organic matter in the Mississippi River plume. *Organic Geochemistry*, 32, 597-611.
- Bhosle, N. B., Bhaskar, P. V., Ramachandran, S. (1998). Abundance of dissolved polysaccharides in the oxygen minimum layer of the Northern Indian Ocean. *Marine Chemistry*, 63, 171-182.
- Bianchi, T. S., Grace, B. L., Carman, K. R., Maulana, I. (2014). Amino acid cycling in the Mississippi River Plume and effects from the passage of Hurricanes Isadore and Lili. *Journal of Marine Systems*, 136, 10-21.
- Carlson, C. A., & Hansell, D. A. (2015). DOM Sources, Sinks, Reactivity, and Budgets, In D. A. Hansell, C. A. Carlson, (Eds.). *Biogeochemistry of Marine Dissolved Organic Matter* (2nd ed.) (65-126). Boston: Academic Press.

- Carlson, C. A., Ducklow, H. W., Hansell, D. A., Smith, W. O. (1998). Organic carbon partitioning during spring phytoplankton blooms in the Ross Sea Polynya and the Sargasso Sea. *Limnology and Oceanography*, 43, 375-386.
- Cauwet, G., Déliat, G., Krastev, A., Shtereva, G., Becquevort, S., Lancelot, C., et al. (2002). Seasonal DOC accumulation in the Black Sea: a regional explanation for a general mechanism. *Marine Chemistry*, 79, 193-205.
- Cava, F., Lam, H., de Pedro, M., Waldor, M. K. (2011). Emerging knowledge of regulatory roles of d-amino acids in bacteria. *Cellular and Molecular Life Sciences*, 68, 817-831.
- Chanudet, V., & Filella, M. (2006). The application of the MBTH method for carbohydrate determination in freshwater revised. *International Journal of Analytical Chemistry*, 86, 693-712.
- Chen, Y., Yang, G. P., Liu, L., Zhang, P. Y., Leng, W. S. (2016b). Sources, behaviors and degradation of dissolved organic matter in the East China Sea. *Journal of Marine Systems*, 155, 84-97.
- Chen, Y., Yang, G. P., Wu, G. W., Gao, X. C., Xia, Q. Y. (2013). Concentration and characterization of dissolved organic matter in the surface microlayer and subsurface water of the Bohai Sea, China. *Continental Shelf Research*, 52, 97-107.
- Chen, Y., Yang, G. P., Xia, Q. Y., Wu, G. Y. (2016a). Enrichment and characterization of dissolved organic matter in the surface microlayer and subsurface water of the South Yellow Sea. *Marine Chemistry*, 182, 1-13.
- Conan, P., Sondergaard, M., Kragh, T., Thingstad, F., Pujo-Pay, M., Williams, P. J. L. B., et al. (2007). Partitioning of organic production in marine plankton communities: the effects of inorganic nutrient ratios and community composition on new dissolved organic matter. *Limnology and Oceanography*, 52, 753-765.

- Cowie, G. L., & Hedges, J. I. (1992). Sources and reactivities of amino acids in a coastal marine environment. *Limnology and Oceanography*, 37, 703-724.
- Cowie, G. L., & Hedges, J. I. (1996). Digestion and alteration of the biochemical constituents of a diatom (*Thalassiosira weissflogii*) ingested by an herbivorous zooplankton (*Calanus pacificus*). *Limnology and Oceanography*, 41, 581-594.
- Dauwe, B., & Middelburg, J. J. (1998). Amino acids and hexosamines as indicators of organic matter degradation state in North Sea sediments. *Limnology and Oceanography*, 43, 782-798.
- Dauwe, B., Middelburg, J. J., Herman, P. M. J., Heip, C. H. R. (1999). Linking Diagenetic Alteration of Amino Acids and Bulk Organic Matter Reactivity. *Limnology and Oceanography*, 44, 1809-1814.
- Davis, J., Kaiser, K., Benner, R. (2009). Amino acid and amino sugar yields and compositions as indicators of dissolved organic matter diagenesis. *Organic Geochemistry*, 40, 343-352.
- Dittmar T., Cherrier J., Ludwighowski K. U. (2009). The analysis of amino acids in seawater. In: O. Wurl, (Ed.), *Practical guidelines for the analysis of seawater* (1st ed.) (67-77). Boca Raton: Taylor & Francis Group.
- Dittmar, T., Fitznar, H. P., Kattner, G. (2001). Origin and biogeochemical cycling of organic nitrogen in the eastern Arctic Ocean as evident from D- and L-amino acids. *Geochimica et Cosmochimica Acta*, 65 (22), 4103-4114.
- Duman, M., Avcı, M., Duman, Ş., Demirkurt, E., Düzbastılar, M. K. (2004). Surficial sediment distribution and net sediment transport pattern in İzmir Bay, western Turkey. *Continental Shelf Research*, 24, 965-981.

- Emelianov, E. M., & Romankevitch, E. A. (1979). In E. A. Romankevich (Ed.). *Geochemistry of Organic Matter in the Ocean* (1st ed.) (127). Berlin: Springer.
- EPA, (1983). *Methods for chemical analysis of water and wastes* (2nd ed.). Washington: EPA.
- Ergin, M., Bodur, M. N., Ediger, D., Ediger, V., Yilmaz, A. (1993). Organic carbon distribution in the surface sediments of the Sea of Marmara and its control by the inflows from the adjacent water masses. *Marine Chemistry*, *41*, 311-326.
- Escoubeyrou, K., & Tremblay, L. (2014). Quantification of free, dissolved combined, particulate, and total amino acid enantiomers using simple sample preparation and more robust chromatographic procedures. *Limnology and Oceanography: Methods*, *12*, 421-431.
- Fitznar, H. P., Lobbes, J. M., Kattner, G. (1999). Determination of enantiomeric amino acids with high performance liquid chromatography and pre-column derivatisation with o-phthaldialdehyde and N-isobutyrylcysteine in seawater and fossil samples (mollusks). *Journal of Chromatography A*, *832*, 123-32.
- Grasshoff, K., Ehrhardt, M., Kremling, K. (1999). *Methods of seawater analysis* (3rd ed.). Wiley-VCH Verlag, Berlin.
- Guo, L., Tanaka, T., Wang, D., Tanaka, N., Murata, A. (2004). Distributions, speciation and stable isotope composition of organic matter in the southeastern Bering Sea. *Marine Chemistry*, *91* (1-4), 211-226.
- Handa, N. (1966). Distribution of dissolved carbohydrate in the Indian Ocean. *Journal of the Oceanographical Society of Japan*, *22* (2), 50-55.

- Handa, N. (1967). The distribution of the dissolved and the particulate carbohydrates in the Kuroshio and its adjacent areas. *Journal of the Oceanographical Society of Japan*, 23 (3), 115-123.
- Harvey, H. R., & Mannino, A. (2001). The chemical composition and cycling of particulate and macromolecular dissolved organic matter in temperate estuaries as revealed by molecular organic tracers. *Organic Geochemistry*, 32, 527-542.
- Hasumi, H., & Nagata, T. (2014). Modeling the global cycle of marine dissolved organic matter and its influence on marine productivity. *Ecological Modelling*, 288, 9-24.
- He, Z., Wang, Q., Yang, G. P., Gao, X. C., Wu, G. W. (2015). Spatiotemporal variation characteristics and related affecting factors of dissolved carbohydrates in the East China Sea. *Continental Shelf Research*, 108, 12-24.
- Hedges, J. I. (2002). Why Dissolved Organics Matter. In D. A. Hansell, C. A. Carlson, (Eds.). *Biogeochemistry of Marine Dissolved Organic Matter* (1st ed.) (1-33). Florida: Academic Press.
- Hedges, J. I., Cowie, G. L., Richey, J. E., Quay, P. D., Benner, R., Strom, M., et al. (1994). Origins and processing of organic matter in the Amazon River as indicated by carbohydrates and amino acids. *Limnology and Oceanography*, 39, 743-761.
- Hopkinson, C. S., & Vallino, J. J. (2005). Efficient export of carbon to the deep ocean through dissolved organic matter. *Nature*, 433, 142-145.
- Hopkinson, C. S., Vallino, J. J., Nolin, A. (2002). Decomposition of dissolved organic matter from the continental margin. *Deep Sea Research Part II*, 49 (20), 4461-4478.



- Hung, C. C., & Santschi, P. H. (2001). Spectrophotometric determination of total uronic acids in seawater using cation-exchange separation and pre-concentration by lyophilization. *Analytica Chimica Acta*, 427, 111-117.
- Hung, C. C., Gong, G. C., Chiang, K. P., Chen, H. Y., Yeager, K. M. (2009). Particulate carbohydrates and uronic acids in the northern East China Sea. *Estuarine, Coastal and Shelf Science*, 84 (4), 565-572.
- Hung, C. C., Guo, L., Santschi, P. H., Alvarado-Quiroz, N., Haye, J. M. (2003). Distributions of carbohydrate species in the Gulf of Mexico. *Marine Chemistry*, 81, 118-135.
- Hung, C. C., Tang, D., Warnken, K. W., Santschi, P. H. (2001). Distributions of carbohydrates, including uronic acids, in estuarine waters of Galveston Bay. *Marine Chemistry*, 73 (3-4), 305-318.
- IMST, (2000). *Monitoring of Izmir Bay after Wastewater Treatment Plant Technical Report*. Institute of Marine Sciences and Technology, Izmir, Turkey (in Turkish)
- İzdar, E. (1971). Introduction to geology and metamorphism of the Menderes massif of western Turkey. In A. S. Campbell, (Ed.). *Geology and History of Turkey. Thirteenth Annual Field Conference, Petroleum Exploration* (1st ed.) (495-500). Tripoli: Society of Libya.
- Jaffé, R., Yamashita, Y., Maie, N., Cooper, W. T., Dittmar, T., Dodds, W. K., et al. (2012). Dissolved organic matter in headwater streams: Compositional variability across climatic regions of North America. *Geochimica Cosmochimica Acta*, 94, 95-108.
- Jang, L. K., Harpt, N., Grasmick, D., Vuong, L. N., Geesey, G. G. (1990). A two-phase model for determining the stability constants for interactions between copper and alginic acid. *Journal of Physical Chemistry*, 94 (1), 482-488.

- Jang, L. K., Nguyen, D., Geesey, G. G. (1995). Selectivity of alginate gel for Cu vs. Co. *Water Research*, 29 (1), 307-313.
- Jørgensen, L., Lechtenfeld, O. J., Benner, R., Middelboe, M., Stedmon, C. A. (2014). Production and transformation of dissolved neutral sugars and amino acids by bacteria in seawater. *Biogeosciences*, 11, 5349-5363.
- Jørgensen, L., Stedmon, C. A., Kragh, T., Markager, S., Middelboe, M., Søndergaard, M. (2011). Global trends in the fluorescence characteristics and distribution of marine dissolved organic matter. *Marine Chemistry*, 126, 139-148.
- Kaiser, D., Unger, D., Qiu, G. (2014). Particulate organic matter dynamics in coastal systems of the northern Beibu Gulf. *Continental Shelf Research*, 82, 99-118.
- Kaiser, K., & Benner R. (2008). Major bacterial contribution to the ocean reservoir of detrital organic carbon and nitrogen. *Limnology and Oceanography*, 53 (1), 99-112.
- Kaiser, K., & Benner R. (2009). Biochemical composition and size distribution of organic matter at the Pacific and Atlantic time-series stations. *Marine Chemistry*, 113, 63-77.
- Kattner, G., Lobbes, J. M., Fitznar, H. P., Engbrodt, R. Nöthig, E.-M., Lara, R. J. (1999). Tracing dissolved organic substances and nutrients from the Lena River through Laptev Sea (Arctic). *Marine Chemistry*, 65, 25-39.
- Khodse, V. B., Bhosle, N. B., Matondkar, S. P. (2010). Distribution of dissolved carbohydrates and uronic acids in a tropical estuary, India. *Journal of Earth System Science*, 119 (4), 519-530.

- Khodse, V. B., Fernandes, L., Gopalkrishna, V. V., Bhosle, N. B., Fernandes, V., Matondkar, S. G. P., et al. (2007). Distribution and seasonal variation of concentrations of particulate carbohydrates and uronic acids in the northern Indian Ocean. *Marine Chemistry*, 103 (3-4), 327-346.
- Kim, T. H., & Kim G. (2013). Factors controlling the C:N:P stoichiometry of dissolved organic matter in the N-limited, cyanobacteria-dominated East/Japan Sea. *Journal of Marine Systems*, 115-116, 1-9.
- Kontas, A, Kucuksezgin, F., Altay, O., Uluturhan, E. (2004). Monitoring of eutrophication and nutrient limitation in the Izmir Bay (Turkey) before and after Wastewater Treatment Plant. *Environment International*, 29, 1057-1062.
- Kucuksezgin, F., Kontas, A., Altay, O., Uluturhan, E. (2005). Elemental composition of particulate matter and nutrient dynamics in the Izmir Bay (Eastern Aegean). *Journal of Marine Systems*, 56, 67-84.
- Lee, C., & Bada, J. L. (1975). Amino acids in equatorial Pacific Ocean water. *Earth and Planetary Science Letters*, 26, 61-68.
- Lee, C., & Bada, J. L. (1977). Dissolved amino acids in the equatorial Pacific, the Sargasso Sea, and Biscayne Bay. *Limnology and Oceanography*, 22, 502-510.
- Lee, J. H., Lee, D, Kang, J. J., Joo, H. T., Lee, J. H., Lee, H. W., et al. (2017). The effects of different environmental factors on the biochemical composition of particulate organic matter in Gwangyang Bay, South Korea. *Biogeosciences*, 14, 1903-1917.
- Leppard, G. G. (1997). Colloidal organic fibrils of acid polysaccharides in surface waters: electron-optical characteristics, activities and chemical estimates of abundance. *Colloids and Surfaces A: Physicochemical and Engineering Aspects*, 120 (1-3), 1-15.

- Letscher, R. T., Hansell, D. A., Kadko, D., Bates, N. R. (2013). Dissolved organic nitrogen dynamics in the Arctic Ocean. *Marine Chemistry*, 148, 1-9.
- Libes, S. M. (2009). *Introduction to Marine Biogeochemistry* (2nd Ed.). California: Academic Press.
- Lin, P., & Guo, L. (2015). Spatial and vertical variability of dissolved carbohydrate species in the northern Gulf of Mexico following the Deepwater Horizon oil spill, 2010-2011. *Marine Chemistry*, 174, 13-25.
- Lindroth, P., & Mopper, K. (1979). High Performance Liquid Chromatographic Determination of Subpicomole Amounts of Amino Acids by Precolumn Fluorescence Derivatization with o-Phthaldialdehyde. *Analytical Chemistry*, 51, 1667-1674.
- Lu, X., Zou, L., Clevinger, C., Liu, Q., Hollibaugh, J. T., Mou, X. (2014). Temporal dynamics and depth variations of dissolved free amino acids and polyamines in coastal seawater determined by high-performance liquid chromatography. *Marine Chemistry*, 163, 36-44
- McCarthy, M. D., & Bronk, D. A. (2008). Analytical Methods for the Study of Nitrogen. In D. G. Capone, D. A. Bronk, M. R. Mulholland, E. J. Carpenter (Eds.). *Nitrogen in the Marine Environment* (2nd ed.). San Diego: Academic Press.
- McCarthy, M. D., Hedges, J. I., Benner, R. (1998). Major bacterial contribution to marine dissolved organic nitrogen. *Science*, 281, 231-234.
- McCarthy, M., Hedges, J., Benner, R. (1996). Major biochemical composition of dissolved high molecular weight organic matter in seawater. *Marine Chemistry*, 55, 281-297.

- Meador, T. B., Gogou, A., Spyres, G., Herndl, G. J., Krasakopoulou, E., Psarra, S., et al. (2010). Biogeochemical relationships between ultrafiltered dissolved organic matter and picoplankton activity in the Eastern Mediterranean Sea. *Deep-Sea Research II*, 57, 1460-1477.
- Meon, B., & Kirchman, D.L. (2001). Dynamic and molecular composition of dissolved organic material during experimental phytoplankton blooms. *Marine Chemistry*, 75, 185-199.
- Mopper, K. & Lindroth, P. (1982). Diel and depth variations in dissolved free amino acids and ammonium in the Baltic Sea determined by shipboard HPLC analysis. *Limnology and Oceanography*, 27, 336-347.
- Murphy, K. R., Stedmon, C. A., Waite, T. D., Ruiz, G. M. (2008). Distinguishing between terrestrial and autochthonous organic matter sources in marine environments using fluorescence spectroscopy. *Marine Chemistry*, 108, 40-58.
- Murrell, M. C. & Hollibaugh, J. T. (2000). Distribution and Composition of Dissolved and Particulate Organic Carbon in Northern San Francisco Bay During Low Flow Conditions. *Estuarine, Coastal and Shelf Science*, 51, 75-90.
- Myklestad, S. M., & Børsheim, K. Y. (2007). Dynamics of carbohydrates in the Norwegian Sea inferred from monthly profiles collected during 3 years at 66°N, 2°E. *Marine Chemistry*, 107 (4), 475-485.
- Myklestad, S. M., Skånøy, E., Hestmann, S. (1997). A sensitive and rapid method for analysis of dissolved mono- and polysaccharides in seawater. *Marine Chemistry*, 56, 279-286.
- Novane, R. (1964). Proposed method for nitrate in potable waters. *American Journal of Water Works Association*, 56, 781.

- Opsahl, S., & Benner, R. (1999). Characterization of carbohydrates during early diagenesis of vascular plant tissues. *Organic Geochemistry*, 30 (1), 83-94.
- Osburn, C. L., & Stedmon, C. A. (2011). Linking the chemical and optical properties of dissolved organic matter in the Baltic-North Sea transition zone to differentiate three allochthonous inputs. *Marine Chemistry*, 126, 281-294.
- Ozkan, E. Y., & Buyukisik, B. (2012). Examination of reactive phosphate fluxes in an eutrophicated coastal area. *Environmental Monitoring and Assessment*, 184, 3443-3454.
- Ozkan, E. Y., Buyukisik, B., Koray, T., Sabancı, F. (2008a). The Influence of Changes in Nutrient Ratios on Several Biological Processes in Inner Bay of Izmir. *Turkish Journal of Fisheries and Aquatic Sciences*, 8, 103-114.
- Ozkan, E. Y., Kocatas, A., Buyukisik, B. (2008b). Nutrient dynamics between sediment and overlying water in the inner part of Izmir Bay, Eastern Aegean. *Environmental Monitoring and Assessment*, 143, 313-325.
- Pakulski, J. D., & Benner, R. (1994). Abundance and distribution of carbohydrates in the ocean. *Limnology and Oceanography*, 39 (4), 930-940.
- Panagiotopoulos, C., Sempéré, R., Jacq, V., Charrière, B. (2014). Composition and distribution of dissolved carbohydrates in the Beaufort Sea Mackenzie margin (Arctic Ocean). *Marine Chemistry*, 166, 92-102.
- Panagiotopoulos, C., Sempéré, R., Para, J., Raimbault, P., Rabouille, C., Charrière, B. (2013). The composition and flux of particulate and dissolved carbohydrates from the Rhone River into the Mediterranean Sea. *Biogeosciences*, 9, 1827-1844.

- Passow, U., Alldredge, A. L., Logan, B. E. (1994). The role of particulate carbohydrate exudates in the flocculation of diatom blooms. *Deep Sea Research Part I: Oceanographic Research Papers*, 41 (2), 335-357.
- Penna, N., Capellacci, S., Ricci, F., Kovac, N. (2003). Characterization of carbohydrates in mucilage samples from the northern Adriatic Sea. *Analytical and Bioanalytical Chemistry*, 376 (4), 436-439.
- Penna, N., Kovač, N., Ricci, F., Penna, A., Capellacci, S., Faganeli, J. (2009). The Role of Dissolved Carbohydrates in the Northern Adriatic Macroaggregate Formation. *Acta Chimica Slovenica*, 56 (2), 305-314.
- Penru, Y., Simon, F. X., Guastalli, A. R., Esplugas, S., Llorens, J., Baig, S. (2013). Characterization of natural organic matter from Mediterranean coastal seawater. *Journal of Water Supply: Research and Technology – Aqua*, 62 (1), 42-51.
- Pettine, M., Casentini, B., Fazi, S., Giovanardi, F., Pagnotta, R. (2007). A revisitiation of TRIX for trophic status assessment in the light of the European water framework directive: application to Italian coastal waters. *Marine Pollution Bulletin*, 54, 1413-1426.
- Pettine, M., Patrolecco, L., Manganelli, M., Capri, S., Farrace, M. G. (1999). Seasonal variations of dissolved organic matter in the northern Adriatic Sea. *Marine Chemistry*, 64 (3), 153-169.
- Redfield, A. C., Ketchum, B. H., Richards, F. A. (1963). The influence of organisms on the composition of seawater. In M. N. Hill, (Ed.). *The Sea* (Vol. 2) (26-77). New York: Interscience.
- Repeta, D. J. (2015). Chemical Characterization and Cycling of Dissolved Organic Matter. In D. A. Hansell, C. A. Carlson, (Eds.). *Biogeochemistry of Marine Dissolved Organic Matter* (2nd ed.) (21-63). Boston: Academic Press.

- Romera-Castillo, C., Álvarez-Salgado, X. A., Galí, M., Gasol, J. M., Marrasé, C. (2013). Combined effect of light exposure and microbial activity on distinct dissolved organic matter pools. A seasonal field study in an oligotrophic coastal system (Blanes Bay, NW Mediterranean). *Marine Chemistry*, 148, 44-51.
- Sambrotto, R. N., Savidge, G., Robinson, C., Boyd, P., Takahashi, T., Karl, D. M., et al. (1993). Elevated consumption of carbon relative to nitrogen in the surface ocean. *Nature*, 363, 248-250.
- Sannigrahi, P., Ingall, E. D., Benner, R. (2006). Nature and dynamics of phosphorus-containing components of marine dissolved and particulate organic matter. *Geochimica et Cosmochimica Acta*, 70, 5868-5882.
- Sayin, E. (2003). Physical features of the Izmir Bay. *Continental Shelf Research*, 23, 957-970.
- Scoullou, M., Plavšić, M., Karavoltzos, S. (2006). Partitioning and distribution of dissolved copper, cadmium and organic matter in Mediterranean marine coastal areas: The case of a mucilage event. *Estuarine, Coastal and Shelf Science*, 67, 484-490.
- Sharp, J. H., Rinker, K. R., Savidge, K. B., Abell, J., Benaim, J. Y., Bronk, D., et al. (2002). A preliminary methods comparison for measurement of dissolved organic nitrogen in seawater. *Marine Chemistry*, 78, 171-184.
- Shin, K. H., Hama, T., Handa, N. (2003). Effect of nutrient conditions on the composition of photosynthetic products in the East China Sea and surrounding waters. *Deep Sea Research II*, 50 (2), 389-401.
- Skoog, A., & Benner, R. (1997). Aldoses in various size fractions of marine organic matter: implications for carbon cycling. *Limnology and Oceanography*, 42 (8), 992-996.



- Skoog, A., Alldredge, A., Passow, U., Dunne, J., Murray, J. (2008). Neutral aldoses as source indicators for marine snow. *Marine Chemistry*, 108 (3-4), 195-206.
- Sohrin, R., Imanishi, K., Suzuki, Y., Kuma, K., Yasuda, I., Suzuki, K., et al. (2014). Distributions of dissolved organic carbon and nitrogen in the western Okhotsk Sea and their effluxes to the North Pacific. *Progress in Oceanography*, 126, 168-179.
- Statham, P. J. & Williams, P. J. le B. (1999). The automated determination of dissolved organic carbon by ultraviolet photooxidation. In K. Grasshoff, K. Kremling, M. Ehrhardt (Eds.). *Methods of Seawater Analysis* (3rd Ed.) (421-436). Weinheim: Wiley-VCH.
- Strickland, J. D. H., & Parsons, T. R. (1972). *A Practical Handbook of Seawater Analysis* (2nd ed.). Ottawa: Fisheries Research Board of Canada.
- Strom, S. L., Benner, R., Ziegler, S, Dagg, M. J. (1997). Plankton grazers are a potential important source of marine dissolved organic carbon. *Limnology and Oceanography*, 42 (6), 1364-1374.
- Suksomjit, M., Nagao, S., Ichimi, K., Yamada, T., Tada, K. (2009). Variation of Dissolved Organic Matter and Fluorescence Characteristics before, during and after Phytoplankton Bloom. *Journal of Oceanography*, 65, 835-846.
- Sunlu, F. S., Sunlu, U., Buyukisik, B., Kukrer, S., Uncumusaoglu, A. (2012). Nutrient and Chlorophyll a Trends after Wastewater Treatment Plant in Izmir Bay (Eastern Aegean Sea). *Journal of Animal and Veterinary Advances*, 11 (1), 113-123.
- Suzuki, M. S., Rezende, C. E., Paranhos, R., Falcão, A. P. (2015). Spatial distribution (vertical and horizontal) and partitioning of dissolved and particulate nutrients (C, N and P) in the Campos Basin, Southern Brazil. *Estuarine, Coastal and Shelf Science*, 166, 4-12.

- Tada, K., Tada, M., Maita, Y. (1998). Dissolved free amino acids in coastal seawater using a modified fluorometric method. *Journal of Oceanography*, 54, 313-321.
- Terzić, S., Ahel, M., Cauwet, G., Malej, A. (1998). Group specific phytoplankton biomass/dissolved carbohydrate relationships in the Gulf of Trieste (Northern Adriatic). *Hydrobiologia*, 363, 191-205.
- Van Beusekom, J. E. E., & de Jonge, V. N. (2012). Dissolved organic phosphorus: An indicator of organic matter turnover? *Estuarine, Coastal and Shelf Science*, 108, 29-36.
- Van Engeland, T., Soetaert, K., Knuijt, A., Laane, R. W. P. M., Middelburg, J. J. (2010). Dissolved organic nitrogen dynamics in the North Sea: A time series analysis (1995-2005). *Estuarine, Coastal and Shelf Science*, 89, 31-42.
- Vollenweider, R. A., Giovanardi, F., Montanari, G., Rinaldi, A. (1998). Characterization of the Trophic Conditions of Marine Coastal Waters with Special Reference to the Nw Adriatic Sea: Proposal for a Trophic Scale, Turbidity and Generalized Water Quality Index. *Environmetrics*, 9, 329-357.
- Voutsinou-Taliadouri, F., & Satsmadjis, J. (1982). Concentration of some metals in east Aegean sediments. *Review International Oceanography Mediterranean* 66-67, 71-76.
- Walinga, I., van Vark, W., Houba, V. J. G., van der Lee, J. J. (1989). Plant Analysis Procedures (1st ed.) (197-200). Wageningen: Wageningen Agricultural University.
- Wang, B. D, Wang, X. L, Zhan, R. (2003). Nutrient conditions in the Yellow Sea and the East China Sea. *Estuarine, Coastal and Shelf Science* 58 (1), 127-136.

- Wang, D, Henrichs, S. M., Guo, L. (2006). Distributions of nutrients, dissolved organic carbon and carbohydrates in the western Arctic Ocean. *Continental Shelf Research*, 26 (14), 1654-1667.
- Wangersky, P. J. (2000). Intercomparisons and Intercalibrations. In P. J. Wangersky, (Ed.). *The Handbook of Environmental Chemistry* (1st ed.) (167-191). Berlin: Springer.
- Wetz, M. S., & Wheeler, P. A. (2007). Release of dissolved organic matter by coastal diatoms. *Limnology and Oceanography*, 52, 798-807.
- Wu Y., Liu, Z., Hu, J., Zhu, Z., Liu, S., Zhang, J. (2016). Seasonal dynamics of particulate organic matter in the Changjiang Estuary and adjacent coastal waters illustrated by amino acid enantiomers. *Journal of Marine Systems*, 154, Part A, 57-65.
- Yamashita, Y., & Tanoue, E. (2003). Distribution and alteration of amino acids in bulk DOM along a transect from bay to oceanic waters. *Marine Chemistry*, 82, 145-160.
- Yang, G. P., Chen, Y., Gao, X. C. (2009). Distribution of dissolved free amino acids, dissolved inorganic nitrogen and chlorophyll  $\alpha$  in the surface microlayer and subsurface water of the Yellow Sea, China. *Continental Shelf Research*, 29, 1737-1747.
- Yang, G. P., Zhang, Y. P., Lu, X. L., Ding, H. B. (2010). Distributions and seasonal variations of dissolved carbohydrates in the Jiaozhou Bay, China. *Estuarine, Coastal and Shelf Science*, 88 (1), 12-20.
- Zhang, Y. P. (2010). *Distributions and Influencing Factors of Dissolved Carbohydrates in the Coastal Waters of China*. Ph.D. Thesis, Ocean University of China, Qingdao.

Zhang, Y., Yang, G, Chen, Y. (2009). Chemical characterization and composition of dissolved organic matter in Jiaozhou Bay. *Chinese Journal of Oceanology and Limnology* 27 (4), 851-858.



## **APPENDICE 1: Abbreviations List**

Ala – Alanine

ANOVA – Analysis of Variance

Arg – Arginine

AS – Amino sugars

Asp – Aspartic Acid

Aut – Autumn

C - Carbon

CaCO<sub>3</sub> – Calcium carbonate

CDOM – Chromophoric Dissolved Organic Matter

Chl-a – Chlorophyll-a

Chl-b – Chlorophyll-b

Chl-c – Chlorophyll-c

CTD – Conductivity, Temperature and Depth profiling system

DCAA – Dissolved Combined Amino Acids

DFAA – Dissolved Free Amino Acids

DI – Degradation Index

DIN – Dissolved Inorganic Nitrogen

DIP – Dissolved Inorganic Phosphorus

DNA – Deoxyribonucleic acid

DO – Dissolved Oxygen

DOC – Dissolved Organic Carbon

DOM – Dissolved Organic Matter

DON – Dissolved Organic Nitrogen

DOP – Dissolved Organic Phosphorus

DTN – Dissolved Total Nitrogen

DTP – Dissolved Total Phosphorus

FA – Factor Analysis

Glu – Glutamic Acid

Gly – Glycine

GRNMS – Gray's Reef National Marine Sanctuary

h – Reduced plate height  
HCl – Hydrochloric acid  
HDPE – High Density Polyethylene  
HMW – High molecular weight  
HPLC – High Performance Liquid Chromatography  
IBDC – N-isobutyryl-D-cysteine  
IBLC – N-isobutyryl-L-cysteine  
Ile – Isoleucine  
k – Retention factor  
LMW – Low molecular weight  
MCHO – Dissolved Free Carbohydrates - Monosaccharides  
MgCO<sub>3</sub> – Magnesium carbonate  
MidIn – Middle-Inner Bays  
MRP – Mississippi River Plume  
N – Nitrogen  
n – Peak capacity  
N – Theoretical plate number  
NH<sub>4</sub><sup>+</sup> – Ammonium  
NMR – Nuclear Magnetic Resonance  
NO<sub>2</sub><sup>-</sup> – Nitrite  
NO<sub>3</sub><sup>-</sup> – Nitrate  
NPIW – North Pacific Intermediate Water  
NS – Neutral sugars  
O<sub>2</sub> – Oxygen  
OPA – o-phthalaldehyde  
OSMW – Okhotsk Sea Mode Water  
Out – Outer Bay  
P – Phosphorus  
p – Significance level  
PA – Short-chained aliphatic polyamine  
PARAFAC – Parallel Factor Analysis  
PC – Principal Component

PCA – Principal Components Analysis  
PCHO – Dissolved Combined Carbohydrates - Polysaccharides  
Pg – Peta gram  
PHAA – Particulate Hydrolyzable Amino Acids  
Phe - Phenylalanine  
PN – Particulate Nitrogen  
 $\text{PO}_4^{3-}$  – Phosphate  
POC – Particulate Organic Carbon  
POM – Particulate Organic Matter  
PP – Particulate Phosphorus  
PTFE – Poly-tetrafluoro ethylene  
QNMR – Quantitative Nuclear Magnetic Resonance  
R – Peak resolution  
RNA – Ribonucleic acid  
Ser – Serine  
SPOM – suspended particulate organic matter  
Spr – Spring  
Sum – Summer  
TDCHO – Total Dissolved Carbohydrates  
TDHAA – Total Dissolved Hydrolyzable Amino Acids  
TDN – Total Dissolved Nitrogen  
Thr – Threonine  
TN – Total Nitrogen  
 $\text{TNO}_x^-$  – Total Nitrite+Nitrate Nitrogen  
TOC - Total Organic Carbon  
TP – Total Phosphorus  
TPTZ – 2,4,6-Tri(2-pyridyl)-s-triazine  
 $t_R$  – Retention time  
Tyr – Tyrosine  
UDOM – Ultrafiltrated Dissolved Organic Matter  
UV – Ultraviolet  
Val – Valine

$w$  – Peak width

Win – Winter

$y$  – Year

$\alpha$  – Separation factor

$\rho$  – Spearman's rank correlation coefficient

